universität wien

DISSERTATION

Titel der Dissertation

Candida spp. and Oxidative Stress Response in Innate Immune Cells

Verfasserin

Mag[a]. Ingrid Frohner

angestrebter akademischer Grad

Doktorin der Naturwissenschaften (Dr. rer.nat.)

Wien, 2010

Studienkennzahl lt. Studienblatt:	A 091 441
Dissertationsgebiet (lt. Studienblatt):	Genetik - Mikrobilogie
Betreuer:	Ao Univ.-Prof. Dr. Karl Kuchler

Table of Contents

Zusammenfassung **1**

Summary **2**

I. Introduction **3**

I.1 Introduction to fungi 3

I.2 Opportunistic fungal pathogens and *Candida* species 3

I.2.1 Virulence factors of *Candida albicans* 4

I.2.1.1 Dimorphism – *C. albicans* a fungus of many faces 4

I.2.1.2 Cell surface 7

I.2.1.3 Infection-related gene expression in *C. albicans* 13

I.2.2 Oxidative stress adaptation in *C. albicans* 14

I.2.2.1 Oxidative stress adaptation via Cap1 14

I.2.2.2 The HOG MAPK pathway 15

I.2.2.3 Antioxidant enzymes 15

I.3 Immunity to *Candida* infections 16

I.3.1 Introduction to the mammalian immune system 16

I.3.2 Recognition of *C. albicans* by the innate immune system 18

I.3.2.1 Pattern recognition receptors and their targets 19

I.3.3 Reactive oxygen species in phagocytic cells 24

I.3.3.1 Oxidative burst – the pathogen "destroyer" 24

I.3.3.2 ROS and cell signalling 28

I.3.3.3 ROS production in response to Candida infection 28

II. Aims of this work **30**

III. Results **31**

III.1 *C. albicans* degrades host-derived ROS to escape innate immune surveillance 31

III.2 PRRs and their adaptor proteins in the activation of the respiratory burst 51

III.2.1 TLRs are not involved in *C. albicans* or zymosan-induced ROS production 52

III.2.2 *C. albicans* ROS induction requires Src/Syk kinases activation but not Dectin-1 54

III.2.3 Heat-killed *C. albicans* induces ROS and MAPK signalling via Dectin-1 56

III.2.4 Dectin-2 is not involved in *C. albicans*- or zymosan-induced ROS production 58

III.2.5 CD11b has an inhibitory effect on zymosan-induced ROS production. 60

III.3 Establishing siRNA knock-down assays in BMDMs. 62

III.3.1 BMDMs are efficiently transfected by siRNA 62

III.3.2 mRNA of the target genes is sufficiently down-regulated 62

III.3.3 Transfection in a 96-well format is not sufficiently down-regulating 64

III.3.4 Transfection in 3.5 cm dishes diminishes Syk protein levels 66

IV. Conclusions and Discussion 69

IV.1 *C. albicans* degrades host-derived ROS to escape innate immune surveillance 69

IV.2 PRRs and their adaptor proteins in the activation of the respiratory burst 70

IV.3 siRNA knock-down in BMDMs 74

V. Materials and Methods 77

V.1 Genomic DNA isolation 77

V.2 Southern blot analysis 77

V.3 RNA extraction, reverse transcription and real-time PCR analysis 77

V.4 Protein extracts and western blot analysis 78

V.5 Cytokine measurements by ELISA 78

V.6 Transfection of siRNAs 78

V.7 In vitro systems for studying the interaction of fungal pathogens with primary cells from the mammalian innate immune system 79

VI. Literature 95

VII. Appendix 111

Zusammenfassung

In dieser Arbeit wurde der „Oxidative Burst“ des angeborenen Immunsystems in der Interaktion mit *Candida albicans* untersucht. Das klinische Spektrum des opportunistischen Pathogens *C. albicans* reicht von mucokutanen Infektionen bis hin zu lebensbedrohlichen, systemischen Krankheiten in immunsupprimierten Patienten. Eine der ersten Reaktionen der Zellen des angeborenen Immunsystems, sogenannte Phagozyten, ist die Produktion von Reaktiven Oxygen Spezies (ROS) wenn sie auf Pathogene stoßen. ROS spielen eine wichtige Rolle bei Entzündungsreaktionen, zum Beispiel zerstören sie eindringende Krankheitserreger. Durch eine Überproduktion von ROS kann aber auch das Endothel beschädigt werden. Frühere Studien haben gezeigt, dass Zymosan, eine Zellwand Aufbereitung von *Saccharomyces cerevisiae*, und *C. albicans* die ROS Produktion in Makrophagen aktivieren. Das *C. albicans* Genom codiert sechs Superoxid Dismutasen (*SOD1* bis *SOD6*), die an der Zersetzung von ROS beteiligt sind, *SOD1* bis *SOD3* sind intrazellular und *SOD4* bis *SOD6* sind wahrscheinlich an der Zellwand von *C. albicans* lokalisiert.

Diese Arbeit zeigt, dass die Co-Kultur von Makrophagen oder myeloischen dendritischen Zellen mit *C. albicans* denen Sod5 genetisch entfernt wurde zu einer massiven extrazellulären Anhäufung von ROS in vitro führt. Diese ROS Akkumulierung ist in der Interaktion mit Makrophagen noch höher wenn *C. albicans* weder Sod4 noch Sod5 haben. Weiteres werden *C. albicans* Sod5 und Sod4 Mutanten von Makrophagen in vitro besser getötet als Wildtyp *C. albicans*. Makrophagen, die einen Defekt im Oxidativen Burst haben weil ihnen das gp91Phox Gen fehlt, können diese Mutanten nicht mehr töten, dies zeigt eine ROS-abhängige Eliminierung von pathogenen Pilzen durch Makrophagen. Diese Daten zeigen die physiologische Rolle der *C. albicans* Zellwand SODs bei der Entgiftung von ROS und weisen auf einen Mechanismus, mit dem *C. albicans* das Immunsystems *in vivo* überlistet, hin.

Im zweiten Teil dieser Arbeit wurden potentielle Rezeptor(en) untersucht, durch die Makrophagen *C. albicans* erkennen, um den oxidative Burst zu induzieren. Die Toll Like Rezeptor-Familie und das intrazelluläre MyD88 Adapter-Protein sind nicht an der ROS-Produktion durch Zymosan oder *C. albicans* Stimulation beteiligt. Wenn der C-Typ-Lectin-Rezeptor Dectin-1 mit Zymosan oder Hitze-getöteter *C. albicans* stimuliert wird, induziert Dectin-1 die ROS Antwort indem die *Src* und Syk-Kinase aktiviert wird. Darüber hinaus aktiviert Zymosan auch die ERK1/2 MAP-Kinasen via Dectin-1. Im Gegensatz dazu ist Dectin-1 nur mäßig an der Aktivierung von ROS und ERK1 beteiligt wenn die Makrophagen mit lebenden *C. albicans* stimuliert werden. Interessanterweise ist die Aktivierung der Src und Syk-Kinasen auch wichtig für ROS Induktion durch Stimulierung mit lebender *C. albicans*. Dies führt zu dem Schluss, dass ein Rezeptor oder Adapter-Protein mit einem ITAM Motif an der Induktion von ROS beteiligt ist. Ein siRNA-basierendes knock-down-Experiment zeigt, dass das ITAM Adapter-Protein DAP12 für die ROS Produktion durch *C. albicans* und Zymosan mitverantwortlich ist.

Summary

In this work the oxidative burst of the innate immune system in response to *Candida albicans* infection was investigated. The clinical spectrum of the human opportunistic pathogen *C. albicans* ranges from mucocutaneous infections to systemic life-threatening diseases in immunocompromised patients. One of the immediate early responses of cells of the innate immune system on encountering microbial pathogens is the production of reactive oxygen species (ROS) by phagocytes. ROS play important roles in inflammatory reactions by destroying invading pathogens. However, overproduction of ROS may also cause endothelial damage, and excessive inflammation. Previous studies have shown that zymosan, a cell wall preparation of *Saccharomyces cerevisiae*, as well as *C. albicans* in the yeast form, strongly induce ROS in macrophages. The *C. albicans* genome harbours six superoxide dismutases (*SOD1-6*) involved in ROS degradation; *SOD1* to *SOD3* are intracellular and *SOD4* to *SOD6* are located in the cell wall.

This work demonstrates that co-culture of macrophages or myeloid dendritic cells with *C. albicans* cells lacking Sod5 leads to massive extracellular ROS accumulation *in vitro*. ROS accumulation was further increased in co-culture with fungal cells lacking both Sod4 and Sod5. Survival experiments show that *C. albicans* Sod5 and Sod4 double mutants exhibit a severe loss of viability in the presence of macrophages *in vitro*. The reduced viability of the mutants relative to wild type is not evident with macrophages from *gp91phox*$^{-/-}$ mice defective in the oxidative burst activity, demonstrating a ROS-dependent killing activity of macrophages targeting fungal pathogens. These data show a physiological role for cell surface SODs in detoxifying ROS, and suggest a mechanism whereby *C. albicans* can evade host immune surveillance in vivo.

The second part of this thesis aims to identify putative receptor(s) by which macrophages recognise *C. albicans* and induce the oxidative burst. The Toll-like receptor family and its MyD88 adaptor protein are not involved in ROS production due to zymosan or *C. albicans* stimulation. The c-type lectin receptor Dectin-1 can induce the ROS response via activation of Syk kinase with its immunoreceptor tyrosine-based activation motif (ITAM)-like domain upon zymosan or heat-killed *C. albicans* stimulation. Furthermore, zymosan also activates extracellular signal related kinase ERK1/2 MAPK dependent on Dectin-1. In contrast, Dectin-1 is only moderately involved in activation of ROS and ERK1/2 when stimulated with live *C. albicans*. Interestingly, activation of *Src* and Syk kinases is essential to induce the ROS response by live *C. albicans*. This leads us to conclude that an ITAM-containing receptor or adaptor protein is involved in the recognition of live *C. albicans*. Using a siRNA-based knock-down assay, we found that one ITAM-containing adaptor protein, DAP12, may contribute to the ROS response upon fungal pathogens such as *C. albicans*.

I. Introduction

I.1 Introduction to fungi

The kingdom of fungi is made up of diverse eukaryotic species. Fungi are heterotrophic organisms composed of rather rigid chitinous cell walls. About 180000 species of fungi have been described, although there are about 1,5 million species estimated (Mueller and Schmit, 2007). Recently, the kingdom of fungi was newly classified, taking molecular phylogenetic analyses and input from diverse members of the fungal taxonomic community into account (Hibbett et al., 2007). Macroscopic fungi such as morels and mushrooms represent only a small fraction of the diversity in the Fungi kingdom. The majority of fungal species, the molds, grow as multicellular filaments. The more phylogenetically primitive molds produce coenocytic filaments, which are multinucleate cells without septa. The more advanced forms grow hyphae with septa that subdivide filaments into uninucleate and multinucleate compartments. Some fungal species, the yeasts, also grow as single cells. Although the yeast form occurs less frequently in nature, it is found in economically very important and scientifically well explored species such as "bakers' yeast" *Saccharomyces cerevisiae* (Carlile and Watkinson, 1994).

I.2 Opportunistic fungal pathogens and *Candida* species

About 300 fungal species are known to cause human infections, and some fungi are economically important as animal and plant pathogens (Taylor et al., 2001). In humans, fungi can cause superficial, cutaneous, subcutaneous, systemic or allergic diseases. In healthy individuals, fungal diseases are benign. However, the few existing life-threatening fungal diseases are of major clinical relevance, since they pose an increasing problem in humans with altered bacterial flora due to antibiotics treatment, as well as in immunocompromised patients. (McGinnis MR., 1996)

There are two main types of fungal infections described. First, in true pathogenic fungal infections, the fungus is virulent regardless of the constitutional adequacy of the host; they include *Histoplasma*, *Coccidioides*, *Blastomyces* and *Paracoccidiodies*. Second, the opportunistic fungal mycoses are caused by organisms which are normally of low virulence. However, disease manifestation is dependent on a reduced host resistance to infection. Common fungi involved in opportunistic infections are *Aspergillus*, *Cryptococcus and Candida* spp.

Aspergillus species are ubiquitous saprophytic fungi found all over the world. They thrive well in soil and decaying vegetation. Of all fungal diseases aspergillosis has been the subject of most intensive studies (Blanco and Garcia, 2008). Cellular characteristics that might cause respiratory aspergillosis have been described in many mammalian species and birds (Tell, 2005). The incidence of invasive aspergillosis in patients with AIDS, chronic granulomatous disease and acute leukaemia are estimated at 0-12%, 25-40% and 5-24 % (Warris and Verweij, 2005).

Two species can be differentiated in the genus *Cryptococcus*. *C. neoformants* infects primarily patients with a compromised immune system, while *C. gattii* infects immunocompetent hosts. Cryptococcal meningitis is a common opportunistic infection in late-stage HIV infections and mortality from HIV-associated cryptococcal meningitis ranges from 10-30% (Bicanic et al., 2005).

Candida species are harmless commensal colonisers of the gastrointestinal and genitourinary tracts and to a lesser extent on the human skin. Approximately 75% of all women experience vaginal infections caused by *Candida spp.* at least once in their lifetime. *Candida albicans* is the causative agent in 85-95 % of these infections (Fidel, 2007). However, in weakened immune systems, for example as a result of cancer chemotherapy, HIV infection or in neonates, *Candida* can colonize, invade and destroy host tissue. In total, there are more than 200 *Candida* spp., but only few of them are of medical relevance. Besides *C. albicans, C. parapsilosis*, *C. glabrata*, *C. tropicalis*, *C. krusei* as well as *C. dubliniensis* can be the cause of candidiasis in humans. *Candida spp.* now rank as the fourth-most common cause of nosocomial bloodstream infections in the United States, with mortalities reaching up to 40% (Pfaller and Diekema, 2007). Incidences of infection have risen with the increased prevalence of immunosuppressive therapies and the use of broad-spectrum antibiotics. Since *C. albicans* has rarely been isolated from the environment, it is considered to be obligatorily associated with mammalian hosts. To fully understand its pathogenicity, a major key is to explore and decipher the regulatory networks that support the transition from the commensal to pathogenic state (Brown et al., 2007; Zakikhany et al., 2008).

I.2.1 Virulence factors of *Candida albicans*

I.2.1.1 Dimorphism – *C. albicans* a fungus of many faces

C. albicans displays a remarkable morphogenetic plasticity (Figure 1). The organism can grow in yeast or hyphal forms or intermediate morphologies such as pseudohyphae (Whiteway and Bachewich, 2007). In the yeast growth form cells are round to ellipsoid single cells, dividing by

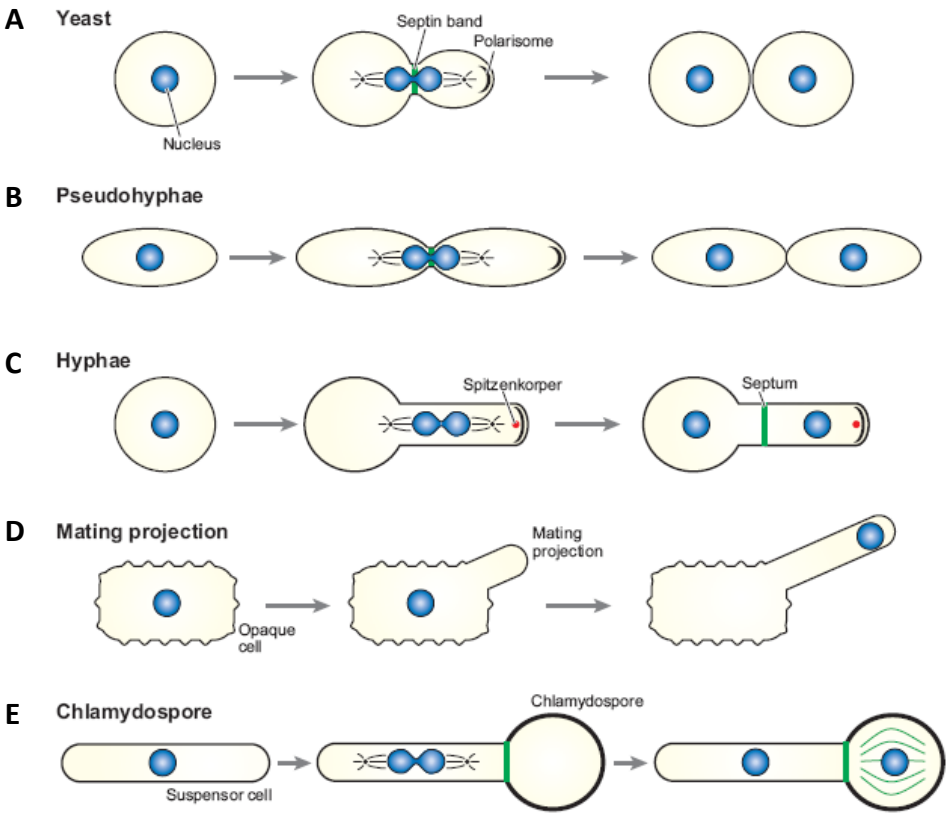

Figure I.I.1: Distinct morphological forms of *C. albicans*.
A In yeast-form a blastospore buds off a new cell, resulting in two discrete cells. **B** In pseudohyphal the cells themselves are more elongated than during yeast growth, and the cells remain attached after cytokinesis. **C** Hyphal growth is defined by a polarisome and a "Spitzenkörper" at the tip of the growing hyphae. **D** Opaque-form cells are capable of responding to mating pheromone by elongating a mating projection or shmoo. **E** Chlamydospores are formed at the end of suspensor cells. They have a thicker cell wall and are larger than blastospores (Whiteway and Bachewich, 2007).

budding to physically separated cells. In contrast, hyphal growth originates from a germ tube that resembles a bud. Upon emergence, it is extended into a long filament where individual cells are separated by septae (Berman and Sudbery, 2002). The switch from yeast growth to hyphal growth is controlled by the environmental state and numerous stimuli. The standard trigger of hyphal growth is nutrient poor media such as Lee's medium and a rise in temperature together with *N*-acetyl-glucosamine (GlcNAc) or serum (Whiteway and Bachewich, 2007). *C. albicans* switches to the hyphal form in the host to adhere to and penetrate through tissues, therefore this switch has been considered important for virulence (Whiteway and Oberholzer, 2004).

The transcriptional control of the yeast-hyphal transition is well explored. The expression of hyphal-specific genes is tightly regulated by a complex network of signal transduction pathways (Biswas et al., 2007). Initially, it was observed that the combined loss of the transcription factors Efg1 and Cph1 blocked the hyphal transition, and *efg1*/*cph1* mutant showed attenuated virulence. This observation suggested importance of the yeast to hyphal transition in

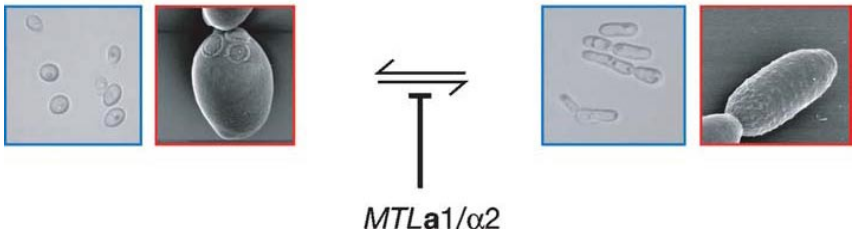

Figure I.2: White-opaque switching in *C. albicans* adapted from (Bennett and Johnson, 2005)

pathogenicity (Lo et al., 1997). External pH is another signal regulating the transition. Rim101 is the main transcription factor involved in the induction of the alkali induced hyphal growth (Davis et al., 2000). The TEA/ATTS transcription factor Tec1 is essential for serum-induced filamentation (Schweizer et al., 2000). Furthermore, there are a number of other transcription factors (Czf1, Flo8, Hap5 Efh1, Ace2 Mcm1, Ash1 and Cph2) involved in filamentation under specific growth conditions (Whiteway and Bachewich, 2007). The cAMP-protein kinase A pathway is involved in regulating morphogenesis on solid medium and the G Protein-coupled receptors Gpr1 and the Gpa2 act through the cAMP pathway to regulate hyphal transition (Maidan et al., 2005; Miwa et al., 2004).

The second-most studied phenotypic switch of *C. albicans* is the transition from white to opaque form. White cells exhibit the classic yeast cell shape and generate dome-shaped colonies with a creamy colour. Opaque cells are elongated with a distinctive pimpled surface (Figure I.2) forming colonies that are more flattened and gray than those of white cells (Lockhart et al., 2002; Slutsky et al., 1987; Soll, 2004). The ability to switch to the opaque form depends on whether the *mating type locus* (*MTL*) is homozygous (Figure I.2, bottom). Most *C. albicans* cells are heterozygous for the MTL (*MTL***a**/*MTL*α) and express the heterodimeric **a**1/α2 repressor, and therefore are unable to switch (Miller and Johnson, 2002). This repressor controls the expression of another transcription factor, the *WOR1* (white opaque regulator) gene product (Huang et al., 2006; Zordan et al., 2006).

The Wor1 transcription factor is the primary regulator in the white opaque switching. Ectopic expression of *WOR1* in *MTL***a**/*MTL*α cells induces a pseudo-opaque state (Zordan et al., 2006). The existing data suggest that once Wor1 is expressed, it is keeping the cells in the opaque state. Nevertheless, once Wor1 levels drop below a critical threshold, cells switch back to the white phase (Zordan et al., 2006). Other players involved in switching are Efg1 and Tup1. Already described above, Efg1 is a positive regulator of the yeast to hyphal transition, while Tup1 is a negative regulator of pseudohyphal development. Efg1 is highly expressed in white form cells but not in opaque cells, and loss of Efg1 causes white cells to display some characteristics of

opaque cells (Sonneborn et al., 1999b). Loss of Tup1 changes the morphology of the opaque cells and deregulates the expression of some phase-specific genes, but permits the mating-competent cell type (Park and Morschhäuser, 2005). Additional transcriptional regulators of white-opaque switching are Czf1 and the white-opaque regulator Wor2 (Zordan et al., 2007). Furthermore, chromatin modifiers were identified as modulators of the white-opaque switching, since they seem to modulate the activity of transcriptional circuitry (Hnisz et al., 2009; Klar et al., 2001; Srikantha et al., 2001).

Like the yeast-hyphae transition, white-opaque phase transition also influences virulence properties. The viability of opaque cells is reduced when compared to white cells under many growth conditions (Slutsky et al., 1987). Furthermore, macrophages seem to preferentially phagocytose white cells (Lohse and Johnson, 2008).

Pseudohyphae and chlamydospores are additional morphological states of *C. albicans* (Staib and Morschhauser, 2007; Whiteway and Bachewich, 2007). Pseudohyphal growth typically shows elongated cells connected in chains, but individual cells are yeast-like (Whiteway and Bachewich, 2007). Chlamydospore formation has served for a long time as identification of the human fungal pathogen *C. albicans*, but the biological function of these structures remains elusive. They have been proposed to allow survival in harsh environmental conditions, but this assumption remains yet to be proven. Chlamydospore formation also requires the transcriptional regulator Efg1 (Sonneborn et al., 1999a) and the MAP kinase Hog1 (Alonso-Monge et al., 2003).

I.2.1.2 Cell surface

The fungal cell surface contributes to pathogenesis by mediating interactions with host-cells and eliciting host immune responses. Fungal cell walls combine skeletal and matrix components. Depending on the method used for analysis of *C. albicans* wall components, it appears to consist of 4 to 8 layers (Poulain et al., 1978). The skeletal component of the cell wall of *C. albicans* is based on a core structure of β-glucans (a network of β-(1,3)-glucan linked with β-(1,6)-glucan) and chitin (a β-(1,4)-linked polymer of *N*-acetylglucosamine (GlcNAc)) (Figure I.3). Other studies suggest that the structure of the β-glucan network is more similar to *S. cerevisiae,* where lateral β-(1,6)-glucan chains are linked with β-(1,3)-glucan (Iorio et al., 2008).

Most models suggest that the skeletal components of the cell wall are close to the membrane forming an inner layer, although chitin and glucan are present throughout the

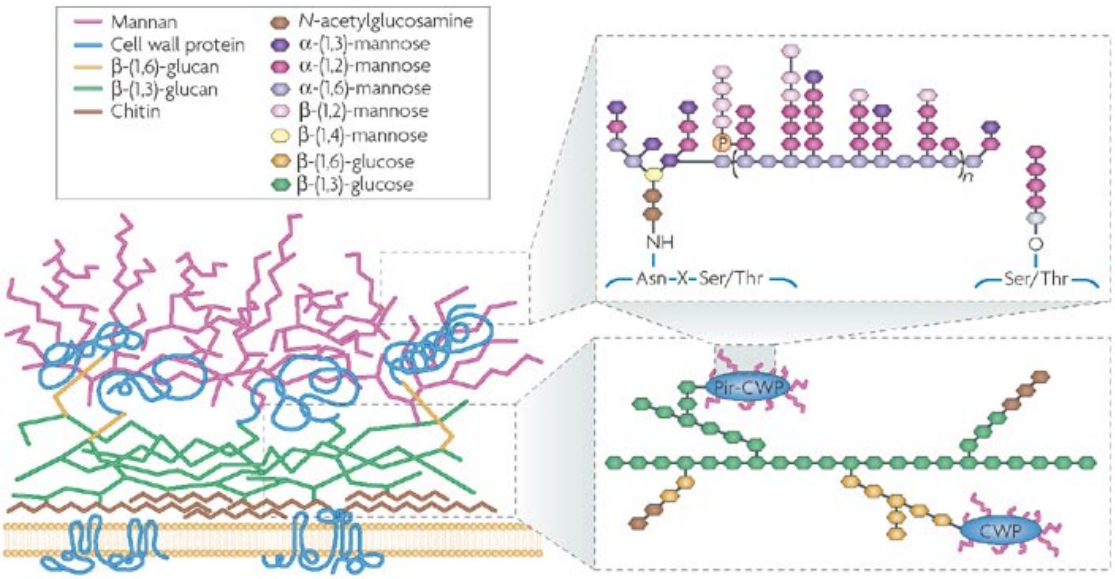

Figure I.3: The components of the cell wall and their localisation.
The main structural components of the cell wall β-(1,3)-glucan and chitin (poly-β-(1,4)-N-acetylglucosamine), are located towards the inside. The outer layer is enriched with cell wall proteins (CWP) that are attached to this skeleton mainly via glycosylphosphatidylinositol remnants to β-(1,6)-glucan or with internal repeat domains (Pir-CWP), via alkali-sensitive linkages to β-(1,3)-glucan. The insets show the structure of the glucan and mannan components (Netea et al., 2008a).

thickness of the wall via bud scars (Gantner et al., 2005). In addition to the skeleton, the cell wall matrix mainly consists of glycosylated proteins, representing 30-40% of the cell wall dry weight (Klis et al., 2001). Mannoproteins are bound to the β-glucan/chitin inner layer through lateral chains of β-(1,6)-glucan or to β-(1,3)-glucan. Very important for the discrimination between fungal species and serotypes are β-(1,2)-mannans. They are present in *C. albicans* but absent in *S. cerevisiae*. Macrophages use this to distinguish these two fungal species via the pattern recognition receptor Galectin-3 (see also Chapter I.3.2.1) (Fradin et al., 2000; Jouault et al., 2006; Kohatsu et al., 2006). Furthermore, three types of β1,2-mannans have been found in different *Candida* species (Shibata et al., 1996a; Shibata et al., 1996b; Suzuki et al., 1996). Lipids are minor components of the cell wall. In *C. albicans,* phospholipomannan reacts with antibodies specific to β-1,2-oligomannosides (Poulain et al., 2002). For phospholipomannan, it has been suggested that it may have relevance in adhesion, protection and signalling (Jouault et al., 2003; Mille et al., 2004).

Chitin

Synthesis of chitin involves a transglycolysation reaction of GlcNAc residues to the growing polysaccharide chain. This reaction is catalysed by chitin synthases (CHS) and requires divalent metal ions (Ruiz-Herrera and Martinez-Espinoza, 1999). Three genes encoding chitin synthases are described in *C. albicans*. *CHS2* is preferentially expressed in the hyphal state although its lack

does not have any effect on chitin levels, the yeast to hyphal transition or virulence in a mouse model (Gow et al., 1994). Chs1 is involved in septum formation and essential for cell integrity and virulence (Mio et al., 1996). Strains defective in Chs3 are less virulent in a mouse model than the parental strain. Deletion of the *C. albicans* homologue of the *S. cerevisiae BNI4* gene, which is the protein responsible for tethering of Chs3 during budding, leads to reduced chitin levels and morphological alterations, but does not affect the chitin ring that separates mother and daughter cell (Ruiz-Herrera et al., 2006). Exposure of *C. albicans* to cell wall stresses such as $CaCl_2$ or Cacofluor White (CFW) can increase the chitin synthase activity (Munro et al., 2007). Additionally, caspofungin treatment, which targets the β-(1,3)-glucan synthesis increases Chs3 levels in the cell (Walker et al., 2008). A fourth Chs was identified by in silico analysis: Csh8, which is similar to Csh2 and is responsible for 25% of the chitin synthase activity but not essential for growth (Munro et al., 2003). The chitin synthase can be used as a target to control mycosis because of the importance of chitin in the structure of the cell wall and its absence in the host. So far, two important inhibitors of chitin synthase have been described: polyoxins and nikkomycins. They are showing high antifungal activity in vitro, however, both do not show effective activities in in vivo studies (Ruiz-Herrera et al., 2006).

Cell wall glucans

β-Glucans are the most abundant polysaccharides of the fungal cell wall. They occur as β-(1-3)-linked glucose polymers with β-(1-6)-linked side chains of varying length and distribution. The synthesis of β-glucans is a complex reaction, involving several enzymes located at different cell compartments. Chain growth of β-(1,3)-glucans involves a transglycolysation reaction of glucosyl residues from the universal donor UDP-glucose to growing polysaccharide chains (Ruiz-Herrera et al., 2006). Genes encoding the β-(1,3)-glucan synthase are named *FKS* in *S. cerevisiae*. The *C. albicans* genome harbours three homologues: *GSC1, GSL1* and *GSL2* (Mio et al., 1996).

Glucans and mannans are released by *C. albicans* in synthetic medium as well as in the blood of infected patients. These molecules can induce anaphylactic shocks and coronary arthritis in murine models (Nakagawa et al., 2003). On the other hand, anti-glucan antibodies contribute to the immune response by recogni*sing* pathogenic fungi (Ishibashi et al., 2005). The ability to modulate host immunity is influenced by polymer length, tertiary structure and degree of branching (Tsoni and Brown, 2008). In general, large particulate β-glucans are able to activate leukocytes directly, triggering phagocytosis, the production of cytokines, chemokines and other inflammatory mediators (Brown and Gordon, 2005). Intermediate-sized β-glucans (glucan phosphate) are active in vivo but do not trigger leukocyte response in vitro. There is evidence

that they can activate *nuclear factor* '*kappa*-light-chain-enhancer' of activated *B*-cells (NF-κB) and modulate inflammation via the phosphoinositol-3-kinase (PI3K) pathway (Adams et al., 1997; Williams et al., 2004). Small and low molecular weight β-glucans, such as laminarin, are recognised by glucan receptors but do not activate downstream signals (Brown and Gordon, 2003). The ability of β-glucans to modulate immune recognition has brought pharmaceutical interest in these compounds (Liu et al., 2009a).

Treatment with β-glucans can reduce microbial burdens and increase survival of infected animals. Although it is not known how they mediate the anti-infective activities, β-glucans are used as immune boosters, and have been assessed in clinical trials with promising results (Brown and Gordon, 2003; Dellinger et al., 1999). The anti-tumour activity is the best-examined property of glucans. They have been shown to inhibit tumour growth and increase survival times, but the success of this treatment is dependent on a number of factors including the type of tumour (Liu et al., 2009b; Ross et al., 1999). In general, β-glucans are considered as safe but they can also have some negative side-effects on the treated host. Intravenous injection of particulate β-glucan causes the formation of granulomas, but this has been overcome by the invention of active soluble glucans. Nevertheless, they have also been implicated in triggering autoimmune diseases such as arthritis and could be involved in respiratory burst disorders (Yoshitomi et al., 2005).

Cell wall proteins

Cell wall proteins can fall into two classes. Class I proteins are not covalently linked to the cell wall and are extractable with detergents or chaotropic agents. They have a signalling domain and a Ser/Th-rich functional and structural domain. Class 2 proteins can only be solubilised after the destruction of structural polysaccharides or by breaking the specific bonds which link them to the polysaccharides (Ruiz-Herrera et al., 2006). These class 2 proteins can again be divided into the "true" wall proteins and "atypical" wall proteins. The true wall proteins include glycosylphosphatidylinositol (GPI)-anchored cell wall proteins (GPI-CWPs) bound to β-(1,6)-glucan (De Groot et al., 2005; de Nobel and Lipke, 1994), proteins with internal repeats (Pir), proteins attached to the cell wall through alkaline-soluble wall bounds (ASL-CWP) (Castillo et al., 2003; De Groot et al., 2005) and reducing agents-extractable wall proteins (RAE-CWPs) (Moukadiri and Zueco, 2001). Atypical wall proteins are lacking a carbohydrate moiety and the mechanism retaining them at the cell wall is not known (Ruiz-Herrera et al., 2006).

GPI –anchored proteins

In *C. albicans*, the major class of cell wall proteins are GPI-CWPs. All are attached through a GPI remnant to β-(1,3)- glucans (90%) or chitin (10%) by a highly branched β-(1,6)-glucan linker. The CWPs are normally highly glycosylated with mannose-containing polysaccharides, which can account for up to 90% of their molecular mass. The core structure linking the C-terminal end of GPI proteins to the lipid moiety (protein-CO-NH-(CH_2)- PO_4-Man-α-1,2-Man-α-1,6-Man-α-1,4-GlcN-α-1,6-inositol-PO_4-lipid) is identical in all GPIs analysed so far, but the side chains linked to this core is differs widley between species (Sipos et al., 1995). The amino acids upstream of the site of GPI anchor addition (ω-site) serve as a signal for the attachment of the protein to the membrane or the cell wall (Frieman and Cormack, 2003). This signal consists of hydrophobic amino acids, followed by a short region of hydrophilic residues and a binding site formed by three residues named ω, ω+1 and ω+2. The protein is cleaved between ω and ω+1 and the GPI-anchor remains bound to the ω amino acid (Nuoffer et al., 1993). The transfer of the GPI moiety to the protein takes place in the lumen of the endoplasmic reticulum. After the cleavage of the carboxy-terminal hydrophobic sequence, an amid linkage between the ethanolamine phosphate of the GPI and the new carboxy-terminal amino acid is formed (Udenfriend and Kodukula, 1995). The transfer is catalysed by a GPI-transamidase. In cell wall proteins, the above described anchor is trimmed, and only a part is retained at their C-terminus, which participates in binding the proteins to β-(1,6)-glucan (Figure I.4) (Lipke and Ovalle, 1998).

The number of putative GPI proteins identified in *C. albicans* (115) is almost twice as high as of those identified in *S. cerevisiae* (58). However, both lists stem from insilico predictions and may have inaccuracies (Richard and Plaine, 2007). The 115 GPI-proteins identified in *C. albicans* can be divided in four classes (Table I-1). The largest class of genes with unknown functions might be relevant for the future discovery of pathogenicity genes. Since GPI proteins are located

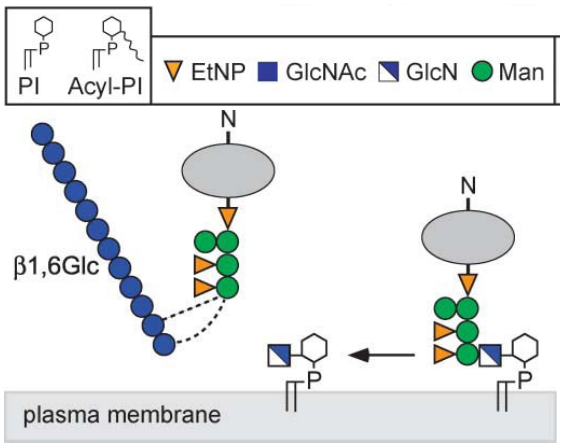

Figure I.4: Postulated transglycosylation reaction in which a GPI-cell wall protein becomes cross-linked to cell wall β-(1,6)-glucan via its GPI glycan. The GPI is likely to be cleaved between Man-1 and glucosamine (GlcN) and transferred to a terminal or an internal β-(1,6)-linked glucan in cell wall. Features of a GPI-glycoprotein that correlate with cell wall anchorage include the presence of serine and threonine-rich regions in the protein and the absence of two basic amino acids from the ω minus region. It is not known whether the presence of ethanolamine phosphate (EtNP) side branches, or of long acyl chains or a ceramide on the GPI, is important for transglycosylation to occur or whether EtNP side branches are retained after cross-linking. Adapted from (Orlean and Menon, 2007)

Table I-1: Classes of GPI-anchored Genes in *C. albicans* (Richard and Plaine, 2007)

Class	Nr genes	% genes	Function
1	76	66	Unknown
2	15	13	Cell wall biogenesis and remodelling
3	13	11	Cell-cell adhesion and interactions
4	11	9.5	Enzymatic properties (e.g. superoxide dismutase and aspartyl protease activity

at the cell surface they are supposed to interact with the host cells. Further, *C. albicans* is highly adapted to its environment compared to other opportunistic fungi (in terms of pH, oxidation, phagosomes, etc.), suggesting that evolutionally, it developed several mechanisms to colonize its host. These unique functions might involve surface proteins of unknown functions.

The agglutinin-like sequence (ALS) gene family encodes eight GPI-anchored proteins which are the most intensively studied GPI proteins in *C. albicans*. They may promote adhesion of *C. albicans* cells to host tissues (Hoyer et al., 2008; Zhao et al., 2005). Immunohistochemical approaches demonstrate expression of Als proteins in *C. albicans* cells infecting the spleen, kidneys, liver, heart and lungs of mice (Hoyer, 2001). In addition, the expression of individual ALS genes has been detected during oral and vaginal infections by RT-qPCR (Cheng et al., 2005; Green et al., 2004; Green et al., 2006). ALS expression patterns in clinical samples were similar to those observed in the corresponding animal models of oral, vaginal and systemic candidiasis, and in reconstituted human epithelial models (Brown et al., 2007). Als3 was found to bind ferritin and allows *C. albicans* to utilise iron in oral cavities (Almeida et al., 2008)

Pir proteins do not contain a GPI anchor domain; they are attached to the cell surface via as yet unknown alkali labile bonds. At least some of the Pir proteins are retained in the wall by disulfide bridges (Castillo et al., 2003). They are highly O-glycosylated and are characterised by the presence of internal repeats in variable numbers (Toh-e et al., 1993). The group of **atypical wall proteins** includes proteins predicted to be cytoplasmic, but those have been detected in large amounts at the cell wall (Ruiz-Herrera et al., 2006).

Many surface proteins are essential for *C. albicans* viability. First, some these proteins have enzymatic activity and degrade large impermeable compounds thereby making products accessible for cell nutrition. For example, the cell wall-linked acid trehalase *ATC1* enables the fungus to grow on trehalose by hydrolysing the latter (Chaffin, 2008; Pedreno et al., 2004). Second, wall proteins mediate interactions with other cells and surfaces. Attachment or adherence is dependent on different recognition systems, the type of host cell, the type of

adhesin and the type of host cell ligand (Calderone, 1993). An example would be the already mentioned ALS family proteins. The third role of wall proteins relates to the pathogenicity of *C. albicans.* Proteins extracted from the cell wall induce arthritis in mice and many *C. albicans* mutants lacking cell wall proteins show reduced virulence (Fradin et al., 2005). Fourth, the antigenic property of *C. albicans* glycoproteins that are differentially present in the yeast or mycelia forms (Sundstrom et al., 1988). Last but not least, surface proteins are important for the structure and morphogenesis of the fungus. For example, the putative surface glycosidase (Csf4) is important for cell wall integrity and maintenance (Alberti-Segui et al., 2004).

I.2.1.3 Infection-related gene expression in *C. albicans*

The adaptation of *C. albicans* to different host niches is very important for a switch to pathogenicity. As a commensal, *C. albicans* colonises the gastrointestinal tract and oral cavity. As a pathogen, it invades vaginal and oral epithelial surfaces, and in immunocompromised patients it can be transported via the bloodstream and invade internal organs (Calderone, 2002). In all niches, *C. albicans* encounters different host stress conditions. The pH can change from acidic to mildly alkaline, and the accessibility of nutrients varies extensively (Brown et al., 2007). When *C. albicans* colonises a niche, it may very well alter that niche by metabolising nutrients thereby changing the ambient pH or damage host tissues (Brown et al., 2007). Numerous proteins expressed during dissemination in the host are associated with major changes at the cellular level including morphogenesis. Other proteins investigated are predicted virulence factors such as secreted aspartyl proteinases (SAPs), phospholipases B (PLBs), secreted lipases (LIPs) and adhesins (described in "Cell surface and adhesion") (Brown et al., 2007).

Proteinase activity of *C. albicans* is linked to a family of 10 members, the secreted aspartyl protease (SAP) family (Monod and Borg-von Zepelin, 2002). While Sap1 - 8 are secreted proteins, Sap9 and Sap10 have C-terminal consensus sequences typical for GPI proteins (Monod et al., 1998; Monod et al., 1994). *SAP2* and *SAP5* are the most commonly expressed ones, *SAP1*, *SAP3*, *SAP4* and *SAP7* are linked to oral disease, while *SAP1*, *SAP3* and *SAP6 - 8* expression is associated with vaginal infections (Naglik et al., 2003). All members of the SAP family are expressed during colonisation and dissemination. Furthermore, certain *SAP* genes might have more important roles specifically during infection and the expression is most likely tightly controlled during the progression from colonisation to infection (Naglik et al., 2004). Recently, it was shown that *SAP1 – SAP6* are not required for the invasion of reconstructed human epithelial tissue (Lermann and Morschhauser, 2008). *C. albicans* secretes proteases that interfere with and inactivate host

innate immune effector components, such as the complement proteins C3b, C4b and C5 (Gropp et al., 2009).

In addition to SAPs, extracelluar phospholipase (PLs) and secreted lipases (LIPs) are also enzymes considered as virulence factors. Two extracellular PLs, *PLB1* and *PLB2,* have been studied (Schaller et al., 2005). Expression has been detected in gastrointestinal, mucosal and systemic infection models (Schaller et al., 2005), with differences in the expression of *PLB1* and *PLB2* in samples of human oral and vaginal infections (Naglik et al., 2003). The secreted LPs consist of at least 10 members (*LIP1* – *LIP10*) (Hube et al., 2000). *LIP5*, *LIP6*, *LIP8* and *LIP9* are expressed during intraperitoneal infection in mice (Hube, 2000). *LIP1*, *LIP3* and *LIP9* are found in infected gastric tissues but undetectable in oral mucosa (Schofield et al., 2005). *LIP4* preferentially plays a role in superficial infections (Stehr et al., 2004).

I.2.2 Oxidative stress adaptation in *C. albicans*

A major mechanism of the host defence system responding to fungal infections is the production of reactive oxygen species (ROS) by phagocytes used to kill invading microbes (for details see Chapter I.3.3). Understanding how fungal cells deal with ROS can provide critical information and be a first step towards designing strategies to enhance host cell- mediated killing of these pathogenic organisms. The oxidative stress response in *C. albicans* involves oxidant sensing and response to oxidative damage via two major pathways that appear to act distinctly: the Cap1p pathway and the high osmolarity glycerol (HOG) mitogen-activated protein kinase (MAPK) pathway (Chauhan et al., 2003; Enjalbert et al., 2006). The regulation of stress adaptation varies according to the concentration of peroxide to which cells were exposed. Cap1 mediates adaptation to both low and high peroxide concentrations, while Hog1 regulates adaptation to high peroxide concentrations (Enjalbert et al., 2006).

I.2.2.1 Oxidative stress adaptation via Cap1

In *S. cerevisiae,* the basic leucine zipper transcription factor Yap1 is required for oxidative-stress tolerance and mediates pleiotropic drug and metal resistance (Wendler et al., 1997; Wysocki et al., 2004). The genes regulated by Yap1 are for example *GPX2* (glutathione peroxidise), *TRX2* (thioredoxin) and *GSH* (glutathione biosynthesis) (Dormer et al., 2002; Tanaka et al., 2005). Cap1 is the *C. albicans* Yap1 homologue, and Cap1-defective cells are hypersensitive to oxidative stress induced by diamide or H_20_2 (Alarco and Raymond, 1999). *CAP1* transcription increases when the fungal cells are phagocytosed by human neutrophils, and deletion of the gene attenuates virulence (Bahn and Sundstrom, 2001; Fradin et al., 2005). Cap1-mediated responses

involve multiple pathways, including the cellular antioxidant system, carbohydrate metabolism and energy metabolism, protein degradation, ATP-dependent RNA helicase, and resistance pathways (Wang et al., 2006b). Recently, a Cap1 regulon consisting of 89 target genes was described, including genes involved in oxidative stress adaptation, drug response, phospholipid transfer and regulation of nitrogen utilisation (Znaidi et al., 2009).

I.2.2.2 The HOG MAPK pathway

One of the major signalling pathways in *C. albicans*, which senses oxidative stress and elicits the transcriptional regulation for the adaptation, is the HOG-MAPK pathway, which is otherwise also involved in osmotic stress adaptation (Moye-Rowley, 2003).This pathway was first described in *S. cerevisiae* with a function in osmo-adaptation (Hohmann et al., 2007). Upstream of the Hog1 MAPK are multistep phosphorylated proteins determining pathway activation. In *C. albicans,* several genes of the HOG MAPK signalling pathway play a role in the adaptation to oxidative stress. The *ssk1* mutant is sensitive to several oxidants, and its survival is reduced in human neutrophils. Furthermore, the mutant strain is avirulent in a mouse model (Chauhan et al., 2003; Du et al., 2005). A *bps2* mutant was sensitive to both osmotic and oxidative stress, as was a *hog1* mutant (Arana et al., 2005). Moreover, the *C. albicans* Skn7 kinase is required for oxidative stress in vitro (Singh et al., 2004).

I.2.2.3 Antioxidant enzymes

In addition to specific oxidative stress signalling pathways, fungi have various antioxidant enzymes to counteract oxidative damage, including superoxide dismutase (SOD), glutathione reductase, thioredoxin, and catalase (Hwang et al., 2003; Hwang et al., 2002; Lamarre et al., 2001; Martchenko et al., 2004; Nakagawa et al., 2003; Wysong et al., 1998). *C. albicans* harbours six SODs (Figure I.5), the cytoplasmic Sod1 (Cu-Zn SOD) and Sod3 (Mn-SOD), the mitochondrial Sod2 (Mn-SOD) and three other potential surface Cu-Zn SODs, Sod4–6, (Hwang et al., 2003; Hwang et al., 2002; Lamarre et al., 2001; Martchenko et al., 2004).

Among the SODs, the best studied ones regarding their role in pathogenesis are Sod1 and Sod5. A *sod1* mutant of *C. albicans* is sensitive to menadione but not to H_2O_2, hyper-sensitive to killing by cultured macrophages when compared to wild type cells, and displays reduced virulence in an invasive mouse model (Hwang et al., 2002). Upregulation of *SOD5* was observed during the yeast-to-hyphal transition in the presence of non-fermentable carbon sources, and when cells grow under conditions of oxidative, osmotic stress or basic pH. A *sod5* deletion mutant of *C. albicans* is sensitive to H_2O_2 when cells grow under nutrient-limiting conditions.

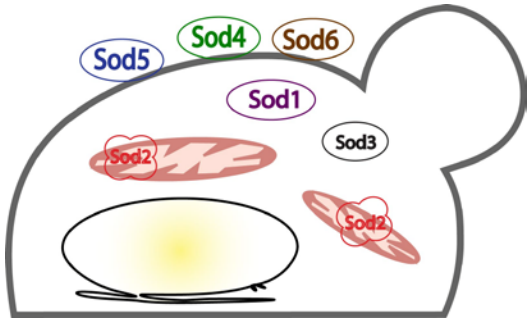

Figure I.5: Localistion of *C. albicans* SODs

SOD5 is also required for virulence in a mouse model (Martchenko et al., 2004). However, the mutant survives in RAW246.7 macrophage cells to the same extent as wild type cells (Martchenko et al., 2004). Transcription profiling of *C. albicans* with neutrophils from whole human blood indicated that *SOD5* is upregulated following phagocytosis (Fradin et al., 2005). In the same study, survival of the *sod5* mutant in human neutrophils cells was significantly reduced when compared with wild type cells. The Sod3 enzyme utilises manganese as a cofactor. However, contrary to other eukaryotic MnSods, it is active in the cytosol and not in the mitochondrial matrix. Furthermore, *SOD3* is expressed during the stationary growth phase of *C. albicans* (Lamarre et al., 2001).

In the *C. albicans* genome, there exist several genes encoding glutaredoxin activity. Ca*GRX2* encodes a putative glutathione reductase, and *grx2* deletion strain is defective in hyphal formation, more susceptible to killing by neutrophils than the wild type strain and sensitive to intracellular superoxide stress (Chaves et al., 2007).

In contrast to *S. cerevisiae* a single catalase exists in *C. albicans* (designated *CTA1*, *CCT1* or *CAT1*). Cta1 protects cells from peroxide stress and is required for virulence in a mouse model of invasive candidiasis (Nakagawa et al., 2003; Wysong et al., 1998). Furthermore, hyphae of a *CTA1* mutant are damaged by human neutrophils, indicating a protective effect of this gene product against polymorphonuclear cells (PMN) (Wysong et al., 1998).

I.3 Immunity to *Candida* infections

I.3.1 Introduction to the mammalian immune system

The physiological principles of the immune system comprise the extinction of pathogenic microbes, the removal of dead cells or the destruction of cancer cells. The innate immunity, which is the phylogenetically oldest mechanism of the defence against pathogens, is operating in

Table I-2: Components of Innate Immunity, adapted from (Abbas et al., 2007)

Type	Components	Principal Functions
Epithelial Barriers	Epithelial layers	Prevent microbial entry
	Defensins/cathelicidin	Microbial killing
	Intraepithelial lymphocytes	Microbial killing
Circulating effector cells	Neutrophils	Early phagocytosis and killing of microbes
	Macrophages	Efficient phagocytosis and killing of microbes, secretion of cytokines that stimulate inflammation
	NK cells	Lysis of infected cells, activation of macrophages
Circulating effector proteins	Complement	Killing of microbes, opsonisation of microbes, activation of leukocytes
	Mannos-binding lectin	Opsonisation of microbes activation of complement
	C-reactive protein (pentraxin)	Opsonisation of microbes activation of complement
Cytokines	TNF, IL-1, chemokines	Inflammation
	IFN-α, -β	Resistance to viral infection
	IFN-γ	Macrophage activation
	IL-12	IFN-γ production by NK cells and T cells
	IL-15	Proliferation of NK cells
	IL-10, TGF-β	Control of inflammation

all multicellular organisms, including plants and insects. By contrast, the more specialised adaptive immunity evolved much later and is present in vertebrates only (Janeway, 2005).

Innate immunity consists of biochemical and cellular defence mechanisms present even before infections and thus can rapidly respond to infections (Table I-2). The innate immune apparatus includes epithelia and antimicrobial substances like defensins, leukocytes or phagocytic cells (neutrophils, macrophages) and natural killer (NK) cells, blood effector protein complexes such as the complement system. Finally, signalling proteins known as cytokines coordinate and regulate the actions of immune cells. The mechanism of innate immunity is specific for structures typical for microbial pathogens and thus are absent in mammalian cells. So-called pathogen-associated molecular patterns (PAMPs) are recognised by the innate immune cells via dedicated pattern recognition receptors (PRRs) (Ausubel, 2005). Innate immunity is hence the first response to microbes, fighting infections of the host. Furthermore, it communicates with the adaptive immune system, and influences the nature of adaptive responses to make them efficient against different types of pathogens, and mounts memory responses (Janeway, 2005).

The adaptive immunity develops in response to an infection, leading to the adjustment to certain infections. The defining features of adaptive immunity are an exquisite specificity for

distinct molecules and the ability to "memorize" and respond more powerfully to repetitive encounters with the same pathogen. The cellular components involved are mainly lymphocytes and their produced cytokines. Adaptive immune responses comprise two major types, cell-mediated and humoral immunity. They are mediated by different machineries of the immune system and eliminate different types of microbes.

Humoral immunity is mediated by mucosal secretions and serum antibodies, produced by B lymphocytes. It is directed against extracellular microbes and their toxins. Antibodies recognise microbial antigens to neutralise the antigenic epitope or target pathogens for elimination by phagocytes (Carroll, 2008).

Cell-mediated immunity is mediated by T lymphocytes, which promote the killing of infected cells or the destruction of pathogens residing in phagocytes. The initiation and development of adaptive immune responses require antigens to be captured, processed and displayed to naive T-cells. This role is served by professional antigen-presenting cells (APCs), of which the most specialized ones are dendritic cells (DCs). Different types of microbes elicit distinct and protective T-cell responses. Elimination of microbes residing within phagosomes of phagocytes is mediated by the subclass of $CD4^+$ T-helper cells by recognising presented antigens and activating phagocytes to kill the ingested microbe. Further, $CD4^+$ T-cells also stimulate growth and differentiation of B-cells. They can be separated into two subsets of effector cells, T_H1 and T_H2, which produce different sets of cytokines and perform different effector functions (Abbas et al., 2007). While the main function of T_H1 cells is in phagocyte-mediated defence against infections, especially in the case of intracellular pathogens, T_H2 cells are responsible for defence against helminthic infections, as well as for allergic reactions. The antibodies stimulated by T_H2 cytokines do not promote phagocytosis and therefore antagonise T_H1 responses.

The adaptive immune responses to pathogens infecting and replicating in the cytoplasm of host cells, including non-phagocytic cells, are mediated by $CD8^+$ cytotoxic T-cells (CTLs), which kill infected cells presenting antigens (Abbas et al., 2007; Janeway, 2005).

I.3.2 Recognition of *C. albicans* by the innate immune system

The host immune responses to fungal infections are diverse and range from the innate immune system to the sophisticated adaptive immune system. The innate immunity effectively discriminates between self and non-self, and activates adaptive immunity through specific cytokine signals (see also I.3). Mammalian innate antifungal defences are mediated by cells (professional phagocytes), cellular receptors and different humoral factors. The innate response

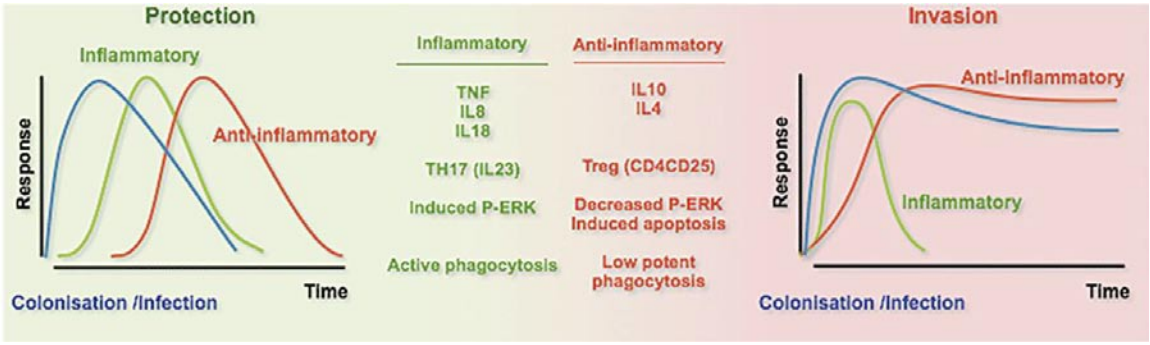

Figure I.6: Initial immune response modulating the protection/invasion towards *C.albicans*
The main immune system activities induced by *C. albicans* leading to either an inflammatory or anti-inflammatory response are shown. An amplified anti-inflammatory response results in an unbalanced immune response which favours the development of infection. Adapted from (Jouault et al., 2009)

to fungi serves two main purposes. First, it shows direct antifungal effector activity by destroying fungi via phagocytosis or through the secretion of microbicidal compounds against indigestible fungal elements. Second, innate immune cells initiate the adaptive immune system via secretion of pro-inflammatory cytokines and chemokines and the presentation of antigens (Romani, 2004). The balance of pro- and anti-inflammatory cytokines produced by the immune cells is important for the outcome of the fungal disease (Figure I.6). For instance, during a *C. albicans* infection the absence of IL-10, an anti-inflammatory cytokine, is beneficial for the host response (Del Sero et al., 1999).

The task of recognising fungal cells and activating the host cell response is initiated by PRRs, which mainly recognise the fungal cell wall components (described in Chapter I.2.1.2) (Figure I.7). Of course, the localisation of mannans and mannoproteins at the outermost part of the cell wall are excellent targets for PRRs, but glucans and perhaps chitin present in bud scars are also likely to be recognised by leukocyte PRRs.

I.3.2.1 Pattern recognition receptors and their targets

Monocytes, neutrophils and macrophages are the first line of defence against invading pathogens. Monocytes express high levels of Toll-like receptors (TLRs) and moderate levels of lectin receptors (LRs). When monocytes differentiate into macrophages, they retain their levels of TLRs and increase their expression of LRs. Neutrophils strongly express phagocytic receptors such as Fc gamma receptors (FcγR) and complement receptor 3 (CR3), but also moderate levels of TLRs. Fungal recognition by DCs is crucial for antigen-processing and presentation to T-cells (Netea et al., 2008a). DCs also express both TLRs and LRs. In the following section, the PRRs and their fungal ligands, as well as the induced signalling cascades and cytokine production are described in more detail.

Toll-like receptors

Lemaitre et al. were the first to describe the functional role of Toll-like receptors in antifungal host defence. *Drosophila* flies deficient of *toll* were rapidly overgrown with *Aspergillus fumigatus* (Lemaitre et al., 1996). In mammalian cells, fungal recognition by TLRs induces the activation of kinase cascades such as the MAPK pathways, as well as the nuclear translocation of transcription factors, such as NF-κB (Akira et al., 2006). At least four TLRs may be involved in the defence against *C. albicans* including TLR2, TLR4, TLR6 and TLR9.

TLR2 inhibition or deletion results in decreased production of proinflammatory cytokines and neutrophil recruitment after stimulation with *C. albicans* (Netea, 2002; Villamon, 2004). However, $TLR2^{-/-}$ mice show increased resistance to candidiasis and decreased production of anti-inflammatory cytokines like IL-10, while increased production of IL-12 and INFγ (Bellocchio et al., 2004; Netea, 2004). Furthermore, TLR2-deficient macrophages were able to clear *C. albicans* infections better than wild type controls (Blasi et al., 2005). This evidence for an anti-inflammatory role for TLR2 in host defence is also supported by a recent study showing that zymosan can induce immunological tolerance through a TLR2-mediated pathway involving MAPK/ERK (Dillon et al., 2006). The TLR2 ligand from *C. albicans* remains elusive, although phospholipomannan might be recognised by TLR2 and TLR6 (Jouault et al., 2003).

TLR4 strongly induces proinflammatory cytokines (TNF-α) via two pathways. First, through the MyD88-Mal mediated induction of NF-κB and p38-mediated cytokine and chemokin production. Second, through TRIF/TRAM-mediated induction of IRF3-dependent release of type I interferons (Toshchakov, 2002). TLR4 is important for *C. albicans* elimination in kidneys, chemokine production and neutrophil recruitment, although no change in cytokine production is observed during infection (Netea, 2002). However, there are controversial studies stating that TLR4 is not relevant for the survival of mice infected with *C. albicans* (Gil and Gozalbo, 2006; Murciano, 2006). TLR4 is also involved in controlling susceptibility to *A. fumigatus* conidia, *Pneumocystis pneumonia* but not *C. neoformans* (Bellocchio et al., 2004; Ding et al., 2005; Nakamura et al., 2006)

TLR4 is the receptor for bacterial lipopolysaccharide (LPS) (Poltorak et al., 1998), however, there is limited knowledge about the nature of fungal PAMPs recognised by TLR4. Recognition of mannan from *C. albicans* and *S. cerevisiae* (Tada et al., 2002), especially recognition of shorter O-bound mannan, is probably performed by TLR4 triggering in cytokine production (Netea et al., 2006).

The role of **TLR6** and **TLR9** in cytokines induction in response to *C. albicans* is less well explored. TLR2/TLR6 heterodimers are involved in zymosan recognition, but cytokine production is only moderately reduced in TLR6$^{-/-}$ macrophages, and TLR6 does not seem to play a role in disseminated *C. albicans* infections (Netea et al., 2008b). The natural ligands for TLR9 are unmethylated CpG sequences. Several reports suggest that TLR9 recognises fungal DNA. Blocking TLR9 in human monocytes and TLR9$^{-/-}$ mouse macrophages reduces cytokine production (IL-10) after stimulation with *C. albicans* (van de Veerdonk et al., 2008). TLR9 also recognises fungal DNA from *A. fumigatus* and *C. neoformans* (Nakamura et al., 2008; Ramirez-Ortiz et al., 2008). A recent study indicates that TLR9 recognises *C. albicans* DNA, and induces MyD88 dependent NF-κB and IL-12 signalling (Miyazato et al., 2009).

C-type lectin receptors (CLRs)

The CLRs known to recognise fungal PAMPs are Dectin-1, Dectin-2, macrophage mannose receptor (MR), galectin-3, dendritic cell-specific ICAM3-grabbing nonintegrin (DC-SIGN) and mincle.

Dectin-1 is the most extensively studied receptor implicated in fungal recognition. Dectin-1 recognises β-1,3 glucans via its extra cellular C-type lectin-like domain (CTLD) (Tsoni and Brown, 2008). Dectin-1 signals via a non-classical immunoreceptor tyrosine-based activation motif (ITAM) through the spleen tyrosine kinase (Syk) and the caspase recruitment domain 9 (CARD9), linking Syk-coupled receptors to the canonical NF-κB pathway (Gross, 2006; Hara et al., 2007). Dectin-1 also activates the non-canonical NF-κB pathway via a Syk-dependent activation of RelB (Gringhuis et al., 2009). Dectin-1 stimulation with curdlan, a linear β-(1,3)-glucan, also stimulates IL-2 and IL-10 in DCs. Isolated spleenocytes from *C. albicans*-infected mice produce CARD9 dependent TH-17 cells (LeibundGut-Landmann et al., 2007). Another study challenges this by stating that Syk-dependent but CARD9-independent pathways lead to ERK induction, mediating the production of IL-2 and IL-10 (Slack et al., 2007). Syk controls CARD9-independent pro-IL-1β synthesis and CARD9-dependent inflammasome activation after stimulation with *C. albicans* (Gross et al., 2009). Interestingly, CARD9 plays a different role in macrophages and dendritic cells. While stimulation of bone marrow derived DCs trigger NF-κB activation and TNF-alpha production via Dectin-1 and CARD9, CARD9 is recruited to the phagosome in bone marrow derived macrophages (BMDMs) and signals to p38 MAPK in a NF-κB independent way (Goodridge et al., 2009).

ROS production upon zymosan and *C. albicans* stimulation requires Dectin-1 and Syk (Gantner et al., 2003; Gantner et al., 2005; Taylor et al., 2007). However, the role in *C. albicans* ROS signalling is still unclear because macrophages from dectin-1$^{-/-}$ mice fail to show alterations in ROS production when challenged with *C. albicans* (Saijo et al., 2007). Details about ROS signalling are discussed in Chapter I.3.3.1: Oxidative burst - the pathogen "destroyer". In addition, Dectin-1 is required for phagocytosis (Gantner et al., 2005; Hernanz-Falcon et al., 2009; Herre et al., 2004). Dectin-1$^{-/-}$ mice are more susceptible to infection with *C. albicans*, resulting in increased fungal burden and lower survival (Taylor et al., 2007). However, another study using a different mouse strain of dectin-1$^{-/-}$ mice found increased susceptibility to *Pneumocystis* but not to *C. albicans* (Saijo et al., 2007).

Dectin-1 can also cooperate with TLRs to induce proinflammatory responses. In macrophages, cooperative signalling through Dectin-1 and TLR2 heterodimers is required for the induction of TNF-α in response to *C. albicans* and zymosan (Brown et al., 2003; Gantner et al., 2003). Notably, Dectin-1 amplifies TLR4-dependent pathways in a Syk-dependent manner (Dennehy et al., 2008). Furthermore, Dectin-1 can couple with other MyD88-dependent TLRs, resulting in the synergistic induction of TNF-α and IL-10 (Ferwerda et al., 2008). In murine macrophages, a collaboration of Dectin-1 and DC-SIGNR1 for fungal binding exists (Taylor et al., 2004), and in human DCs, a costimulation of DC-SIGN and Dectin-1 induces arachidonic acid signalling (Valera et al., 2008).

Dectin-2 has a specificity for high mannose structures (McGreal et al., 2006). The receptor preferentially recognises hyphal forms of fungi such as *C. albicans*, *Trichophyton rubrum* and *Microsporum audouinii.* However, the receptor can also weakly recognise yeast or conidial forms (McGreal et al., 2006; Sato et al., 2006). The cytoplasmic tail of Dectin-2 appears to associate with the FcγR chain, a signalling adaptor associated with several other transmembrane receptors. This induces TNF-α and IL-1R in response to hyphal forms of *C. albicans* (Robinson et al., 2009; Sato et al., 2006). In dendritic cells, Dectin-2 contributes to the activation of p38 and ERK MAPK and the production of IL-2 and IL-10 in response to live or heat-killed *C. albicans,* respectively. Blocking of Dectin-2 in a *C. albicans* infection model abrogated T_H17 response, and in combination with Dectin-1 loss, T_H1 response decreased (Robinson et al., 2009).

Mannose Receptor (MR) has several domains that recognise oligosaccharides, fucose and mannose. The role of MR in *C. albicans* has been investigated using mutant strains of *C. albicans* defective in O-linked and N-linked mannans (Netea et al., 2006). According to this study, the MR recognises branched O-linked mannans. A very recent study indicates that IL-17 production is

induced by the MR, and that Dectin-1/TLR2 amplify the IL-17 production (van de Veerdonk et al., 2009).

Galectin-3 is a receptor mainly expressed by macrophages. It is crucial for the recognition of β-1,2 linked mannosides and collaborates with TLR2 (Fradin et al., 2000; Jouault et al., 2006) Binding of recombinant Galectin-3 to the specific β-1,2 linked mannosides of *C. albicans* directly induces death to a fraction of *C. albicans* cells (Kohatsu et al., 2006).

The human **dendritic cell-specific ICAM3-grabbing nonintegrin (DC-SIGN)** is primarily expressed on immature DCs, but has also been found in macrophage populations (Koppel et al., 2005; Lai et al., 2006). DC-SIGN recognises high mannose structures in a calcium dependent way (Koppel et al., 2005). Similar to Dectin-1, DC-SIGN has a non-classical ITAM, domain but signals independently of this motif (Fuller et al., 2007). Eight orthologues of DC-SIGN exist in mice,

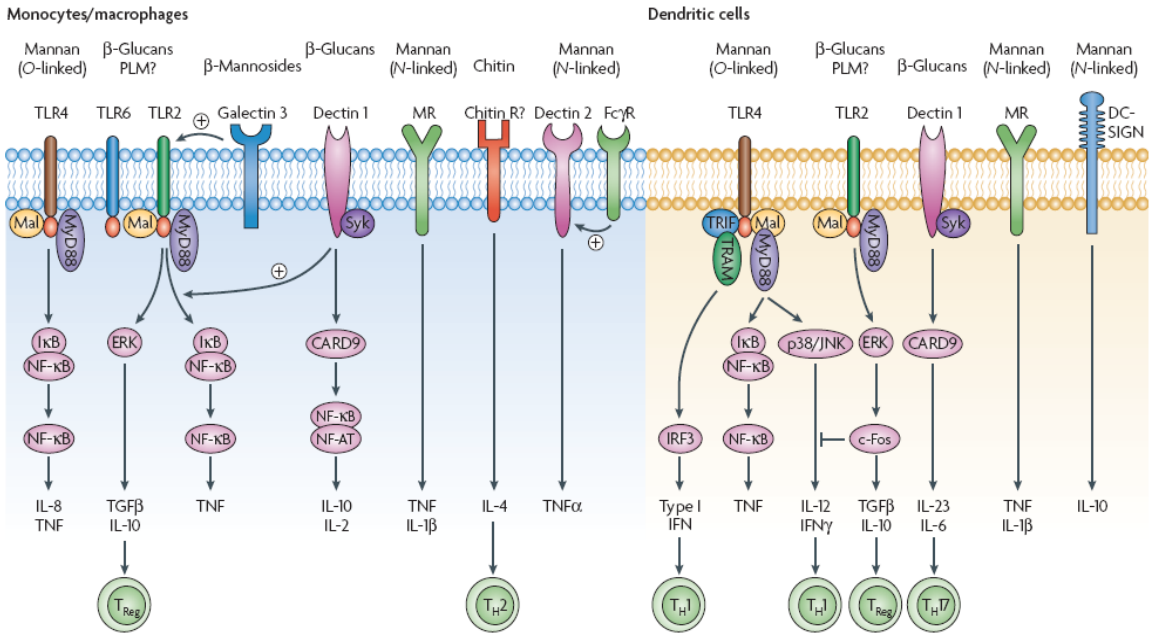

Figure I.7: Recognition of *C. albicans* at the cell membrane is mediated by TLRs and Lectin Receptors. TLR4 induces mainly pro-inflammatory signals in monocytic cell types through the MyD88–Mal-mediated NF-κB and MAPK pathways, while stimulating TH1 responses through IRF3-dependent mechanisms mainly occurs in plasmacytoid DCs. **TLR2** stimulates the production of moderate amounts of pro-inflammatory cytokines and strong IL-10 and TGFβ responses. On the one hand, this leads to the induction of a tolerant phenotype in DCs, through an ERK/MAPK-dependent mechanism. Alternatively, in monocytes and macrophages it induces TGFβ and IL-10, and subsequent proliferation of T_{Reg} cells and immunosuppression. The proinflammatory effects of TLR2 can be amplified by Dectin-1 and **galectin 3** — the latter especially in macrophages. In addition to amplifying the effects of TLR2, the non-classical lectin-like receptor **Dectin-1** induces IL-2, IL-10 and TH17 responses through a Syk–CARD9 cascade, independently of its interaction with TLR2. The classical lectin-like receptor, **MR**, induces pro-inflammatory effects in monocytes and macrophages, whereas chitin-dependent stimulation of these cells induces mainly TH2 responses, although this effect has yet to be demonstrated for *C. albicans*, and the identity of the chitin receptor is unknown. Other less well characterised pathways include stimulation of TNF and IL-1Ra by **Dectin 2**, while engagement of **DC-SIGN** in DCs induces production of the immunosuppressive cytokine IL-10 (Netea et al., 2008a)

although these molecules appear to have different expression profiles and several structural differences (Powlesland et al., 2006). The role of this receptor in response to fungi has not been studied extensively, but DC-SIGN has been proposed to mediate fungal uptake (Cambi et al., 2003). Among the murine homologues, only SIGNR1 (also termed murine DC-SIGN) and SIGNR3 recognise fungal PAMPs(Takahara et al., 2004; Taylor et al., 2004). DC-SIGN can induce intracellular signalling through the Raf-kinase pathway, modulating TLR-mediated responses (Gringhuis et al., 2009).

Mincle appears to be involved in the recognition of *C. albicans* by macrophages. It localises to the phagocytic cup, although it is not essential for phagocytosis. Mincle$^{-/-}$ mice are susceptible to *C. albicans,* and blocking of Mincle in macrophages leads to reduced TNF (Bugarcic et al., 2008; Wells et al., 2008). Like other CLRs, Mincle induces inflammatory cytokines and chemokines via the association with the Fcγ chain (Yamasaki et al., 2008).

Complement receptor 3 (CR3) is a heterodimer of the subunits CD11b and CD18. The CR3 integrin mediates adhesion, chemotaxis and phagocytosis in complement-dependent but also complement-independent ways (Le Cabec et al., 2002; Le Cabec et al., 2000; Ross et al., 1985; Ross and Vetvicka, 1993; Xia and Ross, 1999). CR3 recognises β-glucans of unopsonised yeast via the carbohydrate binding site of the Cd11b subunit (Xia and Ross, 1999). In thioglycollate-elicited peritoneal macrophages CR3 is not actively involved in the phagocytosis of *C. albicans,* but is associated with the phagocytic cup (Heinsbroek et al., 2008). A recent study using human neutrophils suggests that CR3 but not Dectin-1, is the major receptor for β-glucan bearing particles (van Bruggen et al., 2009).

I.3.3 Reactive oxygen species in phagocytic cells

I.3.3.1 Oxidative burst – the pathogen "destroyer"

Phagocytes such as eosinophils, polymorphonuclear neutrophils, monocytes and macrophages comprise one of the most powerful weapons of host defence against bacteria and fungi. One very potent mechanism exploited by phagocytes to destroy invading pathogens is the oxidative burst. Phagocytic cells recognise the pathogen via opsonins, such as the immunoglobulins G and activation of complement system, and also via PAMPs recognised by PRRs (see Chapter above). Recognition is generally followed by engulfment of the particle or the pathogen, leading to the encapsulation of the pathogen by a membrane envelope resulting in a vacuole called the phagosome. This process triggers the production of reactive oxygen species (ROS), and in most cases leads to the destruction of the invading pathogen (Babior, 2002).

The NADPH oxidase

Phagocytes have a membrane-bound multicomponent enzyme complex, termed the NADPH oxidase generating large quantities of ROS (Babior, 2004). Interestingly, a family of NADPH oxidases (NOXs) is also expressed in nonphagocytic cells (Lambeth, 2004). NOXs produce ROS in a regulated manner and at lower levels than the phagocyte NAPDH oxidase (Lambeth, 2004). The NADPH oxidase is dormant in resting cells but be rapidly activated by a variety of soluble mediators (e.g., chemoattractant peptides and chemokines) as well as particulate stimuli (e.g., bacteria and immune complexes) that interact with cell-surface PRRs (Figure I.8). The phagocyte oxidase is an enzyme formed by $gp91^{phox}$ (NOX2), $p22^{phox}$, $p40^{phox}$, $p47^{phox}$, $p67^{phox}$, and Ras-related C3 botulinum toxin substrate 2 (rac2) (Lambeth, 2004). In the resting state, the subunits of the NADPH oxidase are separated. Upon activation, they assemble to a complex and use NADPH as electron donor to convert molecular oxygen into its one-electron reduced product, superoxide ($O^{2-\cdot}$), which is the major end product (Figure I.8). Hydrogen peroxide (H_2O_2) arises from the subsequent dismutation of superoxide by enzymes called superoxide dismutases (SOD). The interaction between H_2O_2 and $O^{2-\cdot}$ can also give rise to the hydroxyl radical (OH°) through the Haber-Weiss reaction in the presence of a transition metal or through the Fenton reaction in the presence of iron. Hypochlorous acid (HOCl) is formed in the presence of a halide such as Cl^- in a reaction catalysed by the granular enzyme myeloperoxidase (MPO), an enzyme present in neutrophils but not in macrophages (El-Benna et al., 2005) (Figure I.8).

This system is also called the phagocyte “respiratory burst” (increased respiration of phagocytosis), and plays a key role in host defence against microbial agents, as evident from a human genetic disorder called chronic granulomatous disease (CGD). A defect in one of the subunits of NADPH oxidase leads to a failure in the production of ROS by phagocytes (Hohn and Lehrer, 1975), resulting in increased bacterial and fungal infections such as pneumonia, abscesses, arthritis and osteomyelitis (Aratani et al., 2002; Dinauer, 1993; Johnston, 2001; Warris et al., 2003). The most frequent form of CGD (approximately 70 % of all cases) is the X-linked gp91phox-deficient form, followed by the autosomal form deficient in p47phox (25%) (Kannengiesser et al., 2008; Meischl and Roos, 1998).

Several receptors, including Fc receptors (FcR) and integrins trigger ROS production in response to microbial pathogens (Berton and Lowell, 1999; Ravetch and Bolland, 2001). All of these receptors have an immunoreceptor tyrosine-based activation motif (ITAM) in their cytoplasmic tail or associate with ITAM containing adaptors such as DAP12 or FcγR (Mocsai et al., 2006; Swanson and Hoppe, 2004). Activation of an ITAM-associated receptor leads to

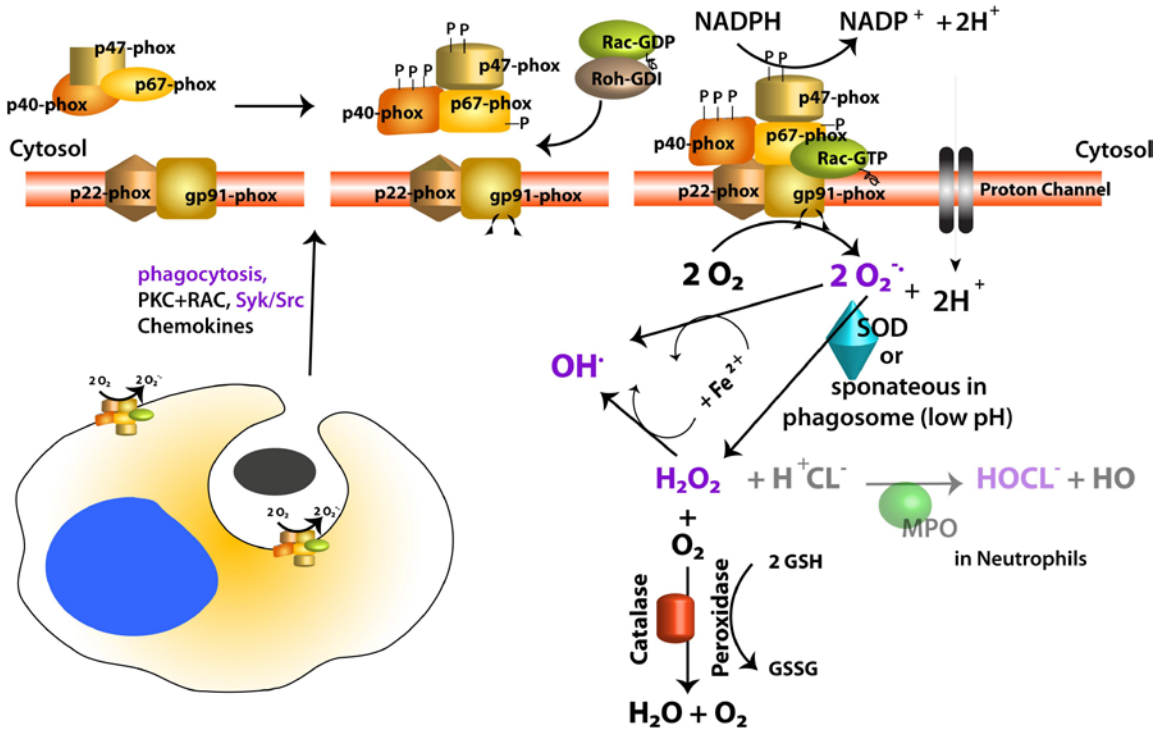

Figure I.8 The NADPH oxidase activation. In resting cells the components of NADPH oxidase are distributed between the cytosol and the membranes. Upon cell activation the cytosolic components p47phox, p67phox, and p40phox are phosphorylated, and migrate to the membranes where they associate with the membrane-bound components gp91phox and p22phox; at the same time, rac 2 exchanges its GDP by GTP, dissociates from its inhibitor rho-GDI, and migrates to the membrane; cytochrome b558 (p22 and gp91phox complex) is then activated by p67phox via its activation domain and rac2. Activated NADPH oxidase then uses cytosolic NADPH to reduce oxygen and to produce superoxide anions adapted from (El-Benna et al., 2005).

phosphorylation by *Src* family kinases (SFK) of the tyrosine residues within the ITAM consensus sequence. Syk family kinases are consequently recruited and activated, inducing signalling through multiple downstream pathways, including phosphatidylinositol (PI) 3-kinase and protein kinase C (PKC). Dectin-1 recognises β-(1,3) glucans in the cell wall of yeasts (Brown, 2006) and regulates ROS production in phagocytes. Dectin-1 contains a noncanonical ITAM motif in its cytoplasmic tail, and crosslinking of Dectin-1 leads to Syk phosphorylation independent of DAP12 and FcγR which results in ROS production (Rogers et al., 2005; Underhill et al., 2005).

TLRs have also been implicated in the ROS response. The MyD88 adaptor protein is needed for the activation of the NADPH oxidase in response to gram-negative bacteria (Laroux et al., 2005; Ryan et al., 2004). The roles of specific TLRs in NADPH oxidase assembly and ROS generation seem to be cell type-dependent. For example, TLR4 is required for NADPH oxidase activation in human neutrophils infected with *Serovar Typhimurium* (van Bruggen et al., 2007), but not in mouse peritoneal macrophages (Laroux et al., 2005). Additionally, the TLR4 ligand LPS does not induce detectable levels of ROS in murine bone marrow-derived macrophages (Charles

et al., 2008). ROS production during *M. tuberculosis* infection is dependent on the interaction of TLR2 and $gp91^{phox}$ (Yang et al., 2009).

The NOX isoenzymes can also be activated by TLR4 (Park et al., 2004; Ryan et al., 2004; Zhang et al., 2006). Stimulation of TLR4 with lipopolysaccharide (LPS) induces ROS generation and NF-κB activation and this process is mediated by the interaction of TLR4 with Nox4 (Park et al., 2004). Furthermore, minimally oxidised LDL (mmLDL) stimulates intracellular reactive oxygen species (ROS) generation in macrophages through ($gp91^{phox}$/Nox2) in a TLR4 and Syk-dependent manner (Bae et al., 2009). In neutrophils, ROS are primarily released into phagosomes where they interact rapidly with microbial proteins and lipids, resulting in their oxidation. They are also released into the cytosol, where they alter the cellular redox state, and oxidise proteins and lipids, which changes their function (Fialkow et al., 2007; Liang and Petty, 1992). Besides the NADPH oxidase, there are additional enzymes capable of generating ROS as side products of electron transfer reactions.

Mitochondrial electron transport

ROS, including $O_2^{\cdot-}$ and H_2O_2 are normally generated as side products of electron transfer reactions that occur during the operation of the mitochondrial electron transport chain. The mechanism of generation of ROS involves “leakage” of electrons from electron carriers that are passed directly to oxygen, reducing it to $O_2^{\cdot-}$. For rapid elimination of intracellular ROS, mitochondria have their own Mn^{2+} dependent SOD enzyme (Fialkow et al., 2007).

Nitric oxide synthase and reactive nitrogen species

Nitric oxide synthase (NOS) catalyses the production of nitric oxide ($NO^{\cdot}$) from L-arginine, oxygen and NADPH (Marletta, 1993). There are two kinds of NOS; the constitutive NO synthases (NOS1 and NOS3) and the inducible NOS2 or iNOS. iNOS is expressed in leukocytes including macrophages and neutrophils, and its activity is Ca^{2+}-dependent. The expression of iNOS is increased by cytokines and other inflammatory stimuli (Evans et al., 1996; Razavi et al., 2004; Wheeler et al., 1997). NO can influence diverse cellular responses, and can have both pro- and anti-inflammatory effects. Similar to ROS, NO participates in diverse cellular processes such as receptor regulation, endocytic pathways, GTP-binding proteins, transcription factors, ion channels and tyrosine kinases (Quijano et al., 2005; Sun et al., 2003; Wang et al., 2006a). There are physiologically important interactions between NO° and ROS such as $O_2^{\cdot-}$. NO can therefore act as an endogenous biologic scavenger or inactivator of ROS (Beckman et al., 1990; McCall et al., 1989). In leukocytes, the reaction between NO and superoxides generates reactive nitrogen

species like peroxynitrite ($ONOO^-$), a cytotoxic compound that can modify signalling molecules by nitrosylation (Beckman et al., 1990). iNOS is not essential for *C. albicans* infections in oral Candidiasis (Farah et al., 2009). Furthermore, *C. albicans* seems to suppress RNS production by IFN-γ (Chinen et al., 1999).

I.3.3.2 ROS and cell signalling

Endogenously produced ROS are involved in several signal transduction pathways. The first signalling components identified to be redox sensitive were transcription factors. ROS induce activation of NF-κB, *c-fos* and *c-jun* (Lo and Cruz, 1995; Schreck et al., 1991). NF-κB mediates the rapid induction of expression of genes involved in the acute inflammatory responses, including cytokines and their receptors, adhesion molecules and MHC antigens (Celec, 2004). In Kupffer cells, production of TNF-alpha is regulated by a ROS-activated NF-κB pathway (Rose et al., 2000). NF-κB activation in alveolar macrophages was altered in a knock-out mouse model lacking $p47^{phox}$ (Koay et al., 2001), indicating the importance of this pathway in lungs. ROS also mediate TNF-α induction of *c-fos* in chondrocytes, which may have important consequences in the development of inflammatory diseases such as arthritis (Lo and Cruz, 1995). In addition, ROS is also produced by binding of TNF-α with its receptor. This ROS is not produced by NADPH oxidase on the cellular membranes but rather in the cytoplasm and in the mitochondria (Forman and Torres, 2002).

MAP kinases are serine-threonine kinases that regulate many key cellular and antimicrobial responses. The signalling module of the ERK pathway is composed of ERK1/2, the dual-specificity kinases MEK1/2. Isoforms of Raf are principally activated by hormones and growth factors (Qi and Elion, 2005). Exogenous H_2O_2 activates ERK1 and ERK2 in many cell types, although this activation appears to be cell type-specific (Abe et al., 1998; Aikawa et al., 1997; Guyton et al., 1996; Torres and Forman, 2003). Further studies indicate that increased intracellular ROS production also activates the ERK pathway (Irani, 2000). Several reports have shown that phosphorylation of tyrosine kinases, including Syk, Hck, Lyn, Fgr, Yes and Btk can be either directly or indirectly modulated by NADPH and endogenously generated ROS (Berton and Lowell, 1999; Brumell et al., 1996).

I.3.3.3 ROS production in response to Candida infection

ROS production upon zymosan stimulation of BMDMs, thioglycollate-elicited macrophages, and mast cells was shown to be Dectin-1 dependent (Gantner et al., 2003; Taylor et al., 2007; Yang and Marshall, 2009). Furthermore, ROS production upon zymosan stimulation is Syk-dependent

(Gantner et al., 2003). However, the role of Dectin-1 in *C. albicans* ROS signalling is still unclear because alveolar macrophages from dectin-$1^{-/-}$ mice fail to show alterations in ROS production when stimulated with *C. albicans* (Saijo et al., 2007). Further inhibition of Dectin-1 with laminarin or anti-Dectin-1 blocking-antibodies inhibits ROS production upon *C. albicans* stimulation (Gantner et al., 2005). Notably, human DCs stimulated with heat-killed *C. albicans* produce ROS in a Dectin-1 and Syk-dependent manner (Skrzypek et al., 2009). Furthermore, *C. albicans* stimulates BMDCs to produce ROS in a Syk-dependent but Card9-independent manner (Gross et al., 2009).

II. Aims of this work

One of the immediate early defence responses of macrophages facing invading fungal cells includes the production of reactive oxygen species (ROS), which play important roles in inflammatory reactions. ROS destroy invading pathogens, but overproduction of ROS may also cause endothelial damage.

Two strategies were chosen to investigate the immunological importance of the respiratory burst, and the upstream factors leading to the production of ROS in innate immune cells when challenged with *C. albicans*.

Generation and analysis of mutant strains of all *C. albicans* superoxide dismutases

On the pathogen side, the aim of this thesis was to generate *C. albicans* mutant strains lacking one or more of the superoxide dismutases (*SOD1-6*) putatively involved in ROS response. Using different stress conditions and a combination of different ROS assays, I addressed the question of whether and how the *C. albicans* SODs are involved in the response to ROS produced by innate immune cells such as bone marrow-derived macrophages or myeloid dendritic cells.

Analysis of putative pattern recognition receptors involved in ROS transduction

We and others have shown that *C. albicans, C. dubliensis (C.d)* and *C. glabrata (C.g)* induce ROS in BMDMs and mDCs to different extents following distinct kinetics. The pattern recognition receptor Dectin-1 is known to be important for ROS production in response to zymosan. So far, Dectin-1 was also implicated to be important for ROS production in response to *C. albicans* although concerning the latter, there are conflicting data in the literature.

The second aim of this work was therefore to elucidate whether or not Dectin-1 is involved in *C. albicans*-induced ROS production in BMDMs, and if there are other pattern recognition receptors engaged in this immune response, which acitvates downstream signalling pathways initiating ROS production. To address these questions, I used knock-out mice of different pattern recognition receptors and specific blocking agents or antibodies. Additionally, I have set up a siRNA knock down assay to reveal new pathways that might be responsible for *Candida* induced ROS in BMDMs.

III. Results

III.1 *C. albicans* degrades host-derived ROS to escape innate immune surveillance

C. albicans Cell Surface Superoxide Dismutases Degrade Host-Derived Reactive Oxygen Species to Escape Innate Immune Surveillance

Ingrid E. Frohner, Christelle Bourgeois, Kristina Yatsyk, Olivia Majer & Karl Kuchler[§]

From the

Medical University Vienna

Christian Doppler Laboratory for Infection Biology, Max F. Perutz Laboratories

Campus Vienna Biocenter; A-1030 Vienna, Austria

Running title:

C. albicans and oxidative burst of innate immune cells

Keywords

Candida albicans, superoxide dismutase, reactive oxygen species, virulence, macrophages, immune evasion

[§]To whom all correspondence should be addressed:

Karl Kuchler

Medical University Vienna

Christian Doppler Laboratory for Infection Biology, Max F. Perutz Laboratories

Dr. Bohr-Gasse 9/2; Campus Vienna Biocenter, A-1030 Vienna, Austria

Ph: +43-1-4277-61807; FAX: +43-1-4277-9618

e-mail: karl.kuchler@meduniwien.ac.at

Molecular Microbiology (2009) 71(1), 240–252 ■
doi:10.1111/j.1365-2958.2008.06528.x
First published online 21 November 2008

Candida albicans cell surface superoxide dismutases degrade host-derived reactive oxygen species to escape innate immune surveillance

Ingrid E. Frohner, Christelle Bourgeois, Kristina Yatsyk, Olivia Majer and Karl Kuchler*
Medical University Vienna, Christian Doppler Laboratory for Infection Biology, Max F. Perutz Laboratories, Campus Vienna Biocenter; A-1030 Vienna, Austria.

Summary

Mammalian innate immune cells produce reactive oxygen species (ROS) in the oxidative burst reaction to destroy invading microbial pathogens. Using quantitative real-time ROS assays, we show here that both yeast and filamentous forms of the opportunistic human fungal pathogen *Candida albicans* trigger ROS production in primary innate immune cells such as macrophages and dendritic cells. Through a reverse genetic approach, we demonstrate that coculture of macrophages or myeloid dendritic cells with *C. albicans* cells lacking the superoxide dismutase (SOD) Sod5 leads to massive extracellular ROS accumulation *in vitro*. ROS accumulation was further increased in coculture with fungal cells devoid of both Sod4 and Sod5. Survival experiments show that *C. albicans* mutants lacking Sod5 and Sod4 exhibit a severe loss of viability in the presence of macrophages *in vitro*. The reduced viability of *sod5*Δ/Δ and *sod4*Δ/Δ *sod5*Δ/Δ mutants relative to wild type is not evident with macrophages from *gp91phox*$^{-/-}$ mice defective in the oxidative burst activity, demonstrating a ROS-dependent killing activity of macrophages targeting fungal pathogens. These data show a physiological role for cell surface SODs in detoxifying ROS, and suggest a mechanism whereby *C. albicans*, and perhaps many other microbial pathogens, can evade host immune surveillance *in vivo*.

Accepted 24 October, 2008. *For correspondence. E-mail karl.kuchler@meduniwien.ac.at; Tel. (+43) 1427 761 807; Fax (+43) 142 779 618.
Re-use of this article is permitted in accordance with the Creative Commons Deed, Attribution 2.5, which does not permit commercial exploitation.

© 2008 The Authors
Journal compilation © 2008 Blackwell Publishing Ltd

Introduction

Invasive *Candida albicans* infections are life-threatening clinical conditions affecting immunosuppressed patients and those with general defects in the immune system. The mortalities associated with disseminated candidiasis can be as high as 30–40%, despite extensive antifungal therapies (Pfaller and Diekema, 2007). Host defences against fungi range from non-specific proteolytic defences to dedicated adaptive immune responses (Romani, 2004; Netea *et al*., 2008). The earliest host response to fungal pathogens, including *C. albicans*, relies on fungal recognition by innate immune cells such as dendritic cells, macrophages and neutrophils and involves pattern recognition receptors, followed by the subsequent phagocytosis and elimination of microbial pathogens (Brown and Gordon, 2005; Akira *et al*., 2006; Jouault *et al*., 2006; Taylor, 2007; Gow *et al*., 2007).

Upon interaction with pathogens, phagocytes rapidly produce reactive oxygen species (ROS), which are thought to aid killing of invading microbes (Dinauer, 1993; Morgenstern *et al*., 1997), and further activate defensive signalling pathways reviewed in Forman and Torres (2002) and Netea *et al*. (2008). ROS production is initiated through assembly and activation of nicotinamide adenine dinucleotide phosphate (NADPH) oxidase in phagocytes (Babior, 2004). This triggers the respiratory burst by generating superoxide anions (O_2^-) (Schrenzel *et al*., 1998), which are subsequently converted to hydrogen peroxide (H_2O_2), hydroxyl radical (OH°) and hypochlorous acid, the latter conversion only taking place in neutrophils.

In *C. albicans*, the Cat1 catalase has been implicated in counteracting the respiratory burst by protecting cells from killing by H_2O_2 stress. Cells lacking Cat1 also display attenuated virulence in an invasive mouse virulence model as reviewed in Chauhan *et al*. (2006). Furthermore, the *C. albicans* genome harbours six genes encoding putative superoxide dismutases (SOD), four of which are copper-zinc (CuZn)-dependent, namely the cytoplasmic Sod1 and the cell surface Sod4, Sod5 and Sod6; two SODs, the mitochondrial Sod2 and cytoplasmic Sod3, are manganese-dependent (Chauhan *et al*., 2006). SODs

convert O_2^- into molecular oxygen and hydrogen peroxide, thereby scavenging the toxic effects of O_2^- and preventing higher H_2O_2 levels by other downstream reactions (Teixeira *et al*., 1998).

The best-studied *C. albicans* SODs with respect to their role in pathogenesis are Sod1 and Sod5, the latter being a GPI-anchored cell surface protein (Fradin *et al*., 2005). Both appear required for virulence of *C. albicans* in invasive mouse models (Hwang *et al*., 2002). Further, fungal cells lacking Sod1 are sensitive to menadione and more sensitive to killing by macrophages than a wild-type strain (Hwang *et al*., 2002). *SOD5* is upregulated under osmotic and oxidative stress conditions, as well as during yeast-to-hyphae transition (Martchenko *et al*., 2004). Moreover, transcriptional profiling indicates that *SOD5* expression is also upregulated by neutrophil contact, in presence of neutrophils and viability of a *sod5*Δ/Δ mutant is reduced relative to the wild type. Notably, both Sod4 and Sod6 are predicted GPI-anchored cell wall proteins reviewed in Richard and Plaine (2007), but their function has not been analysed. The surface location of Sod4, Sod5 and Sod6 prompted the notion that they may protect *C. albicans* against extracellular stress (Fradin *et al*., 2005; Gantner *et al*., 2005).

In this work, we demonstrate a pivotal role for *C. albicans* SODs in destroying host-derived ROS. We show that primary innate immune cells rapidly respond to fungal pathogens by mounting a protective ROS response to destroy invading cells. We exploit a reverse genetic approach to show that certain *C. albicans* SODs counteract the respiratory burst. Strikingly, we demonstrate that Sod5, and to a lesser extent Sod4, catalyses destruction of host-derived ROS. Interestingly, *sod5*Δ/Δ and *sod4*Δ/Δ *sod5*Δ/Δ *C. albicans* show decreased viability in the presence of macrophages. Thus, our data identify *SOD5* as a novel *C. albicans* gene, mediating detoxification of host-derived ROS. The results suggest a molecular mechanism whereby fungal pathogens can escape the immediate early immune response, namely the oxidative burst reaction.

Results

C. albicans *yeast and hyphae forms trigger ROS in macrophages and dendritic cells*

The earliest response of innate immune cells facing pathogens includes the production of ROS (DeLeo *et al*., 1999; Forman and Torres, 2002). Thus, we asked whether *C. albicans* can induce ROS in mouse bone marrow-derived macrophages (BMDMs) as well as myeloid dendritic cells (mDCs). To investigate production of total ROS, we adapted a luminol-dependent, chemiluminescence assay in the presence of horseradish peroxidase (HRP). Oxidation of luminol by ROS leads to chemiluminescence and the luminescence measured is proportional to the ROS produced in the system (Dahlgren and Karlsson, 1999).

In order to determine the optimal ratio of *C. albicans* to host immune cells, we first performed experiments with different multiplicities of infection (MOI). Yeast forms of the clinical isolate *C. albicans* SC5314 induced ROS in BMDMs and mDCs at an MOI ranging from 2:1 (fungi to macrophages) up to 10:1 (Fig. 1A a and b). No ROS were detected with an MOI of 20:1 and higher (data not shown). The optimal ROS response by BMDMs and mDCs was observed with a 5:1 MOI (Fig. 1A). Notably, the oxidative burst of mDCs is more than five times higher than that of BMDMs (Fig. 1A c). Zymosan, a crude cell wall preparation from *Saccharomyces cerevisiae*, served as positive control in all experiments (Gantner *et al*., 2003). Mature hyphal forms of *C. albicans* (up to 12 μg per well dry weight equivalent) also induced ROS in BMDMs (Fig. 1B). To determine whether ROS are produced by immune cells or fungi, we used BMDMs differentiated from *gp91phox*$^{-/-}$ mice lacking an essential NADPH subunit required for ROS production. As expected, no ROS production was observed when *gp91phox*$^{-/-}$ BMDMs were incubated with zymosan. A substantially blunted signal was detected when *C. albicans* interacted with *gp91phox*$^{-/-}$ BMDMs (Fig. 1C). Thus, these data demonstrate that both yeast and hyphal forms of *C. albicans* can trigger ROS production in BMDMs as well as mDCs. Importantly, ROS detected by the assays is mainly derived from mammalian immune cells, as *gp91phox*$^{-/-}$ BMDMs failed to generate ROS.

ROS accumulate when sod5Δ/Δ *cells infect BMDMs*

Like most organisms, fungi possess various antioxidant enzymes to counteract oxidative damage, including thioredoxin, glutathione reductase, catalase, gluthathione peroxidase as well as SODs. The genome of *C. albicans* encodes six putative SODs (*SOD1–6*, reviewed in Chauhan *et al*., 2006).

To clarify which *C. albicans* SODs are involved in the response to innate immune cells, we constructed homozygous deletion strains, each lacking one of the six *C. albicans* SOD genes (*SOD1–6*) in the SN152 genetic background (Noble and Johnson, 2005). To create a *HIS1 LEU2* prototrophic control strain, we integrated the Cd*LEU2* and Cm*HIS1* cassettes at their corresponding genomic loci in the SN152 strain, yielding the strain CA-IF100, hereafter referred to as wild type throughout the text. This wild-type strain induced ROS to levels similar to the clinical isolate SC5314, suggesting that the different genetic backgrounds or auxotrophic markers did not affect ROS release (data not shown). We then tested the phenotypes of mutants lacking SODs concerning

© 2008 The Authors
Journal compilation © 2008 Blackwell Publishing Ltd,

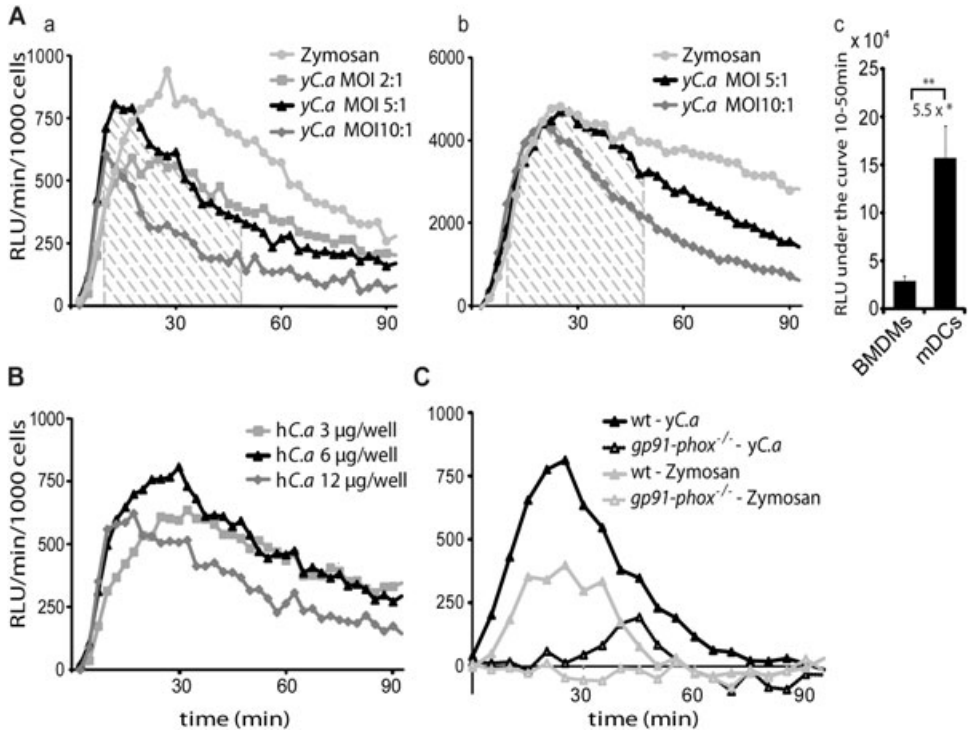

Fig. 1. *C. albicans* induces ROS production in wild-type BMDMs and mDCs.
A–C. ROS measurement by luminol-dependent chemiluminescence at 37°C in 2.5 min intervals over a 90 min period [relative luciferase units (RLU) min^{-1} per 1000 immune cells].
A. Stimulation of BMDMs (a) or mDCs (b) with yeast-form *C. albicans* (y*C.a*) at an MOI of 2:1 (equivalent to 2 µg yeast dry weight per well), 5:1 (5 µg/well) or 10:1 (10 µg/well) or with zymosan (20 µg/well). (c) Quantification of the total ROS release between 10 and 50 min (striped area) by calculating the area under the curve (MOI 5:1). The average of three independent experiments is presented. *mDCs produce 5.5 ± 0.35 times more ROS than BMDMs. **$P < 0.02$.
B. Stimulation of BMDMs with hyphae-form *C. albicans* (h*C.a*) *at* 3 µg dry weight/well, 6 µg/well or 12 µg/well.
C. Stimulation of *gp91phox*$^{-/-}$ and wt BMDMs with yeast-form *C. albicans* at an MOI of 5:1 or zymosan (20 µg/well).
A–C. Results of one experiment per condition are shown. Data were reproduced in at least three independent experiments. Statistical significance was calculated using a two-tailed Student's *t*-test.

intracellular stress such as menadione, which is generating intracellular superoxide radicals, and diamide, a thiol-specific oxidant that can readily oxidize reduced glutathione. We confirmed the previously reported sensitivities of *C. albicans* strains lacking *SOD1* and *SOD2* to menadione, as well as the resistance to diamide, on SD media (Hwang *et al.*, 2002; 2003) (data not shown). Importantly, the absence of extracellular SODs failed to show any sensitivity or resistance to any of the drugs causing intracellular oxidative stress, implying a putative function in extracelluar ROS detoxification.

Next, we tested phenotypes of cells lacking various SODs concerning the activation of ROS production in macrophages or dendritic cells using the luminol assay. The interaction of primary BMDMs with *C. albicans sod1*Δ/Δ or *sod4*Δ/Δ strains did not show any significant changes in ROS levels over a period of 90 min when compared with the wild-type strain CA-IF100 (Fig. 2A a). Similarly, the *sod2*Δ/Δ, *sod3*Δ/Δ and *sod6*Δ/Δ homozygous deletion strains did not show any different ROS production (data not shown). By contrast, ROS accumulated more than fourfold when BMDMs were infected with the *sod5*Δ/Δ deletion strain CA-IF019, but not with the *sod5*Δ/*SOD5* heterozygous strain (Fig. 2A a–c). As a control, we also re-integrated a functional *SOD5* gene into the corresponding genomic locus, *sod5*Δ/Δ::*SOD5* to construct the revertant strain CA-IF070. As expected, ROS levels induced by this strain were similar to those elicited by the wild-type strain. The phorbol ester PMA, a potent ROS inducer, was used as a positive control (Fig. 2A b). Similar results were obtained for ROS induction by mutant and wild-type strain using primary mDCs (Fig. 2B a and b). Furthermore, no ROS accumulation was observed in BMDMs derived from *gp91phox*$^{-/-}$ mice infected with *sod5*Δ/Δ homozygous deletion strains and the wild-type strain, unequivocally demonstrating that ROS accumulation in BMDMs and mDCs requires functional *gp91phox* and the absence of Sod5 (Fig. 2C), suggesting a role for Sod5 in counteracting the oxidative burst of innate immune cells *in vitro*.

© 2008 The Authors
Journal compilation © 2008 Blackwell Publishing Ltd,

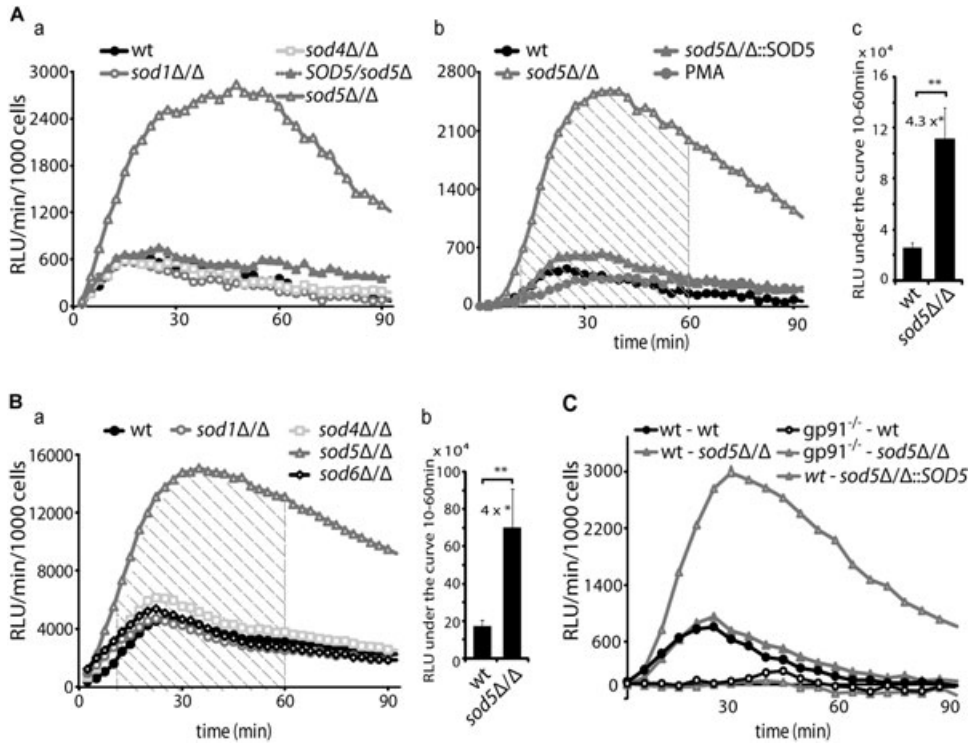

Fig. 2. ROS accumulate when BMDMs or mDCs, but not *gp91phox*$^{-/-}$ BMDMs, are infected with *sod5*Δ/Δ cells.
A–C. ROS measurement by luminol-dependent chemiluminescence at 37°C in 2.5 min intervals over a 90 min period [relative luciferase units (RLU) min^{-1} per 1000 immune cells].
A. (a) Stimulation of BMDMs with either the wild type (CA-IF100) strain or the *sod1*Δ/Δ (CA-IF003), *sod4*Δ/Δ (CA-IF015), *sod5*Δ/Δ (CA-IF019) mutant strains or *sod5*Δ/*SOD5* heterozygous strain (CA-IF017) (MOI 5:1). (b) Stimulation of BMDMs with the *sod5*Δ/Δ::*SOD5* revertant (CA-IF027) (MOI 5:1) or PMA (10 nM). (c) Quantification of the total ROS release between 10 and 60 min (striped area) by calculating the area under the curve (MOI 5:1). The average of three independent experiments is presented. *Infection with *sod5*Δ/Δ yields 4.3 ± 0.68 times more ROS than with wild-type *C. albicans*. **$P < 0.02$.
B. (a) Stimulation of mDCs with either the wild type (CA-IF100) strain, or the *sod1*Δ/Δ (CA-IF003), *sod4*Δ/Δ (CA-IF015), *sod6*Δ/Δ (CA-IF023) or *sod5*Δ/Δ mutant strains. (b) Quantification of the total ROS release between 10 and 60 min (striped area) by calculating the area under the curve. The average of three independent experiments is presented. *Infection with *sod5*Δ/Δ yields 4 ± 0.64 times more ROS than with wild type cells. **$P < 0.05$.
C. Stimulation of *gp91phox*$^{-/-}$ or wild-type BMDMs with either the wild-type (CA-IF100) strain, the *sod5*Δ/Δ (CA-IF019) mutant strain or *sod5*Δ/Δ::*SOD5* re-integrant (CA-IF027).
A–C. Results of one experiment per condition are shown. Data were reproduced in at least three independent experiments. Statistical significances were calculated using a two-tailed Student's *t*-test.

ROS accumulation in vitro *is due to enhanced extracellular superoxide levels*

The SODs are believed to destroy harmful superoxides produced by converting them first to H_2O_2; subsequently catalase converts H_2O_2 into harmless H_2O and O_2. We therefore hypothesized that deletion of an SOD gene should increase superoxide levels. Because the main type of ROS detected by the luminol assay is peroxide but not superoxide, we measured superoxide levels using lucigenin as a luminescence probe (Li *et al.*, 1998). Superoxide accumulation in BMDMs cocultured with the wild-type strain, as well as the *sod4*Δ/Δ strain, was similar. By contrast, the *sod5*Δ/Δ mutant showed a more than threefold superoxide accumulation. As expected, superoxide accumulation was not observed in BMDMs cocultured with the functionally restored *sod5*Δ/Δ::*SOD5* strain (Fig. 3A).

The NADPH-oxidase is believed to assemble either in the plasma membrane or in membranes of phagosomes (Hampton *et al.*, 1998; Kobayashi *et al.*, 1998). Therefore, ROS will either be released from cells or retained inside the phagosomes. To discriminate the locations of ROS accumulation, we measured ROS using isoluminol as a luminescence probe (Lundqvist and Dahlgren, 1996), which, in contrast to luminol, is membrane-impermeable. In BMDMs, ROS accumulated about 10-fold higher in the presence of *sod5*Δ/Δ cells, when compared with macrophages coincubated with *sod6*Δ/Δ cells or the wild-type strain (Fig. 3B).

© 2008 The Authors
Journal compilation © 2008 Blackwell Publishing Ltd,

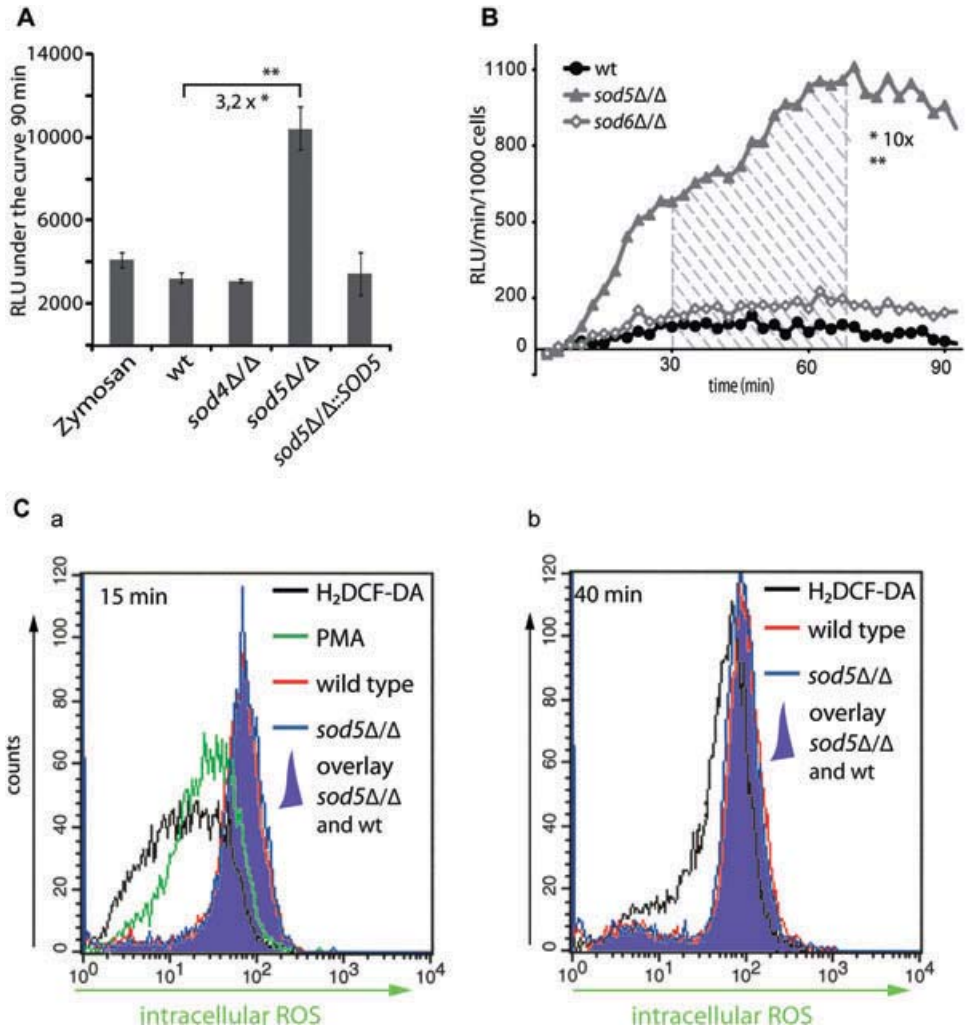

Fig. 3. Extracellular ROS accumulate in the presence of *sod5*Δ/Δ cells.
A. Superoxides measurement by lucigenin-dependent chemiluminescence at 37°C over a 90 min period [relative luciferase units (RLU) under the curve]. Stimulation of BMDMs with either the wild-type (CA-IF100) strain, or the *sod4*Δ/Δ (CA-IF015), *sod5*Δ/Δ (CA-IF019) mutant strain or the *sod5*Δ/Δ::*SOD5* revertant (CA-IF027) (MOI 5:1). *Infection with *sod5*Δ/Δ yields 3.2 ± 0.21 times more superoxides than with wild-type *C. albicans* $^{**}P > 0.005$.
B. Extracellular ROS measurement by isoluminol-dependent chemiluminescence at 37°C in 2.5 min intervals over a 90 min period [relative luciferase units (RLU) min^{-1} per 1000 cells]. Stimulation of BMDMs with either the wild-type (CA-IF100) strain or the *sod5*Δ/Δ (CA-IF019) or *sod6*Δ/Δ (CA-IF023) mutant strains (MOI 5:1). Quantification of the total ROS release between 30 and 70 min (striped area) by calculating the area under the curve. *Infection with *sod5*Δ/Δ yields 10 ± 0.5 times more extracellular ROS than with wild-type cells. $^{**}P > 0.001$.
C. Intracellular ROS production in response to the phorbol ester PMA, wild-type (CA-IF100) strain or *sod5*Δ/Δ (CA-IF019) mutant strain was measured by FACS analysis using H_2DCF-DA staining of BMDMs after 15 min (a) or 40 min (b) of infection.
A–C. Results of one experiment per condition are shown. All data were reproduced in at least three independent experiments. Statistical significances were calculated using a two-tailed Student's *t*-test.

Finally, to visualize intracellular ROS production, we pre-loaded BMDMs with the non-fluorescent dye H_2DCF-DA, which cannot cross cellular compartments after esterase cleavage. Upon oxidation by ROS, H_2DCF-DA is converted to the fluorescent product 2′-7′-dichlorofluorescein (DCF). A limited permeability of DCF retains it preferentially at the site where it was generated (Yeung *et al.*, 2005). Therefore, ROS produced in the phagosomes is not detected by H_2DCF-DA. We then measured the generation of ROS after 15 min (Fig. 3C a) and 45 min (Fig. 3C b) using the standard 5:1 MOI of fungal cells to BMDMs and the phorbol ester PMA as a control (Fig. 3C). FACS analysis showed that intracellular ROS levels were induced at very similar levels by both *sod5*Δ/Δ and the wild-type strains (Fig. 3C, violet overlay). We conclude that Sod5 is involved in the detoxification of extracellular or phagosomal superoxides produced by BMDMs, but has no effect on the intracellular ROS levels.

© 2008 The Authors
Journal compilation © 2008 Blackwell Publishing Ltd,

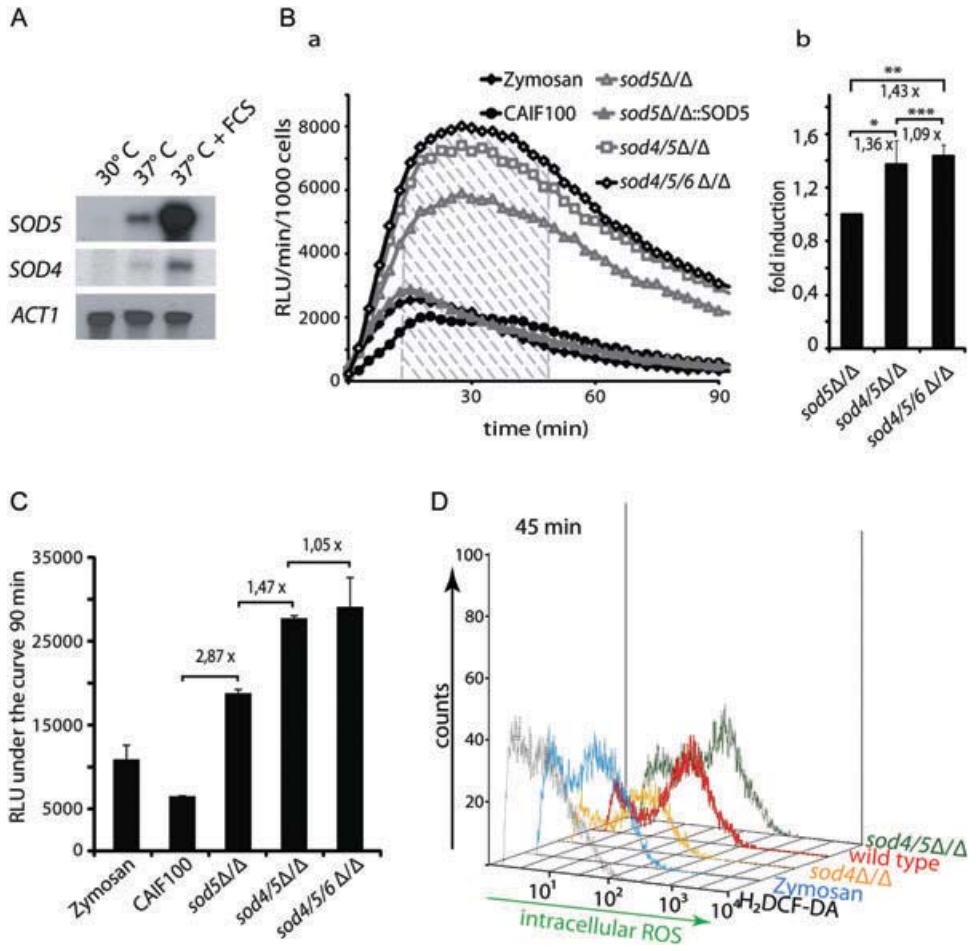

Fig. 4. A *sod4*Δ/Δ deletion in a *sod5*Δ/Δ background boosts ROS accumulation.
A. Northern analysis of *SOD4*, *SOD5* and *ACT1* mRNA. The clinical *C. albicans* SC5314 strain was grown at 30°C, 37°C and 37°C plus 10% FCS.
B. ROS measurement by luminol-dependent chemiluminescence at 37°C in 2.5 min intervals over a 90 min period [relative luciferase units (RLU) min^{-1} per 1000 BMDMs]. Stimulation of BMDMs with either the wild-type (CA-IF100) strain or *sod5*Δ/Δ (CA-IF019), *sod5*Δ/Δ::*SOD5* (CA-IF027), *sod4*Δ/Δ *sod5*Δ/Δ (CA-IF039) and *sod4*Δ/Δ *sod5*Δ/Δ *sod6*Δ/Δ (CA-IF070) mutant strains (MOI 5:1) (a). Quantification of the total ROS release between 10 and 50 min (striped area) by calculating the area under the curve (MOI 5:1) and calculating the fold differences. The average of four independent experiments is presented. Infection with *sod4*Δ/Δ *sod5*Δ/Δ yields 1.36 ± 0.18 times more ROS than by a *sod5*Δ/Δ strain. $^{*}P < 0.05$, *sod4*Δ/Δ *sod5*Δ/Δ *sod6*Δ/Δ triple mutant yields 1.43 ± 0.09 times more ROS than by a *sod5*Δ/Δ strain. $^{*}P < 0.02$; and the *sod4*Δ/Δ *sod5*Δ/Δ *sod6*Δ/Δ triple mutant yields 1.09 ± 0.1 times more ROS than *sod4*Δ/Δ *sod5*Δ/Δ. $^{***}P > 0.09$ (b).
C. Superoxides measurement by lucigenin-dependent chemiluminescence at 37°C over a 90 min period [relative luciferase units (RLU) under the curve]. Stimulation of BMDMs with either zymosan (20 μg/well), the wild-type (CA-IF100) strain, the *sod5*Δ/Δ (CA-IF019), *sod4*Δ/Δ *sod5*Δ/Δ (CA-IF039) and *sod4*Δ/Δ *sod5*Δ/Δ *sod6*Δ/Δ (CA-IF070) mutant strains (MOI 5:1).
A and B. Results of one experiment per condition are shown. All data were reproduced in two independent experiments.
D. Intracellular ROS production in response to wild-type (CA-IF100) strain or *sod4*Δ/Δ (CA-IF015), *sod4*Δ/Δ *sod5*Δ/Δ (CA-IF039) mutant strains (MOI 5:1) or zymosan (100 μg ml^{-1}). ROS was measured by FACS analysis using H_2DCF-DA-staining of BMDMs after 45 min of infection.
A–C. Results of one experiment per condition are shown. All data were reproduced in at least three independent experiments. Statistical significances were calculated using a two-tailed Student's *t*-test.

Sod4 but not Sod6 shares functional overlap with Sod5

A previous report showed that *SOD4* is upregulated in a *sod5*Δ/Δ mutant cocultured with blood cells (Fradin *et al.*, 2005), suggesting that the lack of the *SOD5* gene may result in compensatory upregulation of other functionally overlapping *SOD* genes. Northern analysis demonstrated that *SOD4* mRNA levels in yeast-form *C. albicans* were lower than those of *SOD5*. However, both transcripts were strongly upregulated under conditions promoting hyphal transition, including higher temperature at 37°C or 37°C plus serum (Fig. 4A). While we failed to detect *SOD6*-specific expression via Northern analysis, we used qPCR to detect *SOD6* mRNA in the wild type, the single *sod5*Δ/Δ mutant, as well as in the *sod4*Δ/Δ *sod5*Δ/Δ double deletion strain, all of which were growing at 30°C and 37°C plus

© 2008 The Authors
Journal compilation © 2008 Blackwell Publishing Ltd,

10% FCS. The mRNA levels of *SOD6* were the same under all conditions tested (data not shown), indicating that *SOD6* is not regulated during yeast to hyphae transition or by temperature. We therefore hypothesized that *SOD4* expression may compensate at least partially for the lack of *SOD5*, while *SOD6* is unable to do so. To test this hypothesis, we generated *sod4*Δ/Δ *sod5*Δ/Δ and *sod4*Δ/Δ *sod6*Δ/Δ double mutants and a *sod4*Δ/Δ *sod5*Δ/Δ *sod6*Δ/Δ triple mutant (using the *SAT1*-flipper cassette, Reuss *et al*., 2004), and looked at ROS accumulation after infecting BMDMs. When BMDMs were infected with the *sod4*Δ/Δ *sod5*Δ/Δ double deletion strain, accumulation of ROS was slightly (1.36 times), but significantly higher than in the presence of the respective *sod5*Δ/Δ single deletion strain (Fig. 4B b). By contrast, a *sod4*Δ/Δ *sod6*Δ/Δ double mutant strain did not affect the ROS accumulation relative to single deletions or the wild-type cells (data not shown). The *sod4*Δ/Δ *sod5*Δ/Δ *sod6*Δ/Δ triple mutant slightly increased ROS accumulation when compared with the *sod4*Δ/Δ *sod5*Δ/Δ double mutant, but without a statistical significance (Fig. 4B a + b). Superoxide accumulation in BMDMs cocultured with the *sod5*Δ/Δ deletion strain was again about threefold higher than with the wild-type strain. BMDMs cocultured with the *sod4*Δ/Δ *sod5*Δ/Δ double deletion accumulated about 1.5 times more superoxides than the *sod5*Δ/Δ mutant strain. By contrast, the *sod4*Δ/Δ *sod5*Δ/Δ *sod6*Δ/Δ triple deletion strain showed no increase in superoxide accumulation relative to the *sod4*Δ/Δ *sod5*Δ/Δ double mutant (Fig. 4C).

We then measured the generation of intracellular ROS using the standard 5:1 MOI of fungal cells to BMDMs. FACS analysis showed that after 30 min intracellular ROS were induced at very similar levels by the *sod4*Δ/Δ, *sod4*Δ/Δ *sod5*Δ/Δ mutant and the wild-type strains (data not shown). Notably, after 45 min, the *sod4*Δ/Δ mutant strain exhibited less intracellular ROS than the wild-type control strain, but induced similar ROS levels as zymosan; the *sod4*Δ/Δ *sod5*Δ/Δ mutant strains induced levels of intracellular ROS similar to the wild type (Fig. 4D).

Hence, these data suggest that Sod5 and Sod4 play a major role in the clearance of ROS produced by innate immune cells. Notably, Sod4, although present at very low levels, can at least partially compensate for a loss of Sod5.

Exogenous SOD rescues defects of cells lacking Sod4 and Sod5

Previous work indicated that a *sod5*Δ/Δ deletion strain was attenuated in a mouse model for disseminated infection, and exhibited increased susceptibility to killing by whole human blood cultures and polymorphonuclear neutrophils, but not to human monocytes or the macrophage cell line RAW264.7 (Martchenko *et al*., 2004; Fradin *et al*., 2005). Our data, as well as published virulence data, predict that cells lacking SODs should display higher susceptibilities to killing by immune cells and thus exhibit reduced viability in the presence of host cells. To examine the contribution of all CuZn-dependent SOD mutants to the defence of *C. albicans* against macrophage-derived ROS, the wild-type, *sod4*Δ/Δ, *sod5*Δ/Δ in SN152, *sod5*Δ/Δ::*SOD5*, *sod4*Δ/Δ *sod5*Δ/Δ, *sod4*Δ/Δ *sod6*Δ/Δ strains, the clinical isolate SC5314 and a new *sod5*Δ/Δ mutant generated in the genetic background of the clinical isolate SC5314 were tested for their viability in coculture with primary BMDMs using a modified 'endpoint dilution survival' assay as described earlier (Rocha *et al*., 2001).

As shown in Fig. 5A, the quantification of the survival data of an interaction with BMDMs at the low MOI 1:1024 showed that 66.4% of the wild-type cells survived in the presence of BMDMs. Likewise, *sod4*Δ/Δ, *sod6*Δ/Δ and *sod4*Δ/Δ *sod6*Δ/Δ strains had very similar survival rates as the wild type at all BMDM dilutions. As predicted, the *sod5*Δ/Δ strain was hypersensitive to BMDM killing by almost one order of magnitude, while the *sod5*Δ/Δ::*SOD5* revertant displayed the same viability as the wild-type control (Fig. 5A). When coculturing BMDMs with the *sod4*Δ/Δ *sod5*Δ/Δ double mutant, viability was even further reduced. The *sod4*Δ/Δ *sod5*Δ/Δ *sod6*Δ/Δ triple mutant had a similar survival rate as the *sod4*Δ/Δ *sod5*Δ/Δ double mutant (Fig. 5A a), demonstrating the functional redundancy of at least Sod4 and Sod5. The increased sensitivity of *sod5*Δ/Δ and *sod4*Δ/Δ *sod5*Δ/Δ strains was observed in coincubations with BMDMs at the higher MOI of 1:4 for *sod5*Δ/Δ and 1:1 for *sod4*Δ/Δ *sod5*Δ/Δ cells respectively (data not shown). To reconfirm our findings, we also tested *sod5*Δ/Δ in the SC5314 background strain. When infected with BMDMs, *sod5*Δ/Δ SC5314 cells showed similar survival as the unrelated *sod5*Δ/Δ deletion strain CA-IF019 (Fig. 5A b).

To unequivocally demonstrate the role of SOD in mediating survival in the presence of BMDMs, we spiked survival assays with 10 U commercial bovine erythrocyte SOD enzyme. Strikingly, exogenous SOD fully rescued the viability defect to both *sod5*Δ/Δ and *sod4*Δ/Δ *sod5*Δ/Δ double mutants (Fig. 5A, white bars). Furthermore, ROS accumulation was also suppressed by the exogenous SOD activity when BMDMs were infected with strains lacking Sod5 or both Sod5 and Sod4 (data not shown). Finally, we also used *gp91phox*$^{-/-}$ BMDMs to test whether the absence of ROS production can increase the survival of *sod5*Δ/Δ and *sod4*Δ/Δ *sod5*Δ/Δ strains (Fig. 5B). As expected, in the presence of *gp91phox*$^{-/-}$ BMDMs, both *sod5*Δ/Δ and *sod4*Δ/Δ *sod5*Δ/Δ double mutants showed a survival comparable to the wild-type control. The same results were obtained with the independent *sod5*Δ/Δ mutant and the wild-type SC5314, respectively, in

© 2008 The Authors
Journal compilation © 2008 Blackwell Publishing Ltd,

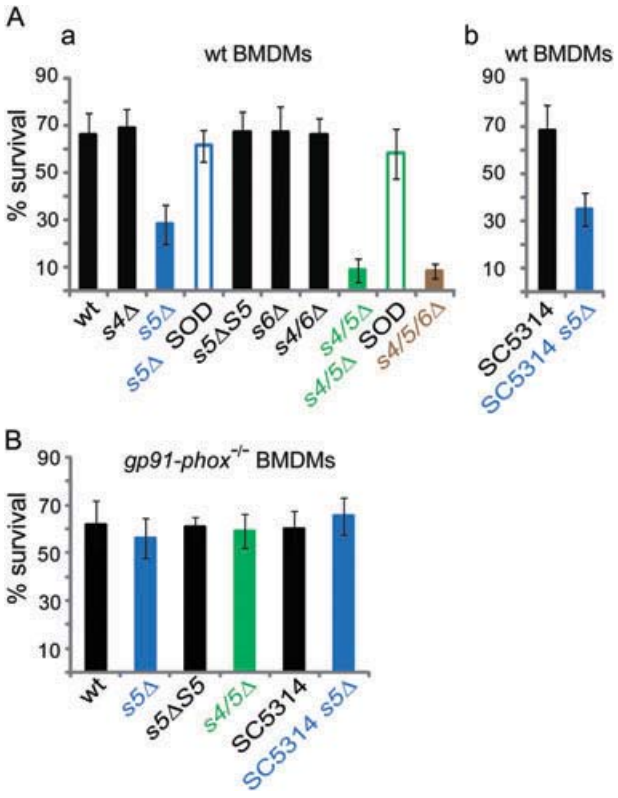

Fig. 5. *sod5*Δ/Δ and *sod4*Δ/Δ *sod5*Δ/Δ strains are hypersensitive to killing by BMDMs.
A and B. Survival of *C. albicans* and isogenic mutant cells was determined using the end-point dilution assay. Mean and standard deviation of three independent experiments are presented.
A. Wild-type BMDMs in medium without (filled bars) or with 10 U commercial erythrocyte SOD (white bar) were coincubated with either wild-type (wt) *C. albicans* strain or strains lacking *SOD4* (*s4*Δ), *SOD5* (*s5*Δ blue), the restored *SOD5* (*s5*Δ*S5*), *SOD6* (*s6*Δ) or strains lacking both *SOD4* and *SOD6* (*s4/6*Δ), *SOD4* and *SOD5* (*s4/5*Δ green) or lacking all three *SOD4*, *SOD5* and *SOD6* (*s4/5/6* brown) (a), or with the clinical isolate SC5314 and the *sod5*Δ/Δ mutant in the SC5314 background (SC5314 *s5*Δ blue) (b) for 48 h at 37°C with 5% CO_2.
B. *gp91phox*$^{-/-}$ BMDMs were infected with the wild type (wt) or strains lacking *SOD4* (*s4*Δ), *SOD5* (*s5*Δ blue), the restored *SOD5* (*s5*Δ*S5*) or strains lacking both *SOD4* and *SOD5* (*s4/5*Δ green), the clinical isolate SC5314 or the *sod5*Δ/Δ mutant in the SC5314 background (SC5314 *s5*Δ). The percentage of survival for each strain was determined as follows (colonies in absence of BMDMs versus colonies in presence of BMDMs × 100).

gp91phox$^{-/-}$ BMDMs. (Fig. 5B). This proves that increased killing of the *sod5*Δ/Δ and *sod4*Δ/Δ *sod5*Δ/Δ by innate immune cells is caused by host-derived ROS. Taken together, our data demonstrate an essential role of *C. albicans* Sod5 in counteracting the host-derived immune defence as mounted through ROS to evade host immune response.

Based on our results, we propose that *C. albicans* can escape host-generated oxidative burst (Fig. 6). Adhesion, recognition and phagocytosis of fungal cells by innate immune cells trigger an immediate and rapid assembly of the ROS machinery at the cell surface or in the forming phagosomal membrane, preceding phagocytosis and persisting throughout phagosomal formation (Nauseef, 2004). Concomitantly, host temperature and adhesion may enhance *SOD4* and *SOD5* expression, followed by the elimination of extracellular and perhaps phagosomal ROS produced by host cells. In our *in vitro* assay during phagocytosis, substrate and enzyme may become trapped in the phagosomes. Hence, ROS production may also continue within the phagosomes. The SOD-mediated decay of host-derived ROS perhaps facilitates intraphagosomal survival of fungal cells, which would facilitate killing of the host cells. Taken together, these data reveal a physiological function of cell surface SODs in evading immune surveillance, thereby facilitating invasion and ultimately dissemination of fungal pathogens in the mammalian host (Fig. 6).

Discussion

In this report, we show that yeast and hyphal forms of *C. albicans* rapidly induce ROS in primary innate immune cells such as macrophages and dendritic cells. We demonstrate that the GPI-anchored Sod5 and Sod4 enzymes act to degrade extracellular ROS produced by innate immune cells. Strikingly, *C. albicans* strains lacking SODs Sod4 and Sod5 fail to counteract the host-derived oxidative burst and are thus hyper-susceptible to killing by

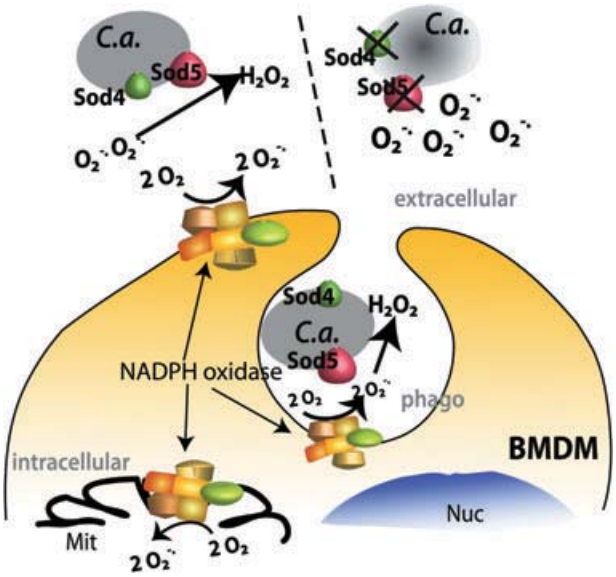

Fig. 6. Model for Sod4 and Sod5-mediated protection against respiratory burst. Upon contact with BMDMs and mDCs, Sod4 and Sod5 anchored at the *C. albicans* (*C.a*) surface (left) degrade superoxide anions (O_2^-) to hydrogen peroxide (H_2O_2). The lack of the Sod4 and Sod5 (right) causes ROS accumulation in the medium and perhaps inside the phagosomes (phago), which results in enhanced killing of *C. albicans*. Production of mitochondrial ROS (Mit) is unaffected.

© 2008 The Authors
Journal compilation © 2008 Blackwell Publishing Ltd,

primary BMDMs, suggesting a physiological role of cell surface SODs in the evasion of immune surveillance.

Yeast and hyphae forms of C. albicans *induce ROS in BMDMs and mDCs*

The ROS induction is independent of morphology as both yeast and filamentous forms of *C. albicans* trigger ROS in BMDMs (Fig. 1A). Our data agree in principle with previous studies showing ROS production upon fungal recognition (Gantner *et al*., 2005), but in contrast to this earlier report, we found that hyphae also have the capacity to trigger ROS in BMDMs (Fig. 1B a). This discrepancy may be due to differences in experimental conditions. Notably, the previous study used higher MOI than our study. In our hands, increasing MOI to similar high levels failed to trigger ROS during the interaction of both yeast and hyphal forms with BMDMs (data not shown), suggesting that higher amounts of *C. albicans* may kill or exceed the macrophage defence capacity.

We observed about 5.5 times more ROS upon interaction of *C. albicans* with mDCs when compared with BMDMs, perhaps as a consequence of higher NADPH oxidase activities in mDCs (Fig. 1A a). Consistent with this notion, similar observations were made in mDC responding to the phorbol ester PMA (Savina *et al*., 2006), one of the strongest ROS triggers known. We unequivocally demonstrate that the majority of ROS produced in response to *C. albicans* is produced through the NADPH oxidase present in immune cells, as ROS release is almost absent in *gp91phox*$^{-/-}$ cells lacking a functional oxidase (Fig. 1C).

Host cells produce ROS in response to *C. albicans*, as well as fungal surface structures, although the molecular identities of ligands triggering ROS signalling remain unknown. Possible candidates include beta1–3 as well as beta 1–6 glucans (Gantner *et al*., 2003; Rubin-Bejerano *et al*., 2007). However, the use of appropriate knock-out mice may allow to answer which pattern recognition receptors contribute to ROS signalling or mediate *C. albicans* uptake into host cells (Netea *et al*., 2008).

C. albicans *Sod5 degrades extracellular ROS produced by immune cells*

Experiments using monocyte-derived dendritic cells from human blood show that *C. albicans* inhibit PMA-induced superoxide production. This inhibition increases with increasing numbers of *C. albicans* cells, whereas heat-killed *C. albicans* fails to do so (Donini *et al*., 2007). Based on our work, we propose that *C. albicans* actively counteracts the oxidative burst of immune cells by expressing and inducing expression of cell surface SODs, which may therefore be considered fungal defence genes (Fig. 6). The GPI-anchored Sod5 and Sod4, as well as Sod6, have only been described in *C. albicans* so far. However, BlastP or tBlastN analysis identified at least one coding sequence potentially encoding putative GPI-anchored homologous of *SOD4*, *SOD5* or *SOD6* in other fungal pathogens, including *Candida dubliniensis*, *Candida tropicalis*, *Candida parapsilosis*, *Candida guilliermondi*, *Debraryomyces hanseii* and *Lodderomyces elongisporus* (data not shown). Hence, these pathogens may rely on similar mechanisms to counteract host-derived oxidative stress. Infecting BMDMs and mDCs with *C. albicans* mutants lacking putative Sod enzymes shows that Sod5 can degrade extracellular and maybe phagosomal superoxides, but not intracellular, superoxides produced by BMDMs and mDCs (Fig. 3 and 4). Thus, to the best of our knowledge, this is the first report that a fungal cell surface SOD degrades extracellular ROS released by host cells.

The ability of *C. albicans* to destroy ROS *in vitro* may explain why despite its cytotoxic potential, macrophages are poor in killing *C. albicans.* Notably, even if only a small fraction of fungal cells survive and escape phagosomal killing to grow within the host, the subsequent filament formation will physically destroy the host cell (Mansour and Levitz, 2002). Furthermore, we and others (Martchenko *et al*., 2004) show that elevated temperature, yeast-to-hyphae transition (Fig. 4A), as well as conditions mimicking the phagosome environment, strongly induce *SOD5*. Similarly, contact with neutrophils strongly activates *SOD5* transcription (Fradin *et al*., 2005). Thus, *SOD5* upregulation is perhaps part of the mechanism whereby the pathogen defence machinery responds to adverse host conditions.

The upregulation of *SOD4* in a *sod5*Δ/Δ deletion strain (Fradin *et al*., 2005) partially compensates for the loss of Sod5, providing redundant function. Indeed, we show that the putative extracellular Sod4 also contributes to ROS degradation, although at much lower capacity (Fig. 4B and C). Interestingly, microarray data and our own preliminary results (data not shown) suggest that Sod4 is also upregulated upon the transition from the white form to the opaque form of *C. albicans* (Lan *et al*., 2002), implying that Sod4 may also play a prominent role in ROS degradation in the opaque form. Opaque phase *C. albicans* cells, for instance, are better colonizers of the skin and are also believed to colonize the anaerobic gastrointestinal tract. Hence, Sod4 could play a more prominent role in the gastrointestinal tract or in skin infections. By contrast, white cells are more prevalent in bloodstream infections (Kvaal *et al*., 1999; Dumitru *et al*., 2007; Ramirez-Zavala *et al*., 2008), providing selective advantages for the survival of opaque versus white cells in different host niches.

Notably, we were unable to detect a role in ROS decay for Sod6, the third *C. albicans* SOD predicted to reside at

© 2008 The Authors
Journal compilation © 2008 Blackwell Publishing Ltd,

the cell surface. We detected *SOD6* mRNA in the wild type, the *sod5* single as well as the *sod4 sod5* double deletion strains in YPD 30°C or YPD + FCS 37°C (data not shown). Furthermore, removal of *SOD6* in the *sod4*Δ/Δ or the *sod4*Δ/Δ *sod5*Δ/Δ deletion strains does not play a role in ROS degradation *in vitro*, at least in the interaction with primary BMDMs. *In vivo* experiments using animal models might provide more details as to a possible protective function of *SOD6*. Moreover, a surface localization of Sod6 has not been demonstrated or published. Therefore, the possibility remains that Sod6 may also reside in another cellular compartment, explaining the lack of ROS recognition during host interaction.

Cells lacking Sod4 and Sod5 are hypersensitive to killing by host ROS

Candida albicans strains lacking the *SOD5* gene display attenuated virulence in mice *in vivo* (Martchenko *et al*., 2004), and contribute to a better survival of *C. albicans* in neutrophils (Fradin *et al*., 2005). This is in agreement with our *in vitro* survival experiments, showing that *sod5*Δ/Δ mutant cells in two independent genetic backgrounds show strongly reduced survival in BMDMs when compared with the wild-type control strain, and the genomically restored *SOD5* revertant (Fig. 5A). However, our results are not in agreement with a previous study, reporting similar survival degrees of the *sod5* mutant when compared with the wild-type strain (Martchenko *et al*., 2004). However, the previous study used the macrophage cell line RAW264.7, whereas we exploited primary macrophages, which are likely to display a pathogen response reminiscent of the normal host situation. Hence, the RAW264.7 tumour cells might very well display a different signalling response to *C. albicans* than unstimulated primary BMDMs. Further, the 'immortalized' tumour RAW264.7 cells in question stem from different progenitors than our BMDMs, as they were isolated from ascites and not from bone marrow. Interestingly, a recent report indicates that *C. albicans* is more susceptible when applying the end-point dilution survival assays with RAW264.7 cells than with BMDMs (Marcil *et al*., 2008).

Cells lacking Sod4 and Sod5 show significantly decreased survival when compared with the single *sod5*Δ/Δ mutant, confirming the importance of Sod4 activity and the functional redundancy with Sod5. Further, complementing the defect with commercial SOD from bovine erythrocytes restores the survival of mutant strains to almost wild-type levels. (Fig. 5A, white bars). Moreover, wild type, *sod5*Δ/Δ and *sod4*Δ/Δ *sod5*Δ/Δ strains are all equally sensitive to killing by *gp91phox*$^{-/-}$ BMDMs defective in ROS release. The remaining 30–40% killing efficiency of *gp91phox*$^{-/-}$ macrophages, as well as the 30–40% killing of wild-type *C. albicans* strains by wild-type BMDMs, may be independent of the oxidative burst and stem from other host defence mechanisms such as acidification of the phagolysosomes (Watanabe *et al*., 1991).

Our results recall previous findings showing that extracellular CuZn SODs of bacteria, for example SodC of *Mycobacterium tuberculosis* and the periplasmic SodC of *Salmonella typhimurium* confer improved survival in macrophages by degrading extracellular superoxides (De Groote *et al*., 1997; Piddington *et al*., 2001). Our current working model suggests that *C. albicans* can eliminate ROS produced in the extracellular space of the macrophages and dendritic cells, including ROS produced during phagosome formation within immune cells (Fig. 6).

Taken together, this work suggests that pathogens able to develop high oxidative stress tolerance are also more resistant to killing by immune cells. Therefore, scavenging ROS produced by the NADPH oxidase reaction through surface SODs may represent a physiological mechanism driving virulence, invasion and efficient survival in the host. The work also suggests a general mechanism whereby *C. albicans* and other fungal pathogens evade the host immune response and surveillance. Hence, inhibiting or blocking the extracellular SOD enzymes of *C. albicans* may be a novel therapeutic approach to combat systemic fungal disease. For instance, specific inhibitors of SODs may prove useful novel drugs to be used alone or in combination with existing antifungals to interfere or block dissemination of fungal pathogens *in vivo*.

Experimental procedures

Reagents, media and growth conditions

Luminol, Lucigenin, Isoluminol, HRP Type VI, PMA, SOD from bovine erythrocytes and zymosan were obtained from Sigma (St Louis, MO). FCS, HBSS, H_2DCF-DA were from Invitrogen Molecular Probes (Oregon). DMEM was purchased from PAA (Vienna, Austria), anti-mouse antibodies CD16/CD32, CD11b-FITC, CD11c-APC, F4/80-PE-Cy5 were obtained from BD Bioscience (Mountain View, CA). Rich medium (YPD) and synthetic complete were prepared essentially as described (Kaiser *et al*., 1994). BMDM media are composed of DMEM, 10% heat-inactivated FCS, 20% L-conditioned medium. mDC media are composed of DMEM, 10% heat-inactivated FCS, 10% X-conditioned medium. *C. albicans* strains were grown at 30°C in YPD medium overnight, diluted to an OD_{600} = 0.2 the next morning, grown to the logarithmic growth phase and used for the experiment unless indicated otherwise. For the preparation of mature filaments, an overnight culture of *C. albicans* was diluted 1:10 in YPD + 10% FCS and grown at 37°C for 3–4 h. For experiments requiring stimulation of macrophages with filaments, an aliquot of each culture was pelleted and the dry weight was determined by routine procedures. Aliquots of cultures equalling the indicated dry weights of yeast or filaments were

© 2008 The Authors

used for experiments. Typically, 4×10^4 yeast cells correspond to 1 μg dry weight.

Fungal strains and construction of C. albicans *deletion mutants*

Candida albicans strains, primers and plasmids used in this study are listed in Tables S1–S3 respectively. The laboratory strain SN152 served as wild-type parental strain to construct single deletion strains (*SOD1* to *SOD6*) using the method described elsewhere (Noble and Johnson, 2005). SN152 is a leucine, histidine, arginine auxotroph derivative of the clinical isolate SC5314 (Gillum *et al*., 1984). The *sod5* deletion was also generated in the SC5314 background. Multiple gene deletion mutants, as well as the *sod5*Δ/Δ in the SC5314 background, were created using the recyclable '*SAT1*-flipping' method (Reuss *et al*., 2004). Transformation was achieved by electroporation (Reuss *et al*., 2004). For all strains used in this study, correct genomic integration was verified by PCR and Southern blotting.

Mouse strains and cell culture of innate immune cells

The 7- to 9-week-old C57BL/6 wild-type mice were used for preparation of BMDMs and mDCs. Frozen bone marrow of 6- to 8-week-old *gp91phox*$^{-/-}$ C57BL/6 mice was kindly provided by Kristina Erikson (George-Chandy *et al*., 2008). Bone marrow was collected from mouse femurs, treated with red blood lysis buffer (8.29 g l^{-1} NH4CL, 1 g l^{-1} KHCO3, 0.0372 g l^{-1} EDTA, pH 7.2–7.4) and re-suspended either in macrophage media to induce differentiation into BMDMs or in mDC media to prepare mDC according to previously described methods (Hume and Gordon, 1983; Inaba *et al*., 1992). After 3 days in culture, fresh medium was added. mDCs were used after 7–8 days in culture. After 7 days, BMDMs cultures were split 1:3 and further cultured up to day 10. BMDMs were used between day 10 and day 13 of differentiation. Cell surface markers of the mDCs and BMDMs cell preparation were assessed by flow cytometry using a panel of marker antibodies. mDCs preparations were negative for F4/80, a macrophage marker, positive for CD11b, and at least 50–60% of the cells were CD11c+. In BMDMs cultures, 95% of the cells expressed CD11b and F4/80 markers.

ROS assays

For the detection of total, extracellular and intracellular ROS, chemiluminescense assays were performed using electron acceptors with various characteristics; luminol- (reacts weakly with O_2^-, strongly with other ROS like H_2O_2, HRP-dependent), isoluminol- (extracellular O_2^-, HRP dependent) and lucigenin- (O_2^-) enhanced chemiluminescence assays were performed as described before (Dahlgren and Karlsson, 1999). Briefly, BMDMs were suspended in culture medium at a density of 4×10^5 cells ml^{-1} and kept warm at 37°C in a water bath for a maximum of 30 min. And 100 μl aliquots of cell suspension were distributed in a 96-well luminometer plate (Nunc, Roskilde, Denmark); 50 μl HBSS medium containing PMA (10 nM) or zymosan (100 μg ml^{-1}) as positive controls and *C. albicans* mutants at the indicated cell numbers were added. Immediately after adding stimuli, 50 μl HBSS containing either 200 μM luminol or 600 μM Isoluminol and 16 U HRP, or 400 μM lucigenin were distributed into each well. Chemiluminescence was measured at 2.5 min intervals at 37°C with a multiplate reader Wallac VictorV^3 (PerkinElmer). Data are expressed as relative luciferase units min^{-1} per 1000 BMDM cells over time, or as total relative luciferase units under curve within 90 min. Area under the curve was calculated using the trapezoidal method. Statistical significances were calculated using two-tailed Student's *t*-test from three wells per condition or from data of three independent experiments.

Intracellular ROS was measured using H_2DCFA-DA dye to determine hydrogen peroxide production. BMDMs were suspended in HBSS at 5×10^6 cells ml^{-1} approximately 30 min before measurements. Just prior to the experiment, cells were loaded with 5 μM H_2DCF-DA in HBSS for 20 min at room temperature in the dark, and pelleted at 300 *g* for 7 min at room temperature. After washing with PBS, cells were carefully re-suspended in HBSS at a density of 5×10^6 cells ml^{-1}. Aliquots of 5×10^5 cells were stimulated with different agents in HBSS. *C. albicans* (MOI 5:1) zymosan (1 mg ml^{-1}), PMA (200 nM) and incubated for 15–45 min at 37°C. After an additional washing step, cells were re-suspended in 400 μl PBS, 0.1% BSA on ice, followed by FACS analysis with FL1-H.

RNA extraction and Northern analysis

Total yeast RNA was isolated by the hot phenol method and quantified exactly as described elsewhere (Kren *et al*., 2003). About 15 μg of total RNA per sample was separated in a 1.4% agarose gel and transferred to nylon membranes (Amersham, Buckinghamshire, UK). Northern blots were hybridized with PCR-amplified probes, which were ^{32}P-dCTP-radiolabelled by using a MegaPrime labelling kit (Amersham) using conditions recommended by the manufacturer. Hybridization with purified probes was performed exactly as previously described (Kren *et al*., 2003). Membranes were washed three times in 2× SSC-1% SDS and three times in 1× SSC-1% SDS at 65°C, and then exposed to X-ray films at –70°C. DNA probes for Northern blots were PCR-amplified from genomic DNA using primers listed in Table S1.

End-point dilution survival assays

End-point dilution survival assays were performed as described previously (Rocha *et al*., 2001) with the following modifications. BMDMs were seeded 1 day before the experiment at 1×10^5 cells per well in every second column of flat-bottom 96-well plates (Greiner, Longwood, Florida) in BMDM medium. Next day, cells were washed twice with PBS and 100 μl DMEM without phenol red containing 10% FCS. Overnight cultures of *C. albicans* cells were washed in PBS, and re-suspended at 2×10^6 cells ml^{-1} DMEM without phenol red but with 10% FCS. Aliquots of 50 μl cell suspensions were added to the first two columns, and serial fourfold dilutions of

© 2008 The Authors
Journal compilation © 2008 Blackwell Publishing Ltd,

C. albicans suspensions were placed in subsequent columns. Plates were spun at 500 *g* for 1 min, followed by incubation at 37°C and 5% CO_2 for 48 h. Yeast colonies were stained in the 96-well plate with Cristal violet, using a 0.2% solution in 20% MeOH exactly as described previously (Stockinger *et al.*, 2002). Viable colonies were counted and compared with equivalent dilutions in wells with macrophages. An assay setup of four to eight plates per day was defined as one experiment. At least three independent experiments were performed per condition. Colonies from a total of at least 25 wells per condition were used to quantify viability data.

Acknowledgements

We thank all laboratory fellows and Bernhard Hube for critical and helpful discussions. We are very grateful to K. Eriksson for the gift of bone marrow from *gp91phox*$^{-/-}$ knock-out mice, Alexander Johnson for providing the SN152 strain, pSN52 and pSN40 plasmids and J. Morschhäuser for providing the pSFS2A plasmid. *C. albicans* sequence data were obtained from the Stanford Genome Center (http://www.candidagenome.org). This work was supported by a grant from the Christian Doppler Research Society to K.K., and in part by a grant from the Vienna Science and Technology Fund WWTF (Project HOPI-LS133). I.E.F. was supported through the Vienna Biocenter PhD Programme WK001.

References

Akira, S., Uematsu, S., and Takeuchi, O. (2006) Pathogen recognition and innate immunity. *Cell* **124:** 783–801.

Babior, B.M. (2004) NADPH oxidase. *Curr Opin Immunol* **16:** 42–47.

Brown, G.D., and Gordon, S. (2005) Immune recognition of fungal [beta]-glucans. *Cell Microbiol* **7:** 471–479.

Chauhan, N., Latge, J.P., and Calderone, R. (2006) Signalling and oxidant adaptation in *Candida albicans* and *Aspergillus fumigatus*. *Nat Rev Microbiol* **4:** 435–444.

Dahlgren, C., and Karlsson, A. (1999) Respiratory burst in human neutrophils. *J Immunol Meth* **232:** 3–14.

De Groote, M.A., Ochsner, U.A., Shiloh, M.U., Nathan, C., McCord, J.M., Dinauer, M.C., *et al.* (1997) Periplasmic superoxide dismutase protects *Salmonella* from products of phagocyte NADPH-oxidase and nitric oxide synthase. *Proc Natl Acad Sci USA* **94:** 13997–14001.

DeLeo, F., Allen, L., Apicella, M., and Nauseef, W. (1999) NADPH oxidase activation and assembly during phagocytosis. *J Immunol* **163:** 6732–6740.

Dinauer, M.C. (1993) The respiratory burst oxidase and the molecular genetics of chronic granulomatous disease. *Crit Rev Clin Lab Sci* **30:** 329–369.

Donini, M., Zenaro, E., Tamassia, N., and Dusi, S. (2007) NADPH oxidase of human dendritic cells: role in *Candida albicans* killing and regulation by interferons, dectin-1 and CD206. *Eur J Immunol* **37:** 1194–1203.

Dumitru, R., Navarathna, D.H., Semighini, C.P., Elowsky, C.G., Dumitru, R.V., Dignard, D., *et al.* (2007) In vivo and in vitro anaerobic mating in Candida albicans. *Eukaryot Cell* **6:** 465–472.

Forman, H.J., and Torres, M. (2002) Reactive oxygen species and cell signaling: respiratory burst in macrophage signaling. *Am J Respir Crit Care Med* **166:** S4–S8.

Fradin, C., De Groot, P., MacCallum, D., Schaller, M., Klis, F., Odds, F.C., and Hube, B. (2005) Granulocytes govern the transcriptional response, morphology and proliferation of *Candida albicans* in human blood. *Mol Microbiol* **56:** 397–415.

Gantner, B.N., Simmons, R.M., Canavera, S.J., Akira, S., and Underhill, D.M. (2003) Collaborative induction of inflammatory responses by dectin-1 and Toll-like receptor 2. *J Exp Med* **197:** 1107–1117.

Gantner, B.N., Simmons, R.M., and Underhill, D.M. (2005) Dectin-1 mediates macrophage recognition of *Candida albicans* yeast but not filaments. *Embo J* **24:** 1277–1286.

George-Chandy, A., Nordstrom, I., Nygren, E., Jonsson, I.M., Postigo, J., Collins, L.V., and Eriksson, K. (2008) Th17 development and autoimmune arthritis in the absence of reactive oxygen species. *Eur J Immunol* **38:** 1118–1126.

Gillum, A.M., Tsay, E.Y., and Kirsch, D.R. (1984) Isolation of the *Candida albicans* gene for orotidine-5′-phosphate decarboxylase by complementation of *S. cerevisiae ura3* and *E. coli pyrF* mutations. *Mol Gen Genet* **198:** 179–182.

Gow, N.A., Netea, M.G., Munro, C.A., Ferwerda, G., Bates, S., Mora-Montes, H.M., *et al.* (2007) Immune recognition of *Candida albicans* beta-glucan by dectin-1. *J Infect Dis* **196:** 1565–1571.

Hampton, M.B., Kettle, A.J., and Winterbourn, C.C. (1998) Inside the neutrophil phagosome: oxidants, myeloperoxidase, and bacterial killing. *Blood* **92:** 3007–3017.

Hume, D.A., and Gordon, S. (1983) Optimal conditions for proliferation of bone marrow-derived mouse macrophages in culture: the roles of CSF-1, serum, Ca2+, and adherence. *J Cell Physiol* **117:** 189–194.

Hwang, C.S., Rhie, G.E., Oh, J.H., Huh, W.K., Yim, H.S., and Kang, S.O. (2002) Copper- and zinc-containing superoxide dismutase (Cu/ZnSOD) is required for the protection of *Candida albicans* against oxidative stresses and the expression of its full virulence. *Microbiology* **148:** 3705–3713.

Hwang, C.S., Baek, Y.U., Yim, H.S., and Kang, S.O. (2003) Protective roles of mitochondrial manganese-containing superoxide dismutase against various stresses in *Candida albicans*. *Yeast* **20:** 929–941.

Inaba, K., Inaba, M., Romani, N., Aya, H., Deguchi, M., Ikehara, S., *et al.* (1992) Generation of large numbers of dendritic cells from mouse bone marrow cultures supplemented with granulocyte/macrophage colony-stimulating factor. *J Exp Med* **176:** 1693–1702.

Jouault, T., El Abed-El Behi, M., Martinez-Esparza, M., Breuilh, L., Trinel, P.A., Chamaillard, M., *et al.* (2006) Specific recognition of *Candida albicans* by macrophages requires galectin-3 to discriminate *Saccharomyces cerevisiae* and needs association with TLR2 for signaling. *J Immunol* **177:** 4679–4687.

Kaiser, C., Michaelis, S., and Mitchell, A. (1994) *Methods in Yeast Genetics: A Laboratory Course Manual*. New York, NY: Cold Spring Harbor Laboratory Press.

Kobayashi, T., Robinson, J.M., and Seguchi, H. (1998) Identification of intracellular sites of superoxide production in stimulated neutrophils. *J Cell Sci* **111:** 81–91.

© 2008 The Authors
Journal compilation © 2008 Blackwell Publishing Ltd,

Kren, A., Mamnun, Y.M., Bauer, B.E., Schuller, C., Wolfger, H., Hatzixanthis, K., *et al.* (2003) War1p, a novel transcription factor controlling weak acid stress response in yeast. *Mol Cell Biol* **23:** 1775–1785.

Kvaal, C., Lachke, S.A., Srikantha, T., Daniels, K., McCoy, J., and Soll, D.R. (1999) Misexpression of the opaque-phase-specific gene *PEP1* (*SAP1*) in the white phase of *Candida albicans* confers increased virulence in a mouse model of cutaneous infection. *Infect Immun* **67:** 6652–6662.

Lan, C.Y., Newport, G., Murillo, L.A., Jones, T., Scherer, S., Davis, R.W., and Agabian, N. (2002) Metabolic specialization associated with phenotypic switching in *Candida albicans*. *Proc Natl Acad Sci USA* **99:** 14907–14912. Epub 12002 October 14923.

Li, Y., Zhu, H., Kuppusamy, P., Roubaud, V., Zweier, J.L., and Trush, M.A. (1998) Validation of lucigenin (bis-N-methylacridinium) as a chemilumigenic probe for detecting superoxide anion radical production by enzymatic and cellular systems. *J Biol Chem* **273:** 2015–2023.

Lundqvist, H., and Dahlgren, C. (1996) Isoluminol-enhanced chemiluminescence: a sensitive method to study the release of superoxide anion from human neutrophils. *Free Radic Biol Med* **20:** 785–792.

Mansour, M.K., and Levitz, S.M. (2002) Interactions of fungi with phagocytes. *Curr Opin Microbiol* **5:** 359–365.

Marcil, A., Gadoury, C., Ash, J., Zhang, J., Nantel, A., and Whiteway, M. (2008) Analysis of *PRA1* and its relationship to *Candida albicans*- macrophage interactions. *Infect Immun* **76:** 4345–4358.

Martchenko, M., Alarco, A.M., Harcus, D., and Whiteway, M. (2004) Superoxide dismutases in *Candida albicans*: transcriptional regulation and functional characterization of the hyphal-induced *SOD5* gene. *Mol Biol Cell* **15:** 456–467.

Morgenstern, D.E., Gifford, M.A., Li, L.L., Doerschuk, C.M., and Dinauer, M.C. (1997) Absence of respiratory burst in X-linked chronic granulomatous disease mice leads to abnormalities in both host defense and inflammatory response to *Aspersillus fumigatus*. *J Exp Med* **185:** 207–218.

Nauseef, W.M. (2004) Assembly of the phagocyte NADPH oxidase. *Histochem Cell Biol* **122:** 277–291.

Netea, M.G., Brown, G.D., Kullberg, B.J., and Gow, N.A. (2008) An integrated model of the recognition of Candida albicans by the innate immune system. *Nat Rev Microbiol* **6:** 67–78.

Noble, S.M., and Johnson, A.D. (2005) Strains and strategies for large-scale gene deletion studies of the diploid human fungal pathogen *Candida albicans*. *Eukaryot Cell* **4:** 298–309.

Pfaller, M.A., and Diekema, D.J. (2007) Epidemiology of invasive candidiasis: a persistent public health problem. *Clin Microbiol Rev* **20:** 133–163.

Piddington, D.L., Fang, F.C., Laessig, T., Cooper, A.M., Orme, I.M., and Buchmeier, N.A. (2001) Cu, Zn superoxide dismutase of *Mycobacterium tuberculosis* contributes to survival in activated macrophages that are generating an oxidative burst. *Infect Immun* **69:** 4980–4987.

Ramirez-Zavala, B., Reuss, O., Park, Y.N., Ohlsen, K., and Morschhauser, J. (2008) Environmental induction of white-opaque switching in *Candida albicans*. *PLoS Pathog* **4:** e1000089.

Reuss, O., Vik, A., Kolter, R., and Morschhauser, J. (2004) The SAT1 flipper, an optimized tool for gene disruption in *Candida albicans*. *Gene* **341:** 119–127.

Richard, M.L., and Plaine, A. (2007) Comprehensive analysis of glycosylphosphatidylinositol-anchored proteins in *Candida albicans*. *Eukaryot Cell* **6:** 119–133.

Rocha, C.R., Schroppel, K., Harcus, D., Marcil, A., Dignard, D., Taylor, B.N., *et al.* (2001) Signaling through adenylyl cyclase is essential for hyphal growth and virulence in the pathogenic fungus *Candida albicans*. *Mol Biol Cell* **12:** 3631–3643.

Romani, L. (2004) Immunity to fungal infections. *Nat Rev Immunol* **4:** 1–13.

Rubin-Bejerano, I., Abeijon, C., Magnelli, P., Grisafi, P., and Fink, G.R. (2007) Phagocytosis by human neutrophils is stimulated by a unique fungal cell wall component. *Cell Host Microbe* **2:** 55–67.

Savina, A., Jancic, C., Hugues, S., Guermonprez, P., Vargas, P., Moura, I.C., *et al.* (2006) NOX2 controls phagosomal pH to regulate antigen processing during crosspresentation by dendritic cells. *Cell* **126:** 205–218.

Schrenzel, J., Serrander, L., Banfi, B., Nusse, O., Fouyouzi, R., Lew, D.P., *et al.* (1998) Electron currents generated by the human phagocyte NADPH oxidase. *Nature* **392:** 734–737.

Stockinger, S., Materna, T., Stoiber, D., Bayr, L., Steinborn, R., Kolbe, T., *et al.* (2002) Production of type I IFN sensitizes macrophages to cell death induced by *Listeria monocytogenes*. *J Immunol* **169:** 6522–6529.

Taylor, P.R. (2007) Dectin-1 is required for [beta]-glucan recognition and control of fungal infection. *Nat Immunol* **8:** 31–38.

Teixeira, H.D., Schumacher, R.I., and Meneghini, R. (1998) Lower intracellular hydrogen peroxide levels in cells overexpressing CuZn-superoxide dismutase. *Proc Natl Acad Sci USA* **95:** 7872–7875.

Watanabe, K., Kagaya, K., Yamada, T., and Fukazawa, Y. (1991) Mechanism for candidacidal activity in macrophages activated by recombinant gamma interferon. *Infect Immun* **59:** 521–528.

Yeung, T., Touret, N., and Grinstein, S. (2005) Quantitative fluorescence microscopy to probe intracellular microenvironments. *Curr Opin Microbiol* **8:** 350–358.

Supporting information

Additional supporting information may be found in the online version of this article.

Please note: Wiley-Blackwell are not responsible for the content or functionality of any supporting materials supplied by the authors. Any queries (other than missing material) should be directed to the corresponding author for the article.

© 2008 The Authors
Journal compilation © 2008 Blackwell Publishing Ltd,

Table S1: Oligonucleotide primers used in this study

Primers to generate deletion cassettes – direction 5' → 3'	
M5	ccgctgctaggcgcgccgtgACCAGTGTGATGGATATCTGC
M3	gcagggatgcggccgctgacAGCTCGGATCCACTAGTAACG
55_caSOD1s	CAAGTCCATCTAAAATGTGTTTG
53_caSOD1as	cacggcgcgcctagcagcggCATTTTTAATTATATATATGTTGATAATTGAAT
35_caSOD1s	gtcagcggccgcatccctgcTGAATAGATGAGCCAAGATTGC
33_caSOD1as	ATGTGGGCATTATATTTGAACC
55_caSOD2s	gtgtgatttctcacacaccaatc
53_caSOD2as	cacggcgcgcctagcagcggCATTGTTAATTATAGTACAATTGTCTTTAAT
35_caSOD2s	gtcagcggccgcatccctgcTAAGTTACTGGACAAAAGTCAAGTACA
33_caSOD2as	GAGTTCTAAACAATGGTACTTATCCTAC
55_caSOD3s	AGGGAAACTTACCATGAATGTG
53_caSOD3as	cacggcgcgcctagcagcggCATGGCGTGGTTGATAAGAG
35_caSOD3s	gtcagcggccgcatccctgcGATACTCTGCGTAACATTGTGTGTA
33_caSOD3as	CCAATTAACCCTTCGGTAGTG
55_caSOD4s	CAGCATAAACCAAATAACATTACTC
53_caSOD4as	cacggcgcgcctagcagcggCATAGTAATAGTGTGTGTGATTAAAAATC
35_caSOD4s	gtcagcggccgcatccctgcTAGATAGAGAATAACTAGAACAATCAAATG
33_caSOD4as	CTTGAAAAAATATCATTAAGTGAACG
55_caSOD5s	CACGGCTGAGAGGTCACTAC
53_caSOD5as	cacggcgcgcctagcagcggCATGATGAATGGTAAGTTAGATTG
35_caSOD5s	gtcagcggccgcatccctgcAGATGAGCCATTTTACTTATTGTG
33_caSOD5as	CATGTCTGTATAGGATAATGAAAGTG
55_caSOD6s	GCTTGGTAGTGGTGGACTAGAG
53_caSOD6as	cacggcgcgcctagcagcggCATCTTGCTGAGACGTTTAGTG
35_caSOD6s	gtcagcggccgcatccctgcTAGTTGAACATAAATACTCTCACCC
33_caSOD6as	CGATTCAGAGCTTGAGATTGAG
Control primers for verifying genomic deletions – direction 5' → 3'	
5_SOD1s	CATTCAAAGACAGGTTGAATACAAC
3_SOD1as	CAACAAAGTGATATTAATCGAATGAC
5_SOD2s	CCAAATAGACATAAATTTCGGTTC
3_SOD2as	TCAATCATAATGTTTATAGGACTGG
5_SOD3s	ATCTACTGGTATGAAGATTTGGTTAG
3_SOD3as	CAAAGCTCCAATCAATCCAAG
5_SOD4s	AACCTCCTAAACGCAACTGC
3_SOD4as	GAACCAAGGAAGCATTGCC
5_SOD5s	CGGCAATTGATTACGACAAG
3_SOD5as	CTCACGTTTGCTTCTCGC
5_SOD6s	GAGGCATCTGTTGCTTCCAC
3_SOD6as	CGGTAGACTATTTGTCATTGGTG
Leu2as	GGAAACATTCACACAACCTGGG
Leu1s	ccggtttacttggatcttcgg
His2as	CCCATACTCCTCACACAACAATCC
His1s	gccatgagcaccataaggacg
Primers to generate deletion cassettes with pSF2a SAT1-FLP – direction 5' → 3'	
55_SacI_SOD4s	GAgagctcCAGCATAAACCAAATAACATTACTC
53_SOD4_NotIas	GAgcggccgcCATAGTAATAGTGTGTGTGATTAAAAATC

35_ApaI_SOD4s	GAgggcccTAGATAGAGAATAACTAGAACAATCAAATG
33_SOD4_KpnIas	GAggtaccCTTGAAAAAATATCATTAAGTGAACG
55_SacI_SOD5s	GAgagctcCACGGCTGAGAGGTCACTAC
53_SOD5_NotIas	GAgcggccgcCATGATGAATGGTAAGTTAGATTG
35_ApaI_SOD5s	GAgggcccAGATGAGCCATTTTACTTATTGTG
33_SOD5_KpnIas	GAggtaccCATGTCTGTATAGGATAATGAAAGTG
55_SacI_SOD6s	GAgagctcGCTTGGTAGTGGTGGACTAGAG
53_SOD6_NotIas	GAgcggccgcCATCTTGCTGAGACGTTTAGTG
35_ApaI_SOD6s	GAgggcccTAGTTGAACATAAATACTCTCACCC
33_SOD6_KpnIas	GAggtaccCGATTCAGAGCTTGAGATTGAG
SAT108as	CTCCATCACCCAGTTTAGTTGTACC
SAT101s	CTCAAGTCTCGAACGAAACAG
Primers for genomic reintegration cassettes at original loci – direction 5' → 3'	
33_SOD5_PvuIs	GAcgatcgCATGTCTGTATAGGATAATGAAAGTG
SOD5_ct_NotAs	GAgcggccgcATTTTATTTTTCTTTTTTAAATCAAGGC
Primers for amplifying probes for Northern analysis – direction 5' → 3'	
Sod5_49s	GATGCACCAATCTCAACTG
Sod5_676as	CAGCAATGACACCAACTAC
Sod4_9s	CTTGTCTATTATTTCAATTGTTGC
Sod4_699as	CTAAATTAAAGCAGCAACAACAC
ACT1_s	ATGGACGGTGGTATGTTTTAGT
ACT1_as	CAGAAGATTGAGAAGAAGTTTGC

Table S2: Plasmids used in this study

Plasmids	Relevant inserts and cloning sites	References
pSFS2a-SAT1-FLP		Reuss et al, 2004
pSN40		Noble & Johnson, 2005
pSN51		Noble & Johnson, 2005
pSFS2a-SOD4	*SacI*5'SOD4*NotI*-SAT1-FLP-*ApaI*3'SOD4*KpnI*	This study
pSFS2a-SOD5	*SacI*5'SOD5*NotI*-SAT1-FLP-*ApaI*3'SOD5*KpnI*	This study
pSFS2a-SOD6	*SacI*5'SOD6ct*NotI*-SAT1-FLP-*ApaI*3'SOD6*KpnI*	This study
pSFS2a-SOD5rev	*SacI*5'SOD5ct*NotI*-SAT1-FLP-*ApaI*3'SOD5*PvuI*	This study

Table S3: Fungal strains used in this study

Strains	Short Names	Genotypes	References
SC5314			Gillum, et al, 1984
SN152	*arg4*Δ/Δ *leu2*Δ/Δ *his1*Δ/Δ	*arg4*Δ/*arg4*Δ, *leu2*Δ/*leu2*Δ, *his1*Δ/*his1*Δ, *URA3*/*ura3*Δ	Noble & Johnson, 2005
CA-IF100	*arg4*Δ/Δ *LEU2 HIS1*	*arg4*Δ/*arg4*Δ, *leu2*Δ/*leu2*Δ::*cmLEU2*, *his1*Δ/*his1*Δ::*cdHIS1*, *URA3*/*ura3*Δ,	This study
CA-IF001	*sod1*Δ	SN152, *sod1*Δ::*cmLEU2*/*SOD1*	This study
CA-IF003	*sod1*Δ/Δ	SN152, *sod1*Δ::*cmLEU2*/*sod1*Δ::*CdHIS1*	This study
CA-IF005	*sod2*Δ	SN152, *sod2*Δ::*cmLEU2*/*SOD1*	This study
CA-IF007	*sod2*Δ/Δ	SN152, *sod2*Δ::*cmLEU2*/*sod2*Δ::*CdHIS1*	This study
CA-IF009	*sod3*Δ	SN152, *sod3*Δ::*cmLEU2*/*SOD2*	This study
CA-IF011	*sod3*Δ/Δ	SN152, *sod3*Δ::*cmLEU2*/*sod3*Δ::*CdHIS1*	This study
CA-IF013	*sod4*Δ	SN152, *sod4*Δ::*cmLEU2*/*SOD4*	This study
CA-IF015	*sod4*Δ/Δ	SN152, *sod4*Δ::*cmLEU2*/*sod4*Δ::*CdHIS1*	This study
CA-IF017	*sod5*Δ	SN152, *sod5*Δ::*cmLEU2*/*SOD5*	This study
CA-IF019	*sod5*Δ/Δ	SN152, *sod5*Δ::*cmLEU2*/*sod5*Δ::*CdHIS1*	This study
CA-IF025	*sod5*Δ/*SOD5*	SN152, *sod5*Δ::*cmLEU1*/*sod5*Δ::*CdHIS1*::*SOD5-SAT1-FLP*	This study
CA-IF027	*sod5*Δ/*SOD5*	SN152, *sod5*Δ::*cmLEU1*/*sod5*Δ::*CdHIS1*::*SOD5-FRT*	This study
CA-IF030	*sod5*Δ/Δ *sod4*Δ	SN152, *sod5*Δ::*cmLEU1*/*sod5*Δ::*CdHIS1* *sod4*Δ::*SAT1*-FLP/*SOD4*	This study
CA-IF033	*sod5*Δ/Δ *sod4*Δ	SN152, *sod5*Δ::cm*LEU1*/*sod5*Δ::*CdHIS1* *sod4*Δ::FRT/*SOD4*	This study
CA-IF036	*sod5*Δ/Δ *sod4*Δ/Δ	SN152, *sod5*Δ::cm*LEU1*/*sod5*Δ::*CdHIS1* *sod4*Δ::FRT/*sod4*Δ::*SAT1*-FLP	This study
CA-IF039	*sod4/5*Δ/Δ	SN152, *sod5*Δ::cm*LEU1*/*sod5*Δ::*Cd HIS1* *sod4*Δ::FRT/*sod4*Δ::FRT	This study
CA-IF021	*sod6*Δ	SN152, *sod6*Δ::cm*LEU2*/*SOD6*	This study
CA-IF023	*sod6*Δ/Δ	SN152, *sod6*Δ::cm*LEU1*/*sod6*Δ::Cd*HIS1*	This study
CA-IF043	*sod6*Δ/Δ *sod4*Δ	SN152, *sod6*Δ::cm*LEU1*/*sod6*Δ::Cd*HIS1* *sod4*Δ::*SAT1-FLP*/*SOD4*	This study
CA-IF046	*sod6*Δ/Δ *sod4*Δ	SN152, *sod6*Δ::cm*LEU1*/*sod6*Δ::Cd*HIS1* *sod4*Δ::FRT/*SOD4*	This study
CA-IF049	*sod6*Δ/Δ *sod4*Δ/Δ	SN152, *sod6*Δ::cm*LEU1*/*sod6*Δ::Cd*HIS1* *sod4*Δ::FRT/*sod4*Δ::*SAT1-FLP*	This study
CA-IF051	*sod4/6*Δ/Δ	SN152, *sod6*Δ::cm*LEU*1/*sod6*Δ::Cd*HIS1* *sod4*Δ::FRT/*sod4*Δ::FRT	This study
CA-IF054	*sod5*Δ	SC5314, *sod5*Δ::*SAT1*-FLP/*SOD5*	This study
CA-IF057	*sod5*Δ	SC5314, *sod5*Δ::FRT/*SOD5*	This study
CA-IF060	*sod5*Δ/Δ	SC5314, *sod5*Δ::FRT/ *sod5*Δ::*SAT1*-FLP	This study
CA-IF063	*sod5*Δ/Δ	SC5314, *sod5*Δ::FRT/*sod5*Δ::FRT	This study
CA-IF067	*sod5*Δ/Δ *sod4*Δ/Δ *sod6*Δ	SN152, *sod5*Δ::cm*LEU1*/*sod5*Δ::*Cd HIS1* *sod4*Δ::FRT/*sod4*Δ::FRT *sod6*Δ::FRT/*SOD6*	This study
CA-IF070	*sod5*Δ/Δ *sod4*Δ/Δ *sod6*Δ/Δ	SN152, *sod5*Δ::cm*LEU1*/*sod5*Δ::*Cd HIS1* *sod4*Δ::FRT/*sod4*Δ::FRT *sod6*Δ::FRT/*sod6*Δ::FRT	This study

III.2 PRRs and their adaptor proteins in the activation of the respiratory burst.

When phagocytic cells encounter and phagocytose pathogenic microbes, the so-called "oxidative burst" is activated. ROS production is mediated by the recruitment of cytosolic subunits of the NADPH oxidase to the phagosomal membrane to generate a functional NADPH oxidase (Babior, 2004). Fc receptors (FcRs) and integrins can trigger ROS production in response to microbial pathogens (Berton and Lowell, 1999; Ravetch and Bolland, 2001). For the initiation of downstream events, an immunoreceptor tyrosine-based activation motif (ITAM) is essential. FcRs contain an ITAM in their cytoplasmic tail or require the ITAM-bearing adapter Fc-gamma receptor (FcγR) for surface expression, phagocytosis, and ROS production (Swanson and Hoppe, 2004). Integrins trigger Syk phosphorylation and ROS production in neutrophils through the ITAM-containing adapters DAP12 and Fcγ (Mocsai et al., 2006). Activation of an ITAM-associated receptor leads to phosphorylation of the tyrosine residues within the ITAM motif by Src family kinases (SFK). This leads to the recruitment and activation of Syk family kinases and induces signalling through multiple downstream pathways, including phosphatidylinositol (PI) 3-kinase and protein kinase C (PKC) activation (Swanson and Hoppe, 2004; Underhill and Goodridge, 2007).

The pattern recognition receptor Dectin-1 recognises β-(1,3)-glucans in the cell wall of yeasts (Brown, 2006). Dectin-1 contains a non-canonical ITAM motif in the cytoplasmic tail, and activation of Dectin-1 leads to Syk phosphorylation independently of DAP12 and FcγR, resulting in activation of ROS production (Rogers et al., 2005; Underhill et al., 2005). In bone marrow derived macrophages (BMDMs) Dectin-1 recognises zymosan and the yeast form of *C. albicans,* thereby inducing ROS production in a TLR2-independent manner (Gantner et al., 2003; Gantner et al., 2005). Conflicting data were reported by a later study, demonstrating that Dectin-$1^{-/-}$ alveolar macrophages are producing the same amount of ROS as wild type cells when stimulated with *C. albicans*. In contrast, *Pneumocystis carni* and zymosan-induced ROS production requires Dectin-1 (Saijo et al., 2007). In mouse mast cells, Dectin-1 is also involved in zymosan-induced intracellular ROS production (Yang and Marshall, 2009).

Toll-like receptors (TLRs) have been implicated in ROS response and the MyD88 adaptor is also needed for the activation of the NADPH oxidase in response to gram-negative bacteria (Laroux et al., 2005; Ryan et al., 2004). The roles of specific TLRs in NADPH oxidase assembly and ROS generation appear to be cell-specific. For example, TLR4 is required for NADPH oxidase

activation in human neutrophils infected with serovar Typhimurium (van Bruggen et al., 2007), but not in mouse peritoneal macrophages (Laroux et al., 2005). Additionally, the TLR4 ligand lipopolysaccharide (LPS) does not induce detectable levels of ROS in murine BMDMs (Charles et al., 2008). ROS production during *M. tuberculosis* infection was recently shown to be dependent on the interaction of TLR2 and gp91phox (Yang et al., 2009).

The integrin CD11b/CD18 (CR3) mediates ROS production in mouse and human macrophages in response to oxidised LDL (Husemann et al., 2001). Superoxide production of human neutrophils in response to either zymosan or beta-glucan particles is also CR3-dependent (Ross et al., 1987). More specifically, in human neutrophils, Cd11b seems to important for ROS production in response to β-1,6-glucans (Rubin-Bejerano et al., 2007). Furthermore, it was shown that costimulation of CR3 and the FcRγ with opsonised zymosan and IgG enhances the superoxide production in bovine neutrophils (Nagahata et al., 2007).

In neutrophils, carcinoembryonic antigen-related cellular adhesion molecule 3 (CEACAM3) has been identified as an ITAM-containing innate immune receptor for *Neisseria gonorrhoeae* that regulates *Neisseria*-induced ROS via a Syk-dependent mechanism (Sarantis and Gray-Owen, 2007).

To elucidate whether or not Dectin-1 is involved in *C. albicans*-induced ROS production in BMDMs and if other receptors are engaged in this immune response, I used specific inhibitors or blocking antibodies and innate immune cells differentiated from the bone marrow of knock-out mice lacking different PPRs. To investigate the mechanisms of ROS induction in innate immune cells elicited by *C. albicans*, we used an *in vitro* cell culture model of primary mouse BMDMs co-cultured with *C. albicans* or zymosan, and measured total ROS production using a luminol-dependent, chemiluminescence assay in the presence of horseradish peroxidase (HRP) (Dahlgren and Karlsson, 1999). To visualize intracellular ROS production, we pre-loaded BMDMs with the non-fluorescent dye H_2DCF-DA, which cannot cross cellular compartments after esterase cleavage. Upon oxidation by ROS, H_2DCF-DA is converted to the fluorescent product 2′-7′-dichlorofluorescein (DCF). A limited permeability of DCF retains it preferentially at the site where it was generated (Yeung et al., 2005). Additionally, I have set up siRNA-based knock down assays to search for new pathways that might be responsible for *Candida*-induced ROS in BMDMs.

III.2.1 TLRs are not involved in *C. albicans* or zymosan-induced ROS production

Phagocytes of the innate immune system such as macrophages and neutrophils trigger ROS production in response to various microbial pathogens reviewed in (El-Benna et al., 2005).

To investigate a possible role of TLRs in *C. albicans*-induced ROS release, we stimulated BMDMs derived from TLR2$^{-/-}$, TLR4$^{-/-}$ and MyD88$^{-/-}$ mice with zymosan or *C. albicans*. To neutralise the stimulatory effects of potential endotoxin contamination in the zymosan or *C. albicans* preparation, we analysed the response in the presence of polymyxin B, an antibiotic which complexes LPS and neutralises its potential biological activity (Cardoso et al., 2007). The stimulation of TLR2, TLR4 or MyD88 knock-out BMDMs with *C. albicans*, or zymosan did not

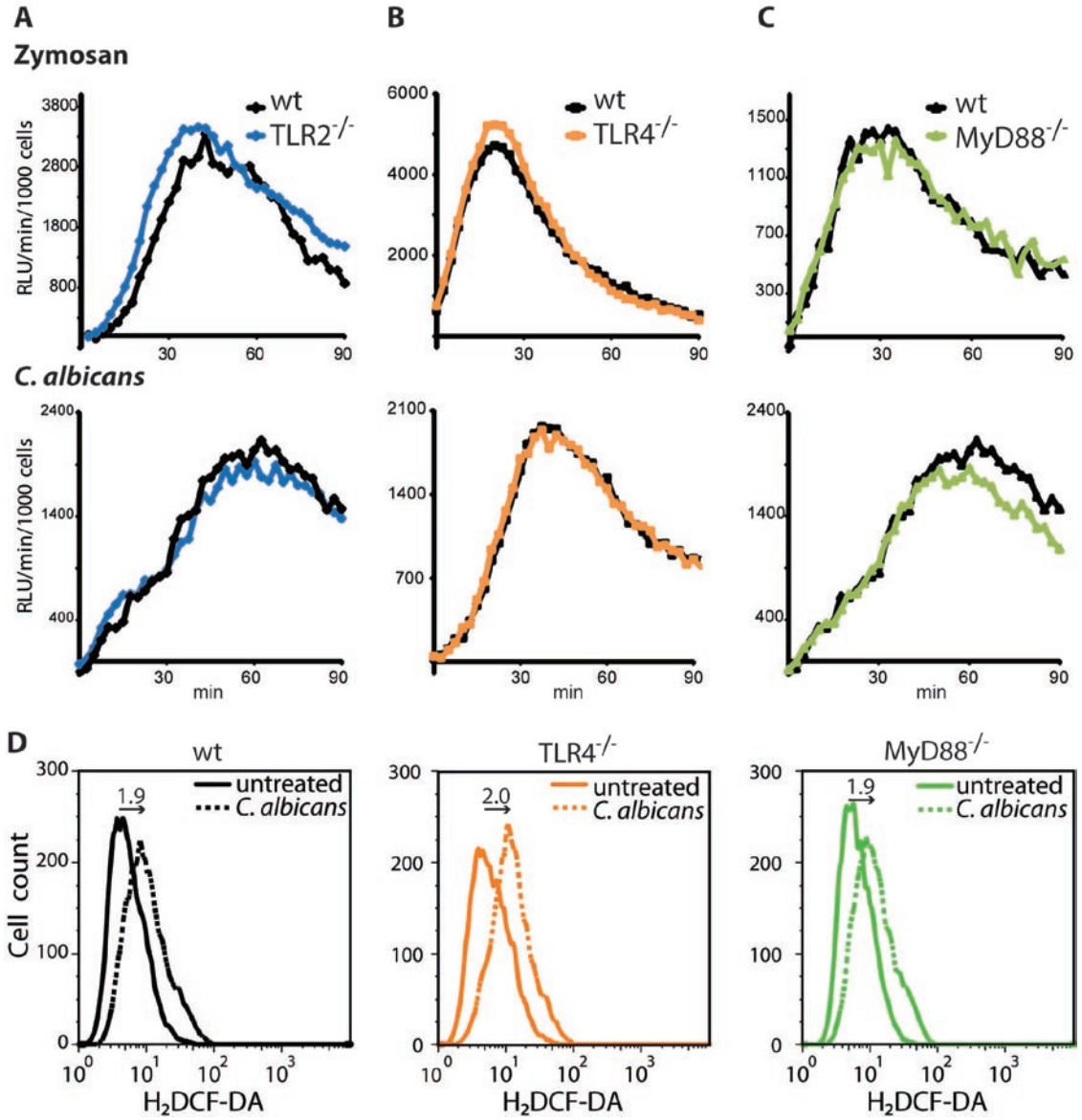

Figure III.1: TLRs are not involved in zymosan or *C. albicans* induced ROS signalling.
A–C. ROS measurement by luminol-dependent chemiluminescence at 37°C in 2.5 min intervals over a 90 min period [relative luciferase units (RLU) min^{-1} per 1000 immune cells], RLU of untreated BMDMs were substracted from stimulated BMDMs. **A.** Stimulation of wild type (C57BL/6) or TLR2$^{-/-}$ BMDMs with either zymosan (100µg/ml) (top) or *C. albicans* (MOI 5:1) (bottom) **B.** Stimulation of wild type(C57BL/6) or TLR4$^{-/-}$ BMDMs with either zymosan (100µg/ml) (top) or *C. albicans* (MOI 5:1) (bottom) **C.** Stimulation of wild type(C57BL/6) or MyD88$^{-/-}$ BMDMs with either zymosan (100µg/ml) (top) or *C. albicans* (MOI 5:1) (bottom) **D.** Intracellular ROS production of wild type(C57BL/6) (left), TLR4$^{-/-}$ (middle) and MyD88$^{-/-}$ (right) BMDMs in response to *C. albicans* after 30 min of infection was measured by FACS analysis using H2DCF-DA staining of BMDMs. Numbers above arrows indicate fold increase in H2DCF-DA fluorescence after stimulation compared to unstimulated fluorescence. **A–C.** Results of one experiment per condition are shown. All data were reproduced in at least three (A-C) or two (D) independent experiments.

show any changes in total ROS levels over a period of 90 min, when compared to wild type BMDMs (Figure III.1 A-C). These results are in line with previous studies showing that in mouse peritoneal macrophages, zymosan-induced ROS production is both MyD88- and TLR2-independent (Gantner et al., 2003), also in alveolar macrophages, *C. albicans*-induced ROS is MyD88 independent (Saijo et al., 2007). Similarly, the production of intracellular ROS by BMDMs lacking TLR4 or MyD88 was unchanged when compared to wild type BMDMs stimulated with *C. albicans* (Figure III.1 D). These results demonstrate that TLR2 and TLR4 are not involved in ROS transduction in BMDMs when stimulated with zymosan or *C. albicans*. Since MyD88 is the adaptor protein of all known TLRs (except TLR3) these results also indicate that other TLR family members do not engage in BMDM ROS production when stimulated with zymosan or *C. albicans.*

III.2.2 *C. albicans* ROS induction requires Src/Syk kinases activation but not Dectin-1

Macrophages, DCs and mouse mast cells treated with zymosan release ROS via stimulation of the beta-glucan receptor Dectin-1 (Saijo et al., 2007; Taylor et al., 2007; Underhill et al., 2005; Yang and Marshall, 2009). ROS production is further dependent on downstream signalling events through phosphorylation of the ITAM-like domain of the cytoplasmic tail of Dectin-1 by Src kinases. This phosphorylation leads to the phosphorylation and activation of the adaptor kinase Syk (Underhill and Goodridge, 2007; Underhill et al., 2005). Concerning *C. albicans*-induced ROS production and the involvement of Dectin-1, the existing literature is conflicting. An anti-Dectin-1 blocking antibody or laminarin - a non signalling agonist of Dectin-1 - showed that the yeast form *C. albicans* induced ROS via the recognition of Dectin-1 in BMDMs (Gantner et al., 2005). In contrast, Dectin-1 deficient alveolar macrophages produce the same amount of ROS as wild type cells when treated with *C. albicans* (Saijo et al., 2007). However, ROS is reduced when the knock-out macrophages are infected with *P. carni*. These differences might be caused by the different types of macrophages, different experimental conditions or *C. albicans* strains used (Gantner et al., 2005; Saijo et al., 2007).

To clarify the role of Dectin-1 in *C. albicans*-induced ROS production, we first investigated the signalling of Dectin-1 and zymosan in our experimental system. Therefore, we stimulated untreated or laminarin-pre-treated BMDMs with zymosan or curdlan, and confirmed that both zymosan- and curdlan-induced ROS in BMDMs was inhibited up to 90 % by laminarin (Figure III.2 A + B). Furthermore, blocking Src and Syk kinases with the inhibitors PP2 and R406 (Braselmann et al., 2006), respectively, substantially reduced ROS production. By contrast, PP3, the inactive

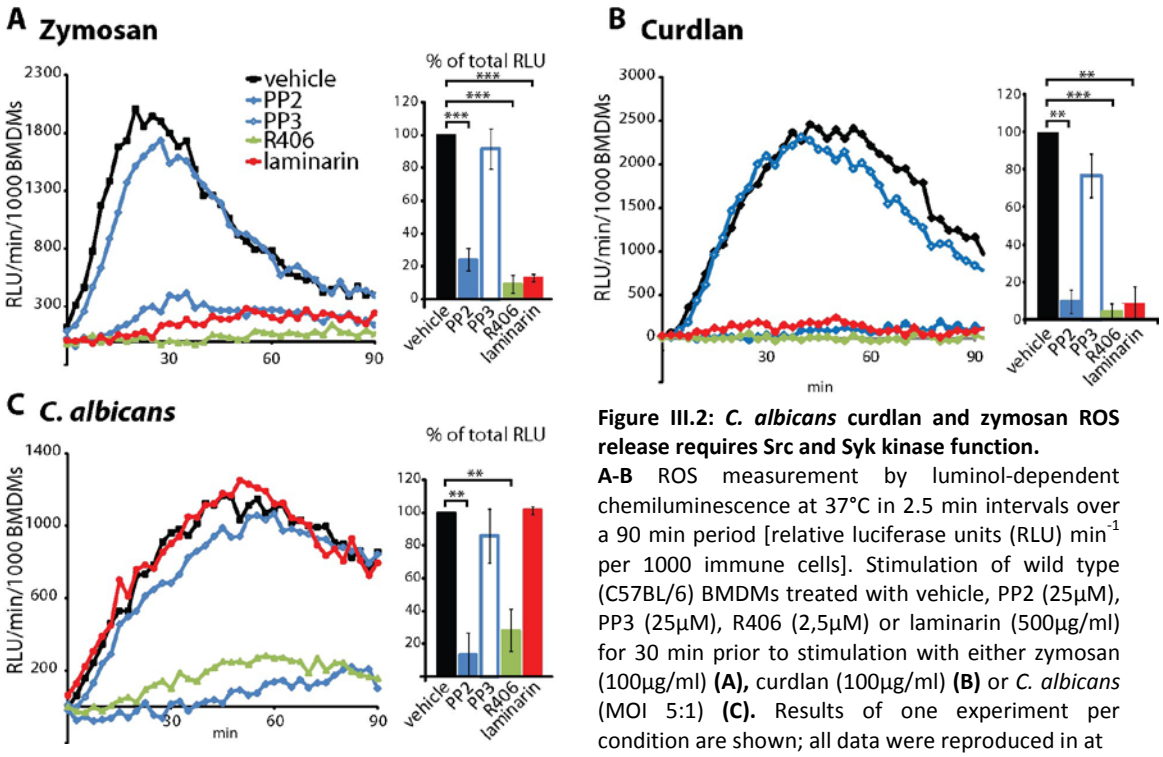

Figure III.2: *C. albicans* curdlan and zymosan ROS release requires Src and Syk kinase function.
A-B ROS measurement by luminol-dependent chemiluminescence at 37°C in 2.5 min intervals over a 90 min period [relative luciferase units (RLU) min^{-1} per 1000 immune cells]. Stimulation of wild type (C57BL/6) BMDMs treated with vehicle, PP2 (25µM), PP3 (25µM), R406 (2,5µM) or laminarin (500µg/ml) for 30 min prior to stimulation with either zymosan (100µg/ml) **(A),** curdlan (100µg/ml) **(B)** or *C. albicans* (MOI 5:1) **(C).** Results of one experiment per condition are shown; all data were reproduced in at least three experiments (left). RLUs of untreated BMDMs were substracted from stimulated BMDMs. The average of three independent experiments is presented and total ROS production by vehicle treated BMDMs in the first 90 min were set to 100%. ** p<0,01 ***p <0,001.

form of PP2, did not have an effect on ROS response. Thus, we verified that zymosan-induced ROS is dependent on Dectin-1 stimulation and proceeds through Src and Syk kinase activation (Figure III.2 A + B). Inhibiting Src and Syk also significantly reduced *C. albicans*-induced ROS production. However, blocking Dectin-1 with laminarin failed to reduce ROS (Figure III.2 C).

To further substantiate our findings that Dectin-1 is not involved in *C. albicans*-stimulated ROS, we generated BMDMs from Dectin-1 deficient bone marrow and the corresponding wild type mice (kindly provided by G. Brown) (Taylor et al., 2007). Dectin-1 deficient BMDMs did not produce ROS in response to zymosan stimulation. However, in response to *C. albicans* BMDMs still released 80% of the ROS produced by the corresponding wild type control BMDMs (Figure III.3 A).

During the activation of the NADPH oxidase, the cytosolic subunits get phosphorylated and migrate to the subunits located at the membrane to assemble the active NAPDH oxidase (El-Benna et al., 2009). p40phox is weakly phosphorylated during activation (Bouin et al., 1998). The role of the phosphorylation is still unclear, since it was reported to play both inhibitory and activatory roles during NADPH oxidase assembly (Kuribayashi et al., 2002; Lopes et al., 2004; Sathyamoorthy et al., 1997). Upon stimulation of wild type BMDMs with zymosan or *C. albicans,* p40phox was phosphorylated at T154 (Figure III.3 B). By contrast, in zymosan-stimulated dectin-

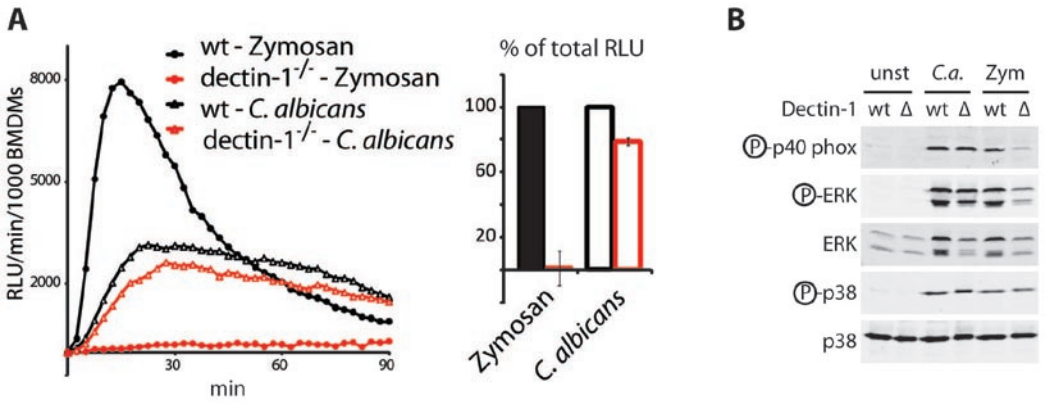

Figure III.3: Zymosan but not live *C. albicans*-induced ROS production is dependent on Dectin-1.
A ROS measurement by luminol-dependent chemiluminescence at 37°C in 2.5 min intervals over a 90 min period [relative luciferase units (RLU) min^{-1} per 1000 immune cells]. The average of two independent experiments is presented and total ROS production by wild type BMDMs in the first 90 min was set as 100%. Stimulation of wild type (129/Sv) (wt black) or *clec7a*$^{-/-}$(Dectin-1$^{-/-}$ red) BMDMs with either zymosan (100µg/ml) or *C. albicans* MOI (5:1), RLUs of untreated BMDMs were substracted from stimulated BMDMs. **B.** Wild type (129/Sv) (wt) or *clec7a*$^{-/-}$ (dectin-1$^{-/-}$) (Δ) BMDMs were left untreated or treated for 30 min with either zymosan (100µg/ml) or live *C. albicans* (MOI 5:1). Phosphorylated p40phox, ERK and p38, were detected by immunoblotting and the blots were re-probed with total ERK and p38 antibodies to assess equal loading between lanes.

1$^{-/-}$ BMDMs, p40phox phosphorylation was undetectable, but was still observed after *C. albicans* stimulation (Figure III.3 B). Similarly, zymosan, but not *C. albicans,* induced ERK1 and ERK2 phosphorylation, which was partially Dectin-1 dependent. On the other hand, p38 phosphorylation was not reduced when Dectin-1 was missing upon zymosan or *C. albicans* stimulation (Figure III.3 B).

Taken together, our data demonstrate that Dectin-1 plays only a limited role - if any - in *C. albicans*-stimulated ROS production, while being the key receptor for zymosan-induced oxidative burst. Furthermore, these results suggest that activation of ERK1/2 and p38 MAPK cascades are partly dependent on Dectin-1 in BMDMs stimulated with zymosan, but are activated independently of Dectin-1 when BMDMs are stimulated with *C. albicans*.

III.2.3 Heat-killed *C. albicans* induces ROS and MAPK signalling via Dectin-1

Previous reports have shown that Dectin-1 recognises β-glucans in the yeast form but not the hyphal form of *C. albicans* (Gantner et al., 2005). We thus used an anti-Dectin-1 blocking antibody to block the receptor. As in previous experiments, blocking Dectin-1 significantly reduced zymosan-induced ROS production by 60% (Figure III.4 A). Likewise, curdlan (β-(1,3)-glucan chains) induced ROS production is Dectin-1 dependent (Figure III.2 B). However, ROS induced by live *C. albicans* in either yeast or hyphal form was not dependent on Dectin-1 (Figure III.4 B+D).

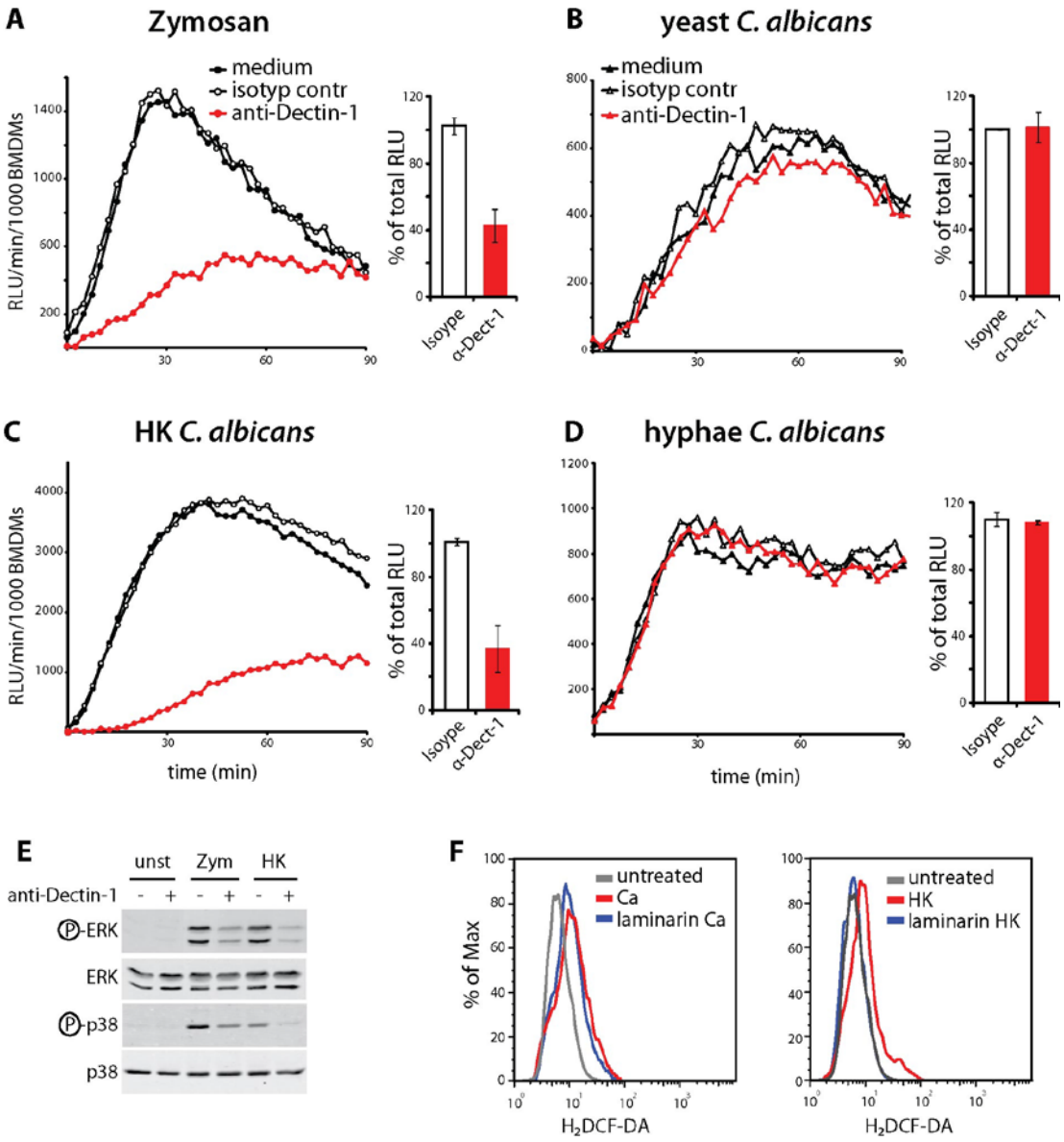

Figure III.4: Heat-killed *C. albicans* and zymosan but not live *C. albicans* signal via Dectin-1.
A-D. ROS measurement by luminol-dependent chemiluminescence at 37°C in 2.5 min intervals over a 90 min period [relative luciferase units (RLU) min^{-1} per 1000 immune cells] (left) The average of three independent experiments is presented and total ROS production in the first 90 min, isotyp control treated BMDMs were set as 100% (right). Stimulation of wt (C57BL/6) BMDMs untreated or pre-treated with anti-Dectin-1 2A11 or IgG2aκ isotype control (10µg/ml) for 30 min prior to stimulation with either zymosan (100µg/ml) **(A)**, live *C. albicans* in yeast form (MOI 5:1) **(B)**, heat-killed *C. albicans* in yeast form (MOI 5:1) **(C),** or live *C. albicans* in hyphae form (6µg dry weight/well) **(D)**. **E.** Wild type (C57BL/6) BMDMs pretreated with anti-Dectin-1 2A11 or IgG2aκ isotype control (10µg/ml) for 30 min were either untreated or treated for 30 min with zymosan (100µg/ml) or HK *C. albicans* (MOI 5:1). Phosphorylated ERK1 and ERK2 and p38 were detected by immunoblotting and the blots were re-probed with total ERK and p38 antibodies to assess equal loading between lanes. **F.** Intracellular ROS production was measured by FACS analysis using H_2DCF-DA staining of BMDMs. BMDMs were either untreated or pre-treated with laminarin (500µg/ml) in response to *C. albicans* live (Ca) or heat-killed (HK) after 45min of infection

Heat-treatment of *C. albicans* has been shown to increase exposure of β-glucans on the cell surface (Wheeler and Fink, 2006). Hence, we used heat-killed *C. albicans* to check whether an unmasked β-glucans would induce ROS via Dectin-1. Indeed, in BMDMs infected with heat-killed *C. albicans,* we observed a 60% reduction of the ROS response when Dectin-1 was blocked with

the neutralising antibodies when compared to the isotype control or untreated BMDMs (Figure III.4 C). In addition, treatment of Dectin-1 blocked BMDMs with heat-killed *C. albicans* reduced ERK1/ERK2 as well as p38 phosphorylation to the same extent as in zymosan-treated cells (Figure III.4 E). Similarly, intracellular ROS staining using H_2DCF-DA revealed that Dectin-1 blocked BMDMs showed a reduced intracellular ROS production when stimulated with heat-killed *C. albicans* but not with live *C. albicans* (Figure III.4 F).

The latter results confirm that the ROS release as well as intracellular ROS production triggered by unmasked β-glucans is Dectin-1-dependent, and demonstrate that neither the hyphal nor the yeast forms of live *C. albicans* induce ROS via Dectin-1.

III.2.4 Dectin-2 is not involved in *C. albicans*- or zymosan-induced ROS production

We have unequivocally shown that Dectin-1 is not the major PRR inducing ROS when macrophages are stimulated with live *C. albicans*. However, the ROS response is dependent on the activation of intracellular Src and Syk kinases, and therefore, most likely proceeds via the activation of an ITAM-signalling motif (Figure III.2). Dectin-2 is a C-type lectin receptor recognising high molecular mannose structures (McGreal et al., 2006). Furthermore, Dectin-2 predominantly recognises the hyphal form of *C. albicans*. Lacking itself an ITAM domain, Dectin-2 couples with FcγR to initiate downstream signalling pathways via the FcγR ITAM domain thereby activating ERK1, ERK2 and p38 MAPK pathways (Robinson et al., 2009; Sato et al., 2006).

To investigate whether Dectin-2 could be the receptor inducing the oxidative burst in response to *C. albicans,* we blocked Dectin-2 with a specific neutralising antibody. However, blocking Dectin-2 failed to reduce the ROS production induced by either zymosan, live or heat-killed *C. albicans* in the yeast form or live *C. albicans* in hyphal form (Figure III.5 A). Nevertheless, after 30 min of infection, there was a high ERK and p38 phosphorylation in BMDMs treated with either zymosan, heat-killed or live *C. albicans* in yeast form. By contrast, *C. albicans* in hyphal form induced only a very weak MAPK response in BMDMs (Figure III.5 B). BMDMs pre-treatment with the anti-Dectin-2 neutralising antibody had no effect on p38 phosphorylation. Conversely ERK phosphorylation was reduced upon stimulation with heat-killed *C. albicans* when Dectin-2 was blocked (Figure III.5.B).

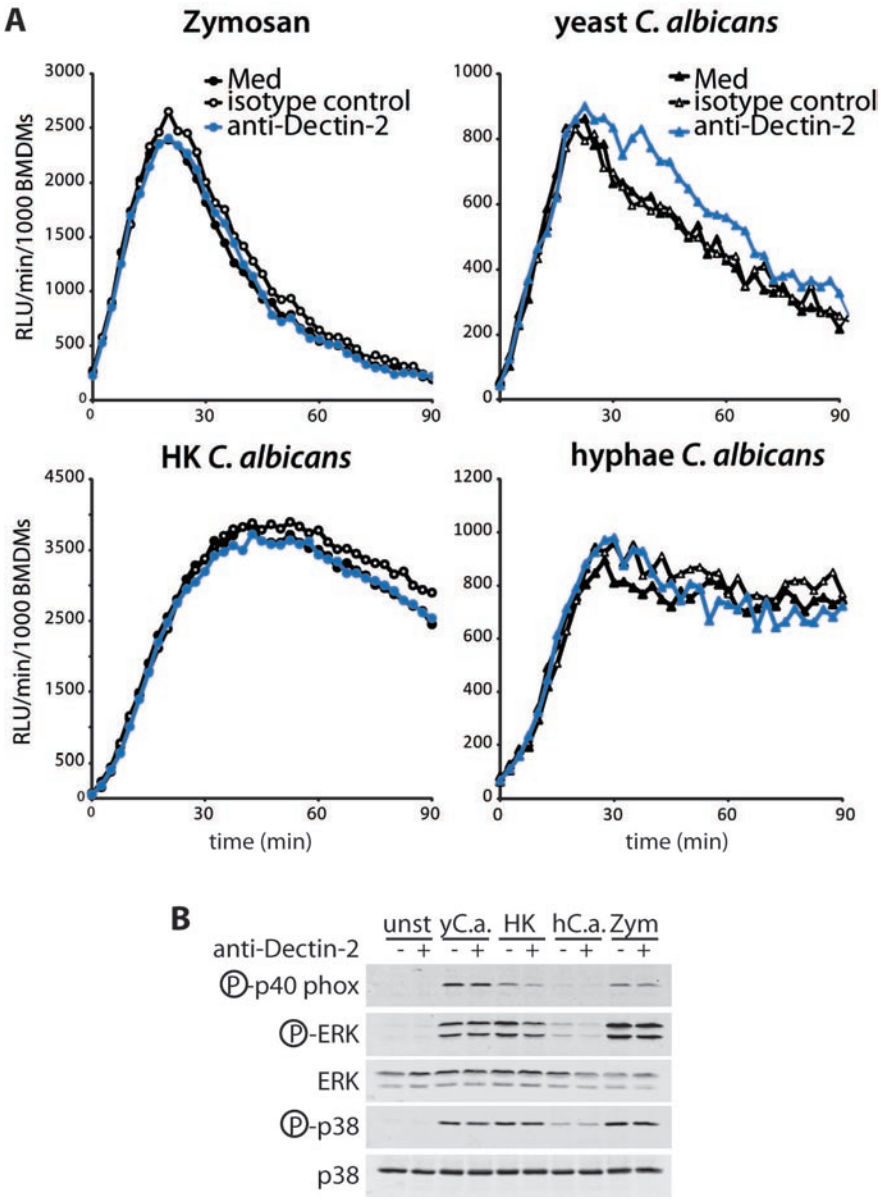

Figure III.5: Dectin-2 is not required for ROS production.
A ROS measurement by luminol-dependent chemiluminescence at 37°C in 2.5 min intervals over a 90 min period [relative luciferase units (RLU) min^{-1} per 1000 immune cells]. Stimulation of wild type (C57BL/6) BMDMs left untreated or pre-treated with anti-Dectin-2 or IgG2aκ isotype control (10µg/ml) for 30 min prior to stimulation with either zymosan (100µg/ml) **(top left)**, live *C. albicans* in yeast form (MOI 5:1) **(top right)**, heat-killed *C. albicans* in yeast form (MOI 5:1) **(bottom left)** or live *C. albicans* in hyphae form (6µg dry weight/well) **(bottom right).** RLUs of unstimulated BMDMs were substracted from stimulated BMDMs. **B** Wild type (C57BL/6) BMDMs pre-treated with anti-Dectin-2 (+) or IgG2aκ isotype control (10µg/ml) (-) were either left untreated or treated for 30 min with either zymosan (100µg/ml) or live *C. albicans* in the yeast (yCa) and hyphae (hCa) form or heat-killed *C. albicans* (HK). Phosphorylated p40phox, ERK and p38, were detected by immunoblotting and the blots were re-probed with total ERK and p38 antibodies to assess equal loading between lanes.

These data demonstrate that Dectin-2 is not involved in ROS response to *C. albicans* or zymosan stimulation in all conditions tested. Furthermore, although it was shown in DCs that crosslinking Dectin-2 with a Dectin-2 specific antibody induces ERK1/2 and p38 phosphorylation (Robinson et al., 2009), blocking Dectin-2 alone is not sufficient to inhibit the MAP kinases

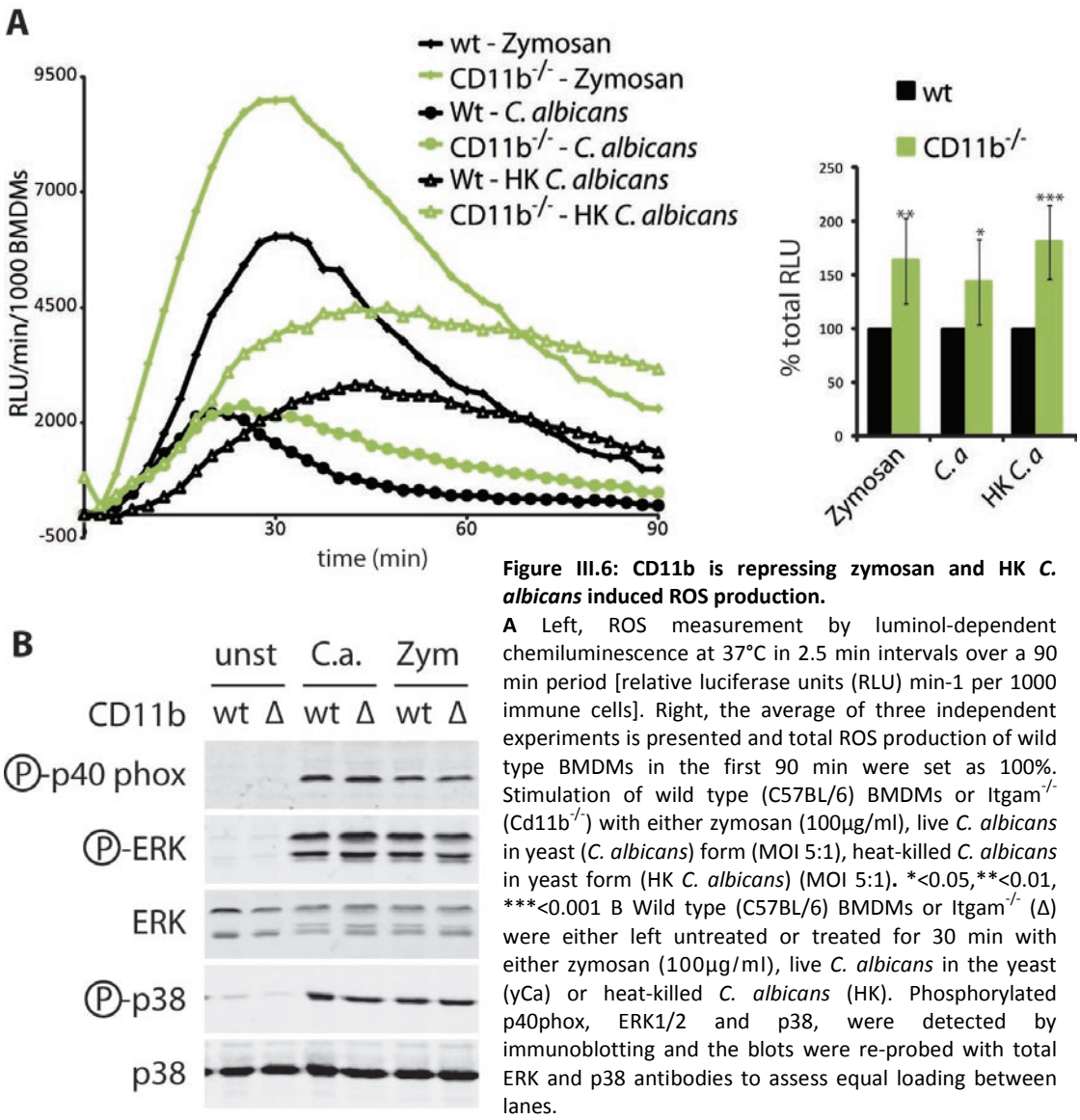

Figure III.6: CD11b is repressing zymosan and HK *C. albicans* induced ROS production.

A Left, ROS measurement by luminol-dependent chemiluminescence at 37°C in 2.5 min intervals over a 90 min period [relative luciferase units (RLU) min-1 per 1000 immune cells]. Right, the average of three independent experiments is presented and total ROS production of wild type BMDMs in the first 90 min were set as 100%. Stimulation of wild type (C57BL/6) BMDMs or Itgam$^{-/-}$ (Cd11b$^{-/-}$) with either zymosan (100µg/ml), live *C. albicans* in yeast (*C. albicans*) form (MOI 5:1), heat-killed *C. albicans* in yeast form (HK *C. albicans*) (MOI 5:1)**.** *<0.05,**<0.01, ***<0.001 B Wild type (C57BL/6) BMDMs or Itgam$^{-/-}$ (Δ) were either left untreated or treated for 30 min with either zymosan (100µg/ml), live *C. albicans* in the yeast (yCa) or heat-killed *C. albicans* (HK). Phosphorylated p40phox, ERK1/2 and p38, were detected by immunoblotting and the blots were re-probed with total ERK and p38 antibodies to assess equal loading between lanes.

activation by live *C. albicans,* although ERK activation is slightly diminished when treated with heat-killed *C. albicans.*

III.2.5 CD11b has an inhibitory effect on zymosan-induced ROS production.

The integrin CD11b/CD18, also known as the complement receptor 3 (CR3), induces ROS production in mouse and human macrophages in response to oxidised LDL (Husemann et al., 2001). Also, ROS production by human neutrophils in response to either zymosan or beta-glucan particles is CR3-dependent (Ross et al., 1987; Rubin-Bejerano et al., 2007). Furthermore, it was shown that co-stimulation of CR3 and FcγR with opsonised zymosan and IgG enhances the superoxide production in bovine neutrophils (Nagahata et al., 2007).

Hence, we investigated whether CR3 is involved in ROS production of BMDMs upon zymosan and *C. albicans* stimulation. Surprisingly, in response to zymosan or heat-killed *C. albicans,* BMDMs lacking Cd11b released about 1.5 times more ROS than wild type BMDMs, whereas ROS production in response to live *C. albicans* was only slightly enhanced (Figure III.6 A). After 30 min of stimulation with zymosan and live *C. albicans* phosphorylation of p40phox, ERK1/2 and p38 was not changed in BMDMs lacking Cd11b compared to wild type BMDMs (Figure III.6 B).

These data indicate that Cd11b may transduce a signal which inhibits ROS response upon stimulation with zymosan and heat-killed *C. albicans,* but does not affect activation of the MAP kinases ERK1, ERK2 and p38.

III.3 Establishing siRNA knock-down assays in BMDMs.

RNA interference (RNAi) is a highly conserved mechanism of transcriptional and post-transcriptional gene silencing, requiring double-stranded (ds) RNA (Hannon, 2002; Meister and Tuschl, 2004; Novina and Sharp, 2004). A long dsRNA is usually digested by Dicer to yield small interfering RNAs (siRNAs) of 21–23 nucleotides (nt) in length (Bernstein et al., 2001; Hammond et al., 2000). A protein complex (RNA-Induced Silencing, RISC) unwinds the siRNAs and uses one strand to anneal to identical sequences in the target mRNA (Hammond et al., 2001). Silencing of mammalian genes by an siRNA-based method is considered more promising than by long dsRNA, as introduction of long dsRNA into mammalian cells frequently induces a fatal interferon response (Hannon and Rossi, 2004).

To identify new and unknown receptors or pathways triggered by *C. albicans* for example the receptor responsible for live *C. albicans*-induced oxidative burst, we decided to establish a siRNA based screening assay.

III.3.1 BMDMs are efficiently transfected by siRNA

To set up the siRNA assay in our BMDMs, we used the siGenome smart pool siRNAs designed by Dharmacon, which consist of 4 different dsRNA sequences per target gene. To find the optimal conditions for RNAi transfection in BMDMs, we first tested different transfection reagents. For efficiency determination, we used green-fluorescent labelled siRNA (siGlo). We tested two different transfection reagents, RNAiMax and Dharmafect4, to determine the transfection efficiency. With the Dharmafect4 and different concentrations of siRNA and different cell density, we did not get higher transfection rates than 35% using 100nM siRNA (data not shown). Using the lipofectamin based RNAiMax, we obtained better transfection rates of about 57% with only 10nM siRNA according to FACS analysis (data not shown). The possible decrease in cell viability upon transfection is a major concern for transfection. Therefore, we also tested for viability using propidium iodine staining after 48 hours of transfection. The transfection with siGlo or the transfection reagent alone did not change the viability of the macrophages when compared to the untreated BMDMs (data not shown).

III.3.2 mRNA of the target genes is sufficiently down-regulated

To check for an efficient down regulation of target genes, quantitative RT PCR was performed on transfection with 6 different siRNAs; gp91phox, MyD88, FcγR, Dectin-1, Dectin-2 and Dap12

(Figure III.7 A). Except for the FcγR, all siRNAs tested reduced the mRNA of the target genes more than 50% when compared to the non-target control (nTG) (Figure III.7 A). Furthermore, MyD88 mRNA expression was unchanged in BMDMs treated with gp91phox siRNA, Dap12 mRNA was not effected in BMDMs treated with Dectin-2 siRNA and Dectin-1 mRNA amounts were unchanged in BMDMs transfected with FcγR siRNA (Figure III.7 A, left column), indicating a target-specific down-regulation.

Since cytotoxic and immunomodulatory activities have been reported for cationic liposome and polyethylenimine-based transfection reagents, we also tested cytokine expression after transfection. About 48 hours after transfection, the cell culture supernatants were analysed for TNFα expression by ELISA. TNFα production was unchanged in BMDMs treated with either the transfection reagent alone, the nTG control or the siRNAs (Figure III.7, B). Previously, we confirmed that ROS production in response to *C. albicans* is dependent on the gp91phox subunit of the NADPH oxidase (see Chapter III.1). To determine whether siRNA-treated cells can be used

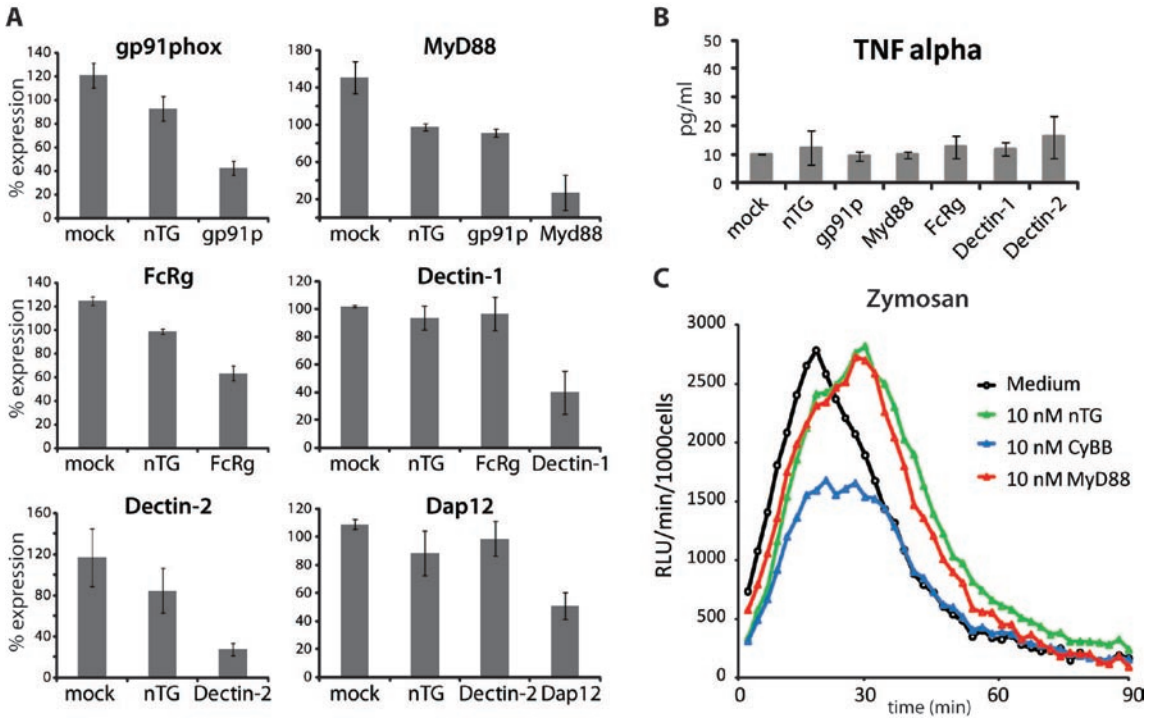

Figure III.7: siRNA knock down is working for BMDMs.
A+B. Transfection of BMDMs in 24 well plate. BMDMs (2 x 10^5/well) were forward transfected with 10nM of the indicated siRNAs. **A**. 48 hours after transfection, total RNAs were isolated and expression of the target genes (gp91phox, MyD88, FcRγ, Dectin-1, Dectin-2 and Dap12) was quantified by real-time PCR. Average of two independent transfections are presented **B.** TNF-alpha production was measured by ELISA after 48 hours of transfection. **C.** Transfection of BMDMs in a white opaque 96 well plate. BMDMs (5 x 10^4/well) were forward transfected with 10nM of the siRNAs indicated. 72 hours post transfection, ROS was measured by luminol-dependent chemiluminescence at 37°C in 2.5 min intervals over a 90 min period [relative luciferase units (RLU)/ min per 1000 immune cells]. Untreated or transfected BMDMs were incubated with zymosan (100µg/ml). RLU values of non-stimulated BMDMs transfected with nTG were subtracted from zymosan stimulated BMDMs. Data are representative of three independent assays.

for our luminol ROS assay, BMDMs were transfected in a 96-well format at the same cell to siRNA and transfection reagent ratio as in the 24-well plate. We used gp91phox siRNA as positive and MyD88 as negative control for the assay. 72 hours after transfection, the ROS assay was performed upon zymosan stimulation. BMDMs transfected with the gp91phox siRNA showed a reduced ROS production when compared to non-treated BMDMs, nTG and MyD88-transfected cells (Figure III.7, C). Similar results were observed with *C. albicans*-treated BMDMs (data not shown). Taken together, these data indicate that siRNA knock down in BMDMs reduces the mRNA and corresponding protein amount of target genes to levels where an effect in the specific immune response, e.g. ROS response, becomes detectable.

III.3.3 Transfection in a 96-well format is not sufficiently down-regulating

To set up a screen in a 96-well format we chose eight additional target genes besides the controls MyD88 and gp91phox: the C-type lectins Dectin-1, Dectin-2, Galectin-3 and Mannose receptor (MRC1), Syk, Card9 and DAP12. Dectin-1 and its adaptor kinase Syk were serving as additional controls. Dectin-2 siRNA was used to reconfirm our previous findings using blocking antibodies. Galectin-3 and MRC1 have so far never been associated with ROS response but are suggested to recognise *C. albicans*. The ITAM-containing adaptors FcγR and Dap12 were previously shown to be important for ROS production during integrin signalling (Mocsai et al., 2006), and Dap12 is needed for *Salmonella-induced* ROS production (Charles et al., 2008). Card9 was chosen as a target, because it was shown to associate with the GDP-dissociation inhibitor LyGDI in phagosomes after bacterial and fungal infections, thereby releasing the Rac1 GTPase from its inhibitor and activating ROS response (Wu et al., 2009).

Untreated and nTG transfected BMDMs produced the same amount of ROS when stimulated with zymosan or *C. albicans*. BMDMs treated with gp91phox siRNA showed a significant reduction in ROS response upon stimulation by both zymosan and *C. albicans,* whereas BMDMs treated with Dectin-1 siRNA produced significantly less ROS when stimulated with zymosan but not when treated with *C. albicans.* These data confirm our studies using dectin-$1^{-/-}$ mice and Dectin-1 blocking reagents (see Chapter III.2). There was no difference in ROS production when cells were transfected with siRNA knocking down Dectin-2, FcRγ, Card9, Syk, Galectin-3 or MRC1 (Figure III.8 A). By contrast, an increase in ROS production was detected when cells were transfected with Dap12 siRNA (Figure III.8 A).

In previous experiments, we have shown Syk inhibition with R406 is blocking ROS production when BMDMs are stimulated with zymosan or *C. albicans*. Therefore we checked for an efficient

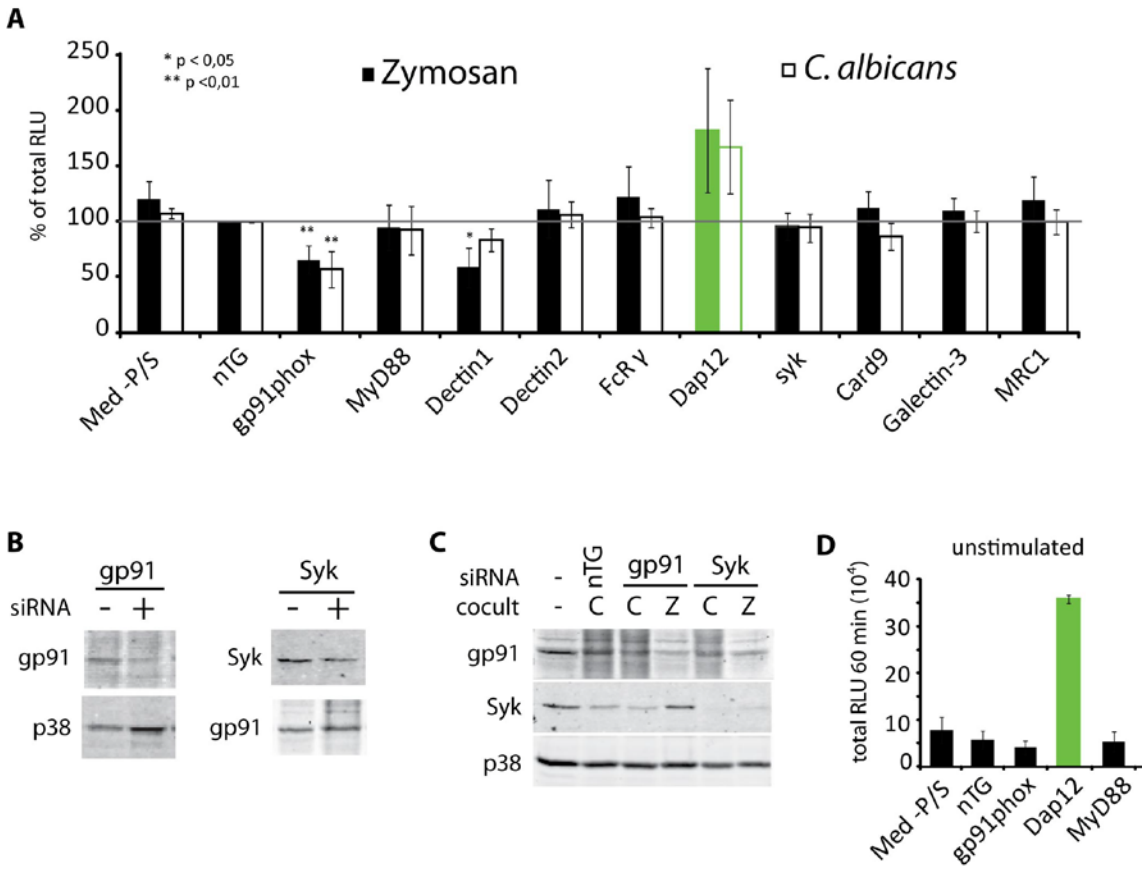

Figure III.8: Transfection in 96 well format is not efficient enough to reduce expression of some target genes.
A In a 96-well plate BMDMs (5 x 10^4/well) were forward transfected with 10nM of either the non targeting control (nTG), gp91phox, MyD88, Dectin-1, Dectin-2, FcR gamma, Dap12, Syk, Card9, Galectin-3 and MRC1 (3 wells per condition). 72 hours post transfection, ROS was measured by luminol-dependent chemiluminescence at 37°C in 2.5 min intervals over a 60 min period. The average of three independent experiments is presented and total ROS production by nTG transfected BMDMs were set as 100%. * p<0,05 **p <0,01. RLU of unstimulated BMDMs transfected with nTG was substracted. Untreated or transfected BMDMs were either incubated with zymosan (100µg/ml) or *C. albicans* (2x10^5 cells/well). **B** Immunoblot analysis of transfected BMDMs. Three wells of either untransfected cells or cells transfected with gp91phox (left) or syk (right) siRNA were pooled together and protein levels were detected via gp91phox (left) or Syk (right) antibodies and the blots were re-probed with p38 and gp91phox antibodies as loading controls. **C.** Immunoblot analysis of BMDMs transfected in 24 well format. Protein levels were detected with gp91phox and Syk antibodies, and the blot was re-probed with p38 antibodies for a loading control. **D** In a 96-well plate BMDMs were either untransfected or transfected with 10nM of nTG, gp91phox, DAP12 or MyD88 (3 wells per condition). 72 hours post transfection, ROS was measured without stimulation. The average of three independent experiments is presented.

down-regulation of gene expression and we determined the protein levels of Syk and gp91phox from samples taken after the ROS assay by immunoblotting. Indeed, gp91phox protein levels were substantially reduced after transfection (Figure III.8 B, left). In the Syk siRNA-treated cells we also observed a decrease in Syk protein. However we still detected the Syk protein with the antibodies (Figure III.8 B, right), which might be sufficient to transduce the signal. Next, we determined whether the down-regulation of Syk is more efficient in 24-well plates. Indeed, transfecting BMDMs in a 24-well plate format reduced the Syk protein to levels which could no longer be detected with anti-Syk antibodies (Figure III.8 C).

Taken together, siRNA transfection and down-regulation of genes in a 96-well format is working for Dectin-1 and gp91phox, but is not efficient enough for the Syk kinase. Thus, only a small fraction of kinase or kinase activity might be needed to transduce the signal. In the 24-well format, the down-regulation of Syk is more efficient, and might therefore lead to a reduced ROS response.

Interestingly, down-regulation of Dap12 led to an enhanced ROS response when the cells were stimulated with zymosan or *C. albicans*. However, in the absence of any stimulation, the DAP12 siRNA-transfected BMDMs already showed highly elevated ROS levels when compared to untranfected, nTG, gp91phox or MyD88 siRNA transfected BMDMs (Figure III.8 D). This suggests that the increase in ROS levels is rather a secondary effect of DAP12 down-regulation than a result of the stimulation with *C. albicans* or zymosan.

III.3.4 Transfection in 3.5 cm dishes diminishes Syk protein levels

To check whether a more efficient down-regulation of Syk inhibits ROS response, we transfected BMDMs with Syk siRNA in 3.5 cm dishes 2 days before performing the ROS assay. 30 min before the assay, the cells were scraped off and distributed in a 96-well luminescence plate. After stimulation with zymosan, we observed a decrease in ROS release by about 40% with gp91phox, 70% with Dectin-1 and 50% with Dap12 siRNA treated cells. No change in ROS production in Syk- or FcRγ-siRNA treated cells was detectable when compared to the nTG control (Figure III.9 A bottom). Protein levels of Syk were reduced although still detectable (Figure III.9 A, top). However, after 75 hours of transfection and *C. albicans* stimulation, Syk siRNA treated BMDMs had a reduced ROS response by about 50% when compared to nTG treated cells. Furthermore, down-regulation of gp91phox reduced the ROS production by about 70%, and Dectin-1 siRNA-treated cells inhibited about 20%, which is comparable to the dectin-$1^{-/-}$ BMDMs. Syk protein was not detectable by immunobloting in the Syk siRNA-transfected BMDMs (Figure III.9 B, top).

Finally, to evaluate the stability of the siRNA-based gene silencing, a ROS assay was performed 96 hours post transfection. BMDMs were stimulated with zymosan and *C. albicans*. After 96 hours of transfection, zymosan-stimulated ROS release was reduced by about 60-70% when BMDMs were transfected with the gp91phox siRNA, by 70% with the Dectin-1 siRNA, about by 50% with the Syk and the Dap12 siRNA, but again no change in ROS production was seen in FcγR siRNA treated BMDMs (Figure III.9 C, left). For the BMDMs stimulated with *C. albicans,* we observed a slight reduction by about 40% in BMDMs transfected with gp91phox siRNA, and a comparable decrease in Syk and Dap12 siRNA-treated cells. As expected Dectin-1

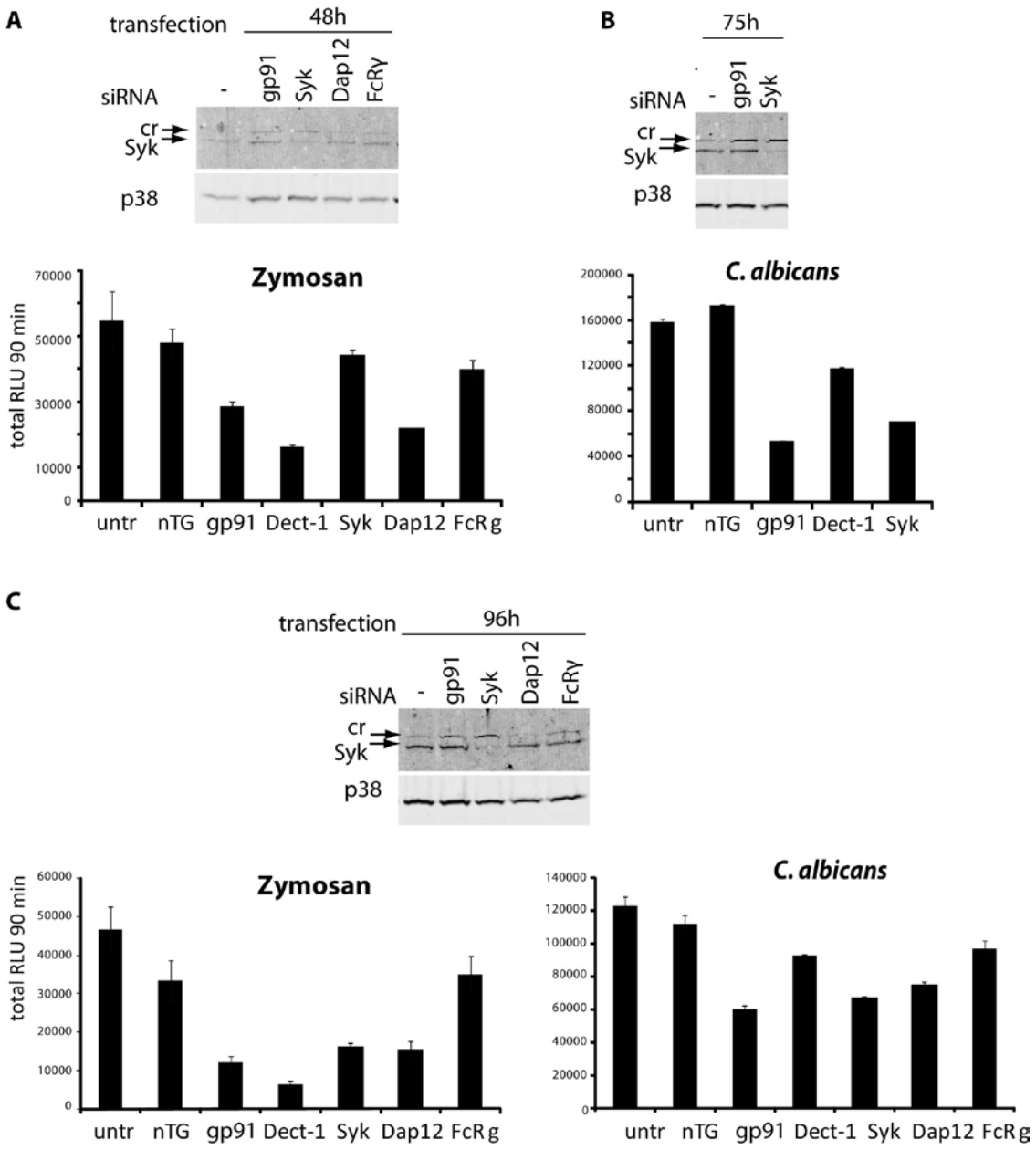

Figure III.9: Transfection in 3.5 cm plates is reducing Syk protein levels efficiently.
A-C BMDMs (1 x 10^6/3.5 cm plate) were forward transfected with 10nM of either the non-target control (nTG), and indicated siRNA. ROS was measured by luminol-dependent chemiluminescence at 37°C in 2.5 min intervals over a 90 min period [total RLU over 90 min was measured]. RLU of unstimulated cells for each condition were subtracted from stimulated cells. 48 hours (A) 75 hours (B) and 96 hours (C) after transfection BMDMs were scraped off, distributed in a 96-well plate and stimulated with either zymosan (A+C) or *C. albicans* (B+C). Protein levels of Syk were detected with anti-Syk antibodies and the blot was re-probed with p38 antibodies for a loading control.

down-regulation again reduced ROS response by about 20% (Figure III.9 C, right). After 96 hours of transfection, protein levels of Syk were no longer detectable by immunoblot analysis in the Syk siRNA transfected BMDMs (Figure III.9 C, top).

These results demonstrate that the transfection efficiency and knock-down of our tested target genes is more efficient in plates with larger surface area, although the ratio of cell amount, transfection reagent and siRNA were not changed. It seems that 75 hours post transfection, the expression of target genes is sufficiently down-regulated, to see a reduced response in a functional assay. In contrast to the 96-well format, in culture plates with larger surfaces the RLU values of untreated BMDMs are only slightly above background in all conditions tested indicating that the BMDMs are less stressed under these culture conditions.

IV. Conclusions and Discussion

Candida albicans, an opportunistic human fungal pathogen, is able to colonise many different body sites and lives as a commensal. Like many other microbial pathogens, *Candida albicans* can cause life-threatening systemic infections in individuals with weakened immune systems. Notably, *C. albicans* can escape the immune surveillance of the host, exploiting several strategies to avoid host clearance (Gropp et al., 2009; Lohse and Johnson, 2008; Lorenz et al., 2004; Marcil et al., 2008). Human immune cells specifically recognise microbial attacks and release highly toxic radicals to kill invading pathogens. This work focuses on one of the immediate early defence mechanism used by macrophages facing fungal challenges, namely the production of reactive oxygen species (ROS) through the "respiratory burst" phenomenon (Babior, 2004).

To investigate the immunological importance of the respiratory burst by innate immune cells in the defence against *C. albicans*, mutant strains of all *C. albicans* superoxide dismutases were generated and analysed in an in vitro interaction model of bone marrow derived macrophages (BMDMs) and myeloid dendritic cells (mDCs) co-cultured with *C. albicans.*

IV.1 *C. albicans* degrades host-derived ROS to escape innate immune surveillance

In the first part of this thesis, we show that both yeast and hyphae forms of *C. albicans* rapidly induce ROS release by primary innate immune cells such as macrophages and dendritic cells. This ROS production is dependent on an active form of the gp91phox subunit of the NADPH oxidase. The GPI-anchored Sod5 and Sod4 enzymes of *C. albicans* are degrading extracellular ROS produced by innate immune cells. Strikingly, *C. albicans* strains lacking superoxide dismutases fail to counteract the host-derived oxidative burst. Furthermore, cells lacking Sod4 and Sod5 are hyper-susceptible to killing by primary BMDMs, suggesting a physiological role of cell surface SODs in the evasion of immune surveillance.

Based on our results, we propose that *C. albicans* can escape the oxidative burst, a host-generated defence mechanism, (Figure IV.1). Adhesion, recognition and phagocytosis of fungi cells by innate immune cells trigger an immediate and rapid assembly of the ROS machinery at the cell surface or in the phagosomal membrane, preceding phagocytosis and persisting throughout phagosomal maturation. Concomitantly, host temperature and adhesion may

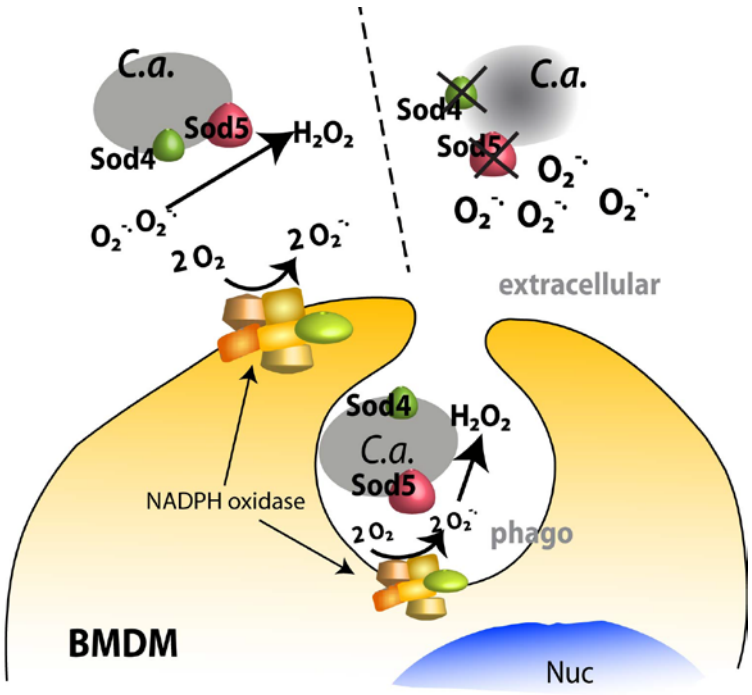

Figure IV.1: Model for Sod4 and Sod5-mediated protection against respiratory burst.
Upon contact with BMDMs and mDCs, Sod4 and Sod5 anchored at the *C. albicans* (C.a) surface (left) degrade superoxide anions (O2 $^{-}$) to hydrogen peroxide (H_2O_2). The lack of the Sod4 and Sod5 (right) causes ROS accumulation in the medium and perhaps inside the phagosomes (phago) which results in enhanced killing of *C. albicans*.

enhance *SOD4* and *SOD5* expression, followed by decaying ROS produced by host cells. The SOD-mediated decomposition of host-derived ROS perhaps facilitates phagosomal survival of fungal cells, which would facilitate killing of the host cells. Taken together, these data reveal a physiological function of cell surface SODs in evading immune surveillance, thereby facilitating invasion and ultimately dissemination of fungal pathogens in the mammalian host.

IV.2 PRRs and their adaptor proteins in the activation of the respiratory burst

To elucidate the signalling pathways and upstream factors leading to the production of ROS in innate immune cells in response to challenge with *C. albicans*, putative pattern recognition receptors (PRRs) and adaptor proteins involved in ROS transduction were investigated.

Toll-like receptors are essential PRRs of the immune system expressed on a large variety of immune cells (Akira, 2006), and involved in the recognition of PAMPs zymosan (Ozinsky et al., 2000). MyD88, an intracellular adaptor protein which is shared by most TLRs is essential for antifungal defence in several in vivo studies (Bellocchio et al., 2004; Biondo et al., 2008; Yauch et

al., 2004). Our data suggest that the TLR family is not involved in the ROS response to *C. albicans* infections and zymosan treatment in BMDMs (Figure III.1). However, since the TLR4 ligand LPS does not induce detectable levels of ROS in murine bone marrow-derived macrophages (Charles et al., 2008), the possibility remains that certain TLRs may still be involved in ROS response in other types of macrophages or phagocytic cells.

Dectin-1 is important for eliminating fungal infections in mice (Taylor et al., 2007), and needed for recognising and phagocytosing *C. albicans* in a variety of human and mouse innate immune cells, including different types of macrophages, mast cells, neutrophils and dendritic cells (Ariizumi et al., 2000; Huysamen and Brown, 2009; Sun and Zhao, 2007; Tsoni and Brown, 2008).

This work confirms previous studies (Saijo et al., 2007; Taylor et al., 2007; Underhill et al., 2005; Yang and Marshall, 2009) showing that efficient zymosan-induced ROS production by macrophages requires Dectin-1 (Figure III.2 –III.4). Furthermore, we show that the activity of intracellular Src and Syk kinases is required for eliciting ROS response (Figure III.2 A). Src kinases are phosphorylating the immunoreceptor tyrosine-based activation motif (ITAM), which in turn binds, phosphorylates and activates Syk (Tohyama and Yamamura, 2009), leading to the induction of several downstream pathways such as the canonical NFκB via CARD9, and the CARD9-independent, non-canonical, NFκB pathway as well as the Nlrp3 inflammasome (Gringhuis et al., 2009; Gross et al., 2009; Ruland, 2008). In addition to getting activated through ITAM motif binding, Syk can also be activated through an autophosphorylation mechanism (Tsang et al., 2008).

Activation of Src and Syk kinases is also essential for *C. albicans*-induced ROS production but Dectin-1 itself only plays a minor role (Figure III.2 B). When macrophages are stimulated with live *C. albicans,* a slightly reduced ROS response is seen with BMDMs lacking Dectin-1 (Figure III.3 B). However, blocking reagents such as laminarin or an anti-Dectin-1 blocking antibodies fail to reduce ROS response upon live *C. albicans* stimulation (Figure III.2 B and Figure III.4 B+D). These data are in line with a previous publication using Dectin-1 knock-out macrophages showing that Dectin-1 is not involved in *C. albicans*-stimulated ROS but is needed for zymosan-stimulated ROS (Saijo et al., 2007). Our results are contradicting earlier work using Dectin-1 blocking reagents to show that Dectin-1 is needed for *C. albicans*-induced ROS (Gantner et al., 2005). Interestingly, ROS production is reduced to the same extent when Dectin-1-blocked macrophages are co-cultured with heat-killed *C. albicans* or treated with zymosan (Figure III.3 C). This data are in line with a recent publication showing that in human DCs, the Dectin-1-Syk pathway is required for *C.*

albicans-induced ROS response using heat-killed yeasts (Skrzypek et al., 2009). Beside its role as intracellular adaptors for immunoreceptors, Syk kinases are also involved in mediating phagocytic processes. Whether its importance for ROS induction occurs through its role in integrin-mediated signal transduction (Van Ziffle and Lowell, 2009), as signalling adaptor of ITAM-bearing receptors or as mediator of phagocytic processes (Tohyama and Yamamura, 2009) will have to be investigated further.

Heat-killing of *C. albicans* results in increased exposure of cell wall β-(1,3)-glucan, which is otherwise only exposed at bud scars in live *C. albicans* (Fradin et al., 1996; Netea et al., 2008a). The β-glucans exposed in the bud scars of live *C. albicans* seem insufficient to stimulate ROS via Dectin-1. Thus *C. albicans* seems to induce ROS via at least one so far undisclosed receptor.

Our preliminary results show an increase in ROS production via zymosan stimulation when the serine-threonine kinase Raf-1 is inhibited. Recently it has been shown in human DCs that Dectin-1 induces Raf-1 in a Syk independent manner, and that an active Raf-1 is needed for the Dectin-1 - TLR crosstalk (Gringhuis et al., 2009). Activation of Raf-1 inhibited the non-canonical NFκB pathway (RelB), thereby stimulating the canonical NFκB pathway and cytokine expression. Interestingly, inhibition of Raf-1 increases IL23p19 transcription (Gringhuis et al., 2009). And elevated IL23p19 levels have previously been associated with patients suffering from rheumatoid arthritis (Kim et al., 2007a; Kim et al., 2007b). This disease results in elevated levels of pro-inflammatory cytokines and increased ROS (Phillips et al., 2009).

Dectin-2 another c-type lectin receptor recognising *C. albicans* is signalling via the ITAM domain of FcRγ (Robinson et al., 2009; Sato et al., 2006). This work suggests that Dectin-2 alone is not involved in ROS response to live and heat-killed *C. albicans* or zymosan stimulation (Figure III.5 A). Furthermore, the MAPK pathways ERK1/2 and p38 are also not induced via Dectin-2 alone when stimulated with live *C. albicans* in yeast or hyphal forms or zymosan (Figure III.5 B). But ERK1/2 phosphorylation is slightly dependent on Dectin-2 when stimulated with heat-killed *C. albicans*. Notably, simultaneous inhibition of Dectin-1 and Dectin-2 in DCs is inhibiting cytokine response more efficiently than inhibiting or deleting one alone (Robinson et al., 2009). Concurrently, we cannot exclude the possibility to see an inhibition of the MAPK pathways only when both receptors are inhibited at the same time.

Furthermore, we also addressed the question whether the integrin **CD11b**, one subunit of the CR3, is involved in *C. albicans* or zymosan-induced ROS response. Interestingly, in BMDMs lacking CD11b, we observe an increased ROS response when cells are stimulated with zymosan,

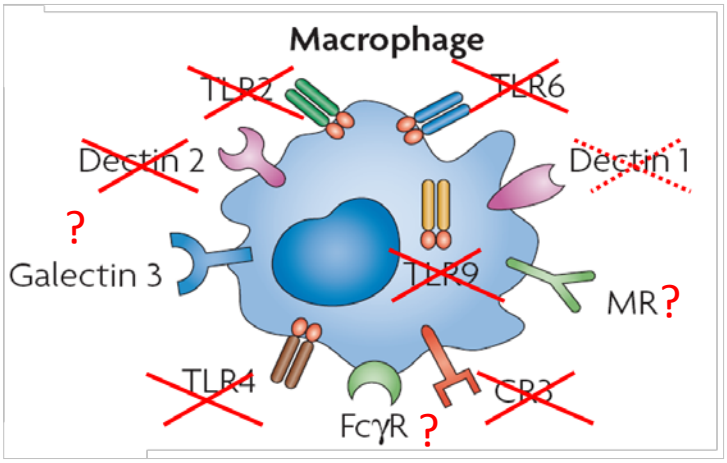

Figure IV.2: Potential receptors involved in ROS production following *C. albicans* recognition.
Using BMDM from knock-out mice we can exclude a possible role of the TLR family in ROS response to zymosan or *C. albicans*. Dectin-1 is signalling zymosan induced ROS and ROS induced by heat-killed *C. albicans* but not by live *C. albicans* in yeast or hyphal form. It also seems unlikely that Dectin-2 is involved in ROS production due to *C. albicans* stimulation. CR3 is also not involved in ROS production but may be involved in down-regulating ROS. Picture adapted from (Netea et al., 2008a)

or heat-killed *C. albicans,* but only a slight increase when BMDMs are infected with live *C. albicans* (Figure III.6 A). Since the level of ROS production is comparable to that of the inhibition of Raf-1, it might be interesting to investigate whether there is a connection between Cd11b and Raf-1 activation. There are reports stating that in neutrophils, Cd11b is crucial for ROS production in response to zymosan and β-glucans (Nagahata et al., 2007; Ross et al., 1987; Rubin-Bejerano et al., 2007). In human neutrophils, Cd11b seems to be even more important than Dectin-1 in the recognition of yeast particles (van Bruggen et al., 2009). This suggests a different recognition process of human neutrophils and mouse macrophages.

Taken together these data show that the TLR family is not involved in ROS production in zymosan or *C. albicans* stimulated BMDMs. Dectin-1 is crucial for zymosan and heat-killed *C. albicans*-induced ROS response and MAPK activation, but is not the primary receptor mediating ROS release by live *C. albicans* in BMDMs. Furthermore, we have confirmed that the activation of Src and Syk kinases is needed for ROS production in response to zymosan and *C. albicans*. In the matter of *C. albicans*-induced ROS response this suggests that there is at least one other receptor involved in ROS response due to live *C. albicans* infection, which is bearing an ITAM or ITAM-like signalling domain or signals via an ITAM containing adaptor protein. In this respect, we have excluded Dectin-2 and Cd11b (CR3) as potential ROS inducing receptors. Cd11b might however be involved in repressing ROS production.

However, there are still some putative receptors expressed on the macrophage cell surface which recognise parts of the *C. albicans* cell wall and might induce ROS production (Figure IV.2). For example the Mannose Receptor (MR) is known to recognise oligosaccharides, like branched O-linked mannans in *C. albicans* and is involved in IL-17 production (van de Veerdonk et al., 2009). Galectin-3 is crucial for the recognition of the β-1,2 linked mannosides and collaborates with TLR2 (Fradin et al., 2000; Jouault et al., 2006). Furthermore, the highly complex *C. albicans* cell surface and multiple receptors known to recognise parts of the *C. albicans* surface, make it likely that ROS activation may be the consequence of stimulating multiple redundant receptors.

IV.3 siRNA knock-down in BMDMs

Inhibition or deletion of receptors or signalling molecules thought to be involved in the recognition of pathogens are beneficial strategies to elucidate the mechanisms of immune host defence. However, the generation of specific high affinity blocking antibodies is very time-consuming, and chemical inhibitors are often not specific enough. Therefore, we decided to establish a siRNA knock-down assay to investigate additional putative receptors involved in ROS transduction. This technique has advantages over other methods such as chemical engineering or blocking antibodies. First, since only a few siRNA copies can degrade the target mRNA sequence in multiple rounds, the blocking is often efficient (Sioud, 2004). Second, a single mismatch between siRNA and mRNA can inhibit cleavage, which makes the siRNA very specific (Ding et al., 2003). Third, once established, the technique is simple and fast, and forth, siRNA libraries containing thousands of sequences make a high-throughput approach of functional screening possible (Gurney and Hunter, 2005).

Of course there are also disadvantages associated with siRNA approches. Especially primary cells are difficult to transfect. It is often necessary to try many different conditions (Gurney and Hunter). Irrespective of how a siRNA is introduced into cells, it can have unspecific off-target effects as a consequence of one of three mechanisms. Because siRNA contains dsRNA it may also trigger nonspecific innate immune responses, as for instance interferon production (Sledz et al., 2003). Introduced siRNAs could saturate the RNAi machinery of cells, thereby inhibiting the function of endogenous miRNAs (Cullen, 2006). Finally, although mature siRNAs are designed to be fully complementary to a single mRNA transcript, they sometimes show significant complementarities to other unrelated non-target mRNAs (Jackson et al., 2006a; Jackson et al., 2006b).

As demonstrated here, we can efficiently down-regulate several target genes in a 24-well plate format (Figure III.7 A) Applying the siRNA assay in 96-well plate and performing a ROS assay we can see a reduction in ROS production for the positive control, gp91phox. The negative control, MyD88 as well as the non-targeting control show similar amounts of ROS production as untreated BMDMs (Figure III.7 C). When we undertook a first small screen using additional controls and putative targets, the gp91phox siRNA decreases ROS production in BMDMs treated with zymosan or *C. albicans.* Likewise, Dectin-1 siRNA is reduces zymosan- but not *C. albicans*-induced ROS production. The ITAM-containing adaptor molecule Dap12 induces more ROS when down-regulated, and other targets such as MyD88, FcγR, MRC1, Card9 and Galectin-3 do not show an effect in ROS production upon down-regulation.

Disturbingly, down-regulating the Syk kinase and stimulating BMDMs with zymosan or *C. albicans* does not show a decrease in ROS production (Figure III.8 A). Analysis of Syk protein levels of the 96-well format transfection however revealed that there is still Syk protein detectable by immunoblotting (Figure III.8 B), which might be sufficient to induce signalling cascade for ROS production. Performing the transfection in a 24-well plate inhibits Syk protein almost completely; this suggests that a 96-well plate is not the ideal choice for transfecting BMDMs.

Transfecting the cells in 3.5 cm plates efficiently reduces Syk protein levels and also reduces ROS production in BMDMs treated with *C. albicans* or zymosan. Surprisingly, in the 3.5 cm plate, we also observe reduced ROS production in response to both stimuli when DAP12 siRNA is transfected. Dectin-1 and gp91phox siRNA treated cells also show a more efficient drop in ROS production in response to *C. albicans* and zymosan, indicating a better transfection rate and higher down-regulation in this format. As in the 96-well plate assay, transfecting FcγR siRNA does not alter zymosan or *C. albicans*-induced ROS levels. TREM2-Dap12 was already shown to be important for ROS production in response to *Salmonella enteric* (Charles et al., 2008) and both Dap12 and FcγR are needed for superoxide production upon integrin stimulation (Mocsai et al., 2006). To my best knowledge Dap12 was until now not associated with *C. albicans* infections, but screening Dap12-associated receptors such as TREM-2 or Oscar (Lanier, 2009), might give us some further information about potential new *Candida albicans* receptors.

When we consider the results we obtained with the siRNA experiments in the light of previous results, we can also exclude the remaining three receptors, namely Galectin-3, MR1 and FcRγ, on the macrophage surface (Figure IV.2) as ROS mediators. However, these data have to be reconfirmed by assessing the knock-down efficiency at the corresponding protein levels. In

conclusion, performing siRNA assays in BMDMs is absolutely feasible in 24-well or 3.5 cm plate, while screening in a 96-well format is neither promising nor feasible. By establishing a screen in a 24-well format it might be possible to screen a couple of hundred putative targets including the Dap12-associated receptors and other receptors, containing ITAM or ITAM like domains.

V. Materials and Methods

This part features methods not described in the following Chapter V.2: In vitro systems for studying the interaction of fungal pathogens with primary cells from the mammalian innate immune system and procedures not described in the Material and Methods part of Chapter III.1.

V.1 Genomic DNA isolation

C. albicans genomic DNA was isolated as described (Sambrook and Russell, 2001) with some modifications. Overnight cultures were grown in 5ml YPD; cells were harvested and resuspended in DNA extraction buffer (2% Triton X-100, 1% SDS, 100mM NaCl, 10 mM Tris pH 8.0, 1mM EDTA). An equal amount of glass beads (250-600µm, Sigma) were added and cells were broken by vortex-mixing for 45min at 4°C. DNA was subsequently isolated by several rounds of Phenol:Choloroform:Isoamylalcohol (Fluka) extractions.

V.2 Southern blot analysis

Southern blotting was performed as previously described (Sambrook and Russell, 2001) with modifications. 20µg of genomic DNA was digested overnight and separated on 0.6% (wt/vol.) agarose gels. DNA was blotted onto a Hybond N+ nylon membrane (Amersham) overnight and cross-linked by UV the following day. Probes were internally labelled with P^{32}-dCTP using the Prime It II, Random Primer Labelling Kit (Stratagene) and hybridised overnight at 65°C. Autoradiography was performed at -70°C using CL-Exposure films (THP).

V.3 RNA extraction, reverse transcription and real-time PCR analysis

Total RNA was isolated from BM-DCs or BMDMs using a centrifugation column-based kit (Promega) according to the manufacturer's instructions. Total RNA samples were eluted in 50µl RNase-free sterile water. RNA concentration was measured using a NanoDrop2000 (Thermo Scientific) and samples were stored at -80°C until further use. Reverse-transcription was performed using a reverse transcription kit (Promega) according to conditions recommended by the manufacturer. Typically, reactions were carried on 0.7-1µg total RNA with oligo-dT primers in a final volume of 40µl. Reverse transcription products were diluted 1:5 with water and stored at –20°C until further use. For the real-time PCR amplification, 5µl of the diluted total cDNAs

were added to 20µl of real-time PCR mix (300nM Forward primer, 300nM Reverse primer, 1X MESA GREEN qPCR MasterMix Plus for SYBR® Assay (Eurogentec) and were submitted to the following cycling conditions: 95°C for 5min, 40 cycles (95°C for 10s, 63°C for 15s, 72°C for 15s) followed by a melting curve analysis. Primers used in this study are listed in Table V-1.

Table V-1: Oligos used for real-time PCR

Forward	Sequence 5'→ 3'	Reverse	Sequence 5'→ 3'
RT_91ph_1522s	GGATGAATCTCAGGCCAATCAC	RT_91ph_1641as	ATGGTCTTGAACTCGTTATCCC
RT_Myd88_808s	TGTCTCCAGGTGTCCAACAG	RT_Myd88_904as	TCGCATATAGTGATGAACCGC
RT_Dec2_429s	CAAGGAGAACTTCTGGAGCAC	RT_Dec2_524as	GTGATGAAATTCTGCTCCGC
RT_Dec1_629s	CCCAACTCGTTTCAAGTCAG	RT_Dec1_789as	TTGCAGATTTGGTTGTAGACCT
RT_DAP12_210s	GTGTTGACTCTGCTGATTGC	RT_DAP12_339as	CCTGAAGCTCCTGATAAGGC
RT_FcRy_167s	CCGCAGCTCTGCTATATCCT	RT_FcRy_257as	TTCGGACCTGGATCTTGAGTC

V.4 Protein extracts and western blot analysis

1 x 10^6 cells were scrapped on ice in 40µl ice-cold protein lysis buffer (Frackelton buffer) (10mM Tris pH7.5, 50mM NaCl, 1% Triton X-100, 1mM PMSF, 0.1mM Na Vanadate, 30mM NaPPi, 50mM NaF, 1X "Complete no EDTA" protease inhibitor cocktail (Roche, Basel, Switzerland)), collected and centrifuged at 15000xg at 4°C for 10 min. Sample supernatants were transferred to fresh tubes containing 15µl of 4X Sample Buffer and heated at 95°C for 5-7min, cooled on ice and stored at -20°C until further use. Aliquots of 15µl of proteins samples were fractionated by SDS-PAGE and transferred onto nitrocellulose membranes. Prior to immunodetection, membranes were blocked for 1-2 hours in 1X TBST with 10% non-fat dry milk. Blots were probed with anti-phospho-ERK antibodies, anti-ERK antibodies, anti-phospho-p38 antibodies, anti phospho-p40phox antibodies (Cell Signalling) or anti-p38 antibodies, (Santa Cruz). An infrared-labeled secondary antibody (LI-Cor,) was used to detect immune complexes and analysis was performed using the infrared imaging system Odyssey (LI-Cor).

V.5 Cytokine measurements by ELISA

Amounts of TNF-α released in cell culture supernatant were assayed using the TNF-α Elisa Kit (BioLegend) according to manufacturer's instructions.

V.6 Transfection of siRNAs

SMARTpool siGENOME siRNAs were obtained from Dharmacon: Dectin-2 (CLECSF10)M-049966-00, Dectin-1 (CLECSF12) M-058470-01; Card9 (LOC332579) M-045760-01; Dap12 (Tyrobp) M-

040951-00; Galectin-3 (LGALS3) M-041097-01; MRC1 M-047522-00; Syk M-041084-01; Fc Receptor γ (FCER1G) M-040340-01; CyBB (gp91phox) M-040340-01; MyD88.

Forward transfection with Dharmafect4 (Dharmacon) or Lipofectamin RNAiMax (Invitrogen) was carried out exactly as described by manufacturers' protocol. For lipofectamin RNAiMax transfection in a 96-well format, 10µM siRNA (final in 120µl) and 0.2 µl transfection reagent in 20µl of OptiMEM (Invitrogen) were distributed in each well. After 15 min of incubation at room temperature 100µl of 4 x 10^4 BMDMs were added in BMDM Med (DMEM incl. 10% FCS and 20% L-cond Medium) were added to the transfection mix for 48 hours. The transfection medium was changed to fresh BMDM-Med and BMDMs were incubated until the experiments were performed. In a 24-well plate, 10µM siRNA (final in 600µl) and 1 µl transfection reagent in 100µl of OptiMEM, 500µl of 2 x 10^5 BMDMs were added as well.

V.7 In vitro systems for studying the interaction of fungal pathogens with primary cells from the mammalian innate immune system

Chapter 11

In Vitro Systems for Studying the Interaction of Fungal Pathogens with Primary Cells from the Mammalian Innate Immune System

Christelle Bourgeois, Olivia Majer, Ingrid Frohner, and Karl Kuchler

Abstract

The incidence of invasive fungal diseases has increased over the past decades, particularly in relation with the increase of immunocompromised patient cohorts (e.g., HIV-infected patients, transplant recipients, immunosuppressed patients with cancer). Opportunistic fungal pathogens such as *Candida* spp. are most often associated with serious systemic infections. Currently available antifungal drugs are rather unspecific, often with severe side effects. In some cases, their prophylactic use has favored emergence of resistant fungal strains. Major antifungal drugs target the biosynthesis of lipid components of the fungal plasma membrane or the assembly of the cell wall. For a more specific and efficient treatment and prevention of fungal infection, new therapeutic strategies are needed, including strengthening or stimulation of the residual host immune response. Achieving such a goal requires a better understanding of factors important for the defense and the survival of the host combating *Candida* spp. Where possible, primary cultures of mammalian immune cells of the innate immune system constitute a better suited model than transformed cell lines to study host-pathogen response and virulence. Hence, *in vitro* primary cell culture systems are a good strategy for a first screening of mutant strains of *Candida* spp. to identify virulence traits with regard to host cell response and pathogen invasion.

Key words: primary cell culture, bone marrow–derived macrophages, myeloid dendritic cells, *Candida* spp., host-pathogen interaction, cell signaling, MAPK, cytokines.

1. Introduction

Candida albicans (C.a) and other *Candida* spp. are harmless commensals in most healthy people. However, they cause both superficial infections and life-threatening systemic candidiasis in immunocompromised patients. Cells of the innate immune system such as dendritic cells, macrophages, or neutrophils comprise the first line of defense against microbial pathogens. *Candida* and other

Steffen Rupp, Kai Sohn (eds.), *Host-Pathogen Interactions*, DOI: 10.1007/978-1-59745-204-5_11,
© 2008 Humana Press, Totowa, NJ

fungi are detected and recognized by the innate immune system through pattern recognition receptors (e.g., *toll*-like receptors, mannose receptor) and coactivators (dectin1, CD14), which recognize pathogen-associated molecular patterns (PAMPs) found in the fungal cell wall.

Mouse models lacking the TLR2,4 or dectin-1 genes indicate a role for these recognition molecules in detecting fungal pathogens and triggering the adaptive cytokine response, which in turn leads to an efficient activation of the acquired immune system. The cytokine response, a consequence of the various combinations of signaling pathways activated by these surface receptors (e.g., mitogen-activated protein kinase [MAPK] pathway, NF-κB activation) drive the host response and determine the outcome of infection (for review, see Refs. *1* and *2*). In the case of *Candida* infections, the balance between the production of inflammatory cytokines (e.g., TNF-α), which promote activation of the immune system and destruction of the pathogen, and the release of anti-inflammatory cytokines (e.g., IL-10), which limits the extent of tissue damage induced by inflammation and activates the adaptive immune response *(3–6)*, appears to be particularly important. To counteract the host response, microbial pathogens have developed escape strategies. In the case of *C.a.*, modulation of the activation of the MAPK/extracellular regulatory kinase (ERK) and p38 pathways may be one of the mechanism by which fungi modulate the cytokine response to its advantage *(7–9)*.

In vitro cell culture models are interesting tools to unravel dynamic changes of signaling activities as they allow for following the initial host attack, with the further goal of identifying downstream factors important for the defense and the survival of the host innate immune cells facing fungal pathogens in general and in particular *Candida* spp. They can be a good compromise for a first screening of virulence properties of fungal mutant strains lacking potential pathogenicity genes affecting host response or pathogen invasiveness even before the use of animal models for *in vivo* studies. Here we describe highly standardized primary cell culture models suitable to study early stages of innate immune cell–*Candida* interaction (e.g., pathogen phagocytosis, MAPK activation, cytokine production) and signaling events driving fungal invasion.

2. Materials and Media Components

2.1. Primary Culture of Bone Marrow–Derived Macrophages

1. High glucose (4.5 g/L) Dulbecco's Modified Eagle's Medium (DMEM) with L-glutamine, without pyruvate (PAA, Vienna, Austria).

2. Sterile PBS.
3. Colony-stimulating-factor 1 (CSF-1)-producing L929 cell line (ATCC no. CCL-1).
4. Bone marrow–derived macrophage (mMP) culture medium, high-glucose DMEM with L-glutamine supplemented with 10% fetal calf serum (FCS), 100 U/mL penicillin, 100 μg/mL streptomycin (Invitrogen, Carlsbad, CA), and 15% to 20% L-conditioned medium, as source of CSF-1 (for preparation, *see* **Notes 1** and **2**).
5. 10 × 10 cm square sterile Petri dishes (nontreated for cell culture; Barloworld Scientific, Stone, UK).
6. Soft-rubber spatula (Deutsch & Neumann, Berlin, Germany).

2.2. Primary Culture of Myeloid Dendritic Cells

1. Red blood-cell lysis buffer, 8.29 g/L NH_4Cl, 1 g/L $KHCO_3$, 0.0372 g/L EDTA, pH 7.2 to 7.4. Adjust pH if necessary, sterile filtrate through 0.2-μm membrane filter, store at 4°C.
2. Granulocyte-macrophage colony-stimulating factor (GM-CSF)-producing X-63 cell line *(10)*.
3. Myeloid DC (mDC) culture medium, high-glucose DMEM with glutamine supplemented with 10% FCS, 100 U/mL penicillin, 100 μg/mL streptomycin, and 5–10% X-conditioned medium as source of GM-CSF (for preparation, *see* **Notes 2** and **3**).
4. Cell-culture treated 24-well plates (NUNC, Roskilde, Denmark).

2.3. Cell Characterization by FACS Analysis

1. FACS buffer, PBS containing 2 g/L sodium azide and 2 g/L BSA, sterile-filtrated through an 0.2-μm filter and stored at 4°C.
2. Anti-mouse antibodies CD16/CD32, CD11b-FITC, CD11c-APC (BD Bioscience, Clontech, Palo Alto, CA).

2.4. Host Cell/Fungi Interaction

1. Laminar hood and 37°C incubator with 5% CO_2, 95% humidity, used only for infection purposes.
2. High glucose (4.5 g/L) DMEM without phenol red (Invitrogen), supplemented with 4 mM L-glutamine.
3. SC5314, clinical isolate of *Candida albicans (11)*.
4. UV-treated *Candida albicans* are prepared by treating an aliquot of the *Candida* infection suspension with 999 μJ/cm^2 in a Stratalinker (Stratagene, La Jolla, CA).
5. YPD agar plates, YPD liquid media for growing and culturing fungi.
6. 2 μM Cytochalasin D (Sigma, St. Louis, MO).
7. Cell scrappers (Becton Dickinson Labware, Franklin Lakes, NJ).

2.5. Microscopic Internalization Assay

1. Autoclaved, 12-mm-diameter glass coverslips, distributed in a 24-well plate.
2. *Candida albicans* strain expressing GFP intrinsically *(12)*.
3. 5 mM Calcofluor White M2R solution (Molecular Probes, Invitrogen, Carlsbad, CA).
4. Nonhardening fluorescence mounting media (Dako, Glostrup, Denmark).

2.6. Protein Extract and Immunoblotting

1. Protein lysis buffer (Frackelton buffer) *(13)*, 10 mM Tris pH 7.5, 50 mM NaCl, 1% Triton X-100, 1 mM PMSF, protease inhibitor cocktail (complete no EDTA; Roche, Basel, Switzerland), phosphatase inhibitors (30 mM NaPPi, 50 mM NaF, 0.1 mM sodium vanadate). Prepare fresh for each experiment and chill on ice.
2. 4x Sample Buffer (SBF), 200 mM Tris pH 6.8, 40% glycerol, 8% SDS, 0.002% bromophenol blue. Add 4% (v/v) β-mercaptoethanol just before use.
3. 1x TBST buffer, 3 g/L Tris-HCl, 8 g/L NaCl, 0.2 g/L KCl, 0.1% (v/v) Tween-20 pH 7.4.
4. Anti-mouse panERK (BD Transduction Laboratories, Palo Alto, CA), anti-mouse phospho-ERK1/2 and anti-mouse p38 (Santa Cruz Biotech Inc., Santa Cruz, CA), anti-mouse phospho-p38 (Cell Signaling Technologies Inc., Danvers, MA).
5. Horseradish peroxidase–coupled secondary antibodies (Merck, Whitehouse Station, NJ).
6. ECL reagents for immunodetection (Pierce, Rockford, IL).

2.7. RNA Extraction Procedure and Real-Time PCR

1. Spin column–based RNA extraction kit (BD Bioscience, Clontech, Palo Alto, CA, or Promega, Madison, WI).
2. First strand cDNA synthesis kit (Fermentas, Hanover, MD).
3. Real-time PCR mix, 75 mM Tris-HCl pH 8.8, 20 mM $(NH_4)_2SO_4$, 0.01% (v/v) Tween-20, 2.5 mM $MgCl_2$, 0.2 mM dNTPs, 300 nM Forward primer, 300 nM Reverse primer, 200 nM SYBR green (Biorad, Hercules, CA), 1 U recombinant Taq DNA polymerase (5 U/μL; Fermentas).
4. Mouse tumor necrosis factor-α (TNF-α); primers used, *forward* 5′-CATCTTCTCAAAATTCGAGTGACAA-3′; and *reverse* 5′-TGGGAGTAGACAAGGTACAACCC-3′ *(14)*.
5. Mouse interleukin 10 (IL-10) primers used: *forward* 5′-GGTTGCCAAGCCTTATCGGA-3′; and *reverse* 5′-ACCTGCTCCACTGCCTTGCT-3′ *(14)*.
6. Mouse GAPDH primers used: *forward* 5′-CATGGCCTTCCGTGTTCCTA-3′; and *reverse* 5′-GCGGCACGTCAGATCCA-3′ (RTPrimerDB, the real-time PCR primer and probe database http://medgen.ugent.be/rtprimerdb/index.php) *(15, 16)*.

3. Methods

3.1. Primary Culture of Bone Marrow–Derived Macrophages (mMPs)

This method is adapted from a protocol published earlier *(17)*.

1. On day 1, dissect mouse tibias and femurs from a 6- to 8-week-old animal in a hood, quickly rinse bones in 70% ethanol, and place in 15 mL ice-cold sterile PBS. When all the limbs are collected, transfer them in fresh 15 mL ice-cold sterile PBS and keep on ice (*see* **Note 4**).
2. To flush out the bone marrow, separate femur from tibia at the knee joint. Holding the bone with forceps above a sterile dish, cut one extremity of the bone and using a 20-mL syringe with a 27GX3/4 needle, flush DMEM with 10% FCS, 100 U/mL penicillin and 100 μg/mL streptomycin, into the medullary cavity until no more cells are coming out.
3. Collect bone marrow suspension and keep it on ice until all bones have been processed. Bone marrow flushing should be performed under semisterile conditions as required for cell culture.
4. To prepare mMPs, centrifuge the collected bone marrow at 300 × *g* for 5 min and resuspend the pellet in 44 mL mMP medium. Distribute the cell suspension equally in four 10 × 10 cm Petri dish (or seven 10-cm-diameter Petri dishes) and transfer to a 37°C incubator with a 5% CO_2, 95% humidity atmosphere (*see* **Notes 5** and **6**).
5. On day 2, add 6 to 8 mL of mMP medium; control for cell density every day.
6. On days 4 to 5, when cells in the plate reach confluency, aspirate the media containing nonadherent cells, gently collect cells by scrapping the plates with a soft rubber spatula, and re-plate at a ratio of 1:2 to 1:3 in square 10 × 10 cm Petri dish (*see* **Note 7**).
7. Let the cells grow for another couple of days, change medium completely every 2 to 3 days.
8. After 9 to 10 days of culture, mMP cell surface markers should be tested before performing interaction experiments (*see* **Section 3.3**).

3.2. Primary Culture of Myeloid Dendritic Cells (mDCs)

This method is based on a method described earlier *(18)* using X-conditioned media as source of GM-CSF.

1. For mouse bone marrow isolation, proceed as described above (*see* **Section 3.1, steps 1** to **3**).
2. To prepare mDCs, centrifuge bone marrow cell suspension at 300 × *g* for 7 min.

3. Resuspend the pellet in 1 mL of room-temperature red cell lysis buffer, and immediately stop the lysis with 1 mL of mDC medium (*see* **Note 5**).
4. Centrifuge cell suspension at 300 × *g* for 7 min. Resuspend pellet in 5 mL mDC medium.
5. Count cells and distribute in a tissue culture–treated 24-well plate, to obtain 10^6 cells/well in 1 mL. Transfer to a 37°C incubator with a 5% CO_2, 95% humidity atmosphere.
6. On day 4, aspirate 0.5 mL of medium from each well with a Gilson pipette and add 1 mL of fresh mDC medium. Under the microscope, loosely attached nodules of mDCs will start appearing as darker mass on the bright layer of adherent cells.
7. On day 7, collect these mDC aggregates by flushing medium against the well wall with a 1 mL Gilson pipette set at 800 μL, in order not to lift up too many of the strongly adherent cells.
8. Pool the cells suspension of each well and re-plate cells at the desired cell density to perform an experiment the next day. Myeloid mDC cell-surface markers should be checked before performing interaction experiments (*see* **Section 3.3**). Myeloid mDCs should be used within 8 days of their preparation.

3.3. Characterization of Cell Markers by FACS Analysis

1. Prepare a 4×10^7 cells/mL suspension in FACS buffer; distribute 12.5 μL (0.5×10^6 cells) in 3 microcentrifuge tubes.
2. Block nonspecific Fc-binding sites with 12.5 μL of CD36/CD32 antibodies diluted 1/25 in FACS buffer.
3. After a 5-min incubation at room temperature, add 25 μL of anti-mouse CD11b-FITC diluted at 1/25 in FACS buffer, or 25 μL of anti-mouse CD11c-APC diluted at 1/25 in FACS buffer, or 25 μL FACS buffer alone for the negative control (*see* **Note 8**).
4. After 15 to 20 min on ice, wash with 800 μL FACS buffer and centrifuge at 300 × *g* for 10 min at 4°C (low-speed centrifugation is important to prevent cell damage). Repeat washing step once.
5. After the second wash, resuspend cell pellet in 500 μL FACS buffer (or less if less cells) and transfer to FACS tube for analysis (*see* **Note 9**).

3.4. Interaction Experiments In Vitro with Candida spp.

1. One day prior to the interaction assay, plate mMPs or mDCs at a density of 1.0×10^5 to 1.25×10^5 cells/cm^2 in a volume of cell culture medium of of 0.2 to 0.4 mL/cm^2 and place them at 37°C in a 5% CO_2, 95% humidity atmosphere.
2. Grow *C.a.* to saturation overnight in 25 mL 1X YPD with continuous shaking at 30°C. The next morning, dilute to 0.2

to 0.3 OD_{600} in 25 mL YPD liquid medium and incubate with continuous shaking at 30°C until the culture reaches 1 OD_{600}.

3. Collect the fungal cells by centrifugation at 1200 × *g* for 5 min at room temperature and rinse the pellet in 50 mL sterile, room temperature H_2O or PBS.
4. Centrifuge again, resuspend the fungal pellet in 1 mL sterile PBS, and determine the fungus counts/mL.
5. Dilute the fungal cell suspension in prewarmed (37°C) high-glucose DMEM without phenol red (*see* **Note 10**) so that fungal-mammalian cell coculture is performed at a ratio of 2 fungal cells per 1 cell mMP or mDC (multiplicity of infection [MOI] 2:1; *see* **Note 11**).
6. Proceed to **step 7** for infection of mMPs or to **step 8** for infection of mDCs.
7. Aspirate the media from mMP culture dishes, replace it with high-glucose DMEM without phenol red with or without *Candida*. Typically, interaction *C.a.*-mMPs are carried out at a 2:1 MOI, either in a 2-mL volume/6-cm dishes or in a 0.5 mL/well volume in 24-well plates. Dishes are maintained at 37°C in a 5% CO_2, 95% humidity atmosphere for a 20 min "infection pulse." Then, media are discarded and replaced with fresh high-glucose DMEM without phenol red and dishes are further incubated at 37°C in a 5% CO_2, 95% humidity atmosphere until collection time.
8. Infection of mDCs is performed as described above for mMPs (**step 7**), except that, because of the poor adhesion properties of inactive mDCs, the *Candida* cell suspension is simply added to the mDC media in a 200-μL volume for 6-cm dishes or in 100 μL/well for 24-well plates. After the 20 min "infection pulse," media of each plate is not discarded but collected and centrifuged at 700 × *g* for 7 min to collect floating cells. After addition of fresh high-glucose DMEM without phenol red, infection plates are further incubated at 37°C in a 5% CO_2, 95% humidity atmosphere until collection time. The cell pellets, kept on ice until collection time, are pooled with the corresponding cell samples.

3.5. Microscopic Internalization Assay (see Note 12)

1. The interaction experiment is performed as described in **Section 3.4**, except that mDCs or mMPs are plated on 12-mm-diameter sterile glass coverslips in 24-well plates 1 day prior to the infection, and a green fluorescent *Candida albicans* strain is used.
2. Terminate infection by carefully transferring each glass coverslip in a new 24-well plate prepared with 0.5 mL ice-cold PBS/well using clamps and guiding with a syringe

needle. Wash gently two more times with 0.5 mL ice-cold sterile PBS.

3. Fix the cells with 200 μL of 1% buffered paraformaldehyde for 5 min on ice. Discard paraformaldehyde solution and wash 3 times with ice-cold sterile PBS.
4. On ice, stain the cell wall of noninternalized fungi with 200 to 300 μL of an ice-cold 15 μM Calcofluor White solution for 5 min in the dark to stain the cell wall. Wash then 3 times with ice-cold sterile PBS.
5. Carefully invert the coverslips onto a drop of mounting medium for fluorescence on a microscopy slide. Observe slides using contrast phase, fluorescein (excitation 485 nm/emission 535 nm) and DAPI (excitation 355 nm/emission 460 nm) filters (**Fig. 11.1**).

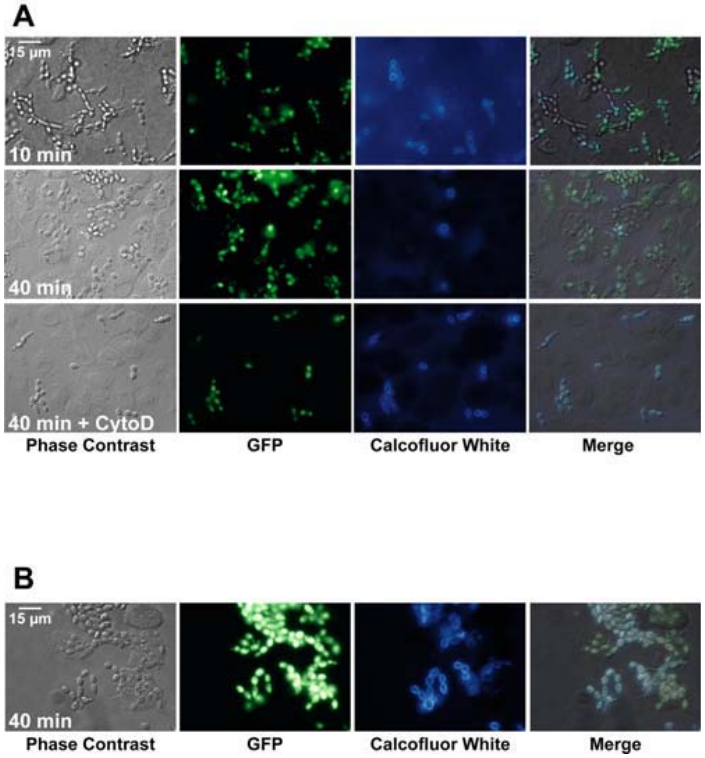

Fig. 11.1. *In vitro* phagocytosis of GFP-labeled *Candida albicans* by mMPs and mDCs. **(A)** mMPs were infected for the indicated time with GFP-*C.a.* at a MOI of 2:1, with or without 2 μM cytochalasin D (cytoD), and processed for Calcofluor White staining (*see* **Section 3.5**). Pictures were obtained on a Zeiss Axioplan2 microscope using a 63× oil-immersion lens, fluorescein and DAPI filters, and a Visitron Imaging System. Phase contrast pictures of the same field at the same magnification are also shown. After a 40-min incubation with GFP-*C.a.*, more "green-only" *C.a.* (internalized) are observed than after 10 min (see merged pictures). As a control for the uptake assay, pretreatment with cytochalasin D is performed as this completely blocks phagocytosis; hence, only double-labeled *C.a.* (noninternalized) are observed. **(B)** representative results of phagocytosis of GFP-*C.a.* by mDCs after infecting for 40 min.

6. For quantification purpose, percentage of internalized fungi can be expressed as (number of Calcofluor White stained fungi)/total of fungi observed in fluorescein channel) × 100.

3.6. Monitoring Activation of Cellular Signaling Pathways

1. Terminate the infection by placing the cell culture dishes on ice and remove media (discard in the case of mMPs, keep and process as described above in **step 8** for mDCs).
2. Scrap the cell layer in 80 μL ice-cold protein lysis buffer, collect in a microcentrifuge tube, and centrifuge at 15,000 × *g* at 4°C for 10 min.
3. Transfer supernatants in fresh tubes containing 30 μL of 4X Sample Buffer.
4. Mix and heat at 95°C for 5 to 7 min, cool on ice, and store at −20°C until further use.
5. After thawing proteins sample at 37°C for 5 min, analyze by SDS-PAGE a 15-μL aliquot on a 10% acrylamide mini gel (0.75 cm) and transfer onto nitrocellulose membrane.
6. Block membranes in 1X TBST containing 10% nonfat dry milk for 1 to 2 h.
7. After a short wash in 1X TBST, probe blots with the primary antibody diluted in 1X TBST with 2% BSA under continuous agitation, at 4°C, overnight (*see* **Note 13**).
8. The next day, wash blots in 1X TBST, and incubate blots with the secondary antibody diluted in 1X TBST with 2% bovine serum albumin (BSA) at room temperature under continuous agitation for 45 min.
9. After 3 to 4 washings in 1X TBST, detect immune complexes using an ECL substrate according to the manufacturer's instructions (**Fig. 11.2**).

3.7. Monitoring Cytokine Gene Expression

1. For RNA isolation from such small amount of mammalian cells, centrifugation column-based kits give very good results. Scraping cells directly in the provided lysis buffer yields a better RNA recovery and better RNA quality.
2. Centrifuge samples at 11,000 × *g* for 8 min and collect supernatants. If too viscous, samples should be passed 4 to 6 times through a syringe fitted with a 20-gauge needle before centrifugation.
3. At that stage, samples can then be kept frozen at −80°C or extraction is pursued according to the manufacturer's instructions.
4. Total RNA samples are eluted in 50 μL RNase-free sterile water.

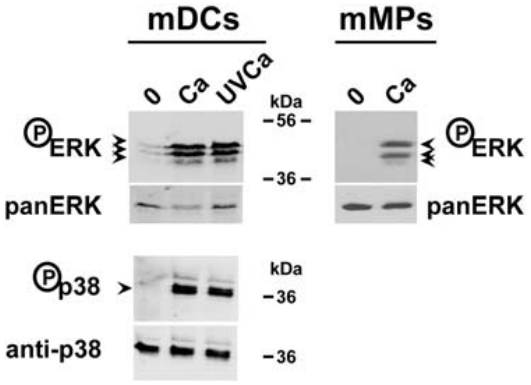

Fig. 11.2. Activation of MAPK in mDCs/mMPs infected with *Candida albicans in vitro*. Cell extracts of mDCs or mMPs incubated with *C.a.* strain SC5314 were collected after 20 and 45 min, respectively, and processed as described in **Section 3.6**. After infecting for 20 min with live SC5314, ERK and p38 activation through phosphorylation was detected in mDCs using phospho-specific antibodies. A similar pattern of MAPK activation was triggered by the UV-killed SC5314 cells, suggesting that early stimulation of these MAPK does not require live fungal cells. ERK phosphorylation is also observed after infecting mMPs for 45 min.

5. Quality control of the samples should include electrophoresis separation of a 5-μL aliquot on a 1% agarose urea-TBE gel for integrity assessment and OD_{260}/OD_{280} measurement of RNA concentration on a 1/20 dilution in Tris 10 mM, pH 7.5.
6. Reverse-transcription is performed on 0.5 to 2 μg total RNA using oligo-dT primers in final volume of 20 μL. The final reverse transcription products are diluted 1:5 with water and stored at −20°C until further use.
7. For the real-time PCR amplification, 5 μL of the diluted cDNAs are added to 20 μL of real-time PCR mix; reactions are submitted to cycling using the following conditions: initial denaturation 95°C for 4 min, followed by 40 cycles (each at 95°C for 10 s, 60°C for 15 s, 72°C for 15 s, and 80°C for 10 s; during these steps, the increase of the fluorescence is recorded); melting curve analysis is done from 60°C to 95°C for 30 min (*see* **Note 14**).
8. For relative quantification, data are analyzed according to the ΔΔCt method and are expressed as the fold-expression (R) of the gene of interest (GOI) versus the expression of a house-keeping gene (GAPDH) in treated (t) versus untreated (ut) conditions. The equation used is $R = 2^{\Delta\Delta Ct}$, where $\Delta\Delta Ct = (\Delta Ct_{GOI}t - \Delta Ct_{GAPDH}t) - (\Delta Ct_{GOI}ut - \Delta Ct_{GAPDH}ut)$ (**Fig. 11.3**).

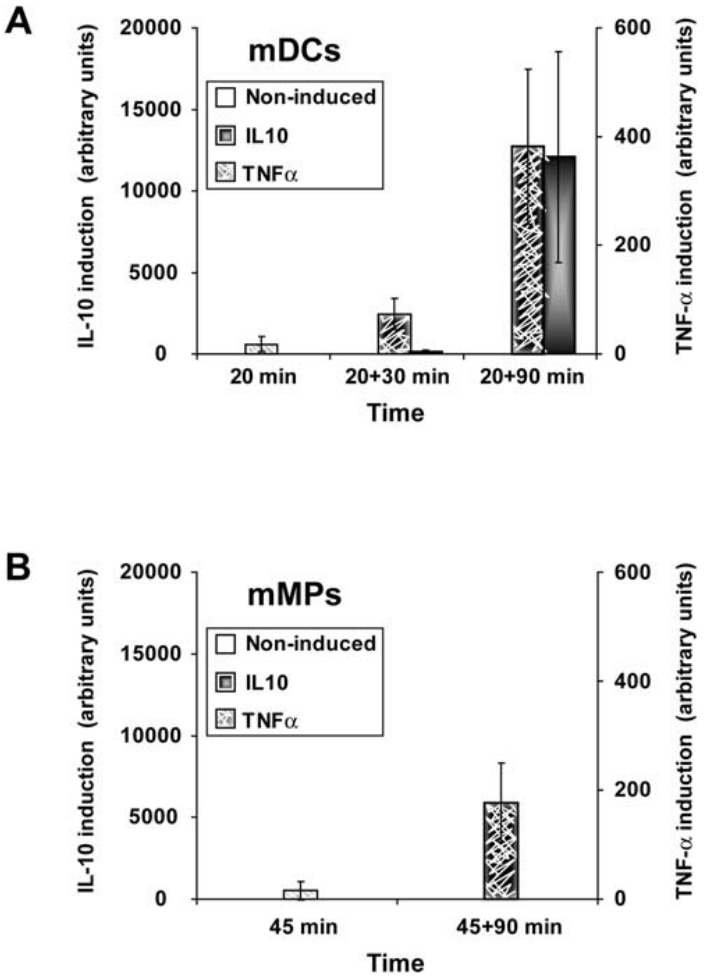

Fig. 11.3. *Candida albicans* triggers TNF-α and IL-10 production in mDCs/mMPs *in vitro*. Cell extracts of mDCs or mMPs incubated with *C.a.* strain SC5314 for a 20-min "pulse" were collected at the indicated times and processed as described in **Section 3.7**. In response to infection, TNF-α mRNA transcription was rapidly activated in both mDCs and mMPs and increased with time. IL-10 mRNA transcription was also induced to a very high extent in mDCs only but not significantly in mMPs.

4. Notes

1. To produce L-conditioned medium, divide 10 confluent 10-cm-diameter dishes of L929 cells (ATCC no. CCL-1) into 20 175-cm^2 flasks with 50 mL/flask of high-glucose DMEM supplemented with 10% FCS without antibiotics. After 36 to 48 hours, when cells are approximately 70% confluent, aspirate the medium and replace it with 100 mL/flask of starving medium (high-glucose DMEM without FCS and antibiotics). After 10 days, collect and filter the conditioned

media on Steritop 0.22-μm GP express PLUS membrane (Millipore, Billerica, MA) to prevent membrane clogging; store 250- to 500-mL aliquots at −20°C. Keep a small aliquot at 4°C for testing (*see* **Note 2**).

2. To test the potency of the L-conditioned media, flush the bones of one mouse as described in **Section 3.1**, divide the cells into five 100 × 100 square Petri dishes. Grow in 11 mL of mMPs cell medium supplemented with 0 to 20% of the fresh batch of L-conditioned medium. As a positive control, also grow two plates in mMPs cell medium supplemented with the optimal concentration of an old batch of L-conditioned medium. After 1 day, add 6 mL of medium. Completely renew the medium every 2 to 3 days. After 5 to 6 days, count the cells at each concentration, and split cells 1:3. Let them grow until confluency and count again. Deduce from the cell count the optimal L-conditioned medium concentration to be used.
3. To produce X-conditioned medium, grow GM-CSF–producing X-63 cell line *(10)* (nonadherent cells) in 10 mL high-glucose DMEM supplemented with 10% FCS, 100 U/mL penicillin, and 100 μg/mL streptomycin in a 75-cm^2 flask until the cell suspension is dense. Dilute the cell suspension at 1:2 with fresh high-glucose DMEM supplemented with 10% FCS, 100 U/mL penicillin, and 100 μg/mL streptomycin. When cells start to become dense again, add 30 mL of starvation media (high-glucose DMEM only) and grow until cells are confluent. Then, transfer into a 250-mL flask and add 50 mL of fresh starvation media. When cells are dense again, add 100 mL of starvation media. After 8 to 10 days, when a large amount of cells are dead, collect X-conditioned medium, centrifuge at 1000 × *g* for 5 min to remove the X-cells, and proceed as described above in **Notes 1 and 2** for sterile-filtration, storage, and testing.
4. Older mice can be used, but the number of bone marrow cells recovered will be smaller.
5. All given volumes are for the limbs of one mouse and should be multiplied according to the number of limbs.
6. Only mMPs will adhere to the non–tissue culture treated plastic, allowing for their separation from other cell types, the latter being eliminated when the media is changed.
7. Alternatively, 4-day-old mMPs can be frozen in FCS with 10% DMSO and stored in liquid nitrogen until use. They should be regrown for about 6 to 7 days in mMPs media before use.
8. To spare cells, double labeling can be performed. In that case, prepare 23 μL FACS buffer + 1 μL from each antibody, and incubate for 15 to 20 min on ice.

9. Typically, mMPs are $CD11^+$ positive and $CD11c^-$ negative. With the above-described method, one can expect to obtain at least 95% pure mMPs in 9- to 10-day-old primary cultures. In our conditions, the expression of mMP cell surface markers is stable up to 14 days after isolation. Myeloid DCs are both $CD11b^+$ positive and $CD11c^+$ positive; this method yields routinely cell preparations of 50% to 70% pure mDCs.
10. Host-pathogen interaction experiments are carried out in DMEM without serum and phenol red to slow hyphae formation of dimorphic fungi (i.e., *C.a.*). For the same reason, the dilution in DMEM should be performed just prior to starting the coculture with mammalian cells, as DMEM rapidly induces hyphae formation.
11. To check the *Candida* suspension used for infection, serial dilutions of the fungal cell suspension are plated on YPD agar plates on the day of the infection assay and incubated at 30°C. After 1 to 2 days, colony-forming units (CFU) are counted in order to control the actual MOI of the *in vitro* infection assay and verify the absence of contaminating microbes.
12. This method uses Calcofluor White (CW), a fluorescent dye (excitation 355 nm/emission 460 nm), which specifically binds to nascent fibrils of chitin in the fungal cell wall *(19)*. CW specifically stains fungal cells but fails to penetrate into mammalian cells. After staining with this dye, cell walls of noninternalized fungi appear as a bright blue ring when inspected by microscopy using appropriate filters.
13. Adding 0.05% sodium azide to primary antibody dilutions and performing incubations at 4°C will allow one to re-use primary antibody dilutions several time if stored at 4°C. Sodium azide should *not* be added to the dilution of horseradish peroxidase–coupled secondary antibodies and washing buffers, as it inhibits the enzyme activity.
14. Better reproducibility is achieved with the real-time PCR analysis when using only 1 to 2 μg of total RNA in the reverse transcription reactions. Each real-time PCR assay data point should be performed at least in triplicate. Recording of the fluorescence increase "in real-time" is performed during the "10 s at 80°C" step to favor the dissociation of possible nonspecific products, leading to a more accurate measurement of the amplicon.

Acknowledgments

We are very grateful to Alexander Johnson for kindly providing us with the GFP-labeled *Candida albicans* strain. We thank the laboratory of Thomas Decker (University of Vienna, Vienna,

Austria) for their technical support and advice. In particular, we acknowledge the invaluable advice and encouragements from Tilo Materna, Sylvia Stockinger, Andreas Pilz, and Katrin Ramsauer. We also thank all lab members for the help with culturing fungal pathogens. This work was supported by the "Wiener Wissenschafts Forschungs- und Technologiefonds" (HOPI-LS133-WWTF) and by the European Union through the funding of the EC Marie Curie Training Network *"CanTrain"* (CT-2004-512481). Additional funds came from the Herzfelder Foundation.

References

1. Roeder A, Kirschning CJ, Rupec RA, Schaller M, Korting HC. *Toll*-like receptors and innate antifungal responses. Trends Microbiol 2004;12:44–9.
2. Netea MG, Van der Graaf C, Van der Meer JW, Kullberg BJ. Recognition of fungal pathogens by *Toll*-like receptors: *Toll*-like receptors and the host defense against microbial pathogens: bringing specificity to the innate-immune system. Eur J Clin Microbiol Infect Dis 2004;23:672–6.
3. Mencacci A, Cenci E, Del Sero G, et al. Defective co-stimulation and impaired Th1 development in tumor necrosis factor/lymphotoxin-alpha double-deficient mice infected with *Candida albicans*. Int Immunol 1998;10:37–48.
4. Vazquez-Torres A, Jones-Carson J, Wagner RD, Warner T, Balish E. Early resistance of interleukin-10 knock-out mice to acute systemic candidiasis. Infect Immun 1999;67:670–4.
5. Farah CS, Hu Y, Riminton S, Ashman RB. Distinct roles for interleukin-12p40 and tumour necrosis factor in resistance to oral candidiasis defined by gene-targeting. Oral Microbiol Immunol 2006;21: 252–5.
6. Vonk AG, Netea MG, van Krieken JH, van der Meer JW, Kullberg BJ. Delayed clearance of intraabdominal abscesses caused by *Candida albicans* in tumor necrosis factor-alpha- and lymphotoxin-alpha-deficient mice. J Infect Dis 2002;186:1815–22.
7. Ibata-Ombetta S, Jouault T, Trinel PA, Poulain D. Role of extracellular signal-regulated protein kinase cascade in macrophage killing of *Candida albicans*. J Leukoc Biol 2001;70:149–54.
8. Zhong B, Jiang K, Gilvary DL, et al. Human neutrophils utilize a Rac/Cdc42-dependent MAPK pathway to direct intracellular granule mobilization toward ingested microbial pathogens. Blood 2003;101:3240–8.
9. Choi JH, Choi EK, Park SJ, et al. Impairment of p38 MAPK-mediated cytosolic phospholipase A(2) activation in the kidneys is associated with pathogenicity of *Candida albicans*. Immunology 2007; 120:173–81.
10. Zal T, Volkmann A, Stockinger B. Mechanisms of tolerance induction in major histocompatibility complex class II-restricted T cells specific for a blood-borne self-antigen. J Exp Med 1994;180: 2089–99.
11. Gillum AM, Tsay EY, Kirsch DR. Isolation of the Candida albicans gene for orotidine-5′-phosphate decarboxylase by complementation of *S. cerevisiae* ura3 and *E. coli pyrF* mutations. Mol Gen Genet 1984;198:179–82.
12. Hull CM, Johnson AD. Identification of a mating type-like locus in the asexual pathogenic yeast *Candida albicans*. Science 1999;285:1271–5.
13. Kovarik P, Stoiber D, Novy M, Decker T. Stat1 combines signals derived from IFN-gamma and LPS receptors during macrophage activation. EMBO J 1998;17: 3660–8.
14. Overbergh L, Giulietti A, Valckx D, Decallonne R, Bouillon R, Mathieu C. The use of real-time reverse transcriptase PCR for the quantification of cytokine gene expression. J Biomol Tech 2003;14:33–43.
15. Pattyn F, Speleman F, De Paepe A, Vandesompele J. RTPrimerDB: the Real-Time PCR primer and probe database. Nucl Acids Res 2003;31:122–3.

16. Pattyn F, Robbrecht P, De Paepe A, Speleman F, Vandesompele J. RTPrimerDB: the real-time PCR primer and probe database, major update 2006. Nucl Acids Res 2006;34:D684–8.
17. Hume DA, Gordon S. Optimal conditions for proliferation of bone marrow-derived mouse macrophages in culture: the roles of CSF-1, serum, Ca^{2+}, and adherence. J Cell Physiol 1983;117: 189–94.
18. Inaba K, Inaba M, Romani N, et al. Generation of large numbers of dendritic cells from mouse bone marrow cultures supplemented with granulocyte/macrophage colony-stimulating factor. J Exp Med 1992; 176:1693–702.
19. Herth W. Calcofluor white and Congo red inhibit chitin microfibril assembly of *Poterioochromonas*: evidence for a gap between polymerization and microfibril formation. J Cell Biol 1980;87:442–50.

VI. Literature

Abbas, A.K., Lichtman, A.H., and Pillai, S. (2007). Cellular and molecular immunology, 6th edn (Philadelphia: Saunders Elsevier).

Abe, M.K., Kartha, S., Karpova, A.Y., Li, J., Liu, P.T., Kuo, W.L., and Hershenson, M.B. (1998). Hydrogen peroxide activates extracellular signal-regulated kinase via protein kinase C, Raf-1, and MEK1. Am J Respir Cell Mol Biol *18*, 562-569.

Adams, D.S., Pero, S.C., Petro, J.B., Nathans, R., Mackin, W.M., and Wakshull, E. (1997). PGG-Glucan activates NF-kappaB-like and NF-IL-6-like transcription factor complexes in a murine monocytic cell line. J Leukoc Biol *62*, 865-873.

Aikawa, R., Komuro, I., Yamazaki, T., Zou, Y., Kudoh, S., Tanaka, M., Shiojima, I., Hiroi, Y., and Yazaki, Y. (1997). Oxidative stress activates extracellular signal-regulated kinases through Src and Ras in cultured cardiac myocytes of neonatal rats. J Clin Invest *100*, 1813-1821.

Akira, S. (2006). TLR signaling. Curr Top Microbiol Immunol *311*, 1-16.

Akira, S., Uematsu, S., and Takeuchi, O. (2006). Pathogen recognition and innate immunity. Cell *124*, 783-801.

Alarco, A.-M., and Raymond, M. (1999). The bZip Transcription Factor Cap1p Is Involved in Multidrug Resistance and Oxidative Stress Response in *Candida albicans*. J. Bacteriol. *181*, 700-708.

Alberti-Segui, C., Morales, A.J., Xing, H., Kessler, M.M., Willins, D.A., Weinstock, K.G., Cottarel, G., Fechtel, K., and Rogers, B. (2004). Identification of potential cell-surface proteins in *Candida albicans* and investigation of the role of a putative cell-surface glycosidase in adhesion and virulence. Yeast *21*, 285-302.

Almeida, R.S., Brunke, S., Albrecht, A., Thewes, S., Laue, M., Edwards, J.E., Filler, S.G., and Hube, B. (2008). the hyphal-associated adhesin and invasin Als3 of *Candida albicans* mediates iron acquisition from host ferritin. PLoS Pathog *4*, e1000217.

Alonso-Monge, R., Navarro-Garcia, F., Roman, E., Negredo, A.I., and Eisman, B. (2003). The Hog1 mitogen-activated protein kinase is essential in the oxidative stress response and chlamydospore formation in *Candida albicans*. Eukaryot. Cell *2*, 351.

Arana, D.M., Nombela, C., Alonso-Monge, R., and Pla, J. (2005). The Pbs2 MAP kinase kinase is essential for the oxidative-stress response in the fungal pathogen *Candida albicans*. Microbiology *151*, 1033-1049.

Aratani, Y., Kura, F., Watanabe, H., Akagawa, H., Takano, Y., Suzuki, K., Dinauer, M.C., Maeda, N., and Koyama, H. (2002). Relative contributions of myeloperoxidase and NADPH-oxidase to the early host defense against pulmonary infections with *Candida albicans* and *Aspergillus fumigatus*. Med Mycol *40*, 557-563.

Ariizumi, K., Shen, G.L., Shikano, S., Xu, S., Ritter, R., 3rd, Kumamoto, T., Edelbaum, D., Morita, A., Bergstresser, P.R., and Takashima, A. (2000). Identification of a novel, dendritic cell-associated molecule, dectin-1, by subtractive cDNA cloning. J Biol Chem *275*, 20157-20167.

Ausubel, F.M. (2005). Are innate immune signaling pathways in plants and animals conserved? Nat Immunol *6*, 973-979.

Babior, B.M. (2002). The leukocyte NADPH oxidase. Isr Med Assoc J *4*, 1023-1024.

Babior, B.M. (2004). NADPH oxidase. Curr Opin Immunol *16*, 42-47.

Bae, Y.S., Lee, J.H., Choi, S.H., Kim, S., Almazan, F., Witztum, J.L., and Miller, Y.I. (2009). Macrophages generate reactive oxygen species in response to minimally oxidized low-density lipoprotein: toll-like receptor 4- and spleen tyrosine kinase-dependent activation of NADPH oxidase 2. Circ Res *104*, 210-218, 221p following 218.

Bahn, Y.S., and Sundstrom, P. (2001). CAP1, an adenylate cyclase-associated protein gene, regulates bud-hypha transitions, filamentous growth, and cyclic AMP levels and is required for virulence of *Candida albicans*. J Bacteriol *183*, 3211-3223.

Beckman, J.S., Beckman, T.W., Chen, J., Marshall, P.A., and Freeman, B.A. (1990). Apparent hydroxyl radical production by peroxynitrite: implications for endothelial injury from nitric oxide and superoxide. Proc Natl Acad Sci U S A *87*, 1620-1624.

Bellocchio, S., Montagnoli, C., Bozza, S., Gaziano, R., Rossi, G., Mambula, S.S., Vecchi, A., Mantovani, A., Levitz, S.M., and Romani, L. (2004). The contribution of the Toll-like/IL-1 receptor superfamily to innate and adaptive immunity to fungal pathogens in vivo. J Immunol *172*, 3059-3069.

Bennett, R.J., and Johnson, A.D. (2005). Mating in Candida albicans and the search for a sexual cycle. Annu. Rev. Microbiol. *59*, 233.

Berman, J., and Sudbery, P.E. (2002). *Candida albicans*: a molecular revolution built on lessons from budding yeast. Nat Rev Genet *3*, 918-930.

Bernstein, E., Caudy, A.A., Hammond, S.M., and Hannon, G.J. (2001). Role for a bidentate ribonuclease in the initiation step of RNA interference. Nature *409*, 363-366.

Berton, G., and Lowell, C.A. (1999). Integrin signalling in neutrophils and macrophages. Cell Signal *11*, 621-635.

Bicanic, T., Wood, R., Bekker, L.G., Darder, M., Meintjes, G., and Harrison, T.S. (2005). Antiretroviral roll-out, antifungal roll-back: access to treatment for cryptococcal meningitis. Lancet Infect Dis *5*, 530-531.

Biondo, C., Midiri, A., Gambuzza, M., Gerace, E., Falduto, M., Galbo, R., Bellantoni, A., Beninati, C., Teti, G., Leanderson, T., and Mancuso, G. (2008). IFN-{alpha}/{beta} Signaling Is Required for Polarization of Cytokine Responses toward a Protective Type 1 Pattern during Experimental Cryptococcosis. J Immunol *181*, 566-573.

Biswas, S., Van Dijck, P., and Datta, A. (2007). Environmental sensing and signal transduction pathways regulating morphopathogenic determinants of *Candida albicans*. Microbiol Mol Biol Rev *71*, 348-376.

Blanco, J.L., and Garcia, M.E. (2008). Immune response to fungal infections. Veterinary Immunology and Immunopathology *125*, 47-70.

Blasi, E., Mucci, A., Neglia, R., Pezzini, F., Colombari, B., Radzioch, D., Cossarizza, A., Lugli, E., Volpini, G., Del Giudice, G., and Peppoloni, S. (2005). Biological importance of the two Toll-like receptors, TLR2 and TLR4, in macrophage response to infection with *Candida albicans*. FEMS Immunol Med Microbiol *44*, 69-79.

Bouin, A.P., Grandvaux, N., Vignais, P.V., and Fuchs, A. (1998). p40(phox) is phosphorylated on threonine 154 and serine 315 during activation of the phagocyte NADPH oxidase. Implication of a protein kinase c-type kinase in the phosphorylation process. J Biol Chem *273*, 30097-30103.

Braselmann, S., Taylor, V., Zhao, H., Wang, S., Sylvain, C., Baluom, M., Qu, K., Herlaar, E., Lau, A., Young, C., *et al.* (2006). R406, an Orally Available Spleen Tyrosine Kinase Inhibitor Blocks Fc Receptor Signaling and Reduces Immune Complex-Mediated Inflammation. J Pharmacol Exp Ther *319*, 998-1008.

Brown, A.J., Odds, F.C., and Gow, N.A. (2007). Infection-related gene expression in *Candida albicans*. Curr Opin Microbiol *10*, 307-313.

Brown, G.D. (2006). Dectin-1: a signalling non-TLR pattern-recognition receptor. Nat Rev Immunol *6*, 33-43.

Brown, G.D., and Gordon, S. (2003). Fungal [beta]-glucans and mammalian immunity. Immunity *19*, 311-315.

Brown, G.D., and Gordon, S. (2005). Immune recognition of fungal [beta]-glucans. Cell Microbiol *7*, 471-479.

Brown, G.D., Herre, J., Williams, D.L., Willment, J.A., Marshall, A.S., and Gordon, S. (2003). Dectin-1 mediates the biological effects of beta-glucans. J Exp Med *197*, 1119-1124.

Brumell, J.H., Burkhardt, A.L., Bolen, J.B., and Grinstein, S. (1996). Endogenous reactive oxygen intermediates activate tyrosine kinases in human neutrophils. J Biol Chem *271*, 1455-1461.

Bugarcic, A., Hitchens, K., Beckhouse, A.G., Wells, C.A., Ashman, R.B., and Blanchard, H. (2008). Human and mouse macrophage-inducible C-type lectin (Mincle) bind *Candida albicans*. Glycobiology *18*, 679-685.

Calderone, R.A. (1993). Recognition between *Candida albicans* and host cells. Trends Microbiol *1*, 55-58.

Calderone, R.A. (2002). Candida and candidiasis (Washington, D.C.: ASM Press).

Cambi, A., Gijzen, K., de Vries, J.M., Torensma, R., Joosten, B., Adema, G.J., Netea, M.G., Kullberg, B.J., Romani, L., and Figdor, C.G. (2003). The C-type lectin DC-SIGN (CD209) is an antigen-uptake receptor for *Candida albicans* on dendritic cells. Eur J Immunol *33*, 532-538.

Cardoso, L.S., Araujo, M.I., Goes, A.M., Pacifico, L.G., Oliveira, R.R., and Oliveira, S.C. (2007). Polymyxin B as inhibitor of LPS contamination of *Schistosoma mansoni* recombinant proteins in human cytokine analysis. Microb Cell Fact *6*, 1.

Carlile, M.J., and Watkinson, S.C. (1994). The fungi (London ; Boston: Academic Press).

Carroll, M.C. (2008). Complement and humoral immunity. Vaccine *26 Suppl 8*, I28-33.

Castillo, L., Martinez, A.I., Garcera, A., Elorza, M.V., Valentin, E., and Sentandreu, R. (2003). Functional analysis of the cysteine residues and the repetitive sequence of *Saccharomyces cerevisiae* Pir4/Cis3: the repetitive sequence is needed for binding to the cell wall beta-1,3-glucan. Yeast *20*, 973-983.

Celec, P. (2004). Nuclear factor kappa B--molecular biomedicine: the next generation. Biomed Pharmacother *58*, 365-371.

Chaffin, W.L. (2008). *Candida albicans* cell wall proteins. Microbiol Mol Biol Rev *72*, 495-544.

Charles, J.F., Humphrey, M.B., Zhao, X., Quarles, E., Nakamura, M.C., Aderem, A., Seaman, W.E., and Smith, K.D. (2008). The innate immune response to *Salmonella enterica serovar Typhimurium* by macrophages is dependent on TREM2-DAP12. Infect Immun *76*, 2439-2447.

Chauhan, N., Inglis, D., Roman, E., Pla, J., Li, D., Calera, J.A., and Calderone, R. (2003). *Candida albicans* response regulator gene *SSK1* regulates a subset of genes whose functions are associated with cell wall biosynthesis and adaptation to oxidative stress. Eukaryot Cell *2*, 1018-1024.

Chaves, G.M., Bates, S., Maccallum, D.M., and Odds, F.C. (2007). *Candida albicans GRX2*, encoding a putative glutaredoxin, is required for virulence in a murine model. Genet Mol Res *6*, 1051-1063.

Cheng, G., Wozniak, K., Wallig, M.A., Fidel, P.L., Jr., Trupin, S.R., and Hoyer, L.L. (2005). Comparison between *Candida albicans* agglutinin-like sequence gene expression patterns in human clinical specimens and models of vaginal candidiasis. Infect Immun *73*, 1656-1663.

Chinen, T., Qureshi, M.H., Koguchi, Y., and Kawakami, K. (1999). *Candida albicans* suppresses nitric oxide (NO) production by interferon-gamma (IFN-gamma) and lipopolysaccharide (LPS)-stimulated murine peritoneal macrophages. Clin Exp Immunol *115*, 491-497.

Cullen, B.R. (2006). Enhancing and confirming the specificity of RNAi experiments. Nat Methods *3*, 677-681.

Dahlgren, C., and Karlsson, A. (1999). Respiratory burst in human neutrophils. J Immunol Methods *232*, 3-14.

Davis, D., Wilson, R.B., and Mitchell, A.P. (2000). RIM101-dependent and-independent pathways govern pH responses in *Candida albicans*. Mol. Cell. Biol. *20*, 971.

De Groot, P.W., Ram, A.F., and Klis, F.M. (2005). Features and functions of covalently linked proteins in fungal cell walls. Fungal Genet Biol *42*, 657-675.

de Nobel, H., and Lipke, P.N. (1994). Is there a role for GPIs in yeast cell-wall assembly? Trends Cell Biol *4*, 42-45.

Del Sero, G., Mencacci, A., Cenci, E., d'Ostiani, C.F., Montagnoli, C., Bacci, A., Mosci, P., Kopf, M., and Romani, L. (1999). Antifungal type 1 responses are upregulated in IL-10-deficient mice. Microbes Infect *1*, 1169-1180.

Dellinger, E.P., Babineau, T.J., Bleicher, P., Kaiser, A.B., Seibert, G.B., Postier, R.G., Vogel, S.B., Norman, J., Kaufman, D., Galandiuk, S., and Condon, R.E. (1999). Effect of PGG-glucan on the rate of serious postoperative infection or death observed after high-risk gastrointestinal operations. Betafectin Gastrointestinal Study Group. Arch Surg *134*, 977-983.

Dennehy, K.M., Ferwerda, G., Faro-Trindade, I., Pyz, E., Willment, J.A., Taylor, P.R., Kerrigan, A., Tsoni, S.V., Gordon, S., Meyer-Wentrup, F.*, et al.* (2008). Syk kinase is required for collaborative cytokine production induced through Dectin-1 and Toll-like receptors. Eur J Immunol *38*, 500-506.

Dillon, S., Agrawal, S., Banerjee, K., Letterio, J., Denning, T.L., Oswald-Richter, K., Kasprowicz, D.J., Kellar, K., Pare, J., van Dyke, T.*, et al.* (2006). Yeast zymosan, a stimulus for TLR2 and dectin-1, induces regulatory antigen-presenting cells and immunological tolerance. J Clin Invest *116*, 916-928.

Dinauer, M.C. (1993). The respiratory burst oxidase and the molecular genetics of chronic granulomatous disease. Crit Rev Clin Lab Sci *30*, 329-369.

Ding, H., Schwarz, D.S., Keene, A., Affar el, B., Fenton, L., Xia, X., Shi, Y., Zamore, P.D., and Xu, Z. (2003). Selective silencing by RNAi of a dominant allele that causes amyotrophic lateral sclerosis. Aging Cell *2*, 209-217.

Ding, K., Shibui, A., Wang, Y., Takamoto, M., Matsuguchi, T., and Sugane, K. (2005). Impaired recognition by Toll-like receptor 4 is responsible for exacerbated murine *Pneumocystis pneumonia*. Microbes Infect *7*, 195-203.

Dormer, U.H., Westwater, J., Stephen, D.W., and Jamieson, D.J. (2002). Oxidant regulation of the Saccharomyces cerevisiae GSH1 gene. Biochim Biophys Acta *1576*, 23-29.

Du, C., Calderone, R., Richert, J., and Li, D. (2005). Deletion of the *SSK1* response regulator gene in *Candida albicans* contributes to enhanced killing by human polymorphonuclear neutrophils. Infect Immun *73*, 865-871.

El-Benna, J., Dang, P.M., Gougerot-Pocidalo, M.A., and Elbim, C. (2005). Phagocyte NADPH oxidase: a multicomponent enzyme essential for host defenses. Arch Immunol Ther Exp (Warsz) *53*, 199-206.

El-Benna, J., Dang, P.M., Gougerot-Pocidalo, M.A., Marie, J.C., and Braut-Boucher, F. (2009). p47phox, the phagocyte NADPH oxidase/NOX2 organizer: structure, phosphorylation and implication in diseases. Exp Mol Med *41*, 217-225.

Enjalbert, B., Smith, D.A., Cornell, M.J., Alam, I., Nicholls, S., Brown, A.J., and Quinn, J. (2006). Role of the Hog1 stress-activated protein kinase in the global transcriptional response to stress in the fungal pathogen *Candida albicans*. Mol Biol Cell *17*, 1018-1032.

Evans, T.J., Buttery, L.D., Carpenter, A., Springall, D.R., Polak, J.M., and Cohen, J. (1996). Cytokine-treated human neutrophils contain inducible nitric oxide synthase that produces nitration of ingested bacteria. Proc Natl Acad Sci U S A *93*, 9553-9558.

Farah, C.S., Saunus, J.M., Hu, Y., Kazoullis, A., and Ashman, R.B. (2009). Gene targeting demonstrates that inducible nitric oxide synthase is not essential for resistance to oral candidiasis in mice, or for killing of *Candida albicans* by macrophages in vitro. Oral Microbiol Immunol *24*, 83-88.

Ferwerda, G., Meyer-Wentrup, F., Kullberg, B.J., Netea, M.G., and Adema, G.J. (2008). Dectin-1 synergizes with TLR2 and TLR4 for cytokine production in human primary monocytes and macrophages. Cell Microbiol *10*, 2058-2066.

Fialkow, L., Wang, Y., and Downey, G.P. (2007). Reactive oxygen and nitrogen species as signaling molecules regulating neutrophil function. Free Radic Biol Med *42*, 153-164.

Fidel, P.L. (2007). History and update on host defense against vaginal candidiasis. Am. J. Reprod. Immunol. *57*, 2-12.

Forman, H.J., and Torres, M. (2002). Reactive oxygen species and cell signaling: respiratory burst in macrophage signaling. Am J Respir Crit Care Med *166*, S4-8.

Fradin, C., De Groot, P., MacCallum, D., Schaller, M., Klis, F., Odds, F.C., and Hube, B. (2005). Granulocytes govern the transcriptional response, morphology and proliferation of *Candida albicans* in human blood. Mol Microbiol *56*, 397-415.

Fradin, C., Jouault, T., Mallet, A., Mallet, J.M., Camus, D., Sinay, P., and Poulain, D. (1996). Beta-1,2-linked oligomannosides inhibit *Candida albicans* binding to murine macrophage. J Leukoc Biol *60*, 81-87.

Fradin, C., Poulain, D., and Jouault, T. (2000). beta-1,2-linked oligomannosides from *Candida albicans* bind to a 32-kilodalton macrophage membrane protein homologous to the mammalian lectin galectin-3. Infect Immun *68*, 4391-4398.

Frieman, M.B., and Cormack, B.P. (2003). The omega-site sequence of glycosylphosphatidylinositol-anchored proteins in *Saccharomyces cerevisiae* can determine distribution between the membrane and the cell wall. Mol Microbiol *50*, 883-896.

Fuller, G.L., Williams, J.A., Tomlinson, M.G., Eble, J.A., Hanna, S.L., Pohlmann, S., Suzuki-Inoue, K., Ozaki, Y., Watson, S.P., and Pearce, A.C. (2007). The C-type lectin receptors CLEC-2 and Dectin-1, but not DC-SIGN, signal via a novel YXXL-dependent signaling cascade. J Biol Chem *282*, 12397-12409.

Gantner, B.N., Simmons, R.M., Canavera, S.J., Akira, S., and Underhill, D.M. (2003). Collaborative induction of inflammatory responses by dectin-1 and Toll-like receptor 2. J Exp Med *197*, 1107-1117.

Gantner, B.N., Simmons, R.M., and Underhill, D.M. (2005). Dectin-1 mediates macrophage recognition of *Candida albicans* yeast but not filaments. Embo J *24*, 1277-1286.

Gil, M.L., and Gozalbo, D. (2006). TLR2, but not TLR4, triggers cytokine production by murine cells in response to *Candida albicans* yeasts and hyphae. Microbes Infect *8*, 2299-2304.

Goodridge, H.S., Shimada, T., Wolf, A.J., Hsu, Y.M., Becker, C.A., Lin, X., and Underhill, D.M. (2009). Differential use of CARD9 by dectin-1 in macrophages and dendritic cells. J Immunol *182*, 1146-1154.

Gow, N.A., Robbins, P.W., Lester, J.W., Brown, A.J., Fonzi, W.A., Chapman, T., and Kinsman, O.S. (1994). A hyphal-specific chitin synthase gene (*CHS2*) is not essential for growth, dimorphism, or virulence of *Candida albicans*. Proc Natl Acad Sci U S A *91*, 6216-6220.

Green, C.B., Cheng, G., Chandra, J., Mukherjee, P., Ghannoum, M.A., and Hoyer, L.L. (2004). RT-PCR detection of *Candida albicans* ALS gene expression in the reconstituted human epithelium (RHE) model of oral candidiasis and in model biofilms. Microbiology *150*, 267-275.

Green, C.B., Marretta, S.M., Cheng, G., Faddoul, F.F., Ehrhart, E.J., and Hoyer, L.L. (2006). RT-PCR analysis of *Candida albicans* ALS gene expression in a hyposalivatory rat model of oral candidiasis and in HIV-positive human patients. Med Mycol *44*, 103-111.

Gringhuis, S.I., den Dunnen, J., Litjens, M., van der Vlist, M., Wevers, B., Bruijns, S.C., and Geijtenbeek, T.B. (2009). Dectin-1 directs T helper cell differentiation by controlling noncanonical NF-kappaB activation through Raf-1 and Syk. Nat Immunol *10*, 203-213.

Gropp, K., Schild, L., Schindler, S., Hube, B., Zipfel, P.F., and Skerka, C. (2009). The yeast *Candida albicans* evades human complement attack by secretion of aspartic proteases. Mol Immunol *47*, 465-475.

Gross, O. (2006). Card9 controls a non-TLR signalling pathway for innate anti-fungal immunity. Nature *442*, 651-656.

Gross, O., Poeck, H., Bscheider, M., Dostert, C., Hannesschlager, N., Endres, S., Hartmann, G., Tardivel, A., Schweighoffer, E., Tybulewicz, V.*, et al.* (2009). Syk kinase signalling couples to the Nlrp3 inflammasome for anti-fungal host defence. Nature *459*, 433-436.

Gurney, A.M., and Hunter, E. (2005). The use of small interfering RNA to elucidate the activity and function of ion channel genes in an intact tissue. Journal of Pharmacological and Toxicological Methods *51*, 253-262.

Guyton, K.Z., Liu, Y., Gorospe, M., Xu, Q., and Holbrook, N.J. (1996). Activation of mitogen-activated protein kinase by H_2O_2. Role in cell survival following oxidant injury. J Biol Chem *271*, 4138-4142.

Hammond, S.M., Bernstein, E., Beach, D., and Hannon, G.J. (2000). An RNA-directed nuclease mediates post-transcriptional gene silencing in Drosophila cells. Nature *404*, 293-296.

Hammond, S.M., Boettcher, S., Caudy, A.A., Kobayashi, R., and Hannon, G.J. (2001). Argonaute2, a link between genetic and biochemical analyses of RNAi. Science *293*, 1146-1150.

Hannon, G.J. (2002). RNA interference. Nature *418*, 244-251.

Hannon, G.J., and Rossi, J.J. (2004). Unlocking the potential of the human genome with RNA interference. Nature *431*, 371-378.

Hara, H., Ishihara, C., Takeuchi, A., Imanishi, T., Xue, L., Morris, S.W., Inui, M., Takai, T., Shibuya, A., Saijo, S*., et al.* (2007). The adaptor protein CARD9 is essential for the activation of myeloid cells through ITAM-associated and Toll-like receptors. Nat Immunol *8*, 619-629.

Heinsbroek, S.E.M., Taylor, P.R., Martinez, F.O., Martinez-Pomares, L., Brown, G.D., and Gordon, S. (2008). Stage-Specific Sampling by Pattern Recognition Receptors during *Candida albicans* Phagocytosis. PLoS Pathogens *4*, e1000218-e1000218.

Hernanz-Falcon, P., Joffre, O., Williams, D.L., and Reis, E.S.C. (2009). Internalization of Dectin-1 terminates induction of inflammatory responses. Eur J Immunol *39*, 507-513.

Herre, J., Marshall, A.S., Caron, E., Edwards, A.D., Williams, D.L., Schweighoffer, E., Tybulewicz, V., Reis e Sousa, C., Gordon, S., and Brown, G.D. (2004). Dectin-1 uses novel mechanisms for yeast phagocytosis in macrophages. Blood *104*, 4038-4045.

Hibbett, D.S., Binder, M., Bischoff, J.F., Blackwell, M., Cannon, P.F., Eriksson, O.E., Huhndorf, S., James, T., Kirk, P.M., Lucking, R*., et al.* (2007). A higher-level phylogenetic classification of the Fungi. Mycol Res *111*, 509-547.

Hnisz, D., Schwarzmüller, T., and Kuchler, K. (2009). Transcriptional loops meet chromatin: a dual-layer network controls white-opaque switching in *Candida albicans*. Mol Microbiol *74*, 1-15.

Hohmann, S., Krantz, M., and Nordlander, B. (2007). Yeast osmoregulation. Methods Enzymol *428*, 29-45.

Hohn, D.C., and Lehrer, R.I. (1975). NADPH oxidase deficiency in X-linked chronic granulomatous disease. J Clin Invest *55*, 707-713.

Hoyer, L.L. (2001). The ALS gene family of *Candida albicans*. Trends Microbiol. *9*, 176.

Hoyer, L.L., Green, C.B., Oh, S.H., and Zhao, X. (2008). Discovering the secrets of the *Candida albicans* agglutinin-like sequence (ALS) gene family--a sticky pursuit. Med Mycol *46*, 1-15.

Huang, G., Wang, H., Chou, S., Nie, X., Chen, J., and Liu, H. (2006). Bistable expression of WOR1, a master regulator of white-opaque switching in *Candida albicans*. Proc. Natl. Acad. Sci. USA *103*, 12813.

Hube, B. (2000). Extracellular proteinases of human pathogenic fungi. Contrib Microbiol *5*, 126-137.

Hube, B., Stehr, F., Bossenz, M., Mazur, A., Kretschmar, M., and Schafer, W. (2000). Secreted lipases of *Candida albicans*: cloning, characterisation and expression analysis of a new gene family with at least ten members. Arch Microbiol *174*, 362-374.

Husemann, J., Obstfeld, A., Febbraio, M., Kodama, T., and Silverstein, S.C. (2001). CD11b/CD18 mediates production of reactive oxygen species by mouse and human macrophages adherent to matrixes containing oxidized LDL. Arterioscler Thromb Vasc Biol *21*, 1301-1305.

Huysamen, C., and Brown, G.D. (2009). The fungal pattern recognition receptor, Dectin-1, and the associated cluster of C-type lectin-like receptors. FEMS Microbiol Lett *290*, 121-128.

Hwang, C.S., Baek, Y.U., Yim, H.S., and Kang, S.O. (2003). Protective roles of mitochondrial manganese-containing superoxide dismutase against various stresses in *Candida albicans*. Yeast *20*, 929-941.

Hwang, C.S., Rhie, G.E., Oh, J.H., Huh, W.K., Yim, H.S., and Kang, S.O. (2002). Copper- and zinc-containing superoxide dismutase (Cu/ZnSOD) is required for the protection of *Candida albicans* against oxidative stresses and the expression of its full virulence. Microbiology *148*, 3705-3713.

Iorio, E., Torosantucci, A., Bromuro, C., Chiani, P., Ferretti, A., Giannini, M., Cassone, A., and Podo, F. (2008). *Candida albicans* cell wall comprises a branched beta-D-(1-6)-glucan with beta-D-(1-3)-side chains. Carbohydr Res *343*, 1050-1061.

Irani, K. (2000). Oxidant signaling in vascular cell growth, death, and survival : a review of the roles of reactive oxygen species in smooth muscle and endothelial cell mitogenic and apoptotic signaling. Circ Res *87*, 179-183.

Ishibashi, K., Yoshida, M., Nakabayashi, I., Shinohara, H., Miura, N.N., Adachi, Y., and Ohno, N. (2005). Role of anti-beta-glucan antibody in host defense against fungi. FEMS Immunol Med Microbiol *44*, 99-109.

Jackson, A.L., Burchard, J., Leake, D., Reynolds, A., Schelter, J., Guo, J., Johnson, J.M., Lim, L., Karpilow, J., Nichols, K.*, et al.* (2006a). Position-specific chemical modification of siRNAs reduces "off-target" transcript silencing. RNA *12*, 1197-1205.

Jackson, A.L., Burchard, J., Schelter, J., Chau, B.N., Cleary, M., Lim, L., and Linsley, P.S. (2006b). Widespread siRNA "off-target" transcript silencing mediated by seed region sequence complementarity. RNA *12*, 1179-1187.

Janeway, C. (2005). Immunobiology : the immune system in health and disease, 6th edn (New York: Garland Science).

Johnston, R.B., Jr. (2001). Clinical aspects of chronic granulomatous disease. Curr Opin Hematol *8*, 17-22.

Jouault, T., El Abed-El Behi, M., Martinez-Esparza, M., Breuilh, L., Trinel, P.A., Chamaillard, M., Trottein, F., and Poulain, D. (2006). Specific recognition of *Candida albicans* by macrophages requires galectin-3 to discriminate *Saccharomyces cerevisiae* and needs association with TLR2 for signaling. J Immunol *177*, 4679-4687.

Jouault, T., Ibata-Ombetta, S., Takeuchi, O., Trinel, P.A., Sacchetti, P., Lefebvre, P., Akira, S., and Poulain, D. (2003). *Candida albicans* phospholipomannan is sensed through toll-like receptors. J Infect Dis *188*, 165-172.

Jouault, T., Sarazin, A., Martinez-Esparza, M., Fradin, C., Sendid, B., and Poulain, D. (2009). Host responses to a versatile commensal: PAMPs and PRRs interplay leading to tolerance or infection by *Candida albicans*. Cell Microbiol *11*, 1007-1015.

Kannengiesser, C., Gerard, B., El Benna, J., Henri, D., Kroviarski, Y., Chollet-Martin, S., Gougerot-Pocidalo, M.A., Elbim, C., and Grandchamp, B. (2008). Molecular epidemiology of chronic granulomatous disease in a series of 80 kindreds: identification of 31 novel mutations. Hum Mutat *29*, E132-E149.

Kim, H.R., Cho, M.L., Kim, K.W., Juhn, J.Y., Hwang, S.Y., Yoon, C.H., Park, S.H., Lee, S.H., and Kim, H.Y. (2007a). Up-regulation of IL-23p19 expression in rheumatoid arthritis synovial fibroblasts by IL-17 through PI3-kinase-, NF-kappaB- and p38 MAPK-dependent signalling pathways. Rheumatology (Oxford) *46*, 57-64.

Kim, H.R., Kim, H.S., Park, M.K., Cho, M.L., Lee, S.H., and Kim, H.Y. (2007b). The clinical role of IL-23p19 in patients with rheumatoid arthritis. Scand J Rheumatol *36*, 259-264.

Klar, A.J., Srikantha, T., and Soll, D.R. (2001). A histone deacetylation inhibitor and mutant promote colony-type switching of the human pathogen Candida albicans. Genetics *158*, 919-924.

Klis, F.M., de Groot, P., and Hellingwerf, K. (2001). Molecular organization of the cell wall of *Candida albicans*. Med. Mycol. *39*, 1-8.

Koay, M.A., Christman, J.W., Segal, B.H., Venkatakrishnan, A., Blackwell, T.R., Holland, S.M., and Blackwell, T.S. (2001). Impaired pulmonary NF-kappaB activation in response to lipopolysaccharide in NADPH oxidase-deficient mice. Infect Immun *69*, 5991-5996.

Kohatsu, L., Hsu, D.K., Jegalian, A.G., Liu, F.T., and Baum, L.G. (2006). Galectin-3 induces death of *Candida* species expressing specific [beta]-1, 2-linked mannans. J. Immunol. *177*, 4718-4726.

Koppel, E.A., van Gisbergen, K.P., Geijtenbeek, T.B., and van Kooyk, Y. (2005). Distinct functions of DC-SIGN and its homologues L-SIGN (DC-SIGNR) and mSIGNR1 in pathogen recognition and immune regulation. Cell Microbiol *7*, 157-165.

Kuribayashi, F., Nunoi, H., Wakamatsu, K., Tsunawaki, S., Sato, K., Ito, T., and Sumimoto, H. (2002). The adaptor protein p40(phox) as a positive regulator of the superoxide-producing phagocyte oxidase. EMBO J *21*, 6312-6320.

Lai, W.K., Sun, P.J., Zhang, J., Jennings, A., Lalor, P.F., Hubscher, S., McKeating, J.A., and Adams, D.H. (2006). Expression of DC-SIGN and DC-SIGNR on human sinusoidal endothelium: a role for capturing hepatitis C virus particles. Am J Pathol *169*, 200-208.

Lamarre, C., LeMay, J.D., Deslauriers, N., and Bourbonnais, Y. (2001). *Candida albicans* expresses an unusual cytoplasmic manganese-containing superoxide dismutase (*SOD3* gene product) upon the entry and during the stationary phase. J Biol Chem *276*, 43784-43791.

Lambeth, J.D. (2004). NOX enzymes and the biology of reactive oxygen. Nat Rev Immunol *4*, 181-189.

Lanier, L.L. (2009). DAP10- and DAP12-associated receptors in innate immunity. Immunological Reviews *227*, 150-160.

Laroux, F.S., Romero, X., Wetzler, L., Engel, P., and Terhorst, C. (2005). Cutting edge: MyD88 controls phagocyte NADPH oxidase function and killing of gram-negative bacteria. J Immunol *175*, 5596-5600.

Le Cabec, V., Carreno, S., Moisand, A., Bordier, C., and Maridonneau-Parini, I. (2002). Complement receptor 3 (CD11b/CD18) mediates type I and type II phagocytosis during nonopsonic and opsonic phagocytosis, respectively. J Immunol *169*, 2003-2009.

Le Cabec, V., Cols, C., and Maridonneau-Parini, I. (2000). Nonopsonic phagocytosis of zymosan and *Mycobacterium kansasii* by CR3 (CD11b/CD18) involves distinct molecular determinants and is or is not coupled with NADPH oxidase activation. Infect Immun *68*, 4736-4745.

LeibundGut-Landmann, S., Gross, O., Robinson, M.J., Osorio, F., Slack, E.C., Tsoni, S.V., Schweighoffer, E., Tybulewicz, V., Brown, G.D., Ruland, J., and Reis e Sousa, C. (2007). Syk- and CARD9-dependent coupling of innate immunity to the induction of T helper cells that produce interleukin 17. Nat Immunol *8*, 630-638.

Lemaitre, B., Nicolas, E., Michaut, L., Reichhart, J.M., and Hoffmann, J.A. (1996). The dorsoventral regulatory gene cassette spatzle/Toll/cactus controls the potent antifungal response in Drosophila adults. Cell *86*, 973-983.

Lermann, U., and Morschhauser, J. (2008). Secreted aspartic proteases are not required for invasion of reconstituted human epithelia by *Candida albicans*. Microbiology *154*, 3281-3295.

Liang, B., and Petty, H.R. (1992). Imaging neutrophil activation: analysis of the translocation and utilization of NAD(P)H-associated autofluorescence during antibody-dependent target oxidation. J Cell Physiol *152*, 145-156.

Lipke, P.N., and Ovalle, R. (1998). Cell wall architecture in yeast: new structure and new challenges. J Bacteriol *180*, 3735-3740.

Liu, J., Gunn, L., Hansen, R., and Yan, J. (2009a). Combined yeast-derived beta-glucan with anti-tumor monoclonal antibody for cancer immunotherapy. Exp Mol Pathol *86*, 208-214.

Liu, J., Gunn, L., Hansen, R., and Yan, J. (2009b). Yeast-derived beta-glucan in combination with anti-tumor monoclonal antibody therapy in cancer. Recent Pat Anticancer Drug Discov *4*, 101-109.

Lo, H.J., Köhler, J.R., DiDomenico, B., Loebenberg, D., Cacciapuoti, A., and Fink, G.R. (1997). Nonfilamentous *C. albicans* mutants are avirulent. Cell *90*, 939-949.

Lo, Y.Y., and Cruz, T.F. (1995). Involvement of reactive oxygen species in cytokine and growth factor induction of c-fos expression in chondrocytes. J Biol Chem *270*, 11727-11730.

Lockhart, S.R., Pujol, C., Daniels, K.J., Miller, M.G., Johnson, A.D., Pfaller, M.A., and Soll, D.R. (2002). In *Candida albicans*, white-opaque switchers are homozygous for mating type. Genetics *162*, 737-745.

Lohse, M.B., and Johnson, A.D. (2008). Differential phagocytosis of white versus opaque *Candida albicans* by Drosophila and mouse phagocytes. PLoS ONE *3*, e1473.

Lopes, L.R., Dagher, M.C., Gutierrez, A., Young, B., Bouin, A.P., Fuchs, A., and Babior, B.M. (2004). Phosphorylated p40PHOX as a negative regulator of NADPH oxidase. Biochemistry *43*, 3723-3730.

Lorenz, M.C., Bender, J.A., and Fink, G.R. (2004). Transcriptional response of Candida albicans upon internalization by macrophages. Eukaryot Cell *3*, 1076-1087.

Maidan, M.M., De Rop, L., Serneels, J., Exler, S., Rupp, S., Tournu, H., Thevelein, J.M., and Van Dijck, P. (2005). The G protein-coupled receptor Gpr1 and the Galpha protein Gpa2 act through the cAMP-protein kinase A pathway to induce morphogenesis in *Candida albicans*. Mol Biol Cell *16*, 1971-1986.

Marcil, A., Gadoury, C., Ash, J., Zhang, J., Nantel, A., and Whiteway, M. (2008). Analysis of *PRA1* and its relationship to *Candida albicans*- macrophage interactions. Infect Immun *76*, 4345-4358.

Marletta, M.A. (1993). Nitric oxide synthase: function and mechanism. Adv Exp Med Biol *338*, 281-284.

Martchenko, M., Alarco, A.M., Harcus, D., and Whiteway, M. (2004). Superoxide dismutases in *Candida albicans*: transcriptional regulation and functional characterization of the hyphal-induced *SOD5* gene. Mol Biol Cell *15*, 456-467.

McCall, T.B., Boughton-Smith, N.K., Palmer, R.M., Whittle, B.J., and Moncada, S. (1989). Synthesis of nitric oxide from L-arginine by neutrophils. Release and interaction with superoxide anion. Biochem J *261*, 293-296.

McGinnis MR., T.S. (1996). Introduciton to Mycology. In Medical Microbiology, B. Samuel, ed. (Texas: Universtiy of Texas Medical Branch at Galveston).

McGreal, E.P., Rosas, M., Brown, G.D., Zamze, S., Wong, S.Y., Gordon, S., Martinez-Pomares, L., and Taylor, P.R. (2006). The carbohydrate-recognition domain of Dectin-2 is a C-type lectin with specificity for high mannose. Glycobiology *16*, 422-430.

Meischl, C., and Roos, D. (1998). The molecular basis of chronic granulomatous disease. Springer Semin Immunopathol *19*, 417-434.

Meister, G., and Tuschl, T. (2004). Mechanisms of gene silencing by double-stranded RNA. Nature *431*, 343-349.

Mille, C., Janbon, G., Delplace, F., Ibata-Ombetta, S., Gaillardin, C., Strecker, G., Jouault, T., Trinel, P.A., and Poulain, D. (2004). Inactivation of CaMIT1 inhibits *Candida albicans* phospholipomannan beta-mannosylation, reduces virulence, and alters cell wall protein beta-mannosylation. J Biol Chem *279*, 47952-47960.

Miller, M.G., and Johnson, A.D. (2002). White-opaque switching in *Candida albicans* is controlled by mating-type locus homeodomain proteins and allows efficient mating. Cell *110*, 293-302.

Mio, T., Yabe, T., Sudoh, M., Satoh, Y., Nakajima, T., Arisawa, M., and Yamada-Okabe, H. (1996). Role of three chitin synthase genes in the growth of *Candida albicans*. J Bacteriol *178*, 2416-2419.

Miwa, T., Takagi, Y., Shinozaki, M., Yun, C.W., Schell, W.A., Perfect, J.R., Kumagai, H., and Tamaki, H. (2004). Gpr1, a putative G-protein-coupled receptor, regulates morphogenesis and hypha formation in the pathogenic fungus *Candida albicans*. Eukaryot Cell *3*, 919-931.

Miyazato, A., Nakamura, K., Yamamoto, N., Mora-Montes, H.M., Tanaka, M., Abe, Y., Tanno, D., Inden, K., Gang, X., Ishii, K*., et al.* (2009). Toll-like receptor 9-dependent activation of myeloid dendritic cells by deoxynucleic acids from *Candida albicans*. Infect Immun.

Mocsai, A., Abram, C.L., Jakus, Z., Hu, Y., Lanier, L.L., and Lowell, C.A. (2006). Integrin signaling in neutrophils and macrophages uses adaptors containing immunoreceptor tyrosine-based activation motifs. Nat Immunol *7*, 1326-1333.

Monod, M., and Borg-von Zepelin, M. (2002). Secreted proteinases and other virulence mechanisms of *Candida albicans*. Chem Immunol *81*, 114-128.

Monod, M., Hube, B., Hess, D., and Sanglard, D. (1998). Differential regulation of *SAP8* and *SAP9*, which encode two new members of the secreted aspartic proteinase family in *Candida albicans*. Microbiology *144 (Pt 10)*, 2731-2737.

Monod, M., Togni, G., Hube, B., and Sanglard, D. (1994). Multiplicity of genes encoding secreted aspartic proteinases in *Candida* species. Mol Microbiol *13*, 357-368.

Moukadiri, I., and Zueco, J. (2001). Evidence for the attachment of Hsp150/Pir2 to the cell wall of *Saccharomyces cerevisiae* through disulfide bridges. FEMS Yeast Res *1*, 241-245.

Moye-Rowley, W.S. (2003). Regulation of the transcriptional response to oxidative stress in fungi: similarities and differences. Eukaryot Cell *2*, 381-389.

Mueller, G., and Schmit, J. (2007). Fungal biodiversity: what do we know? What can we predict? Biodiversity and Conservation *16*, 1-5.

Munro, C.A., Selvaggini, S., de Bruijn, I., Walker, L., Lenardon, M.D., Gerssen, B., Milne, S., Brown, A.J.P., and Gow, N.A.R. (2007). The PKC, HOG and Ca2+ signalling pathways co-ordinately regulate chitin synthesis in *Candida albicans*. Molecular Microbiology *63*, 1399-1413.

Munro, C.A., Whitton, R.K., Hughes, H.B., Rella, M., Selvaggini, S., and Gow, N.A. (2003). *CHS8*-a fourth chitin synthase gene of *Candida albicans* contributes to in vitro chitin synthase activity, but is dispensable for growth. Fungal Genet Biol *40*, 146-158.

Murciano, C. (2006). Toll-like receptor 4 defective mice carrying point or null mutations do not show increased susceptibility to *Candida albicans* in a model of hematogenously disseminated infection. Med. Mycol. *44*, 149-157.

Nagahata, H., Higuchi, H., Inanami, O., and Kuwabara, M. (2007). Costimulatory effects of complement receptor type 3 and Fc receptor for IgG (FcgammaR) on superoxide production and signal transduction in bovine neutrophils. J Vet Med Sci *69*, 993-997.

Naglik, J., Albrecht, A., Bader, O., and Hube, B. (2004). *Candida albicans* proteinases and host/pathogen interactions. Cell Microbiol *6*, 915-926.

Naglik, J.R., Rodgers, C.A., Shirlaw, P.J., Dobbie, J.L., Fernandes-Naglik, L.L., Greenspan, D., Agabian, N., and Challacombe, S.J. (2003). Differential expression of *Candida albicans* secreted aspartyl proteinase and phospholipase B genes in humans correlates with active oral and vaginal infections. J Infect Dis *188*, 469-479.

Nakagawa, Y., Kanbe, T., and Mizuguchi, I. (2003). Disruption of the human pathogenic yeast *Candida albicans* catalase gene decreases survival in mouse-model infection and elevates susceptibility to higher temperature and to detergents. Microbiol Immunol *47*, 395-403.

Nakamura, K., Miyagi, K., Koguchi, Y., Kinjo, Y., Uezu, K., Kinjo, T., Akamine, M., Fujita, J., Kawamura, I., Mitsuyama, M*., et al.* (2006). Limited contribution of Toll-like receptor 2 and 4 to the host response to a fungal infectious pathogen, *Cryptococcus neoformans*. FEMS Immunol Med Microbiol *47*, 148-154.

Nakamura, K., Miyazato, A., Xiao, G., Hatta, M., Inden, K., Aoyagi, T., Shiratori, K., Takeda, K., Akira, S., Saijo, S*., et al.* (2008). Deoxynucleic acids from *Cryptococcus neoformans* activate myeloid dendritic cells via a TLR9-dependent pathway. J Immunol *180*, 4067-4074.

Netea, M.G. (2002). The role of Toll-like receptors in the defense against disseminated candidiasis. J. Infect. Dis. *185*, 1483-1489.

Netea, M.G. (2004). Toll-like receptor 2 inhibits cellular responses against *Candida albicans* through pathways mediated by IL-10 and CD4+CD25+ regulatory T cells. J. Immunol. *172*, 3712-3718.

Netea, M.G., Brown, G.D., Kullberg, B.J., and Gow, N.A. (2008a). An integrated model of the recognition of *Candida albicans* by the innate immune system. Nat Rev Microbiol *6*, 67-78.

Netea, M.G., Gow, N.A., Munro, C.A., Bates, S., Collins, C., Ferwerda, G., Hobson, R.P., Bertram, G., Hughes, H.B., Jansen, T*., et al.* (2006). Immune sensing of *Candida albicans* requires cooperative recognition of mannans and glucans by lectin and Toll-like receptors. J Clin Invest *116*, 1642-1650.

Netea, M.G., van de Veerdonk, F., Verschueren, I., van der Meer, J.W., and Kullberg, B.J. (2008b). Role of TLR1 and TLR6 in the host defense against disseminated candidiasis. FEMS Immunol Med Microbiol *52*, 118-123.

Novina, C.D., and Sharp, P.A. (2004). The RNAi revolution. Nature *430*, 161-164.

Nuoffer, C., Horvath, A., and Riezman, H. (1993). Analysis of the sequence requirements for glycosylphosphatidylinositol anchoring of *Saccharomyces cerevisiae* Gas1 protein. J Biol Chem *268*, 10558-10563.

Orlean, P., and Menon, A.K. (2007). Thematic review series: lipid posttranslational modifications. GPI anchoring of protein in yeast and mammalian cells, or: how we learned to stop worrying and love glycophospholipids. J Lipid Res *48*, 993-1011.

Ozinsky, A., Underhill, D.M., Fontenot, J.D., Hajjar, A.M., Smith, K.D., Wilson, C.B., Schroeder, L., and Aderem, A. (2000). The repertoire for pattern recognition of pathogens by the innate immune system is defined by cooperation between toll-like receptors. Proc Natl Acad Sci U S A *97*, 13766-13771.

Park, H.S., Jung, H.Y., Park, E.Y., Kim, J., Lee, W.J., and Bae, Y.S. (2004). Cutting edge: direct interaction of TLR4 with NAD(P)H oxidase 4 isozyme is essential for lipopolysaccharide-induced production of reactive oxygen species and activation of NF-kappa B. J Immunol *173*, 3589-3593.

Park, Y.N., and Morschhäuser, J. (2005). *Candida albicans* MTLalpha tup1Delta mutants can reversibly switch to mating-competent, filamentous growth forms. Mol. Microbiol. *58*, 1288.

Pedreno, Y., Maicas, S., Arguelles, J.C., Sentandreu, R., and Valentin, E. (2004). The *ATC1* gene encodes a cell wall-linked acid trehalase required for growth on trehalose in *Candida albicans*. J Biol Chem *279*, 40852-40860.

Pfaller, M.A., and Diekema, D.J. (2007). Epidemiology of invasive candidiasis: a persistent public health problem. Clin Microbiol Rev *20*, 133-163.

Phillips, D.C., Dias, H.I., Kitas, G.D., and Griffiths, H.R. (2009). Aberrant Reactive Oxygen and Nitrogen Species generation in Rheumatoid Arthritis (RA): Causes and Consequences for Immune Function, Cell Survival and Therapeutic Intervention. Antioxid Redox Signal. 12, 743-785

Poltorak, A., He, X., Smirnova, I., Liu, M.Y., Van Huffel, C., Du, X., Birdwell, D., Alejos, E., Silva, M., Galanos, C*., et al.* (1998). Defective LPS signaling in C3H/HeJ and C57BL/10ScCr mice: mutations in Tlr4 gene. Science *282*, 2085-2088.

Poulain, D., Slomianny, C., Jouault, T., Gomez, J.M., and Trinel, P.A. (2002). Contribution of phospholipomannan to the surface expression of beta-1,2-oligomannosides in *Candida albicans* and its presence in cell wall extracts. Infect Immun *70*, 4323-4328.

Poulain, D., Tronchin, G., Dubremetz, J.F., and Biguet, J. (1978). Ultrastructure of the cell wall of *Candida albicans* blastospores: study of its constitutive layers by the use of a cytochemical technique revealing polysaccharides. Ann Microbiol (Paris) *129*, 141-153.

Powlesland, A.S., Ward, E.M., Sadhu, S.K., Guo, Y., Taylor, M.E., and Drickamer, K. (2006). Widely divergent biochemical properties of the complete set of mouse DC-SIGN-related proteins. J Biol Chem *281*, 20440-20449.

Qi, M., and Elion, E.A. (2005). MAP kinase pathways. J Cell Sci *118*, 3569-3572.

Quijano, C., Romero, N., and Radi, R. (2005). Tyrosine nitration by superoxide and nitric oxide fluxes in biological systems: modeling the impact of superoxide dismutase and nitric oxide diffusion. Free Radic Biol Med *39*, 728-741.

Ramirez-Ortiz, Z.G., Specht, C.A., Wang, J.P., Lee, C.K., Bartholomeu, D.C., Gazzinelli, R.T., and Levitz, S.M. (2008). Toll-like receptor 9-dependent immune activation by unmethylated CpG motifs in *Aspergillus fumigatus* DNA. Infect Immun *76*, 2123-2129.

Ravetch, J.V., and Bolland, S. (2001). IgG Fc receptors. Annu Rev Immunol *19*, 275-290.

Razavi, H.M., Wang le, F., Weicker, S., Rohan, M., Law, C., McCormack, D.G., and Mehta, S. (2004). Pulmonary neutrophil infiltration in murine sepsis: role of inducible nitric oxide synthase. Am J Respir Crit Care Med *170*, 227-233.

Richard, M.L., and Plaine, A. (2007). Comprehensive analysis of glycosylphosphatidylinositol-anchored proteins in *Candida albicans*. Eukaryot Cell *6*, 119-133.

Robinson, M.J., Osorio, F., Rosas, M., Freitas, R.P., Schweighoffer, E., Gross, O., Verbeek, J.S., Ruland, J., Tybulewicz, V., Brown, G.D.*, et al.* (2009). Dectin-2 is a Syk-coupled pattern recognition receptor crucial for Th17 responses to fungal infection. J Exp Med *206*, 2037-2051.

Rogers, N.C., Slack, E.C., Edwards, A.D., Nolte, M.A., Schulz, O., Schweighoffer, E., Williams, D.L., Gordon, S., Tybulewicz, V.L., Brown, G.D., and Reis e Sousa, C. (2005). Syk-dependent cytokine induction by Dectin-1 reveals a novel pattern recognition pathway for C type lectins. Immunity *22*, 507-517.

Romani, L. (2004). Immunity to fungal infections. Nat Rev Immunol *4*, 1-13.

Rose, M.L., Rusyn, I., Bojes, H.K., Belyea, J., Cattley, R.C., and Thurman, R.G. (2000). Role of Kupffer cells and oxidants in signaling peroxisome proliferator-induced hepatocyte proliferation. Mutat Res *448*, 179-192.

Ross, G.D., Cain, J.A., and Lachmann, P.J. (1985). Membrane complement receptor type three (CR3) has lectin-like properties analogous to bovine conglutinin as functions as a receptor for zymosan and rabbit erythrocytes as well as a receptor for iC3b. J Immunol *134*, 3307-3315.

Ross, G.D., Cain, J.A., Myones, B.L., Newman, S.L., and Lachmann, P.J. (1987). Specificity of membrane complement receptor type three (CR3) for beta-glucans. Complement *4*, 61-74.

Ross, G.D., and Vetvicka, V. (1993). CR3 (CD11b, CD18): a phagocyte and NK cell membrane receptor with multiple ligand specificities and functions. Clin Exp Immunol *92*, 181-184.

Ross, G.D., Vetvicka, V., Yan, J., Xia, Y., and Vetvickova, J. (1999). Therapeutic intervention with complement and beta-glucan in cancer. Immunopharmacology *42*, 61-74.

Rubin-Bejerano, I., Abeijon, C., Magnelli, P., Grisafi, P., and Fink, G.R. (2007). Phagocytosis by human neutrophils is stimulated by a unique fungal cell wall component. Cell Host Microbe *2*, 55-67.

Ruiz-Herrera, J., Elorza, M.V., Valentin, E., and Sentandreu, R. (2006). Molecular organization of the cell wall of *Candida albicans* and its relation to pathogenicity. FEMS Yeast Res *6*, 14-29.

Ruiz-Herrera, J., and Martinez-Espinoza, A.D. (1999). Chitin biosynthesis and structural organization in vivo. EXS *87*, 39-53.

Ruland, J. (2008). CARD9 signaling in the innate immune response. Ann N Y Acad Sci *1143*, 35-44.

Ryan, K.A., Smith, M.F., Jr., Sanders, M.K., and Ernst, P.B. (2004). Reactive oxygen and nitrogen species differentially regulate Toll-like receptor 4-mediated activation of NF-kappa B and interleukin-8 expression. Infect Immun *72*, 2123-2130.

Saijo, S., Fujikado, N., Furuta, T., Chung, S.H., Kotaki, H., Seki, K., Sudo, K., Akira, S., Adachi, Y., Ohno, N.*, et al.* (2007). Dectin-1 is required for host defense against *Pneumocystis carinii* but not against *Candida albicans*. Nat Immunol *8*, 39-46.

Sambrook, J., and Russell, D.W. (2001). Molecular cloning : a laboratory manual, 3rd edn (Cold Spring Harbor, N.Y.: Cold Spring Harbor Laboratory Press).

Sarantis, H., and Gray-Owen, S.D. (2007). The specific innate immune receptor CEACAM3 triggers neutrophil bactericidal activities via a Syk kinase-dependent pathway. Cell Microbiol *9*, 2167-2180.

Sathyamoorthy, M., de Mendez, I., Adams, A.G., and Leto, T.L. (1997). p40(phox) down-regulates NADPH oxidase activity through interactions with its SH3 domain. J Biol Chem *272*, 9141-9146.

Sato, K., Yang, X.L., Yudate, T., Chung, J.S., Wu, J., Luby-Phelps, K., Kimberly, R.P., Underhill, D., Cruz, P.D., Jr., and Ariizumi, K. (2006). Dectin-2 is a pattern recognition receptor for fungi that couples with the Fc receptor gamma chain to induce innate immune responses. J Biol Chem *281*, 38854-38866.

Schaller, M., Borelli, C., Korting, H.C., and Hube, B. (2005). Hydrolytic enzymes as virulence factors of *Candida albicans*. Mycoses *48*, 365-377.

Schofield, D.A., Westwater, C., Warner, T., and Balish, E. (2005). Differential *Candida albicans* lipase gene expression during alimentary tract colonization and infection. FEMS Microbiol Lett *244*, 359-365.

Schreck, R., Rieber, P., and Baeuerle, P.A. (1991). Reactive oxygen intermediates as apparently widely used messengers in the activation of the NF-kappa B transcription factor and HIV-1. EMBO J *10*, 2247-2258.

Schweizer, A., Rupp, S., Taylor, B.N., Rollinghoff, M., and Schroppel, K. (2000). The TEA/ATTS transcription factor CaTec1p regulates hyphal development and virulence in *Candida albicans*. Mol Microbiol *38*, 435-445.

Shibata, N., Akagi, R., Hosoya, T., Kawahara, K., Suzuki, A., Ikuta, K., Kobayashi, H., Hisamichi, K., Okawa, Y., and Suzuki, S. (1996a). Existence of novel branched side chains containing beta-1,2 and alpha-1,6 linkages corresponding to antigenic factor 9 in the mannan of *Candida guilliermondii*. J Biol Chem *271*, 9259-9266.

Shibata, N., Onozawa, M., Tadano, N., Hinosawa, Y., Suzuki, A., Ikuta, K., Kobayashi, H., Suzuki, S., and Okawa, Y. (1996b). Structure and antigenicity of the mannans of *Candida famata* and *Candida saitoana*: comparative study with the mannan of *Candida guilliermondii*. Arch Biochem Biophys *336*, 49-58.

Singh, P., Chauhan, N., Ghosh, A., Dixon, F., and Calderone, R. (2004). *SKN7* of *Candida albicans*: mutant construction and phenotype analysis. Infect Immun *72*, 2390-2394.

Sioud, M. (2004). Therapeutic siRNAs. Trends Pharmacol Sci *25*, 22-28.

Sipos, G., Puoti, A., and Conzelmann, A. (1995). Biosynthesis of the side chain of yeast glycosylphosphatidylinositol anchors is operated by novel mannosyltransferases located in the endoplasmic reticulum and the Golgi apparatus. J Biol Chem *270*, 19709-19715.

Skrzypek, F., Cenci, E., Pietrella, D., Rachini, A., Bistoni, F., and Vecchiarelli, A. (2009). Dectin-1 is required for human dendritic cells to initiate immune response to *Candida albicans* through Syk activation. Microbes Infect *11*, 661-670.

Slack, E.C., Robinson, M.J., Hernanz-Falcon, P., Brown, G.D., Williams, D.L., Schweighoffer, E., Tybulewicz, V.L., and Reis e Sousa, C. (2007). Syk-dependent ERK activation regulates IL-2 and IL-10 production by DC stimulated with zymosan. Eur J Immunol *37*, 1600-1612.

Sledz, C.A., Holko, M., de Veer, M.J., Silverman, R.H., and Williams, B.R. (2003). Activation of the interferon system by short-interfering RNAs. Nat Cell Biol *5*, 834-839.

Slutsky, B., Staebell, M., Anderson, J., Risen, L., Pfaller, M., and Soll, D.R. (1987). "White-opaque transition": a second high-frequency switching system in *Candida albicans*. J Bacteriol *169*, 189-197.

Soll, D.R. (2004). Mating-type locus homozygosis, phenotypic switching and mating: a unique sequence of dependencies in *Candida albicans*. BioEssays *26*, 10-20.

Sonneborn, A., Bockmuhl, D.P., and Ernst, J.F. (1999a). Chlamydospore formation in *Candida albicans* requires the Efg1p morphogenetic regulator. Infect. Immun. *67*, 5514.

Sonneborn, A., Tebarth, B., and Ernst, J.F. (1999b). Control of white-opaque phenotypic switching in *Candida albicans* by the Efg1p morphogenetic regulator. Infect Immun *67*, 4655-4660.

Srikantha, T., Tsai, L., Daniels, K., Klar, A.J., and Soll, D.R. (2001). The histone deacetylase genes *HDA1* and *RPD3* play distinct roles in regulation of high-frequency phenotypic switching in *Candida albicans*. J Bacteriol *183*, 4614-4625.

Staib, P., and Morschhauser, J. (2007). Chlamydospore formation in *Candida albicans* and *Candida dubliniensis* - an enigmatic developmental programme. Mycoses *50*, 1-12.

Stehr, F., Felk, A., Gacser, A., Kretschmar, M., Mahnss, B., Neuber, K., Hube, B., and Schafer, W. (2004). Expression analysis of the *Candida albicans* lipase gene family during experimental infections and in patient samples. FEMS Yeast Res *4*, 401-408.

Sun, J., Xu, L., Eu, J.P., Stamler, J.S., and Meissner, G. (2003). Nitric oxide, NOC-12, and S-nitrosoglutathione modulate the skeletal muscle calcium release channel/ryanodine receptor by different mechanisms. An allosteric function for O_2 in S-nitrosylation of the channel. J Biol Chem *278*, 8184-8189.

Sun, L., and Zhao, Y. (2007). The biological role of dectin-1 in immune response. Int Rev Immunol *26*, 349-364.

Sundstrom, P.M., Tam, M.R., Nichols, E.J., and Kenny, G.E. (1988). Antigenic differences in the surface mannoproteins of *Candida albicans* as revealed by monoclonal antibodies. Infect Immun *56*, 601-606.

Suzuki, A., Shibata, N., Suzuki, M., Saitoh, F., Takata, Y., Oshie, A., Oyamada, H., Kobayashi, H., Suzuki, S., and Okawa, Y. (1996). Characterization of alpha-1,6-mannosyltransferase responsible for the synthesis of branched side chains in *Candida albicans* mannan. Eur J Biochem *240*, 37-44.

Swanson, J.A., and Hoppe, A.D. (2004). The coordination of signaling during Fc receptor-mediated phagocytosis. J Leukoc Biol *76*, 1093-1103.

Tada, H., Nemoto, E., Shimauchi, H., Watanabe, T., Mikami, T., Matsumoto, T., Ohno, N., Tamura, H., Shibata, K., Akashi, S*., et al.* (2002). *Saccharomyces cerevisiae*- and *Candida albicans*-derived mannan induced production of tumor necrosis factor alpha by human monocytes in a CD14- and Toll-like receptor 4-dependent manner. Microbiol Immunol *46*, 503-512.

Takahara, K., Yashima, Y., Omatsu, Y., Yoshida, H., Kimura, Y., Kang, Y.S., Steinman, R.M., Park, C.G., and Inaba, K. (2004). Functional comparison of the mouse DC-SIGN, SIGNR1, SIGNR3 and Langerin, C-type lectins. Int Immunol *16*, 819-829.

Tanaka, T., Izawa, S., and Inoue, Y. (2005). GPX2, encoding a phospholipid hydroperoxide glutathione peroxidase homologue, codes for an atypical 2-Cys peroxiredoxin in *Saccharomyces cerevisiae*. J Biol Chem *280*, 42078-42087.

Taylor, L.H., Latham, S.M., and Woolhouse, M.E. (2001). Risk factors for human disease emergence. Philos Trans R Soc Lond B Biol Sci *356*, 983-989.

Taylor, P.R., Brown, G.D., Herre, J., Williams, D.L., Willment, J.A., and Gordon, S. (2004). The role of SIGNR1 and the beta-glucan receptor (dectin-1) in the nonopsonic recognition of yeast by specific macrophages. J Immunol *172*, 1157-1162.

Taylor, P.R., Tsoni, S.V., Willment, J.A., Dennehy, K.M., Rosas, M., Findon, H., Haynes, K., Steele, C., Botto, M., Gordon, S., and Brown, G.D. (2007). Dectin-1 is required for beta-glucan recognition and control of fungal infection. Nat Immunol *8*, 31-38.

Tell, L.A. (2005). Aspergillosis in mammals and birds: impact on veterinary medicine. Med Mycol *43 Suppl 1*, S71-73.

Toh-e, A., Yasunaga, S., Nisogi, H., Tanaka, K., Oguchi, T., and Matsui, Y. (1993). Three yeast genes, *PIR1*, *PIR2* and *PIR3*, containing internal tandem repeats, are related to each other, and *PIR1* and *PIR2* are required for tolerance to heat shock. Yeast *9*, 481-494.

Tohyama, Y., and Yamamura, H. (2009). Protein tyrosine kinase, syk: a key player in phagocytic cells. J Biochem *145*, 267-273.

Torres, M., and Forman, H.J. (2003). Redox signaling and the MAP kinase pathways. Biofactors *17*, 287-296.

Toshchakov, V. (2002). TLR4, but not TLR2, mediates IFN[beta]-induced STAT I [alpha]/[beta]-dependent gene expression in macrophages. Nature Immunol. *3*, 392-398.

Tsang, E., Giannetti, A.M., Shaw, D., Dinh, M., Tse, J.K., Gandhi, S., Ho, H., Wang, S., Papp, E., and Bradshaw, J.M. (2008). Molecular mechanism of the Syk activation switch. J Biol Chem *283*, 32650-32659.

Tsoni, S.V., and Brown, G.D. (2008). beta-Glucans and dectin-1. Ann N Y Acad Sci *1143*, 45-60.

Udenfriend, S., and Kodukula, K. (1995). How glycosylphosphatidylinositol-anchored membrane proteins are made. Annu Rev Biochem *64*, 563-591.

Underhill, D.M., and Goodridge, H.S. (2007). The many faces of ITAMs. Trends Immunol *28*, 66-73.

Underhill, D.M., Rossnagle, E., Lowell, C.A., and Simmons, R.M. (2005). Dectin-1 activates Syk tyrosine kinase in a dynamic subset of macrophages for reactive oxygen production. Blood *106*, 2543-2550.

Valera, I., Fernandez, N., Trinidad, A.G., Alonso, S., Brown, G.D., Alonso, A., and Crespo, M.S. (2008). Costimulation of dectin-1 and DC-SIGN triggers the arachidonic acid cascade in human monocyte-derived dendritic cells. J Immunol *180*, 5727-5736.

van Bruggen, R., Drewniak, A., Jansen, M., van Houdt, M., Roos, D., Chapel, H., Verhoeven, A.J., and Kuijpers, T.W. (2009). Complement receptor 3, not Dectin-1, is the major receptor on human neutrophils for beta-glucan-bearing particles. Mol Immunol.

van Bruggen, R., Zweers, D., van Diepen, A., van Dissel, J.T., Roos, D., Verhoeven, A.J., and Kuijpers, T.W. (2007). Complement receptor 3 and Toll-like receptor 4 act sequentially in uptake and intracellular killing of unopsonized *Salmonella enterica serovar Typhimurium* by human neutrophils. Infect Immun *75*, 2655-2660.

van de Veerdonk, F.L., Marijnissen, R.J., Kullberg, B.J., Koenen, H.J., Cheng, S.C., Joosten, I., van den Berg, W.B., Williams, D.L., van der Meer, J.W., Joosten, L.A., and Netea, M.G. (2009). The macrophage mannose receptor induces IL-17 in response to *Candida albicans*. Cell Host Microbe *5*, 329-340.

van de Veerdonk, F.L., Netea, M.G., Jansen, T.J., Jacobs, L., Verschueren, I., van der Meer, J.W., and Kullberg, B.J. (2008). Redundant role of TLR9 for anti-Candida host defense. Immunobiology *213*, 613-620.

Van Ziffle, J.A., and Lowell, C.A. (2009). Neutrophil-specific deletion of Syk kinase results in reduced host defense to bacterial infection. Blood *114*, 4871-4882.

Villamon, E. (2004). Toll-like receptor-2 is essential in murine defenses against *Candida albicans* infections. Microbes Infect. *6*, 1-7.

Walker, L.A., Munro, C.A., de Bruijn, I., Lenardon, M.D., McKinnon, A., and Gow, N.A. (2008). Stimulation of chitin synthesis rescues *Candida albicans* from echinocandins. PLoS Pathog *4*, e1000040.

Wang, G., Moniri, N.H., Ozawa, K., Stamler, J.S., and Daaka, Y. (2006a). Nitric oxide regulates endocytosis by S-nitrosylation of dynamin. Proc Natl Acad Sci U S A *103*, 1295-1300.

Wang, Y., Cao, Y.-Y., Jia, X.-M., Cao, Y.-B., Gao, P.-H., Fu, X.-P., Ying, K., Chen, W.-S., and Jiang, Y.-Y. (2006b). Cap1p is involved in multiple pathways of oxidative stress response in *Candida albicans*. Free Radical Biology and Medicine *40*, 1201-1209.

Warris, A., Netea, M.G., Wang, J.E., Gaustad, P., Kullberg, B.J., Verweij, P.E., and Abrahamsen, T.G. (2003). Cytokine release in healthy donors and patients with chronic granulomatous disease upon stimulation with *Aspergillus fumigatus*. Scand J Infect Dis *35*, 482-487.

Warris, A., and Verweij, P.E. (2005). Clinical implications of environmental sources for Aspergillus. Medical Mycology *43*, 59 - 65.

Wells, C.A., Salvage-Jones, J.A., Li, X., Hitchens, K., Butcher, S., Murray, R.Z., Beckhouse, A.G., Lo, Y.L., Manzanero, S., Cobbold, C*., et al.* (2008). The macrophage-inducible C-type lectin, mincle, is an essential component of the innate immune response to *Candida albicans*. J Immunol *180*, 7404-7413.

Wendler, F., Bergler, H., Prutej, K., Jungwirth, H., Zisser, G., Kuchler, K., and Högenauer, G. (1997). Diazaborine resistance in the yeast *Saccharomyces cerevisiae* reveals a link between *YAP1* and the pleiotropic drug resistance genes *PDR1* and *PDR3*. J Biol Chem *272*, 27091-27098.

Wheeler, M.A., Smith, S.D., Garcia-Cardena, G., Nathan, C.F., Weiss, R.M., and Sessa, W.C. (1997). Bacterial infection induces nitric oxide synthase in human neutrophils. J Clin Invest *99*, 110-116.

Wheeler, R.T., and Fink, G.R. (2006). A drug-sensitive genetic network masks fungi from the immune system. PLoS Pathog. *2*, 328-339.

Whiteway, M., and Bachewich, C. (2007). Morphogenesis in *Candida albicans*. Annu Rev Microbiol *61*, 529-553.

Whiteway, M., and Oberholzer, U. (2004). Candida morphogenesis and host-pathogen interactions. Curr Opin Microbiol *7*, 350-357.

Williams, D.L., Li, C., Ha, T., Ozment-Skelton, T., Kalbfleisch, J.H., Preiszner, J., Brooks, L., Breuel, K., and Schweitzer, J.B. (2004). Modulation of the phosphoinositide 3-kinase pathway alters innate resistance to polymicrobial sepsis. J Immunol *172*, 449-456.

Wu, W., Hsu, Y.-M.S., Bi, L., Songyang, Z., and Lin, X. (2009). CARD9 facilitates microbe-elicited production of reactive oxygen species by regulating the LyGDI-Rac1 complex. Nat Immunol *advance online publication*.

Wysocki, R., Fortier, P.K., Maciaszczyk, E., Thorsen, M., Leduc, A., Odhagen, A., Owsianik, G., Ulaszewski, S., Ramotar, D., and Tamas, M.J. (2004). Transcriptional activation of metalloid tolerance genes in *Saccharomyces cerevisiae* requires the AP-1-like proteins Yap1p and Yap8p. Mol Biol Cell *15*, 2049-2060.

Wysong, D.R., Christin, L., Sugar, A.M., Robbins, P.W., and Diamond, R.D. (1998). Cloning and sequencing of a *Candida albicans* catalase gene and effects of disruption of this gene. Infect Immun *66*, 1953-1961.

Xia, Y., and Ross, G.D. (1999). Generation of recombinant fragments of CD11b expressing the functional beta-glucan-binding lectin site of CR3 (CD11b/CD18). J Immunol *162*, 7285-7293.

Yamasaki, S., Ishikawa, E., Sakuma, M., Hara, H., Ogata, K., and Saito, T. (2008). Mincle is an ITAM-coupled activating receptor that senses damaged cells. Nat Immunol *9*, 1179-1188.

Yang, C.S., Shin, D.M., Kim, K.H., Lee, Z.W., Lee, C.H., Park, S.G., Bae, Y.S., and Jo, E.K. (2009). NADPH oxidase 2 interaction with TLR2 is required for efficient innate immune responses to mycobacteria via cathelicidin expression. J Immunol *182*, 3696-3705.

Yang, Z., and Marshall, J.S. (2009). Zymosan treatment of mouse mast cells enhances dectin-1 expression and induces dectin-1-dependent reactive oxygen species (ROS) generation. Immunobiology *214*, 321-330.

Yauch, L.E., Mansour, M.K., Shoham, S., Rottman, J.B., and Levitz, S.M. (2004). Involvement of CD14, toll-like receptors 2 and 4, and MyD88 in the host response to the fungal pathogen *Cryptococcus neoformans* in vivo. Infect. Immun. *72*, 5373-5382.

Yeung, T., Touret, N., and Grinstein, S. (2005). Quantitative fluorescence microscopy to probe intracellular microenvironments. Curr Opin Microbiol *8*, 350-358.

Yoshitomi, H., Sakaguchi, N., Kobayashi, K., Brown, G.D., Tagami, T., Sakihama, T., Hirota, K., Tanaka, S., Nomura, T., Miki, I.*, et al.* (2005). A role for fungal {beta}-glucans and their receptor Dectin-1 in the induction of autoimmune arthritis in genetically susceptible mice. J Exp Med *201*, 949-960.

Zakikhany, K., Thewes, S., Wilson, D., Martin, R., Albrecht, A., and Hube, B. (2008). From attachment to invasion: infection associated genes of Candida albicans. Nippon Ishinkin Gakkai Zasshi *49*, 245-251.

Zhang, X., Shan, P., Jiang, G., Cohn, L., and Lee, P.J. (2006). Toll-like receptor 4 deficiency causes pulmonary emphysema. J Clin Invest *116*, 3050-3059.

Zhao, X., Oh, S.H., Yeater, K.M., and Hoyer, L.L. (2005). Analysis of the *Candida albicans* Als2p and Als4p adhesins suggests the potential for compensatory function within the Als family. Microbiology *151*, 1619-1630.

Znaidi, S., Barker, K.S., Weber, S., Alarco, A.M., Liu, T.T., Boucher, G., Rogers, P.D., and Raymond, M. (2009). Identification of the *Candida albican*s Cap1p regulon. Eukaryot Cell *8*, 806-820.

Zordan, R.E., Galgoczy, D.J., and Johnson, A.D. (2006). Epigenetic properties of white-opaque switching in *Candida albicans* are based on a self-sustaining transcriptional feedback loop. Proc. Natl. Acad. Sci. USA *103*, 12807.

Zordan, R.E., Miller, M.G., Galgoczy, D.J., Tuch, B.B., and Johnson, A.D. (2007). Interlocking transcriptional feedback loops control white-opaque switching in *Candida albicans*. PLoS Biol *5*, e256.

VII. Appendix

Abbreviations

CARD9	caspase recruitment domain protein 9
CFW	cacofluor white
CGD	chronic granulomatous disease
CLR	c-type lectin receptor
DC	dendritic cell
DC-SIGN	dendritic cell-specific ICAM3-grabbing nonintegrin
ERK	extracellular signal related kinase
Etn-P	ethanolamine phosphate
FcγR	Fcγ receptor
GlcN	glucosamine
GlcNAc	*N*-acetyl-glucosamine
IFN	interferon
IL	interleukin
IL-1Ra	interleukin-1 receptor antagonist
IRF3	interferon regulatory factor 3
ITAM	immunoreceptor tyrosine-based activation motif
JNK	Jun N-terminal kinase
LIP	secreted lipases
LR	lectin receptor
MAPK	mitogen-activated protein kinase
MPO	myeloperoxidase
MR	mannose receptor
MyD88	myeloid differentiation primary response gene 88
NADPH	nicotinamide adenine dinucleotide phosphate
NF-κB	*nuclear factor* '*kappa*-light-chain-enhancer' of activated *B*-cells
NOS	nitroc oxide synthase
NOX	NADPH Oxidase
PAMP	pathogen associated molecular patterns
PI3K	phosphoinositol-3-kinase
PL	phospholipase
PLM	phospholipomannan
PMN	polymorphonuclear
PRR	pattern recognition receptor
ROS	reactive oxygen species
SAP	secreted aspartyl proteinases
SOD	superoxide dismutase
Src	sarcoma
Syk	spleen tyrosine kinase
TGFβ	transforming growth factor-β
TH	T helper
TLR	toll-like receptor
TNF	tumour necrosis factor
TReg	regulatory T-cell
WOR	white opaque regulator

Candida spp trigger a type I interferon-response in conventional dendritic cells requiring a novel phagosomal TLR7 & TLR9-mediated IFNβ signaling

Christelle Bourgeois[1], Olivia Majer[1], **Ingrid E. Frohner**[1], Iwona Lesiak-Markowicz[1], Kwang-Soo Hildering[1], Walter Glaser[1], Silvia Stockinger[&#], Thomas Decker[&], Shizuo Akira[*], Mathias Müller[+] & Karl Kuchler[1§]

From the
[1] Medical University Vienna - Max F. Perutz Laboratories
Christian Doppler Laboratory for Infection Biology
Campus Vienna Biocenter, A-1030 Vienna, Austria

Present address: Institut für Medizinische Mikrobiologie und Krankenhaushygiene
D-30625 Hannover, Germany

[&] University of Vienna – Max F. Perutz Laboratories
Department of Microbiology & Genetics, A-1030 Vienna, Austria

[+] University of Veterinary Medicine Vienna
Department of Animal Breeding and Genetics, A-1210 Vienna, Austria

*Osaka University, Research Institute for Microbial Diseases,
Department of Host Defense, Osaka 565-0871, Japan

Running title - *Candida spp* drive phagosomal type I-IFN host response

Keywords - *Candida,* pathogenesis, β-glucans, type I-IFN response, dendritic cells

[§]To whom all correspondence should be addressed:

Karl Kuchler

Medical University Vienna

Christian Doppler Laboratory for Infection Biology, Max F. Perutz Laboratories

Dr. Bohr-Gasse 9/2; Campus Vienna Biocenter, A-1030 Vienna, Austria

Ph: +43-1-4277-61807; FAX: +43-1-4277-9618 e-mail:

karl.kuchler@meduniwien.ac.at

Abstract

Whereas a type-I interferon (IFN-I) response is a hallmark immune response to bacteria and viruses, a function in fungal pathogenesis has remained unknown. Here, we demonstrate a strong IFNβ response in mouse myeloid dendritic cells (BM-DCs) challenged by *Candida* spp, subsequently orchestrating an IFNAR1-dependent intracellular STAT1 activation and IRF7 expression. Interestingly, the initial IFNβ release bypasses the *toll*-like receptor (TLR) 4 and TLR2, the TLR adaptor TRIF, and the β-glucan/phagocytic receptors dectin-1 and CD11b. Notably, Candida-induced IFNβ release is strongly impaired by Src- and Syk-family kinase inhibitors, but strictly requires dynamin-dependent phagocytosis as well as phagosomal acidification. Strikingly, TLR7 and TLR9, as well as MyD88, are essential for IFNβ release. Our work uncovers for the first time a pivotal role for endosomal TLR7 signaling in fungal pathogen recognition and consequently, draw attention to Candida-derived nucleic acids as pathogen-associated molecular patterns eliciting the innate host immune response.

Introduction

Invasive Candida infections are life-threatening clinical conditions, primarily affecting immunosuppressed patient cohorts, and those with general defects in the immune system .(Pfaller and Diekema, 2007). Mortalities associated with disseminated candidemia can exceed 30–40%, despite extensive antifungal therapies (Lewis, 2009). The dimorphic *Candida albicans* (Ca) is most frequent cause of fungal infections. Ca can switch between a yeast and a filamentous (hyphae) form upon host or environmental stimuli, including temperature, pH, lack of nutrients, interaction with host cells and tissues. The inherently drug-tolerant yeast-like *Candida glabrata* (Cg) is the second-most prevalent fungal pathogen humans encounter (Lewis, 2009).

Initial colonization and subsequent development of disseminated diseases are determined by the nature of the interaction of *Candida* spp with host immune cells and tissues (Gow et al., 2002). The rate of clearance by the host immune surveillance versus the fungal fitness and growth in organs and tissues determines the outcome such as cure or death. Early recognition of pathogens by immune cells is mediated by dedicated pattern recognition receptors (PRRs), including *Toll*-like receptors (TLRs) and lectins expressed at the surface of innate cells, mainly monocytes, macrophages, neutrophils and dendritic cells (Netea et al., 2008). PRRs recognize microbe-specific pathogen-associated molecular patterns (PAMPs), and trigger a variety of intracellular signaling pathways to orchestrate an efficient and pathogen-specific host immune response (van de Veerdonk et al., 2008a).

The sugar polymers (e.g. chitin, β-D-glucans, mannan) and proteins forming the fungal cell surface are considered the prime source of fungal PAMPs. Notably, β-D-glucans seem preferential ligands for the dectin-1 receptor, which mediates fungal recognition and signaling alone, as well as with the phospholipomannan receptor TLR2 as a co-receptor. By contrast, mannose-sensing receptors include the mannan R, TLR4, dectin-2, mincle, the SIGNR receptor family, galectin3, while TLR6 may use peptido-

glycan recognition (reviewed in:(Netea et al., 2008; Willment and Brown, 2008)). Deficiency in certain PRRs, including TLR4, TLR2, mincle, dectin-1, (Netea et al., 2002; Taylor et al., 2007; Villamon, 2004; Villamon et al., 2004; Wells et al., 2008) or their intracellular signaling adaptors such as MyD88 and CARD9 (Bellocchio et al., 2004; Gross et al., 2006; Villamon et al., 2004) strongly impairs survival of mice to Candida infections, emphasizing the essential role of early pathogen recognition for mounting efficient host immune responses. Nevertheless, conflicting reports on individual contributions of certain PRRs (Murciano et al., 2006; Netea et al., 2002; Saijo et al., 2007; Taylor et al., 2007) hint the enormous underlying complexity, and may stem from strain-dependent genetic factors and most likely complex genetic interactions.

In addition to cell surface PAMPS, nucleic acids from Candida may also stimulate or modulate the dynamic host response during infection. Indeed, double-stranded DNA from *Candida albicans* elicits cytokine release in mice (Miyazato et al., 2009; Yordanov et al., 2005) in a TLR9–dependent fashion (Miyazato et al., 2009). Single-stranded RNA induces a Th1 response normally associated with protection (Bacci et al., 2002), although a lack of TLR9 alone does not impair survival (Bellocchio et al., 2004; Miyazato et al., 2009; van de Veerdonk et al., 2008b)

Binding of fungal PAMPs to PRRs preludes phagocytosis, stimulates the release of reactive oxygen species (ROS) (Frohner et al., 2009), and specific cytokines, ultimately triggering the activation of innate effectors cells. Among others, dendritic cells (DCs) are instrumental in relaying pathogen information from the innate response to the adaptive response through their ability to act as professional antigen-presenting cells. PAMP recognition stimulates DCs to produce signal cytokines, including type I-interferons (IFNs-I) through the so-called first wave (Stetson and Medzhitov, 2006). Extracellular IFNβ subsequently activates its cognate receptor, the IFNα/β receptor (IFNAR) in an autocrine/paracrine fashion, driving the second wave, massive release of IFNα/β triggering the subsequent expression of IFN-stimulated genes (reviewed in (Stetson and Medzhitov, 2006)) many of which drive maturation of DCs both *in vivo* and *in vitro* (Fitzgerald-Bocarsly and Feng, 2007).

Lack of a functional IFNAR receptor increases the susceptibility of mice to a number of viral and bacterial pathogens. However, in certain cases, IFNβ can also cause deleterious effects for the host, creating a ying-yang situation for the host and the pathogen (Decker et al., 2005). Interestingly, Flt3-induced DCs release IFNs-I in response to Ca (Bonifazi et al., 2009), and a recent report suggests that IFNs-I are implicated in the *in vivo* response of mice to *Cryptococcus neoformans* (Biondo et al., 2008). However, the molecular mechanisms by which fungal pathogens induce the IFN-I response in DCs has remained ill-defined. Hence, our work aimed to decipher the molecular basis of the initial IFNβ release by innate immune cells.

Here, we show that bone marrow-derived conventional dendritic cells (BM-DCs) challenged with *Candida* spp release high levels of IFNβ, which subsequently drives a IFNAR1-dependent activation of intracellular STAT1 and IRF7 expression. Further, IFNβ release by BM-DCs requires dynamin-dependent phagocytosis of fungal cells, the recognition of fungal PAMPs by the endosomal TLR7&9 machinery, activation of the TLR-specific MyD88 adaptor, as well as intracellular Src-family/Syk kinase signaling

pathways. This is the first demonstration of a role for TLR7 in fungal recognition and cooperation between TLR7 &9 in inducing an IFN-I response to *Candida* spp. Our results also highlight the importance of the spatio-temporal order of events in orchestrating the host immune response to *Candida* spp and show that nucleic acids serve as fungal PAMPs at later stages of host invasion.

Results

Candida *spp trigger IFNβ release in BM-DCs and induce IFN-type I-specific genes*

Phagocytes of the innate immune system such as macrophages and dendritic cells can release type-I IFNs in response to various microbial pathogens (Decker et al., 2005). To investigate the molecular mechanisms of IFN-I response elicited by *Candida* spp, we used an *in vitro* cell culture model of primary mouse bone marrow-derived conventional dendritic cells (BM-DCs) or bone marrow-derived macrophages (BMDMs) challenged with *Candida* spp. Mouse innate immune cells were differentiated from bone-marrow as described in the "Material and Methods" section and co-cultured at a multiplicity of infection of one BM-DC or BMDM per two Candida cells (MOI 1:2). We used either, *C. albicans* and *C. dubliniensis*, two dimorphic *Candida* species, or *C. glabrata*, a species found only in the yeast form. Messenger RNA levels, as well as IFNβ protein release, was measured by quantitative real-time PCR or ELISA, respectively. All three *Candida* species strongly stimulated IFNβ mRNA expression in BM-DCs after three hours, whereas no induction was observed in unstimulated BM-DCs (Figure 1A). ELISA assays confirmed that the increase in IFNβ gene expression correlated with the release of IFNβ by Candida-infected BM-DCs (Figure 1B). Notably, both UV-inactivated Ca cells and the yeast, *Saccaromyces cerevisiae* (Figure S1A), triggered the IFNβ release. Interestingly, however, the response was cell-specific and restricted to certain innate immune cells, since we failed to detect IFNβ mRNA induction in bone marrow-derived (although they responded to LPS) or in peritoneal macrophages, in neutrophils or splenic DCs co-cultured with Cg (Figure S1B and C). Remarkably, Cg consistently showed the highest potency in stimulating IFNβ mRNA expression and subsequent cytokine release (Figure 1A and B). Hence, we chose Cg cells as the main pathogen stimulus in further experiments to investigate the mechanisms of IFN-I response in this study.

A hallmark of the IFN-I response is its ability to induce the expression of a large number of downstream effector genes (i.e. IFN-I stimulated genes). Indeed, IFNβ released during the first wave recognizes its own receptor IFNAR (a heterodimer of the IFNAR1 and IFNAR2 subunits), activating the intracellular STAT1 and STAT2 transcription factors ultimately triggering expression of typical IFN-I target genes such as IRF7.

Since mouse BM-DCs are known to express the IFNAR receptor, we asked whether the initial IFNβ release triggered by *Candida* spp can induce IFN-I signaling in an autocrine / paracrine fashion by binding to, and activation of, the IFNAR receptor. Thus, BM-DCs were differentiated from either wild type (WT) bone marrow or from mouse bone marrow lacking the IFNAR1 subunit ($IFNAR1^{-/-}$). Immune cells were co-cultured with *Candida* spp or left unstimulated for 2 hours, after which protein extracts were prepared and STAT1 activation was verified by immunodetection using phospho-specific antibodies. In WT BM-DCs

co-cultured with Candida, IFNβ release correlated with STAT1 phosphorylation and thus activation (Figure 1C), as well as activation of IRF7 transcription (Figure 1D). By contrast, when IFNAR1$^{-/-}$ BM-DCs were co-cultured with Cg, no STAT1 phosphorylation was observed (Figure 1C), and IRF7 transcription was also not enhanced (Figure 1D). Notably, STAT1 activation was still detected in BM-DCs lacking the IFNγ receptor (IFNγ$^{-/-}$), which may also trigger STAT1 phosphorylation (Figure S1D). Consistent with the absence of IFNβ release in BMDMs co-cultured with Cg, no STAT1 activation was observed under these conditions (Figure S1B, right panel). All together, these data demonstrate that the *Candida* spp trigger a first wave of IFNβ in BM-DCs, thereby activating an IFN-I response in an IFNAR1-dependent fashion.

Cg-induced IFNß release is partially dependent on Src/Syk kinase signaling

The main PRRs involved in Candida recognition belong to the C-type lectin and TLR families (Netea et al., 2008). C-type lectins, like other ITAM-bearing receptors, signal through intracellular Syk and Src-family kinases (Underhill and Goodridge, 2007). We thus reasoned that PP2, an inhibitor of Src-family kinases and R406, a highly specific inhibitor of the Syk kinase, may impair the IFNβ response to *Candida* spp. Indeed, pre-treatment of BM-DCs with R406 prior to Cg stimulation, significantly decreased the IFNβ release by 50% (Figure 2A, left panel). Likewise, PP2 strongly inhibited the Cg-triggered IFNβ release to about 12% of the level observed when BM-DCs were pretreated with DMSO vehicle alone; as a control PP3, the inactive analog of PP2, had no significant effect (Figure 2A, right panel). Thus, these results unequivocally show that both intracellular Src and Syk signaling pathways are required to drive the IFNβ release in response to fungal cells. Moreover, the data imply the involvement of ITAM-bearing receptors in this process.

The C-type lectin dectin-1, a β-1,3 glucan receptor, is known as one of the major receptors for *Candida* spp recognition (Dennehy and Brown, 2007). Surprisingly, however, BM-DCs lacking the dectin-1 receptor, still released IFNβ upon Cg challenge (Figure 2B left panel). Thus, these results show that dectin-1 is not involved in mediating the Candida-induced IFNβ release. In addition to dectin-1, CD11b, also known as integrin α_M, can function as a receptor for β-glucans, since it binds Ca (Forsyth et al., 1998) (van Bruggen et al., 2009), is present in the phagosome upon Candida phagocytosis (Heinsbroek et al., 2008), and it also activates the Src-family and Syk kinases (Nakayama et al., 2008). Thus, we investigated the potential role of CD11b in the IFNβ-response. We challenged CD11b-deficient BM-DCs with Cg but even in absence of CD11b, IFNβ-release was observed albeit slightly reduced, suggesting that this β-glucan receptor is also not involved in triggering the initial IFNβ-release in BM-DC infected with Cg. Furthermore, no significant IFNβ-release was observed when BM-DCs were treated with β-glucan extract from *Saccaromyces cerevisiae* or Curdlan (Figure 2C). However, these cells readily responded to LPS, which was used as a positive control for PRR signalling via TLR4. Additional potential PAMPs such as chitin or mannan failed to induce detectable IFNβ levels in BM-DCs (data not shown). Thus, our data show that neither dectin-1 nor CD11b or other PRRs for known cell wall PAMPs are mediating the initial IFNβ release triggered by *Candida* spp. However, it requires activation of Src-family and Syk kinase signaling pathways.

Beside their role as intracellular adaptors for certain PRRs, Src-family and Syk kinases are also involved in mediating phagocytic processes. Therefore, we assayed their involvement in phagocytosis using a flow-cytometry-based analysis of the percentage of BM-DCs having phagocytosed at least one Alexa-480-labelled Cg with or without inhibitor pre-treatment. However, pre-treatment with the Src kinase inhibitor PP2 had no significant effect on the phagocytic properties of BM-DCs (data not shown). By contrast, only 60% of the BM-DCs pre-treated with the Syk inhibitor R406 contained at least one Cg cell when compared to 100% of BM-DCs having engulfed at least one Cg in vehicle (DMSO)-treated BM-DCs (Figure 2D). Therefore, these data suggest that Syk kinase activation promotes IFNβ release by contributing to the phagocytic process in BM-DCs challenged by fungal pathogens.

The Cg-induced IFNβ release is TLR2 and TLR4-independent

The second main class of PRRs involved in sensing and recognizing *Candida* spp is the *toll*-like receptor family. In particular, TLR2 and TLR4 are involved in Candida recognition and reported to be essential for survival to Candida infection in mice. Thus, we investigated whether these receptors were involved in the IFNβ response to Candida using BM-DCs derived from the bone marrow of wild type (WT) or from mice lacking either TLR2 ($TLR2^{-/-}$) or TLR4 ($TLR4^{-/-}$) receptors. Surprisingly, when wild type and mutant BM-DCs were infected with Cg, the IFNβ release was stimulated to similar or even higher levels (Figure 3A and B left panels). Accordingly, a strong STAT1 activation was observed in both wild type and mutant BM-DCs (Figure 3B and B right panel), demonstrating that IFN-I response to fungal pathogens must proceed independently of the known TLR2 or TLR4 signaling pathways.

The IFNβ release of BM-DCs requires phagocytosis and MyD88 activation

Toll-like receptors use as signaling adaptors either, MyD88 (e.g. TLR1, 2, 7, 9), or TRIF (in the case of TLR3) or both as in the case of TLR4. To further investigate the possible involvement of TLR signaling in the Cg-induced IFNβ release, we used BM-DCs lacking either one of these signaling adaptors. Markedly, BM-DCs lacking MyD88 ($MyD88^{-/-}$) were completely unable to release IFNβ following Cg challenge (Figure 4A, left panel). Accordingly, $MyD88^{-/-}$ BM-DCs co-cultured with Cg also failed to mount the subsequent IFN-I response, as evident from a much weaker STAT1 phosphorylation in these cells when compared to wild type BM-DCs (Figure 4A right panel). By sharp contrast, a lack of TRIF did not impair the IFNβ release following Candida challenge (Figure 4B). These data demonstrate a strict requirement for TLR/MyD88 signaling in triggering the first wave of IFNβ release in BM-DCs facing fungal invasion hence excluding any participation of TLR3.

In mice, several surface TLRs (TLR1, 2, 4,5, 6) as well as phagosomal TLRs (TLR7, 9) signal through the MyD88 adaptor. To further narrow down the list of candidate TLRs recognizing *Candida* spp to drive IFNβ, we used dynasore, a specific small molecule inhibitor of the GTP-binding protein, dynamin. Proper constriction of clathrin-coated vesicles during endocytosis and phagocytosis requires dynamin, a process which can be efficiently inhibited by dynasore (Macia et al., 2006).Strikingly, dynasore pre-treatment of BM-DCs prior to Cg addition completely abolished IFNβ release to the level of unstimulated BM-DCs. No

inhibition was observed in BM-DCs pretreated with vehicle (DMSO) only (Figure 4C). The effect of dynasore treatment was not caused by loss of cell viability, as verified by life-staining (data not shown), and since treated BM-DCs still showed intracellular ERK-phosphorylation upon Cg challenge (Figure S2A). Thus, our data demonstrate that IFNβ induction by Cg in BM-DCs requires the completion of dynamin-dependent phagocytosis, strongly suggesting that the activation of MyD88 demands recognition of PAMPs through intracellular TLRs.

The* Candida*-induced IFNβ release requires phagosome acidification and TLR7 & TLR9

Endosomal TLRs have to be processed by proteases in the endolysosome to undergo conformational changes enabling them to recruit and activate MyD88 upon PAMP recognition inside the endolysosome. This proteolytic maturation can be prevented by inhibiting the endosome acidification (Ewald et al., 2008 ; Hacker et al., 1998). Thus, we asked whether bafilomycin A1 or the antimalarial drug chloroquine, both compounds inhibiting endosome acidification, would also block Candida-induced IFNβ release. Strikingly, pre-treatment of BM-DCs with 25µg/ml (50µM) Chloroquine or only 5nM bafilomycin A1 completely abrogated the ability of BM-DCs to release IFNβ upon stimulation with Cg (Figure 5A), demonstrating a role for endosomal TLRs in mediating the Cg-induced IFNβ release in BM-DCs. The effect of bafilomycin A1 or chloroquine treatment was not caused by loss of cell viability, as shown by life-staining (data not shown). Consistent with this treated BM-DCs still activated intracellular ERK upon Cg challenge (Figure S2B).

In mice, endosomal TLRs signaling through MyD88 requires TLR7, TLR8 and TLR9. To specifically block the activation of these receptors, we used the synthetic oligodeoxynucleotides IRS661, an antagonists of TLR7, ODN2088, an antagonist of TLR9 or IRS954, which inhibits both TLR7&9. Blocking of either TLR7 or TLR9 strongly decreased IFNβ production upon Cg challenge by at least 50% ($p \leq 0.0001$), and simultaneous blocking of both TLR receptor subtypes completely abolished IFNβ release ($p \leq 0.0001$) (Figure 5B). The unspecific control oligodeoxynucleotides CTL_IRS and CTL_ODN had no detectable or significant effect on IFNβ production (Figure 5B).

Integrated model of type I response triggered by fungal pathogens in conventional BM-DCs

Based on our collective data presented in this work, we propose the following model for the Candida-induced IFNβ signaling in conventional BM-DCs (Figure 6). Adhesion and recognition of *Candida* spp at the surface of innate immune cells initiates dynamin-dependent phagocytosis. Maturation and acidification of the phagosome enables processing of the TLR7 & TLR9 receptors, which are subsequently activated by their PAMP ligands, most likely fungal nucleic acids, to recruit and activate cytoplasmic MyD88, ultimately triggering the IFNβ release. Other as yet unknown pathways acting through Syk/Src-family kinase signaling may also contribute to the induction of IFN-I response in BM-DCs.. Taken together, the results provide the first demonstration of an IFNβ release by conventional BM_DCs in response to phagosomal Candida recognition, hence, revealing a thus far unrecognized role for endosomal TLRs in fungal recognition.

Discussion

In this report, we show for the first time that *Candida* species trigger an IFN-I response in mouse conventional BM-DCs. We identify TLR7&9 as the essential PRRs activating this response in a MyD88-dependent fashion from within maturing phagosomes. Because of the phagocytic and microbicidal properties, innate immune cells are the first line of defence against many microbial pathogens. In addition, they are producers of IFNs-I, a family of cytokines specialised in coordinating the cross-talk between the innate and adaptive immune response to microbial or viral infections. Therefore, we studied the capabilities of several innate immune cell types, bone marrow-derived neutrophils or macrophages, peritoneal macrophages, and splenic or bone marrow-derived conventional dendritic cells (BM-DCs) to respond to fungal challenges by producing IFNβ using an *in vitro* co-culture interaction system. We demonstrate that mouse BM-DCs rapidly release IFNβ, while only little IFNα is released in response to *Candida* spp. Notably, others also observed detectable IFNβ induction upon challenge with Ca in *flt3*-differentiated DCs and only a weak but significant induction of IFNα gene transcription in BM-DCs stimulated with the yeast form of Ca. This discrepancy may be caused by differences in the protocols used to prepare the conventional BM-DCs (Bonifazi et al., 2009). Notably, both BMDMs and BM-DCs release IFNβ when challenged with another prominent fungal pathogen, *Cryptococcus neoformans* (Biondo et al., 2008). Under our experimental conditions, the IFN-I response to Candida is highly cell-type specific within innate immune cells, since peritoneal or bone marrow-derived macrophages (BMDMs) as well as neutrophil or splenic DCs challenged by Cg fail to release detectable amounts of IFNβ. Nevertheless, our results are consistent with reports about distinct cytokine responses between BMDMs and myeloid dendritic cells (Goodridge et al., 2009; Rosas et al., 2008), suggesting that different innate immune cells may have distinct repertoires to respond to fungal PAMPs, depending on the differentiation procedure used to obtain the cells *in vitro*, or the host tissue environment *in vivo*. This may help fine-tuning the anti-fungal defence and immune surveillance.

We show here that IFNβ is also induced by other *Candida* species such as Cd and Cg. Interestingly, Cg, a non-dimorphic yeast-like species, appears as a much better trigger for IFNβ than the pleomorphic filamentous species Ca or Cd. Notably, Cg can persist in the host {Jacobsen, #1754;Roetzer, #1966}, whereas Ca can escape and normally efficiently kills host cells (Fernandez-Arenas et al., 2009; Marcil et al., 2008). Hence, it is tempting to speculate that the ability of Ca to escape the phagosome and cause host cell lysis may explain the weaker induction of IFN-I response versus Cg favoring a strong IFNβ release by its persistence in the host.

β-glucan preparations stimulate the release by innate immune cells of a number of cytokines such as TNFα, IL2 or IL12 (Hernanz-Falcon et al., 2009), and can induce BM-DC maturation in humans (Carmona et al., 2006), as well as in mice (Yoshitomi et al., 2005). β-glucan drives BM-DC maturation in part through dectin-1, which is considered a major PRR for glucans (Dennehy and Brown, 2007). However, we show here that the Cg-induced IFNβ release does not require dectin-1 and CD11b, both acting as β-glucan receptors accumulating at the site of Candida uptake by macrophage phagocytosis (Heinsbroek et

al., 2008). Furthermore, we tend to exclude the involvement of other unknown beta-glucan receptors, since none of the β-glucan preparations we used, namely β1-3 and β1-6-glucan extracts obtained from the Sc cell wall, and Curdlan, a linear β1-3 glucan polymer, are able to trigger IFNβ release in BM-DCs. Likewise, mannan and chitin are also inactive under these conditions. Hence, in contrast to LPS from Gram-negative bacterial cell walls, fungal cell wall extracts do not induce IFN release in innate immune cells, despite being a rich source of fungal PAMPs for other cytokine responses (Netea et al., 2008). However, care has to be taken when performing these experiments, since many commercial and custom-made cell wall preparations contain minute LPS contaminations, which may lead to conflicting interpretations of results. Therefore, all of our cytokine experiments in primary cells were carried out in the presence of polymyxin B, which alleviates the LPS contamination problem (Cardoso et al., 2007)

By specifically inhibiting dynamin, we demonstrate that Cg phagocytosis is a mandatory prerequisite for IFNβ release. Similarly, inhibition of Src family kinase also strongly blocks Cg-induced IFNβ-release. Notably, phosphorylation of cortactin and dynamin by Src kinase is required for activation of endocytosis in epithelial cells (Cao et al., 2010), and both cortactin and dynamin are essential for Ca internalisation in epithelial cells (Moreno-Ruiz et al., 2009). Furthermore, Syk kinase activation is at least partially necessary for IFNβ production. Although in this context, Syk function on IFNβ release is not dectin-1 or CD11b-dependent, it is relevant for mediating Candida phagocytosis. Whether it occurs through its role in integrin-mediated signal transduction (Van Ziffle and Lowell, 2009), as signaling adaptor of ITAM-bearing receptors or as mediator of phagocytic processes (Tohyama and Yamamura, 2009) will be a matter of further experiments. Nonetheless, our data emphasize the pivotal importance of the phagocytic process for orchestrating the IFN-I host response to *Candida* spp.

Using BM-DCs lacking the TLR adaptors TRIF or MyD88, we demonstrate that the Cg-induced IFNβ release requires MyD88 signaling. Hence, our findings are consistent with the model of a MyD88 pathway mediating the cytokine response of inflammatory DCs to yeast (Bonifazi et al., 2009). Our data further strengthen the importance of inflammatory DCs in the response against Candida infection as major producers of IFNβ. Surprisingly, however, the lack of neither TLR2 nor TLR4 impairs the IFNβ release, although these PRRs appear critical for survival to Candida dissemination in mouse models (Netea et al., 2002; Villamon, 2004; Villamon et al., 2004).

Unexpectedly, our results demonstrate that (i) TLR7 or TLR9 alone trigger an initial IFNβ release upon Candida recognition by BM-DCs, and (ii) the full IFNβ release is only achieved when stimulating both TLR7 and TLR9. Spatial recognition of microbial single-stranded RNA by TLR7 within endosomes was first observed for viruses (Fitzgerald-Bocarsly and Feng, 2007; Gilliet et al., 2008). More recently, this mechanism was found to apply to bacterial recognition in mice and humans (Eberle et al., 2009; Mancuso et al., 2009). However, this is the first report of fungal recognition by TLR7 within the endosomal compartments, thus linking spatio-temporal recognition of fungi to stimulation of the host immune response. Although a lack of TLR9 decreases survival to *Aspergillus fumigatus* or *Cryptoccocus neoformans* in mice (Nakamura et al., 2008; Ramirez-Ortiz et al., 2008), $TLR9^{-/-}$ mice show no significant alterations in survival to Ca (Bellocchio et al., 2004; Miyazato et al., 2009; van de Veerdonk et al., 2008b). A potential

role of TLR7 in survival to Ca or any fungal microbe has yet to be further explored. Given the redundant roles of TLR7 & TLR9 in inducing IFN-type I response in BM-DCs in response to Candida, mice lacking both PRRs may be a better suited model to study the role of endosomal TLRs and IFN-I response in the survival to Candida infection. Since TLR7 and TLR9 recognise guanosine and uridine–rich single-stranded RNA, and unmethylated CpG, respectively, the present report also hints the importance of Candida-derived-nucleic acids as potential PAMP sources for host immune cell activation through the IFN-I response. In agreement, recognition of Ca DNA by TLR9 triggers release of IL12 in BM-DCs (Miyazato et al., 2009). Interestingly, Ca RNA-pulsed BM- and spleen-DCs undergo activation and confer protection against systemic Ca infection in mice (Bacci et al., 2002). Whether these properties resulted from activation of an IFN-I response in these innate immune cells is unknown.

Activation of the IFN-I response is critical for the maturation of DCs into professional antigen-presenting cells to help shaping magnitude and duration of the adaptive immune response by inducing the differentiation of T helper cells (Fitzgerald-Bocarsly and Feng, 2007). Remarkably, IFNs-I can function as pro-inflammatory and anti-inflammatory cytokines, but the contribution of each property to the overall host response is not well understood (Fitzgerald-Bocarsly and Feng, 2007; Kovarik et al., 2007). In human and mice, IFNs-I inhibit the DC-mediated Th17 cell differentiation (Guo et al., 2008; Moschen et al., 2008; Shinohara et al., 2008; Zhang et al., 2009). The role of the IL-17 pathway in antifungal defense is rather controversial. A lack of Th17 cells results in persistent mucocutaneous candidiasis in humans (Curtis and Way, 2009) and impaired survival in mice (Huang et al., 2004; van de Veerdonk et al.). Conversely, other studies suggest that IL-17 may contribute to inflammatory pathology and worsening of fungal disease in mice (De Luca et al., 2007; Zelante, 2007). Furthermore, by stimulating expression of IL10 and down-regulation of IL12, IFNs-I appear to also modulate the Th1/Th2 balance toward a reduced inflammation and host tissue damage, indicating a protective role (Byrnes et al., 2002; Zhang et al., 2009).

In vivo challenges of mice lacking the IFNAR in mouse intraperitoneal inflammation model, suggest that IFNs-I can exert a protective role against local, inflammatory Candida infections. Remarkably, IFNs-I act as chemoattractants, as they appear to stimulate the recruitment and migration of other immune cells to the site of infection (Majer et al., in preparation).. Taken together, our results presented here hint a crucial and as yet unrecognized role for endosomal TLRs in *fungal* recognition and induction of IFN-I response in mouse BM-DCs challenged with *Candida* spp. .Furthermore, our findings stress the importance of fungal nucleic acids as a source for microbial PAMPs in BM-DCs dedicated to recognize and respond to microbial pathogens.

Experimental Procedures

Fungal strains, growth conditions

Fungal strains used in this study were the *Candida albicans* clinical isolate SC5314 (Gillum et al., 1984), the *Candida glabrata* clinical isolate ATCC2001 (CBS138) (Espinel-Ingroff et al., 1998) and the *Candida dubliniensis* clinical isolate CD36 (Sullivan et al., 1995). Fungal cells in the logarithmic growth phase were collected by centrifugation, washed in sterile PBS and diluted at the required cell number for co-culture with innate immune cells. UV-treated *Candida* suspensions were prepared by treating an aliquot of the *Candida* infection suspension with 999μJ/cm2 in a Stratalinker (Stratagene).

Mouse genetic backgrounds

All mice were derived from the C57BL/6 background and housed under specific pathogen-free conditions according to FELASA guidelines (Nicklas et al., 2002). IFNAR1$^{-/-}$ mice (Muller et al., 1994), TLR2$^{-/-}$ (Takeuchi et al., 1999), TLR4$^{-/-}$ (Hoshino et al., 1999), MyD88$^{-/-}$ (Adachi et al., 1998) and TRIF$^{-/-}$ mice (Yamamoto et al., 2003) were kindly provided by Dr. Shizuo Akira, Osaka University, Japan. Bone marrow from dectin-1$^{-/-}$ (Taylor et al., 2007) and corresponding wild type mice were generously supplied by Dr. G. Brown University of Aberdeen, UK . CD11b$^{-/-}$ mice were purchased from the Jackson Laboratory.

Cell culture of primary innate immune cells differentiated from bone marrow

For the preparation of BM-DCs, bone marrow was collected from femurs of 7-9 week old C57BL/6 wild type or knock-out mice, and grown in DMEM supplemented with 10% heat-inactivated FCS and15 % GM-CSF-containing X-conditioned medium (Zal et al., 1994). BM-DCs were used after 7-8 days for co-culture with whole Candida or fungal extracts. Cell surface markers of the BM-DCs preparations were assessed by flow cytometry using a panel of marker antibodies. BM-DCs were F4/80^{-}, CD11b^{+}, and at least 50–60% of the cells were CD11c^{+}.

Co-culture of innate immune cells with fungi or cell wall extracts

Fungal-mammalian cell co-culture was performed exactly as previously described (Bourgeois et al., 2009). Briefly, BM-DCs were plated at a density of 1.0-1.25x10^{5} cells/cm^{2} and incubated with fungal cells at a target to effector ratio of 2:1 at 37°C (5% CO_2) for the indicated time periods. Pre-treatment of BM-DCs with inhibitor molecules (dynasore, PP2, PP3, R406, bafilomycin A1 or chloroquine) or vehicle, were carried out at 37°C (5% CO_2) for 30 min prior to stimulation. Inhibitor final concentrations were 80μM for dynasore (Sigma), 25μM for PP2 and PP3 (Calbiochem), 4μM for R406 (Rigel Pharmaceuticals Inc.), 5 or 1 nM for bafilomycin A1 (Sigma), and 50 or 10 μM for chloroquine (Sigma,). Pre-treatment of BM-DCs with 20μg/ml synthetic oligodeoxynucleotides (IRS661, IRS954, ODN2088) or non-specific oligonucleotide controls were carried out at 37°C for 60 min prior to stimulation. ODN2088 and controls were from InvivoGen, IRS661, IRS954 and control (CTL_IRS) were synthesized by TIB-Molbiol as previously described (Barrat et al., 2005). Stimulation of BM-DCs also used 100μg/ml β-glucans from *S. cerevisiae* (Calbiochem),

Zymosan from 100µg/ml Curdlan, a high-molecular weight β-1-3 glucan from *Alcalagines faecalis* (WAKO Chemicals) or 0.1µg/ml "TLR-grade" LPS from *Salmonella minnesota* (Sigma). All treatments with Candida or fungal cell wall-derived components were carried out in the presence of 30µg/ml polymyxin B (Sigma) to neutralize LPS endotoxin contaminants (Cardoso et al., 2007).

Reverse transcription and real-time PCR analysis

RNA samples preparation reverse transcription and real-time PCR were performed using the methods described in the Supplemental Experimental Procedures using the following primers: Mouse GAPDH: *for* 5'-CATGGCCTTCCGTGTTCCTA-3'; and *rev* 5'-GCGGCACGTCAGATCCA-3' (RTPrimerDB, http://medgen.ugent.be/rtprimerdb /index.php); Mouse IFNβ: *for* 5`TCA GAA TGA GTG GTG GTT GC 3` and *rev* 5`GAC CTT TCA AAT GCA GTA GAT TCA 3` (Stockinger et al., 2004); Mouse IRF7 *for* 5'-CTG-GAG-CCA-TGG-GTA-TGC-A-3'; and *rev* 5'-AAGCACAAGCCGAGACTGCT-3' as determined using the sequence analysis software Vector NTI (Invitrogen).

For relative quantification purpose, efficiencies of the individual PCR reactions were determined by the LinReg method (Ramakers et al., 2003). Results are expressed as the fold-expression (R) of the gene of interest (IFNβ) versus the expression of a house-keeping gene (GAPDH) in treated (t) versus untreated (ut) conditions. The equation used for normalization was: $R = \mathbf{(}E_{IFN\beta(ut)}^{Ct\ IFN\beta(ut)} / E_{GAPDH(ut)}^{CtGAPDH(ut)}\mathbf{)\ /\ (}E_{IFN\beta(t)}^{C\ IFN\beta(t)} / E_{GAPDH(t)}^{CtGAPDH(t)}\mathbf{)}$, where E is the PCR efficiency and Ct, the number of cycles to the threshold fluorescence.

Immunodetection

Sample preparation and immunoblotting were performed using the methods described in the Supplemental Experimental Procedures. Blots were probed with anti-STAT1 antibodies recognizing phospho-Tyr201, anti-phospho-ERK antibodies (Cell Signaling), anti-IRF3 and anti-p38 antibodies, (Santa Cruz), or anti-C-terminal STAT1 sera (a kind gift from Pavel Kovarik (Kovarik et al., 1998)) An infrared-labeled secondary antibody (LI-Cor,) was used to detect immune complexes and analysis was performed using the infrared imaging system Odyssey (LI-Cor) according to conditions recommend by the manufacturer.

Cytokine measurements by ELISA and phagocytosis assays

The amount of IFNβ released in cell culture supernatants was assayed using the Verikine mouse IFNβ ELISA kit (R&D systems) according to manufacturer's instructions.

Phagocytosis assay was performed as previously described (Herre et al., 2004) using the following modifications. Briefly, Cg cells prepared as for interactions experiments were labeled with 10mM Alexa488 C5 maleimide (Invitrogen), in 100mM HEPES buffer, pH 7,5 for 15 min at room temperature in the dark under constant shaking. Labeled Cg were washed twice in HEPES buffer and kept at 4°C until use. BM-DCs plated at density of 1.0-1.25x10^5 cells/cm^2 one day prior to the assay were treated with inhibitors or

vehicle 30 minutes 37°C (5% CO_2) prior to the assay and then pre-cooled on ice. After 20 min, Alexa488-labeled Cg in ice-cold DMEM was added at a target to effector ratio of 2:1, and samples were incubated at 37°C (5% CO_2) for 45 min to allow for phagocytosis to occur.

Phagocytosis was terminated by chilling plates on ice, where they remained during detaching and fixation in 1% formaldehyde. Fluorescence of extracellular Cg was quenched by addition of 0.4% trypan blue. Negative controls for phagocytosis were left on ice during the whole process. Duplicate samples were subjected to flow cytometry analysis, gating on Alexa488/BM-DCs cell populations with internalized Cg. The percentage of phagocytosis was determined as follows: (inhibitor-treated BM-DCs with Cg at 37°C minus inhibitor-treated BM-DCs with Cg at 4°C)/(vehicle-treated BM-DCs with Cg at 37°C minus vehicle-treated BM-DCs with Cg at 4°Cx100. Results are expressed as the mean ± SD of the percentage of ingestion (the percentage of BM-DC containing one or more yeast cells).

Statistical analysis - Statistical analysis of data was performed using the Prism graphing and analysis software. Comparison of two groups was done with the Student's t test. $P < 0{\cdot}05$ was considered significant.

Acknowledgements

We thank all laboratory members for helpful discussions and many critical comments on the manuscript. Further, we thank Pavel Kovarik for providing us with anti-STAT1 antibodies, and Gordon Brown for supplying us with bone marrow from dectin1$^{-/-}$ and corresponding wild-type mice. We highly appreciate the gift of the *Syk* kinase inhibitor R406 from Rigel Pharmaceutical Inc. We are indebted to Anita Sil and Diane Inglis for sharing unpublished data and for exchanging manuscripts before submission.

Authors contributions

CB, OM & KK conceived and designed experiments; CB, OM IF, IL& KSH performed experiments; CB, OM, WG & KK analyzed data; CB & KK wrote the manuscript; WG, SS, TD, SA & MM contributed reagents/materials/analysis tools/experimental advices; OM, IF, WG, SS, TD, AS, & MM commented and contributed to writing the manuscript.

Grant Support

This work was funded by grants from the Christian Doppler Research Society and the Vienna Science & Technology Fund WWTF (Project HOPI-LS133) to KK, MM and TD, from the Austrian Science Foundation (FWF) to MM and TD (SFB28) and to TD (AP20522). Moreover, CB was supported by the EC Marie Curie Training Network *"CanTrain"* (CT-2004-512481), IEF by the VBC PhD Programme WK001, OM by a DOC-*fFORTE* Stipend from the Austrian Academy of Sciences (OeAW). These funding agencies had no role in study design, data collection and analysis, decision to publish, or preparation of the manuscript.

Competing interests: The authors have declared that no competing interests exist.

References

Adachi, O., Kawai, T., Takeda, K., Matsumoto, M., Tsutsui, H., Sakagami, M., Nakanishi, K., and Akira, S. (1998). Targeted disruption of the MyD88 gene results in loss of IL-1- and IL-18-mediated function. Immunity *9*, 143-150.

Bacci, A., Montagnoli, C., Perruccio, K., Bozza, S., Gaziano, R., Pitzurra, L., Velardi, A., d'Ostiani, C.F., Cutler, J.E., and Romani, L. (2002). Dendritic cells pulsed with fungal RNA induce protective immunity to *Candida albicans* in hematopoietic transplantation. J Immunol *168*, 2904-2913.

Barrat, F.J., Meeker, T., Gregorio, J., Chan, J.H., Uematsu, S., Akira, S., Chang, B., Duramad, O., and Coffman, R.L. (2005). Nucleic acids of mammalian origin can act as endogenous ligands for Toll-like receptors and may promote systemic *lupus erythematosus*. J Exp Med *202*, 1131-1139.

Bellocchio, S., Montagnoli, C., Bozza, S., Gaziano, R., Rossi, G., Mambula, S.S., Vecchi, A., Mantovani, A., Levitz, S.M., and Romani, L. (2004). The contribution of the *Toll*-like/IL-1 receptor superfamily to innate and adaptive immunity to fungal pathogens in vivo. J Immunol *172*, 3059-3069.

Biondo, C., Midiri, A., Gambuzza, M., Gerace, E., Falduto, M., Galbo, R., Bellantoni, A., Beninati, C., Teti, G., Leanderson, T.*, et al.* (2008). IFN-{alpha}/{beta} signaling is required for polarization of cytokine responses toward a protective type 1 pattern during experimental cryptococcosis. J Immunol *181*, 566-573.

Bonifazi, P., Zelante, T., D'Angelo, C., De Luca, A., Moretti, S., Bozza, S., Perruccio, K., Iannitti, R.G., Giovannini, G., Volpi, C.*, et al.* (2009). Balancing inflammation and tolerance in vivo through dendritic cells by the commensal *Candida albicans*. Mucosal Immunol *2*, 362-374.

Bourgeois, C., Majer, O., Frohner, I., and Kuchler, K. (2009). In vitro systems for studying the interaction of fungal pathogens with primary cells from the mammalian innate immune system. Methods Mol Biol *470*, 125-139.

Byrnes, A.A., McArthur, J.C., and Karp, C.L. (2002). Interferon-beta therapy for multiple sclerosis induces reciprocal changes in interleukin-12 and interleukin-10 production. Ann Neurol *51*, 165-174.

Cao, H., Chen, J., Krueger, E.W., and McNiven, M.A. (2010). SRC-mediated phosphorylation of dynamin and cortactin regulates the "constitutive" endocytosis of transferrin. Mol Cell Biol *30*, 781-792.

Cardoso, L.S., Araujo, M.I., Goes, A.M., Pacifico, L.G., Oliveira, R.R., and Oliveira, S.C. (2007). Polymyxin B as inhibitor of LPS contamination of *Schistosoma mansoni* recombinant proteins in human cytokine analysis. Microb Cell Fact *6*, 1.

Carmona, E.M., Vassallo, R., Vuk-Pavlovic, Z., Standing, J.E., Kottom, T.J., and Limper, A.H. (2006). Pneumocystis cell wall beta-glucans induce dendritic cell costimulatory molecule expression and inflammatory activation through a Fas-Fas ligand mechanism. J Immunol *177*, 459-467.

Curtis, M.M., and Way, S.S. (2009). Interleukin-17 in host defence against bacterial, mycobacterial and fungal pathogens. Immunology *126*, 177-185.

De Luca, A., Montagnoli, C., Zelante, T., Bonifazi, P., Bozza, S., Moretti, S., D'Angelo, C., Vacca, C., Boon, L., Bistoni, F.*, et al.* (2007). Functional yet balanced reactivity to *Candida albicans* requires TRIF, MyD88, and IDO-dependent inhibition of Rorc. J Immunol *179*, 5999-6008.

Decker, T., Muller, M., and Stockinger, S. (2005). The yin and yang of type I interferon activity in bacterial infection. Nat Rev Immunol *5*, 675-687.

Dennehy, K.M., and Brown, G.D. (2007). The role of the {beta}-glucan receptor Dectin-1 in control of fungal infection. J Leukoc Biol *82*, 253-258.

Eberle, F., Sirin, M., Binder, M., and Dalpke, A.H. (2009). Bacterial RNA is recognized by different sets of immunoreceptors. Eur J Immunol *39*, 2537-2547.

Espinel-Ingroff, A., Stockman, L., Roberts, G., Pincus, D., Pollack, J., and Marler, J. (1998). Comparison of RapID yeast plus system with API 20C system for identification of common, new, and emerging yeast pathogens. J Clin Microbiol *36*, 883-886.

Ewald, S.E., Lee, B.L., Lau, L., Wickliffe, K.E., Shi, G.P., Chapman, H.A., and Barton, G.M. (2008). The ectodomain of *Toll*-like receptor 9 is cleaved to generate a functional receptor. Nature *456*, 658-662.

Fernandez-Arenas, E., Bleck, C.K., Nombela, C., Gil, C., Griffiths, G., and Diez-Orejas, R. (2009). Candida albicans actively modulates intracellular membrane trafficking in mouse macrophage phagosomes. Cell Microbiol *11*, 560-589.

Fitzgerald-Bocarsly, P., and Feng, D. (2007). The role of type I interferon production by dendritic cells in host defense. Biochimie *89*, 843-855.

Forsyth, C.B., Plow, E.F., and Zhang, L. (1998). Interaction of the fungal pathogen *Candida albicans* with integrin CD11b/CD18: recognition by the I domain is modulated by the lectin-like domain and the CD18 subunit. J Immunol *161*, 6198-6205.

Gilliet, M., Cao, W., and Liu, Y.J. (2008). Plasmacytoid dendritic cells: sensing nucleic acids in viral infection and autoimmune diseases. Nat Rev Immunol *8*, 594-606.

Gillum, A.M., Tsay, E.Y., and Kirsch, D.R. (1984). Isolation of the *Candida albicans* gene for orotidine-5'-phosphate decarboxylase by complementation of *S. cerevisiae ura3* and *E. coli pyrF* mutations. Mol Gen Genet *198*, 179-182.

Goodridge, H.S., Shimada, T., Wolf, A.J., Hsu, Y.M., Becker, C.A., Lin, X., and Underhill, D.M. (2009). Differential use of CARD9 by dectin-1 in macrophages and dendritic cells. J Immunol *182*, 1146-1154.

Gow, N.A., Brown, A.J., and Odds, F.C. (2002). Fungal morphogenesis and host invasion. Curr Opin Microbiol *5*, 366-371.

Gross, O., Gewies, A., Finger, K., Schafer, M., Sparwasser, T., Peschel, C., Forster, I., and Ruland, J. (2006). Card9 controls a non-TLR signalling pathway for innate anti-fungal immunity. Nature *442*, 651-656.

Guo, B., Chang, E.Y., and Cheng, G. (2008). The type I IFN induction pathway constrains Th17-mediated autoimmune inflammation in mice. J Clin Invest *118*, 1680-1690.

Hacker, H., Mischak, H., Miethke, T., Liptay, S., Schmid, R., Sparwasser, T., Heeg, K., Lipford, G.B., and Wagner, H. (1998). CpG-DNA-specific activation of antigen-presenting cells requires stress kinase activity and is preceded by non-specific endocytosis and endosomal maturation. EMBO J *17*, 6230-6240.

Heinsbroek, S.E., Taylor, P.R., Martinez, F.O., Martinez-Pomares, L., Brown, G.D., and Gordon, S. (2008). Stage-specific sampling by pattern recognition receptors during *Candida albicans* phagocytosis. PLoS Pathog *4*, e1000218.

Hernanz-Falcon, P., Joffre, O., Williams, D.L., and Reis, E.S.C. (2009). Internalization of dectin-1 terminates induction of inflammatory responses. Eur J Immunol *39*, 507-513.

Herre, J., Marshall, A.S., Caron, E., Edwards, A.D., Williams, D.L., Schweighoffer, E., Tybulewicz, V., Reis e Sousa, C., Gordon, S., and Brown, G.D. (2004). Dectin-1 uses novel mechanisms for yeast phagocytosis in macrophages. Blood *104*, 4038-4045.

Hoshino, K., Takeuchi, O., Kawai, T., Sanjo, H., Ogawa, T., Takeda, Y., Takeda, K., and Akira, S. (1999). Cutting Edge: *Toll*-like receptor 4 (TLR4)-deficient mice are hyporesponsive to lipopolysaccharide: evidence for TLR4 as the LPS gene product. J Immunol *162*, 3749-3752.

Huang, W., Na, L., Fidel, P.L., and Schwarzenberger, P. (2004). Requirement for interleukin-17A for systemic anti-*Candida albicans* host defense in mice. J Infect Dis *190*, 524-631.

Jacobsen, I.D., Brunke, S., Seider, K., Schwarzmuller, T., Firon, A., d'Enfert, C., Kuchler, K., and Hube, B. (2010). *Candida glabrata* persistence in mice does not depend on host immunosuppression and is unaffected by fungal amino acid auxotrophy. Infect Immun *78*, 1066-1077.

Kovarik, P., Sauer, I., and Schaljo, B. (2007). Molecular mechanisms of the anti-inflammatory functions of interferons. Immunobiology *212*, 895-901.

Kovarik, P., Stoiber, D., Novy, M., and Decker, T. (1998). STAT1 combines signals derived from IFN-gamma and LPS receptors during macrophage activation. EMBO J *17*, 3660-3668.

Lewis, R.E. (2009). Overview of the changing epidemiology of candidemia. Curr Med Res Opin *25*, 1732-1740.

Macia, E., Ehrlich, M., Massol, R., Boucrot, E., Brunner, C., and Kirchhausen, T. (2006). Dynasore, a cell-permeable inhibitor of dynamin. Developmental Cell *10*, 839-850.

Mancuso, G., Gambuzza, M., Midiri, A., Biondo, C., Papasergi, S., Akira, S., Teti, G., and Beninati, C. (2009). Bacterial recognition by TLR7 in the lysosomes of conventional dendritic cells. Nat Immunol *10*, 587-594.

Marcil, A., Gadoury, C., Ash, J., Zhang, J., Nantel, A., and Whiteway, M. (2008). Analysis of *PRA1* and its relationship to *Candida albicans*-macrophage interactions. Infect Immun *76*, 4345-4358.

Miyazato, A., Nakamura, K., Yamamoto, N., Mora-Montes, H.M., Tanaka, M., Abe, Y., Tanno, D., Inden, K., Gang, X., Ishii, K.*, et al.* (2009). *Toll*-like receptor 9-dependent activation of myeloid dendritic cells by deoxynucleic acids from *Candida albicans*. Infect Immun *77*, 3056-3064.

Moreno-Ruiz, E., Galan-Diez, M., Zhu, W., Fernandez-Ruiz, E., d'Enfert, C., Filler, S.G., Cossart, P., and Veiga, E. (2009). *Candida albicans* internalization by host cells is mediated by a clathrin-dependent mechanism. Cell Microbiol *11*, 1179-1189.

Moschen, A.R., Geiger, S., Krehan, I., Kaser, A., and Tilg, H. (2008). Interferon-alpha controls IL-17 expression in vitro and in vivo. Immunobiology *213*, 779-787.

Muller, U., Steinhoff, U., Reis, L.F., Hemmi, S., Pavlovic, J., Zinkernagel, R.M., and Aguet, M. (1994). Functional role of type I and type II interferons in antiviral defense. Science *264*, 1918-1921.

Murciano, C., Villamon, E., Gozalbo, D., Roig, P., O'Connor, J.E., and Gil, M.L. (2006). Toll-like receptor 4 defective mice carrying point or null mutations do not show increased susceptibility to *Candida albicans* in a model of hematogenously disseminated infection. Med Mycol *44*, 149-157.

Nakamura, K., Miyazato, A., Xiao, G., Hatta, M., Inden, K., Aoyagi, T., Shiratori, K., Takeda, K., Akira, S., Saijo, S*., et al.* (2008). Deoxynucleic acids from *Cryptococcus neoformans* activate myeloid dendritic cells via a TLR9-dependent pathway. J Immunol *180*, 4067-4074.

Nakayama, H., Yoshizaki, F., Prinetti, A., Sonnino, S., Mauri, L., Takamori, K., Ogawa, H., and Iwabuchi, K. (2008). Lyn-coupled LacCer-enriched lipid rafts are required for CD11b/CD18-mediated neutrophil phagocytosis of nonopsonized microorganisms. J Leukoc Biol *83*, 728-741.

Netea, M.G., Brown, G.D., Kullberg, B.J., and Gow, N.A. (2008). An integrated model of the recognition of *Candida albicans* by the innate immune system. Nat Rev Microbiol *6*, 67-78.

Netea, M.G., Van Der Graaf, C.A., Vonk, A.G., Verschueren, I., Van Der Meer, J.W., and Kullberg, B.J. (2002). The role of *toll*-like receptor (TLR) 2 and TLR4 in the host defense against disseminated candidiasis. J Infect Dis *185*, 1483-1489.

Nicklas, W., Baneux, P., Boot, R., Decelle, T., Deeny, A.A., Fumanelli, M., and Illgen-Wilcke, B. (2002). Recommendations for the health monitoring of rodent and rabbit colonies in breeding and experimental units. Lab Anim *36*, 20-42.

Pfaller, M.A., and Diekema, D.J. (2007). Epidemiology of invasive candidiasis: a persistent public health problem. Clin Microbiol Rev *20*, 133-163.

Ramakers, C., Ruijter, J.M., Deprez, R.H., and Moorman, A.F. (2003). Assumption-free analysis of quantitative real-time polymerase chain reaction (PCR) data. Neurosci Lett *339*, 62-66.

Ramirez-Ortiz, Z.G., Specht, C.A., Wang, J.P., Lee, C.K., Bartholomeu, D.C., Gazzinelli, R.T., and Levitz, S.M. (2008). *Toll*-like receptor 9-dependent immune activation by unmethylated CpG motifs in *Aspergillus fumigatus* DNA. Infect Immun *76*, 2123-2129.

Rosas, M., Liddiard, K., Kimberg, M., Faro-Trindade, I., McDonald, J.U., Williams, D.L., Brown, G.D., and Taylor, P.R. (2008). The induction of inflammation by dectin-1 in vivo is dependent on myeloid cell programming and the progression of phagocytosis. J Immunol *181*, 3549-3557.

Saijo, S., Fujikado, N., Furuta, T., Chung, S.H., Kotaki, H., Seki, K., Sudo, K., Akira, S., Adachi, Y., Ohno, N*., et al.* (2007). Dectin-1 is required for host defense against *Pneumocystis carinii* but not against *Candida albicans*. Nat Immunol *8*, 39-46.

Shinohara, M.L., Kim, J.H., Garcia, V.A., and Cantor, H. (2008). Engagement of the type I interferon receptor on dendritic cells inhibits T helper 17 cell development: role of intracellular osteopontin. Immunity *29*, 68-78.

Stetson, D.B., and Medzhitov, R. (2006). Type I interferons in host defense. Immunity *25*, 373-381.

Stockinger, S., Reutterer, B., Schaljo, B., Schellack, C., Brunner, S., Materna, T., Yamamoto, M., Akira, S., Taniguchi, T., Murray, P.J*., et al.* (2004). IFN regulatory factor 3-dependent induction of type I IFNs by intracellular bacteria is mediated by a TLR- and Nod2-independent mechanism. J Immunol *173*, 7416-7425.

Sullivan, D.J., Westerneng, T.J., Haynes, K.A., Bennett, D.E., and Coleman, D.C. (1995). *Candida dubliniensis* sp. nov.: phenotypic and molecular characterization of a novel species associated with oral candidosis in HIV-infected individuals. Microbiology *141 (Pt 7)*, 1507-1521.

Takeuchi, O., Hoshino, K., Kawai, T., Sanjo, H., Takada, H., Ogawa, T., Takeda, K., and Akira, S. (1999). Differential roles of TLR2 and TLR4 in recognition of Gram-negative and Gram-positive bacterial cell wall components. Immunity *11*, 443-451.

Taylor, P.R., Tsoni, S.V., Willment, J.A., Dennehy, K.M., Rosas, M., Findon, H., Haynes, K., Steele, C., Botto, M., Gordon, S*., et al.* (2007). Dectin-1 is required for beta-glucan recognition and control of fungal infection. Nat Immunol *8*, 31-38.

Tohyama, Y., and Yamamura, H. (2009). Protein tyrosine kinase, Syk: a key player in phagocytic cells. J Biochem *145*, 267-273.

Underhill, D.M., and Goodridge, H.S. (2007). The many faces of ITAMs. Trends Immunol *28*, 66-73.

van Bruggen, R., Drewniak, A., Jansen, M., van Houdt, M., Roos, D., Chapel, H., Verhoeven, A.J., and Kuijpers, T.W. (2009). Complement receptor 3, not dectin-1, is the major receptor on human neutrophils for beta-glucan-bearing particles. Mol Immunol *47*, 575-581.

van de Veerdonk, F.L., Kullberg, B.J., van der Meer, J.W.M., Gow, N.A.R., and Netea, M.G. (2008a). Host-microbe interactions: innate pattern recognition of fungal pathogens. Current Opinion in Microbiology *11*, 305-312.

van de Veerdonk, F.L., Kullberg, B.J., Verschueren, I.C., Hendriks, T., van der Meer, J.W., Joosten, L.A., and Netea, M.G. (2010). Differential effects of IL-17 pathway in disseminated candidiasis and zymosan-induced multiple organ failure. Shock.

van de Veerdonk, F.L., Netea, M.G., Jansen, T.J., Jacobs, L., Verschueren, I., van der Meer, J.W., and Kullberg, B.J. (2008b). Redundant role of TLR9 for anti-Candida host defense. Immunobiology *213*, 613-620.

Van Ziffle, J.A., and Lowell, C.A. (2009). Neutrophil-specific deletion of Syk kinase results in reduced host defense to bacterial infection. Blood *114*, 4871-4882.

Villamon, E. (2004). *Toll*-like receptor-2 is essential in murine defenses against *Candida albicans* infections. Microbes Infect *6*, 1-7.

Villamon, E., Gozalbo, D., Roig, P., Murciano, C., O'Connor, J.E., Fradelizi, D., and Gil, M.L. (2004). Myeloid differentiation factor 88 (MyD88) is required for murine resistance to *Candida albicans* and is critically involved in Candida-induced production of cytokines. Eur Cytokine Netw *15*, 263-271.

Wells, C.A., Salvage-Jones, J.A., Li, X., Hitchens, K., Butcher, S., Murray, R.Z., Beckhouse, A.G., Lo, Y.L., Manzanero, S., Cobbold, C*., et al.* (2008). The macrophage-inducible C-type lectin, mincle, is an essential component of the innate immune response to *Candida albicans*. J Immunol *180*, 7404-7413.

Willment, J.A., and Brown, G.D. (2008). C-type lectin receptors in antifungal immunity. Trends Microbiol *16*, 27-32.

Yamamoto, M., Sato, S., Hemmi, H., Hoshino, K., Kaisho, T., Sanjo, H., Takeuchi, O., Sugiyama, M., Okabe, M., Takeda, K*., et al.* (2003). Role of adaptor TRIF in the MyD88-independent *toll*-like receptor signaling pathway. Science *301*, 640-643.

Yordanov, M., Dimitrova, P., Danova, S., and Ivanovska, N. (2005). *Candida albicans* double-stranded DNA can participate in the host defense against disseminated candidiasis. Microbes Infect *7*, 178-186.

Yoshitomi, H., Sakaguchi, N., Kobayashi, K., Brown, G.D., Tagami, T., Sakihama, T., Hirota, K., Tanaka, S., Nomura, T., Miki, I*., et al.* (2005). A role for fungal {beta}-glucans and their receptor Dectin-1 in the induction of autoimmune arthritis in genetically susceptible mice. J Exp Med *201*, 949-960.

Zal, T., Volkmann, A., and Stockinger, B. (1994). Mechanisms of tolerance induction in major histocompatibility complex class II-restricted T cells specific for a blood-borne self-antigen. J Exp Med *180*, 2089-2099.

Zelante, T. (2007). IL-23 and the Th17 pathway promote inflammation and impair antifungal immune resistance. Eur J Immunol *37*, 2695-2706.

Zhang, X., Jin, J., Tang, Y., Speer, D., Sujkowska, D., and Markovic-Plese, S. (2009). IFN-beta1a inhibits the secretion of Th17-polarizing cytokines in human dendritic cells via TLR7 up-regulation. J Immunol *182*, 3928-3936.

Figure Legends

Figure 1. *Candida* species induce a IFN-I response in mouse conventional BM-DCs

(A, D) Wild-type BM-DCs or BM-DCs lacking the IFNAR1 subunit of the IFN-I receptor (IFNAR1$^{-/-}$) were infected with the indicated *Candida* species (Ca, *Candida albicans;* Cg*, Candida glabrata;* Cd*, Candida dublinienesis*) or left untreated for the indicated time, after which cell lysates were harvested and RNA or protein extracts prepared.

(A, B) IFNβ expression was measured (A) by real-time PCR after 4h of co-culture or (B) by ELISA after 24h of co-culture.

(C) Phosphorylated STAT1 was detected by immunoblotting of protein extracts prepared after 2 hours of *Candida* species-BM-DC co-culture (upper panel) and blots were re-probed with polyclonal anti-STAT1 antibodies to assess equal loading between lanes (lower panel).
(D) IRF7 gene expression was measured by real-time PCR after 24h of co-culture. Real-time PCR results are expressed as fold increase of mRNA expression over untreated BM-DCs. ELISA results are expressed as pg IFNβ/ml cell culture supernatant. Data presented are from one experiment representative of at least three independent experimental repeats.

Figure 2. Role of Syk/Src kinases and β-glucan receptors

(A) Wild-type BM-DCs were pre-incubated with either, a Syk kinase inhibitor (R406), an inhibitor of Src-family kinases (PP2) and an inactive homologue (PP3) or vehicle (DMSO) for 30min at 37°C prior to co-culture with Cg or media alone for 6 hours. IFNβ release into the cell culture medium was measured by ELISA.
(B) Wild-type BM-DCs (WT) or BM-DCs lacking dectin1 (dectin1$^{-/-}$) or CD11b (CD11b$^{-/-}$) were co-cultured for 6 hours with Cg or left unstimulated, and IFNβ release was measured by ELISA.
(C) BM-DCs were stimulated with either β-glucan preparations (Sc-β-glucans) or Curdlan in media containing polymyxin B (30μg/ml), or with LPS (0.1μg/ml) for 4 hours, or left untreated as control. IFNβ release into the cell culture medium was measured by ELISA. ELISA Results are expressed as pg of IFNβ/ml supernatant. Data presented are from one experiment representative of three independent experimental repeats
(D) Wild-type BM-DCs were pre-incubated with a Syk kinase inhibitor (R406) or vehicle (DMSO) prior to co-culture with Alexa480-labelled Cg for 45min at 37°C or 4°C (adherence control). Cells were collected and the number of BM-DCs containing at least one Cg was analysed by flow cytometry. Results are expressed as percentage of ingestion (the percentage of BM-DC containing one or more yeast cells). Data presented are the means ± SD of data from at least two independent experiments (***$p \leq 0{,}0005$ based on unpaired, two-tailed t test).

Figure 3. IFNβ release triggered by *Cg* is TLR2 andTLR4-independent

(A, B) Wild-type BM-DCs or BM-DCs lacking the TLR2 (TLR2$^{-/-}$) or TLR4 receptor (TLR4$^{-/-}$) were co-cultured for 4 hours with Cg or left unstimulated, and IFNβ release was measured by ELISA (left panel) or phosphorylated STAT1 was detected by immunoblotting of extracts prepared after 2 hours of Cg-BM-DC co-culture; blots were re-probed with polyclonal anti-STAT1 antibodies to verify equal loading (right panel). ELISA results are expressed as pg of IFNβ/ml cell culture medium. Data presented are from one experiment representative of at least two or three independent experimental repeats.

Figure 4. IFNβ release requires phagocytosis and MyD88 activation

(A) Wild-type BM-DCs or BM-DCs lacking the MyD88 signaling adaptor (MyD88$^{-/-}$) were co-cultured for 4 hours with Cg or left unstimulated, and IFNβ release was measured by ELISA (left panel) or

phosphorylated STAT1 was detected by immunoblotting of protein extracts prepared after 2 hours of Cg-BM-DC co-culture and blots were re-probed with polyclonal anti-STAT1 antibodies to assess equal loading between lanes (right panel).

(B) Wild-type BM-DCs or BM-DCs lacking the TRIF signaling adaptor ($TRIF^{-/-}$) were co-cultured with Cg or left unstimulated, and IFNβ release was measured by ELISA after 4 hours.

(C) Wild-type BM-DCs pre-treated with dynasore or vehicle (DMSO) for 30 min were co-cultured with Cg or left untreated; IFNβ production was measured by ELISA after 4 hours. ELISA results are expressed as pg of IFNβ/ml cell culture medium. Data presented are from one experiment representative of at least three independent experimental repeats.

Figure 5. IFNβ release requires activation of phagosomal TLR7 and TLR9

(A) BM-DCs pre-treated for 30 min with either bafilomycin A1 (bafiloA1), chloroquine (ChQ) or vehicle alone, were co-cultured with Cg for 6 hours or left untreated. IFNβ release was measured by ELISA and results expressed as pg of IFNβ/ml cell culture medium. Data presented are from one experiment representative of two independent experimental repeats.

(B) BM-DCs were pre-treated for 60 min with the indicated synthetic inhibitory oligodeoxynucleotides (IRS661, ODN2088 or IRS954) or with unspecific oligodeoxynucleotides (CTL_IRS, CTL_ODN) as controls. Subsequently, BM-DCs were co-cultured for 6 hours with Cg or left unstimulated; IFNβ release was measured by ELISA and results are expressed as pg of IFNβ/ml cell culture medium. Values represent the means ± SD of three independent experiments. *** $p \leq 0.0001$ (unpaired, two-tailed t test).

Figure 6: Model of IFNβ response to Candida spp in mouse conventional BM-DCs

In BM-DCs, a dynamin-dependent phagocytosis step, a Syk/Src-dependent-signalling, followed by endosome acidification, leads to the simultaneous activation of TLR7 and TLR9 by Candida nucleic acids, thereby stimulating an MyD88-dependent signaling pathway required for the initial release of IFNβ, and the subsequent induction of a IFN-I response to fungal infection. Action of inhibitors (dynasore, R406, PP2, bafilomycin A1, chloroquine) used in this study are indicated on their specific targets.

Figure 1

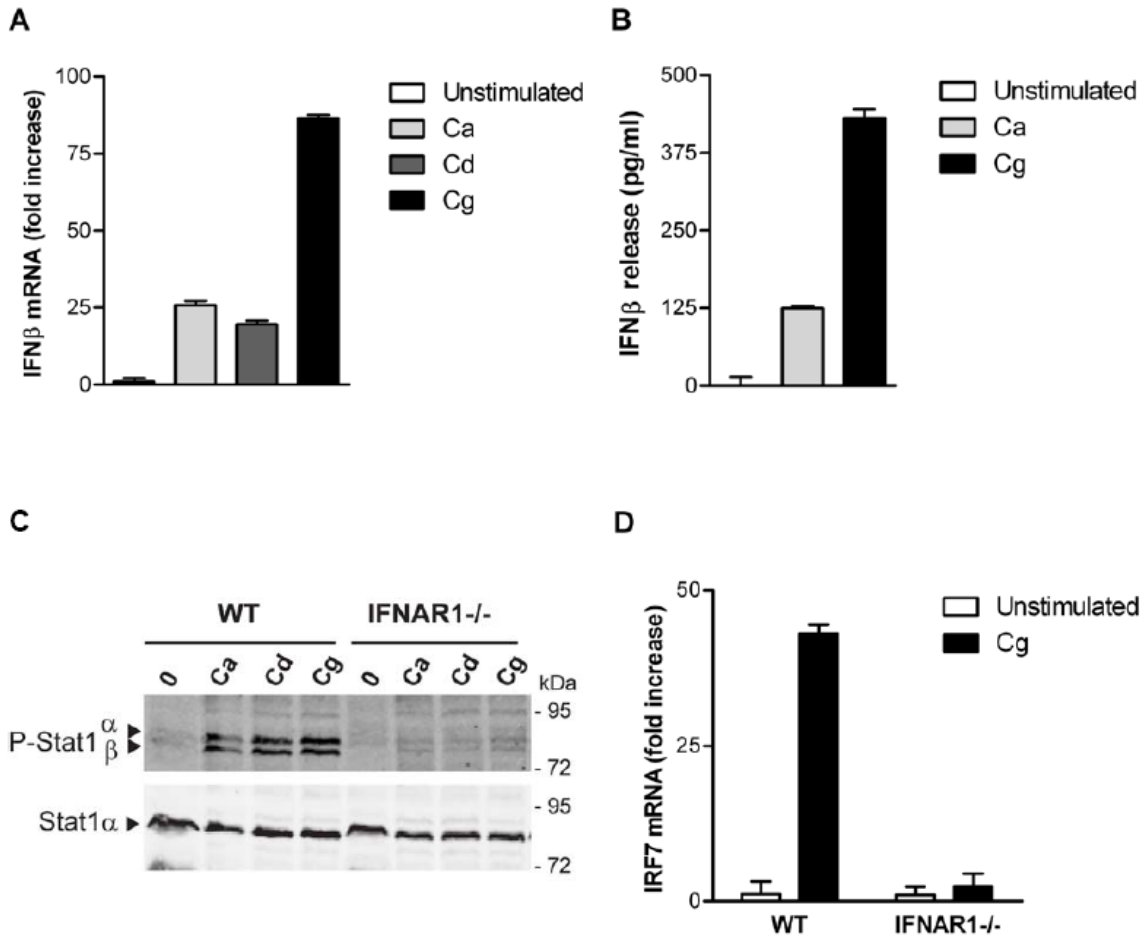
A
IFNβ mRNA (fold increase)
100
75
50
25
0
Unstimulated
Ca
Cd
Cg
B
IFNβ release (pg/ml)
500
375
250
125
0
Unstimulated
Ca
Cg
C
WT
IFNAR1-/-
0
Ca
Cd
Cg
0
Ca
Cd
Cg
kDa
P-Stat1 α β
Stat1α
95
72
95
72
D
IRF7 mRNA (fold increase)
50
25
0
Unstimulated
Cg
WT
IFNAR1-/-

Figure 2

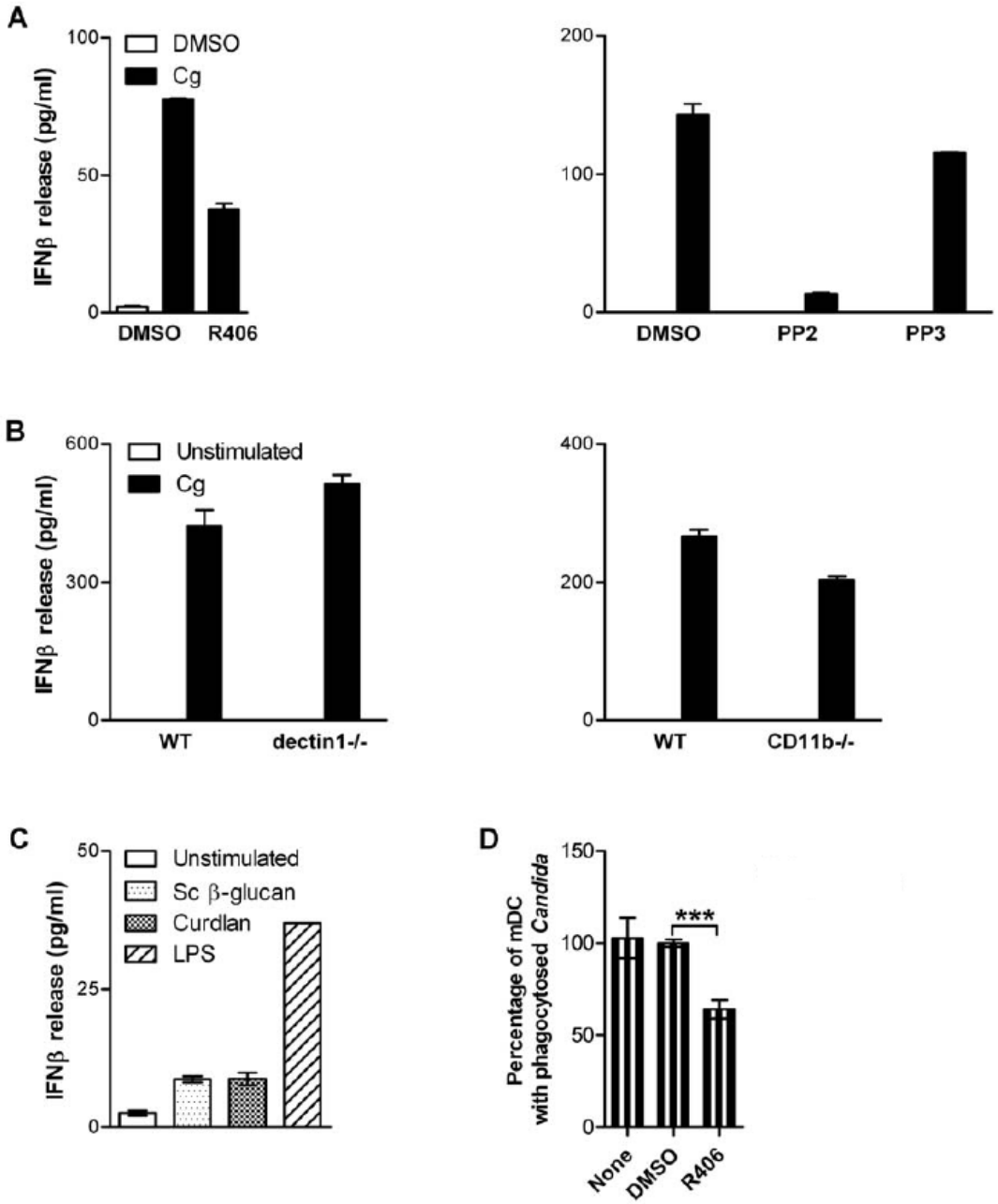
A
IFNβ release (pg/ml)
100
50
0
DMSO
Cg
DMSO
R406
200
100
0
DMSO
PP2
PP3
B
IFNβ release (pg/ml)
600
300
0
Unstimulated
Cg
WT
dectin1-/-
400
200
0
WT
CD11b-/-
C
IFNβ release (pg/ml)
50
25
0
Unstimulated
Sc β-glucan
Curdlan
LPS
D
Percentage of mDC with phagocytosed Candida
150
100
50
0
***
None
DMSO
R406

Figure 3

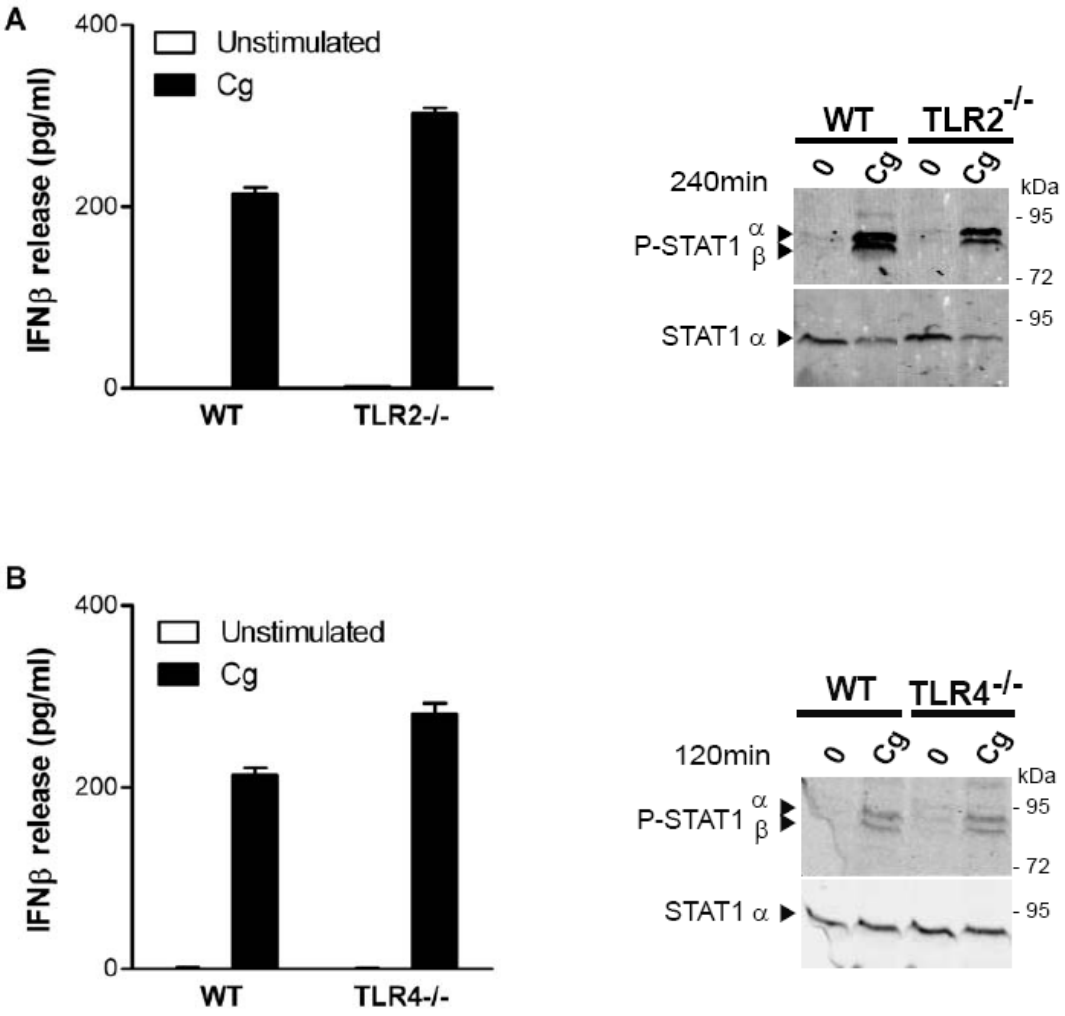
A
400
200
0
IFNβ release (pg/ml)
Unstimulated
Cg
WT
TLR2-/-
WT
TLR2-/-
240min
0
Cg
0
Cg
kDa
P-STAT1 α β
- 95
- 72
STAT1 α
- 95
B
400
200
0
IFNβ release (pg/ml)
Unstimulated
Cg
WT
TLR4-/-
WT
TLR4-/-
120min
0
Cg
0
Cg
kDa
P-STAT1 α β
- 95
- 72
STAT1 α
- 95

Figure 4

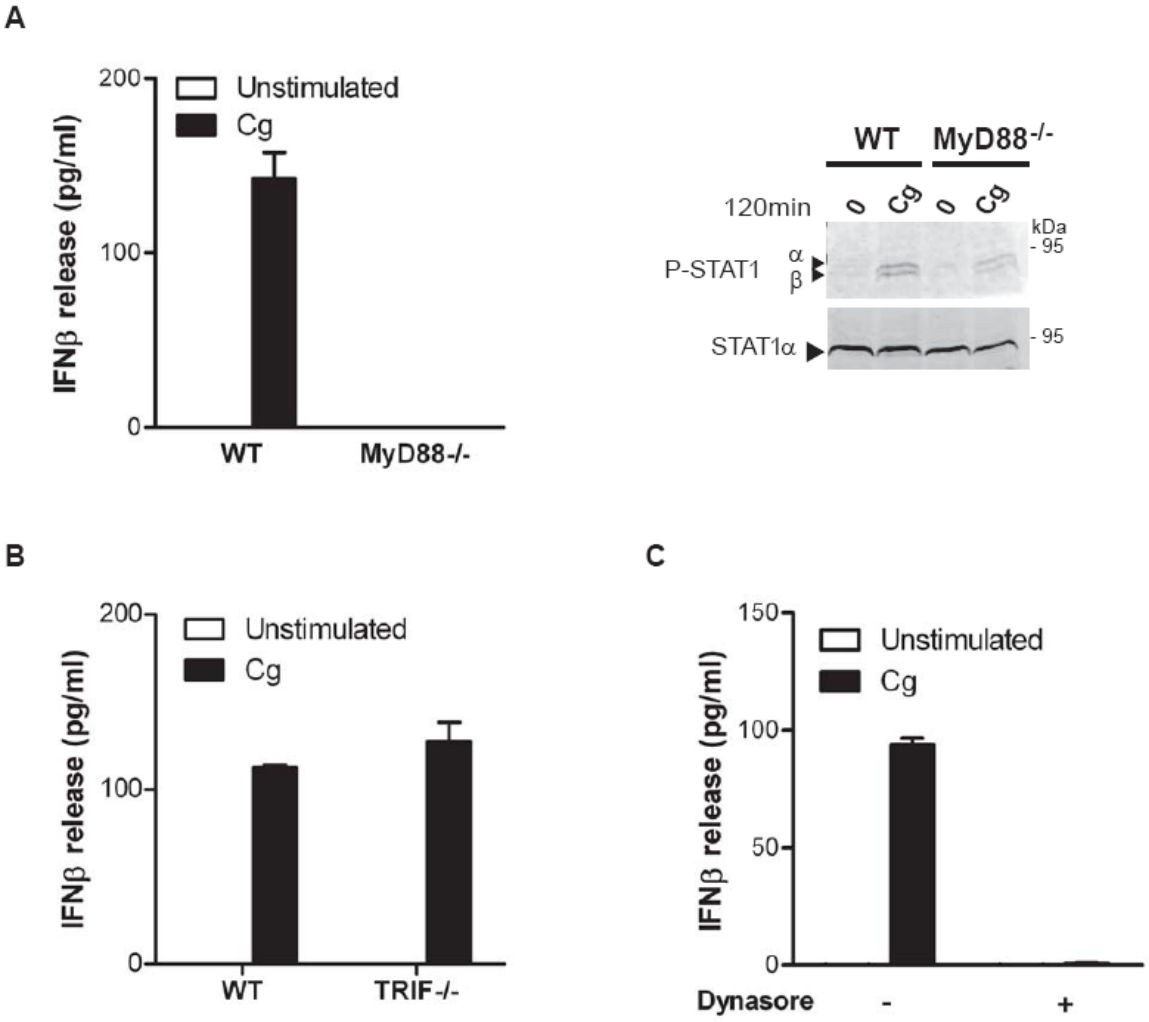
A
200
100
0
IFNβ release (pg/ml)
Unstimulated
Cg
WT
MyD88-/-
WT
MyD88-/-
120min
0
Cg
0
Cg
kDa
- 95
P-STAT1
α
β
STAT1α
- 95
B
200
100
0
IFNβ release (pg/ml)
Unstimulated
Cg
WT
TRIF-/-
C
150
100
50
0
IFNβ release (pg/ml)
Unstimulated
Cg
Dynasore
-
+

Figure 5

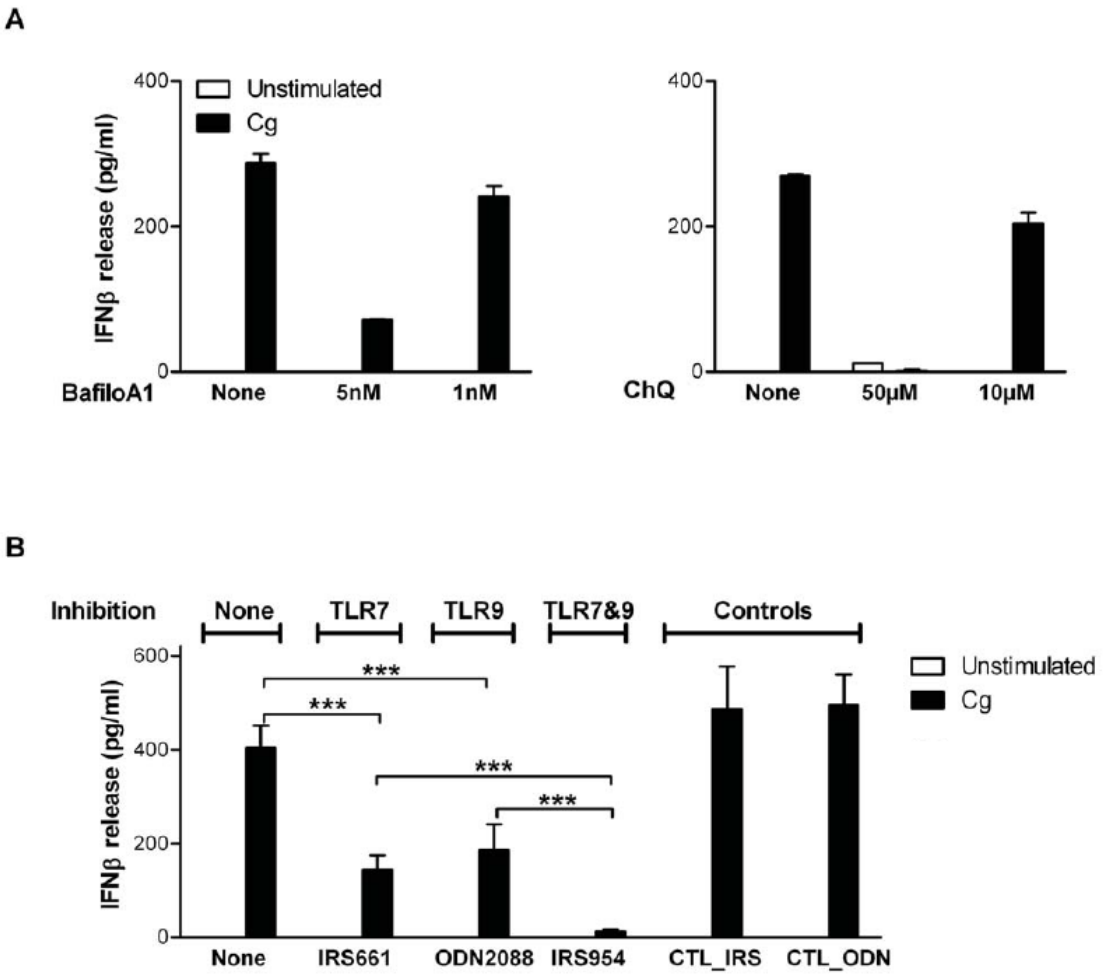
A
400
200
0
IFNβ release (pg/ml)
Unstimulated
Cg
BafiloA1
None
5nM
1nM
ChQ
None
50µM
10µM
B
Inhibition
None
TLR7
TLR9
TLR7&9
Controls
600
400
200
0
IFNβ release (pg/ml)
***
***
***
***
Unstimulated
Cg
None
IRS661
ODN2088
IRS954
CTL_IRS
CTL_ODN

Figure 6

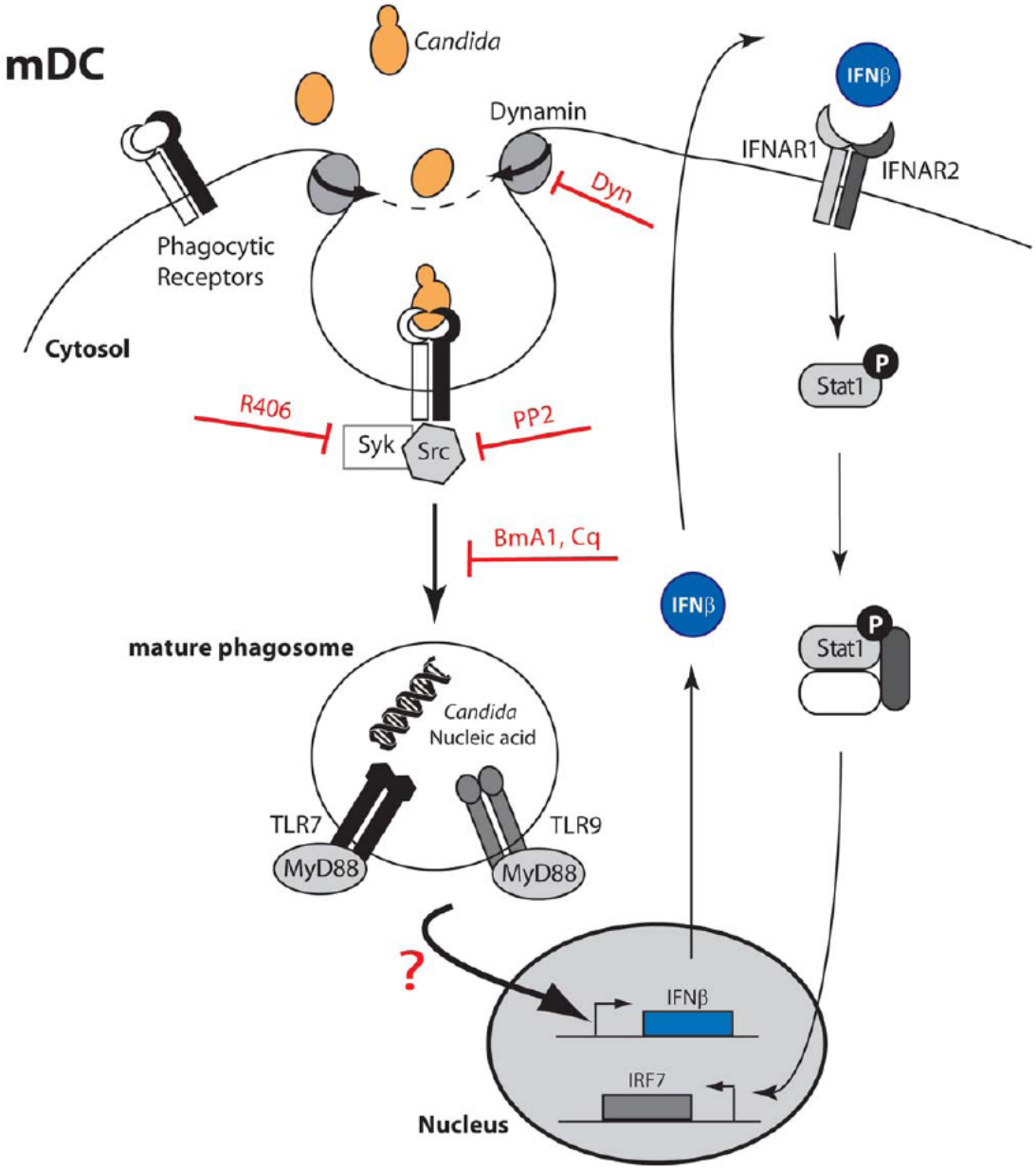
mDC
Candida
Dynamin
IFNβ
IFNAR1
IFNAR2
Dyn
Phagocytic
Receptors
Cytosol
Stat1
P
R406
Syk
Src
PP2
BmA1, Cq
IFNβ
mature phagosome
Stat1
P
Candida
Nucleic acid
TLR7
TLR9
MyD88
MyD88
?
IFNβ
IRF7
Nucleus

The Efg1 Transcription Factor Controls Echinocandin Susceptibility and Caspofungin-Induced Flocculation of *Candida albicans*

Christa Gregori[§], Walter Glaser[§], **Ingrid E. Frohner**[§], Cristina Reinoso-Martín[§], Steffen Rupp[&], Christoph Schüller* & Karl Kuchler[§ $]

From

[§] Medical University of Vienna, Max F. Perutz Laboratories,
Christian Doppler Laboratory for Infection Biology, A-1030 Vienna, Austria

* University of Vienna, Max F. Perutz Laboratories, A-1030 Vienna, Austria

[&]Fraunhofer Institute for Interfacial Engineering and Biotechnology, D-70569 Stuttgart, Germany

Key words: *C. albicans*, Caspofungin, PKC signaling, cell wall remodeling, candin tolerance, flocculation,

Running title: *C. albicans* response to cell wall stress

[$]To whom correspondence and reprint requests should be addressed:
Karl Kuchler
Medical University of Vienna; Max F. Perutz Laboratories
Department of Medical Biochemistry; Campus Vienna Biocenter
Dr. Bohr-Gasse 9/2; A-1030 Vienna, Austria
Phone: +43-1-4277-61807; Fax: +43-1-4277-9618
e-mail:karl.kuchler@meduniwien.ac.at

Submitted to Molecular Biology of the Cell in April 2010

SUMMARY

Echinocandin drugs such as caspofungin (CASP), micafungin, and anidulafungin target fungal cell wall biogenesis by inhibiting Fks1-mediated β-glucan deposition into the cell wall. In addition to cell wall damage, however, CASP triggers several intracellular stress responses. Here, we discover a novel CASP-induced flocculation phenotype of *C. albicans* cells. In liquid YPD medium supplemented with CASP, cells rapidly flocculate forming large cell aggregates. Interestingly, high concentrations of sugars such as mannose or glucose inhibit CASP-induced flocculation and improve survival of *C. albicans* to CASP killing. Hence, increasing external osmolarity stabilizes fungal cells with damaged cell walls, thereby opposing CASP-mediated fungicidal activity. Notably, sublethal concentrations of CASP triggered an Efg1-dependent expression of the adhesin *ALS1*, as well as other Efg1-regulated genes. Hence, CASP challenge triggers an Efg1-dependent transcriptional response, implying that the multifunctional regulator Efg1, which is otherwise involved in filamentation and white – opaque switching, also modulates cell wall homeostasis or remodelling upon CASP challenge. Indeed, cells lacking either Efg1 or Als1 show strongly diminished CASP-induced flocculation. Furthermore, the lack of Efg1 leads to CASP hypersensitivity. Our data suggest that CASP induces parallel activation of the Efg1 and the PKC cell integrity pathway to coordinate cell wall remodeling.

INTRODUCTION

Human fungal pathogens have emerged as an important public health problem during the past decades. Systemic or disseminated infections in immunocompromised individuals caused by fungi such as *Candida*, *Aspergillus*, and *Cryptococcus spp* are often associated with high mortality rates (Pfaller and Diekema, 2007). The clinical therapy for invasive fungal infections has been using a classical repertoire of antifungal drugs, including amphotericin B, fluconazole and itraconazole. However, a number of adverse side effects, fungistatic rather than fungicidal activity, and increasing drug resistance led to the development of second generation azoles like voriconazole, posaconazole, ravuconazole, but also compounds with a novel action mechanism such as the echinocandins (De Pauw, 2000; Denning, 2003). Echinocandins, such as caspofungin, micafungin, and anidulafungin are semisynthetic lipopeptides produced via chemical modification of fungal secondary metabolites. Caspofungin (CASP), for example, is synthesized from pneumocandin B0 from *Glarea lozoyensis* (Leonard *et al.*, 2007). In contrast to azoles acting on the ergosterol biosynthesis pathway, the fungal-specific and fungicidal mode of action of echinocandins is the inhibition of the biosynthesis of β-(1,3)-D-glucan, an essential cell wall component unique to all fungi but absent in the mammalian host (Douglas *et al.*, 1997; Kurtz and Douglas, 1997).

Candida spp represent major fungal pathogens affecting humans. In addition to superficial mucosal conditions such as thrush and vaginitis, they can cause life-threatening systemic infections (Calderone and Fonzi, 2001) with mortality rates exceeding 50% (Pfaller and Diekema, 2007). Thus, *Candida spp* are able to infect a variety of host niches, which in turn impose diverse stresses on fungal

cells, including variable pH, temperature changes, oxidative stress or nutrient limitation. Furthermore, *C. albicans* has to cope with the host immune surveillance, as well as antifungal drugs, posing additional survival stress. Thus, fungal cells have to adapt constantly to these changing conditions, mainly by activating signaling pathways inducing a multitude of adaptive stress responses (Monge *et al.*, 2006).

The molecular target of echinocandins in *C. albicans* is the *FKS1* subunit of the β-(1,3)-D-glucan synthase (Douglas *et al.*, 1997). Resistance to CASP is frequently associated with mutations in the *FKS1* gene (Balashov *et al.*, 2006; Garcia-Effron *et al.*, 2009). Efflux-based mechanism through the Cdr2 ABC transporter may also contribute to CASP tolerance, at least *in vitro* (Schuetzer-Muehlbauer *et al.*, 2003). *C. albicans* cells rapidly respond to CASP treatment, since the cell wall stress triggers signal transduction pathways such as the *C. albicans* cell wall integrity protein kinase C pathway (PKC). Within a few minutes following exposure to CASP, phosphorylation of the MAPK Mkc1 occurs (Walker *et al.*, 2008). Consequently, homozygous deletion of *MKC1* causes CASP-hypersensitivity. Notably, Mkc1, the *C. albicans* orthologue of the *S. cerevisiae* Slt2 MAPK (Reinoso-Martin *et al.*, 2003), is also phosphorylated in response to a variety of other conditions like oxidative stress, osmotic stress, calcium ions and low-temperature shocks (Navarro-Garcia *et al.*, 2005). In addition, Mkc1 is activated when cells are grown on a surface. *C. albicans mkc1*Δ/*mkc1*Δ mutants are defective in two contact-dependent responses, invasive hyphal growth and biofilm formation, indicating that the PKC signaling plays a role in contact-sensing (Kumamoto, 2005). Further, *CHS* gene expression and chitin synthesis is stimulated by CASP. This induction of chitin synthesis is regulated by the high osmolarity glycerol (HOG) pathway, as well as the PKC and Ca^{2+}/calcineurin signaling pathways. However, the Ca^{2+} signaling pathway perhaps plays the major role in this response. Pretreatment of cells with $CaCl_2$ and calcofluor white elevates chitin levels but reduces CASP sensitivity of *mkc1*Δ/*mkc1*Δ as well as wild type cells (Munro *et al.*, 2007; Walker *et al.*, 2008). Notably, calcineurin is a Hsp90 client protein in *C. albicans* and Hsp90 is mediating echinocandin tolerance through calcineurin (Singh *et al.*, 2009). Furthermore, the so-called Psk1-Sko1 pathway may also be involved in CASP response (Rauceo *et al.*, 2008). Recently, the zinc finger regulator Cas5, a transcription factor involved in the CASP response has been identified, but the upstream regulatory elements remain undisclosed (Bruno *et al.*, 2006).

Here, we investigate a novel flocculation phenotype evoked in CASP-exposed *C. albicans* cells. Interestingly, sugars like mannose or glucose acted as inhibitors of CASP-induced flocculation and high concentrations of sugars in the growth medium considerably reduced fungicidal activity of CASP towards *C. albicans* cells. CASP toxicity was also reduced by simultaneous exposure to osmotic stress such as high NaCl concentrations. Exposure of *C. albicans* to sub-inhibitory CASP concentrations resulted in Efg1-dependent expression of the adhesin gene *ALS1,* as well as other Efg1 regulated genes. Interestingly, we identify Als1 as the major factor required for CASP-induced flocculation. These data show an Efg1-regulated response to CASP challenge of *C. albicans*. Our data suggest that CASP-induced cell wall damage triggers parallel activation of the Efg1 and Mkc1 signaling pathways to coordinate cell wall remodeling.

EXPERIMENTAL PROCEDURES

C. albicans strains, growth conditions & growth inhibition assays

C. albicans strains used in this study are listed in Table 1. Gene deletions were created by using the *C.m.LEU2* and *C.d.HIS1* marker cassettes as described in (Noble and Johnson, 2005). C-terminal GFP-tagging of chromosomal *RCT1* was performed as described in (Gerami-Nejad *et al.*, 2001) using plasmid pGFP-HIS1 as PCR-template. Unless otherwise indicated, strains were grown routinely at 30°C in YPD (1% yeast extract, 2% peptone, and 2% glucose) medium. Caspofungin (Merck & Co, Whitehouse Station, NJ, USA) and Posaconazole (kindly provided by Dominique Sanglard) were prepared as stock solutions in sterile water or DMSO, respectively, and added to the medium at the desired concentrations. Sensitivity phenotypes were assayed with cells grown to the exponential growth phase and diluted to an optical density at 600nm (OD_{600nm}) of 0.1. Identical volumes of cultures, as well as 1:10, 1:100 and 1:1,000 serial dilutions, were spotted onto agar plates containing various drug concentrations. Colony growth was inspected and recorded after 48 h incubation at 30°C.

RNA isolation, and Northern analysis

Total yeast RNA was isolated by the hot phenol method. About 20µg of total RNA were fractionated in a 1.4 % agarose gel and transferred to nylon membranes (Amersham Biosciences, Little Chalfont, Buckinghamshire, England). Northern blots were hybridized with PCR-amplified probes, radiolabeled by incorporation of 32P-dCTP and a MegaPrime labeling kit (Amersham). Methylene blue staining was used as control for equal RNA loading. The radiolabeled probes were added to the prehybridization solution after purification on a NICK column (Amersham). Membranes were washed at 65°C three times in 2x SSC-1% SDS, and three times in 1x SSC-1% SDS, and then exposed to X-ray films at -70°C for appropriate time periods.

DNA microarray experiments

30 ml cultures of *C. albicans* strains were grown in YPD to an OD_{600nm} of about 0.5 -1 before treatment with 10ng/ml CASP. After a 60min treatment, cells were harvested, washed and immediately shock-frozen. Total RNA was prepared by hot phenol method followed by LiCl precipitation. RNA concentration was measured at 260nm in TE pH 7. Samples of 30µg total RNA were used for cDNA synthesis, using 200U of Superscript III reverse transcriptase (Invitrogen, Carlsbad, Calif.) with either Cy3-dCTP or Cy5-dCTP. Labeled cDNAs were pooled, and RNA hydrolyzed for 20 minutes in 50 mM NaOH at 65°C. After neutralization with acetic acid, cDNAs were purified using the GFX purification Kit (GE Healthcare).

Hybridization to whole-genome cDNA microarrays was done after a 45min prehybridisation with 4x SSC, 0.1 % SDS, 10 mg/ml BSA at 42°C in 40µl 4x SSC, 0.1 % SDS at 65°C overnight. Microarrays were washed 5 min in 2x SSC-0.1% SDS at 42°C, 10 min in 0.1x SSC-0.1% SDS at room temperature, followed by a 2-minute wash in 0.1x SSC and 15sec in 0.01xSSC at room temperature. Glass slides were spun dry for 3 minutes at 500 rpm in a table top centrifuge, scanned on an Axon 4000B scanner (Molecular Devices).

Gridding and spot identification were performed using Gene Pix Pro4.1 software (Axon). The arrays were subsequently analysed with the limma Bioconductor/R package (Wettenhall and Smyth, 2004). The background was corrected with the norm-exp method and subsequently normalized using the print-tip loess and scale methods. To identify differentially expressed genes, a linear model (Smyth, 2004) and empirical Bayesian- moderated F-statistics were used with cut-off values of 0.01 for the adjusted p-value and either 1,5 or 2-fold expression changes, as well as A-values ≥ 7. DNA microarrays and protocols were obtained from Steffen Rupp, Fraunhofer IGB, Stuttgart. All microarray experiments were carried out with three independent RNA preparations. All microarray datasets are fully MIAME-compliant and have been submitted to Arrays Express, awaiting accession number. Cluster analysis (Eisen *et al.*, 1998) was performed using Cluster3 (http://bonsai.ims.u-tokyo.ac.jp/~mdehoon/software/cluster/software.htm) and visualized with TreeView (Saldanha, 2004) (http://jtreeview.sourceforge.net).

Preparation of yeast extracts and immunoblotting

For immunoblotting cell-free extracts were prepared by the TCA method exactly as previously described (Mamnun *et al.*, 2004). Overnight cultures were diluted to OD_{600nm} of 0.2 and grown until an OD_{600} of 1, before CASP addition to the cultures. Aliquots were harvested after the indicated time intervals. Cell lysates equivalent to 0.5 OD_{600nm} units were separated in 10% SDS-PAGE gels and transferred to nitrocellulose membranes (Protran; Schleicher & Schuell, Dassel, Germany). Phosphorylated Mkc1 was detected using an anti-phospho-p44/42 MAPK (Thr^{202}/Tyr^{204}) antibody (Cell Signaling Technologies, Beverley, USA) to detect dually phosphorylated, activated Mkc1. To detect Rct1-GFP, we used monoclonal anti-GFP antibodies (Roche, Basel Switzerland). Immunoblots were developed with the ECL chemiluminescence detection system and conditions recommended by the manufacturer (Amersham).

Microscopy and viability assay

Fluorescence microscopy was performed using a Zeiss Axioplan 2 fluorescence microscope. Images were captured with a Spot Pursuit (Sony) CCD camera using MetaVue (Molecular Devices) and Spotbasic software. For viability assays, untreated and CASP-treated cells were stained with FUN1 and Calcofluor White using the LIVE/DEAD yeast viability kit (Molecular Probes, Eugene, Oregon, USA) as recommended by the manufacturer. Plasma membrane integrity and metabolic function of yeast convert yellow-green–fluorescent intracellular staining of FUN 1 into red-orange–fluorescent intravacuolar structures; Calcofluor White M2R labels cell-wall chitin with blue fluorescence regardless of metabolic state. For quantification of live and dead cells, 15 pictures were taken for each condition, and cells were counted according to vacuolar (living) or cytoplasmic (dead) staining. To monitor localization of Rct1-GFP, we used an Olympus Cell R live imaging station.

RESULTS

CASP treatment causes flocculation of *C. albicans*

During our experiments with drug-treated cells, we observed a strong flocculation phenotype of *C. albicans* in presence of CASP. Cells grown in liquid YPD or RPMI medium started to flocculate approximately 60 min after addition of CASP. In glass tubes, this effect is clearly visible macroscopically after 2h treatment with 50ng/ml CASP. Aggregated clumps of cells settled at the bottom of culture tubes within a few minutes when shaking was stopped (Figure 1A). This phenotype was evident in commonly used *C. albicans* laboratory strains such as SC5314, CAI4 or SN152, as well as a number of clinical isolates (data not shown).

Cell aggregation might be an active response by *C. albicans* to cope with cell wall stress or for example a consequence of cell death. Induced cell-cell adhesion in fungi usually requires cell-surface proteins, so called 'adhesins' or 'flocculins' that specifically bind amino acid or sugar residues on the surface of neighbouring cells. Lectin-like adhesion requires the lectin-like binding of the adhesin to sugar residues on the surface of other cells, which can be competitively inhibited by certain sugars (Verstrepen and Klis, 2006). To characterize the *C. albicans* flocculation response to CASP, we increased the sugar content of the YPD-medium using different concentrations of mannose, as well as other sugars. After a 3h exposure to CASP, we quantified the degree of flocculation by measuring the drop in of the optical density within a 15min period. In drug-treated, flocculating cultures, cells rapidly aggregated at the bottom of the cuvette with a 40% decrease of the OD_{600nm}. In untreated control cultures, the optical density only decreased by about 3% within 15min (Figure 1B). Notably, 2% and 4% mannose only slightly influenced flocculation, but cellular aggregation was strongly reduced in cultures supplemented with 8.5% and 17% mannose (Figure 1B). A similar effect on flocculation was observed in the presence of high glucose levels (data not shown). Hence, high concentrations of sugars significantly inhibited CASP- induced aggregation. These data suggest that CASP-induced flocculation is the consequence of increased cell-cell adhesion mediated by certain lectin-like adhesins.

Furthermore, we reasoned that high sugar concentrations may also reduce the antifungal potency of CASP. Hence, we investigated cell survival following CASP treatment in the presence and absence of high sugar concentrations using FUN1 staining. The metabolic activities of yeast cells convert the intracellular yellow-green–fluorescent FUN 1 staining into red-orange–fluorescent, intravacuolar signals (Molecular probes Eugene, Oregon, USA). Fluorescence microscopy pictures were taken after a 3h drug treatment, and viability was determined according to red vacuolar staining. Dead cells show green to yellow cytoplasmatic staining in the overlay microscopy pictures. In normal YPD supplemented with 100ng/ml CASP, the majority of cells showed yellow-green straining, indicating mainly dead cells. However, by contrast, most cells grown in YPD plus 10% mannose retained their metabolic activity at the same CASP concentrations indicating a better survival (Figure 1C).

To quantify survival, we split exponentially growing cultures of wild type *C. albicans* grown in YPD or in YPD supplemented with additional sugar (+10% glucose or mannose) in two halves; one half was

treated with CASP for 5h, whereas the second half remained untreated as a control. All cultures were then diluted 1:1000 into normal YPD and incubated overnight at 30°C, followed by measuring the optical density of overnight cultures. This additional overnight growth step was required because of difficulties to obtain reliable cell counts of flocculating cultures. Even though cells cultured in high sugar medium reached slightly lower optical densities than the YPD culture in the absence of CASP, they reached a five times higher optical density in the presence of CASP (Figure 1D).

Interestingly, we observed a similar increase in survival to CASP treatment in the presence of high salt concentrations. We treated cells with CASP in YPD, YPD +10% glucose as well as YPD+ 0.5 M NaCl for 16 hours. As shown in Figure 2, a culture simultaneously exposed to osmotic stress and CASP reached a similar optical density as a culture exposed to CASP in the presence of high glucose. CASP-treatment in YPD alone strongly inhibited growth. To compare the degree of cell aggregation between different cultures, we took pictures within a 5 min time-frame without swirling. In the presence of 0.5M NaCl cells still aggregated and rapidly settled at the bottom of the culture tube within a few minutes (Figure 2). This clearly demonstrates that in contrast to high sugar concentrations, flocculation itself is not inhibited by NaCl. Hence, we reason that inhibition of flocculation and increased survival in the presence of glucose and CASP are independent events. High external osmolarity stabilizes weakened cell walls, thereby increasing survival of *C. albicans* cells in the presence of CASP. Notably, Hog1 is also involved in the response to CASP (Munro *et al.*, 2007; Walker *et al.*, 2008), and we think that osmotic stress induces a Hog1-mediated response that might also increase CASP resistance.

Transcriptional response to CASP

To further investigate the mechanisms underlying CASP-dependent flocculation, we first focused on the *C. albicans* PKC-pathway. From *S. cerevisiae,* it is known that this pathway is involved in mediating CASP tolerance (Reinoso-Martin *et al.*, 2003). Likewise, this pathway is also activated in CASP-treated *C. albicans* cells and its MAPK Mck1 is required for *C. albicans* CASP tolerance (Walker *et al.*, 2008). Indeed, we observed strongly induced Mkc1 activation in the presence of CASP both in normal YPD and in high sugar medium (Figure 3A). We then tested the viability and flocculation of the wild type cells compared to a homozygous *mkc1*Δ/Δ mutant strain using FUN1 staining. We used CASP at a subinhibitory concentration (10ng/ml) and a concentration of 80ng/ml, which strongly impairs growth of the wild type SN152 strain in dose-response curves (data not shown). Fluorescence microscopy pictures were taken after a 3h treatment (Figure 3B). In wild type cells, as well as in the *mkc1*Δ/Δ mutant, only few small cell aggregates were observed at a CASP concentration of 10ng/ml, whereas at concentrations of 80ng/ml large cell aggregates consisting of up to several hundred clumped cells were observed. Whereas in the wild type situation mainly cells with metabolic activity were detected, a large number of dead cells were found in the *mkc1*Δ/Δ cell aggregates. We quantified the live/dead cell ratio in a set of microscopy pictures for each condition. In the presence of 10ng/ml, about 90% of *mkc1*Δ/*mkc1*Δ mutants survived a 3h CASP treatment, whereas only about 30% showed metabolic activity at a concentration of 80ng/ml. In contrast, still 80% of wild type cells survived CASP treatment with the high drug concentration (Figure 3C). Hence,

even though Mkc1 mediates CASP tolerance and is activated in response to the drug, the flocculation response appears independent of Mkc1.

Next, we analyzed the transcriptional response to CASP. While a role for the PKC-pathway in cell-cell adhesion was not observed, we included the homozygous *mkc1* deletion strain (*mkc1* Δ/Δ) strain in our studies to elucidate the impact of the PKC pathway in the general CASP response. Based on transcriptional changes upon CASP treatment, we aimed to identify genes involved in drug resistance as well as cellular aggregation. We used a concentration of 10ng/ml CASP, which is sufficient to activate the PKC pathway, but allows for survival of the majority of cells. Furthermore, at this concentration, we observed only a marginal flocculation. Cells trapped in large cell aggregates might show additional stress phenotypes that are more related to starvation conditions than to drug treatment itself. Therefore, we consider low CASP concentrations at which formation of cell aggregates just starts as suitable for microarray experiments to identify genes involved in flocculation and cell wall stress response.

For microarray experiments, total RNA was isolated from wild type and *mkc1*Δ/Δ mutant cells after a 60 min drug treatment. Transcript profiles were determined by hybridization to genome-wide *C. albicans* microarrays. Hybridizations were repeated with dye colour swaps and expression data were filtered and averaged. Based upon statistical confidence (p 0.01) and an arbitrary expression change of more than 2-fold, we found 246 CASP-responsive genes, out of which 77 were up-regulated and some 169 down-regulated (Dataset S1). This set partially overlaps with published CASP-responsive genes (Liu *et al.*, 2005; Bruno *et al.*, 2006). Among CASP-induced genes, we found *RTA2, RTA3, ECM331, DDR48, orf19.675* and *orf19.6877* upregulated, while repressed ones included *ERG251, ENG1, PGA45, SCW11, CDR4, DAK2* and *OSM1*. Among the highest induced genes, we found a number of putative GPI-anchored genes from the cell surface (*PGA23, PGA31, ECM331, PGA6*), as well as putative cell wall genes or genes involved in cell wall maintenance (*CHS4, PGA6, orf19.765*). Another offset of genes is known to be induced during the response to azole antifungal drugs (*RTA2, orf19.7350, orf19.6877, ENA21, RTA3*) (Copping *et al.*, 2005; Liu *et al.*, 2005) and other types of stress (*RTA2, ENA21*). However, for a large number of CASP-regulated genes the function is not known (Table 2).

The role of Mkc1 in this response was determined by analyzing data sets obtained from wild type and the mutant strain for co-regulated genes. A very small set of genes was found differentially regulated between wild type and the mutant strain in response to CASP. Selecting for genes more than 1.5-fold upregulated upon CASP in wild type but significantly lower expressed in the mutant strain, yielded a list of 23 genes potentially regulated in a Mkc1-dependent manner (Figure 4A, Table S1). A set of genes was found to be exclusively induced in the wild type but not induced or even slightly repressed in the mutant strain (e.g. *PGA31, orf19.1208, orf19.727, CRH11*). Another subset of genes upregulated in the *mkc1* mutant, but to significantly lower levels when compared to the wild type included *LEU4, orf19.2125,* and *PGA6*. Notably, induction of *MKC1* cannot be seen in microarray experiments, since the corresponding cDNA was not spotted onto these batch of arrays. However, Northern analysis revealed a significant up-regulation of *MCK1* under conditions used for transcriptional profiling of CASP-responsive genes (Figure 4B). For instance, *CRH11* and *PGA31* are two putative GPI-anchored proteins significantly upregulated in

wild type cells but not at all in the *mkc1* mutant strain. *CRH11* encoding a putative transglycosidase localizes to the cell wall, and *PGA31*, which was also classified as cell wall protein (Castillo *et al.*, 2008), is strongly upregulated during cell wall regeneration (Castillo *et al.*, 2006). The Mkc1-dependent induction of both genes was further confirmed by Northern blotting experiments (Figure 4B). Together with *UTR2* and *CRH12,* Crh11 plays a role in cell wall organization and integrity. Indeed, a strain lacking Crh11 shows increased susceptibility to Congo Red (Pardini *et al.*, 2006). However, a *crh11*Δ/Δ strain did not show a detectable hypersensitivity to CASP when compared to the mutant containing reintroduced *CRH11* (data not shown). In contrast, *pga31*Δ/Δ cells display CASP-hypersensitivity (Plaine *et al.*, 2008). This sensitivity phenotype may relate to a lower chitin content and a thinner cell wall found in this mutant strain, indicating an important role for Pga31 in cell wall biosynthesis and cell integrity (Plaine *et al.*, 2008). Hence, we propose that increased Pga31 levels are mediating CASP tolerance, while a lack of Pga31 induction, as obvious in the *mkc1* deletion strain, might contribute to the CASP-hypersensitivity due to thinner cell wall structures.

Efg1 is required for CASP tolerance and CASP-induced flocculation

Aggregation of CASP-treated cells suggests overexpression of some adhesin proteins in the cell wall. Notably, our gene expression data showed a pronounced induction of *ALS1* by CASP (Table 2). Als1 is a cell surface protein mediating cell-cell adhesion and was identified as a downstream effector of the *EFG1* regulatory pathway (Fu *et al.*, 2002). These results suggested a role for Als1 in CASP-induced flocculation. Indeed, an *als1*Δ/Δ strain showed strongly reduced flocculation in liquid medium (Figure 5A+B), confirming that the observed cellular aggregation in the presence of CASP requires *ALS1.* Northern blot experiments confirmed that this induction of *ALS1* requires functional Efg1 (Figure 5C), since flocculation is almost completely suppressed in cells lacking Efg1 (Figure 5D+E).

A small set of genes with increased expression in CASP-treated cultures (*ALS1, orf19.7350, CZF1, PTP3*) requires the transcriptional regulator Efg1 (Fu *et al.*, 2002; Harcus *et al.*, 2004; Vinces *et al.*, 2006). Notably, Efg1 is a central regulator of many biological processes, including morphogenesis (Stoldt *et al.*, 1997) or white-opaque switching (Sonneborn *et al.*, 1999; Hnisz *et al.*, 2009). Efg1 also plays a major role in the regulation of cell wall genes and in further consequence in cell wall organization of *C. albicans* (Sohn *et al.*, 2003). We therefore tested two independent *EFG1* deletion strains in different genetic backgrounds for CASP susceptibility, and found that lack of Efg1 leads to pronounced CASP hypersensitivity (Figure 5F). Whereas CASP sensitivity can be linked to the function of Efg1 in cell wall gene regulation, and might be caused by an altered cell wall composition of the mutant, the lack of flocculation suggests an active role of Efg1 in the cellular response to CASP by regulating expression of adhesins.

***orf19.7350* is a antifungal drug-induced gene required for CASP tolerance**

Interestingly, we found *orf19.7350*, an as yet largely uncharacterized ORF, among the highest induced genes upon CASP-induced cell wall stress. Indeed, expression of *orf19.7350* is reduced in an *efg1*Δ/Δ strain (Harcus *et al.*, 2004). We named the protein encoded by *orf19.7350* Rct1 for **R**equired for **C**aspofungin

Tolerance (see below). We verified induction of *RCT1* in response to CASP by Northern analysis and detected reduced upregulation of *RCT1* mRNA levels in a CASP-treated *efg1*Δ/Δ strain when compared to the wild type (Figure 6A). Furthermore, a Rct1-GFP variant was strongly upregulated by CASP treatment by immunoblotting (Figure 6B). Interestingly, the gene is also induced by fluconazole (Copping *et al.*, 2005) and we observed a strong upregulation of the *RCT1* mRNA upon Posaconazole treatment (Figure 6C).

To test whether *RCT1* is required for drug resistance, we generated a *rct1*Δ/Δ strain and tested the growth on CASP to find increased CASP-sensitivity (Figure 6D), which was fully restored to wild type susceptibility in the reconstituted *rct1*Δ/Δ::*RCT1* strain. Thus, *RCT1* is induced by CASP treatment and necessary for mediating CASP tolerance.

To investigate the subcellular localization of Rct1*,* we again used the strain expressing a GFP-tagged Rct1-GFP variant. For fluorescence experiments, cells were grown in YPD and either treated with 10ng/ml CASP for 2 h or left untreated. Due to lower expression levels of the GFP-fusion protein in unstressed cells, brightness and contrast of the GFP-picture had to be increased when compared to the picture of stressed cells. Under both growth conditions, the signal of Rct1-GFP was found mainly cytoplasmic. However, staining was also visible in the nucleus in spots that co-localised with nuclear DAPI staining (Figure 6E). Since nuclear staining was increased in CASP-treated cells, we reasoned that Rct1 may undergo nuclear-cytoplasmic distribution or shuttling upon CASP stress. However, the molecular function of the *RCT1* gene product has remained unknown, and no significant homologies or conserved domains have been identified in the databases.

Taken together, our data show that Efg1 is a major regulator of cell wall biogenesis following CASP-induced cell wall remodeling. Moreover, our data indicate that Efg1 regulates important target genes which contribute to the survival of *C. albicans* cells experiencing cell wall damage and thus have an important function for survival of CASP treated cells.

DISCUSSION

CASP treatment affects the fungal cell wall by interfering with cell wall biosynthesis, thereby activating several mechanisms of cellular stress responses. This is consistent with the fact that cell wall biogenesis and maintenance in *C. albicans* is regulated by a complex network of signaling cascades and downstream effector molecules. Our findings provide novel insights into the mechanisms that contribute to CASP-induced stress response. Here, we show that (i) Mkc1 is required for the up-regulation of cell-wall genes in the presence of CASP, (ii) CASP triggers an Efg1-dependent response mediating increased flocculation and cell-cell adhesion, (iii) Efg1 is required for CASP tolerance, and (iv) high osmolarity reduces the antifungal potency of CASP. Based on our data, we propose the following model for *C. albicans* response to cell wall damage (Figure 7). CASP induces several parallel signaling pathways such as the HOG-and PKC pathway as well as calcineurin-mediated signaling, to ensure proper repair of cell wall damage. The signaling mechanisms upstream of Efg1 may be involved in cross-talk but also utilize Efg1 as downstream effector of cell wall remodeling.

CASP induces the Mkc1-dependent upregulation of cell wall remodelling genes

In several pilot microarray experiments, we readily observed an immediate response to CASP at the transcriptional level. A core set of genes consisting of *RTA2, RTA3, ORF19.7350, ORF19.7296* was found immediately upregulated 10min after exposure to 10ng/ml CASP (data not shown), indicating very rapid sensing and signaling mechanisms activated by CASP exposure. Indeed, the MAPK Mkc1 is rapidly phosphorylated in the presence of CASP (Walker *et al.*, 2008). This activation and the requirement for a functional PKC-pathway to survive in the presence of CASP indicate a significant contribution of the PKC-pathway to the CASP stress response. Interestingly, *C. albicans* rapidly elevates the cell wall chitin content upon CASP, which protects cells from extensive surface damage due to persistent inhibition of □(1,3)-glucan synthesis. The PKC-, the HOG- as well as the calcineurin pathways contribute to this adaptive response (Walker *et al.*, 2008). Notably, a lack of Mkc1 reduces the cell wall chitin (Munro *et al.*, 2007). Likewise, strains lacking the putative GPI-anchored protein Pga31 have lower chitin content and thinner cell walls, indicating that the CASP hypersensitivity of this mutant results from altered cell wall composition (Plaine *et al.*, 2008).

Here, we identify *PGA31* as a downstream target gene of the PKC pathway, which is strongly induced in the presence of CASP. Deletion of *MKC1* leads to both reduced basal mRNA levels and lack of *PGA31* upregulation (Figure 4B). Taken together, this indicates that reduced Pga31 levels in a *mkc1*Δ/Δ strain contribute to its CASP hypersensitivity. Furthermore, with *CRH11,* we identified another Mkc1-dependent gene involved in cell wall integrity (Figure 4B). Even though deletion of the putative transglycosidase gene *CRH11* alone has no direct effect on CASP tolerance in growth inhibition tests (data not shown), Crh11 might well contribute to CASP tolerance in synergy with other cell wall related factors. *CRH11* is also a major target of the Sko1 transcription factor in response to CASP (Rauceo *et al.*, 2008). We verified Mkc1-dependent upregulation of *CRH11* in a second independent *mkc1*Δ/Δ background strain (Diez-Orejas *et al.*, 1997) (data not shown). By contrast, we observed only a very moderate induction of Sko1 in the presence of subinhibitory concentrations of CASP (1,5-fold) perhaps because we used significantly lower, sublethal CASP concentrations. Likewise, Cas5 regulates *CRH11* expression in response to high CASP concentrations (Bruno *et al.*, 2006). Hence, *CRH11* might be co-regulated by several response pathways. Alternatively, activation of different regulators follows distinct drug concentrations. Major components and molecules of the newly identified Psk1-Sko1 signaling pathway remain unknown and the upstream factors regulating Cas5 have not been identified so far. Therefore, it is tempting to speculate about an involvement of the PKC pathway in the Sko1 response or Cas5 activation, which will be addressed in further studies.

Flocculation is an Efg1-dependent response to cell wall stress in *C. albicans*

Treatment of *C. albicans* with CASP results in rapid cell-clumping. In liquid YPD medium supplemented with CASP, cells flocculate and large cell aggregates can be observed under the microscope (Figure 1A+3B). A similar cell aggregation occurs in the presence of Calcofluor White (data not shown), while

others observed clumping of *C. albicans* cells in the presence of micafungin (Singh *et al.*, 2009). This indicates that cell wall stress changes the cell surface hydrophobicity and adhesion properties in a way that cell-cell adhesion is strongly favored. Our data demonstrate that clumping occurs already in living cells and must therefore be an active response rather than a consequence of cell death.

Our data show that the major adhesin responsible for CASP-induced flocculation and clumping is *ALS1*, since mRNA levels are strongly upregulated after addition of CASP. As predicted, deletion of Als1 results in strongly diminished flocculation (Figure 5A, B, C). Furthermore, our studies implicate a novel role for Efg1 as downstream regulator of the CASP response, since upregulation of *ALS1* requires functional Efg1 (Figure 5C). This is consistent with previous data that identified Efg1 as regulator of *ALS1* expression under filamentation-inducing conditions (Fu *et al.*, 2002), as well as in the presence of rapamycin (Bastidas *et al.*, 2009).

In addition, strains lacking Efg1 exhibit CASP hypersensitivity (Figure 5F). *EFG1* is known to play an important role in regulating several cell wall genes during morphogenesis. However, already in the *C. albicans* yeast form, lower transcriptional levels of several cell wall genes are observed in an *efg1*Δ/Δ strain (Sohn *et al.*, 2003). Hence, this major role of Efg1 in regulating cell wall genes and the upregulation of Efg1-targets in the presence of CASP clearly implicates Efg1 as important regulator of the CASP signaling network, involved in CASP resistance and cell-cell adhesion.

Among Efg1 target genes which are upregulated in response to CASP *ORF19.7350/RCT1* represents the most highly induced gene. This gene has remained largely uncharacterized to date, but appears upregulated at the mRNA level and/or protein level (Copping *et al.*, 2005; Kusch *et al.*, 2007; Yin *et al.*, 2009) by several stress conditions, implying a general involvement of Rct1 in the environmental stress response in a broad sense. However, despite a pronounced CASP sensitivity, cells lacking Rct1 do not display any other stress hypersensitivity phenotypes (data not shown). *YNL208W*, the closest homologue of Rct1 in baker's yeast is upregulated in response to Zymolyase treatment, a drug which also introduces severe cell wall damage (Garcia *et al.*, 2009). However, a function for *YNL208W* has not been described. In summary, *Candida albicans* Rct1 is required for CASP tolerance and its expression is strongly upregulated by CASP, implicating a rather specific role for Rct1 in the echinocandin response of *C. albicans*. A potentially changing subcellular localization from the cytoplasm to the nucleus might imply a regulatory function of Rct1, but further studies are on the way to answer this question.

High external osmolarity increases *C. albicans* survival in the presence of CASP

Experiments in *S. cerevisiae* showed that flocculation mediated by the *FLO1* adhesin is a major mechanism protecting cells from environmental stress conditions (Smukalla *et al.*, 2008). Whether cell wall stress-induced flocculation is a protective response in *C. albicans* is not clear yet and requires further studies to obtain an answer. With our experimental set up, we fail to observe a direct link between flocculation and increased survival within the first hours of drug treatment. We rather hypothesize that flocculation is a consequence of dynamic changes in the cell wall composition to compensate defects in cell wall

biosynthesis as caused by echinocandins. However, the effect of long-time CASP exposure on cells within cell aggregates has not been investigated so far but will be subject of further studies.

Even though *C. albicans ALS* gene products were previously considered as sugar-independent adhesins (Klotz *et al.*, 2004), we observe that addition of sugars strongly inhibit flocculation (Figures 1B+2). Initially, we thought if aggregation would protect cells located in the center of large cell aggregates, presence of high sugar would reduce survival of CASP-treated cells rather than the opposite. However, we observe that high concentrations of sugars such as mannose or glucose greatly improve survival of *C. albicans* cells to CASP killing (Figure 1C+D) and thus reduce CASP potency. Hence, our analysis has uncovered a protective function of high sugar concentrations in response to CASP. This is also true for cultures supplemented with NaCl, pointing to a role for osmolarity signaling in diminishing CASP killing (Figure 2). Furthermore, increased external osmolarity reduces the CASP hypersensitivity of *efg1* mutant strains (data not shown). Hence, high external osmolarity stabilizes damaged cell walls, thereby opposing CASP activity. Furthermore, a Hog1-mediated response, as transiently activated in cells pre-treated with high osmolarity, might lead to cross-protection against cell wall stress.

In summary, our results link Efg1, which is otherwise involved in filamentation, white – opaque switching as well as other cellular processes, to several genetic networks responding to CASP treatment (Munro *et al.*, 2007; Xu *et al.*, 2007; Rauceo *et al.*, 2008). Furthermore, we identify novel genes activated by the PKC pathway in response to CASP stress, thereby further completing the picture of the important role of the cell wall integrity pathway in the response to CASP-induced cell wall damage. Therefore, our results are consistent with a model that involves activation of parallel signaling pathways to respond to CASP-induced cell wall stress (Figure 7). Moreover, it will be very interesting to test to what extent, if at all, the cAMP/PKA or TOR signaling pathways contribute to the CASP response, since both signaling pathways also use Efg1 as downstream transducer and effector (Bockmuhl and Ernst, 2001; Harcus *et al.*, 2004; Bastidas *et al.*, 2009) Likewise, the sodium chloride suppression of CASP-activity implies a role for the HOG pathway, which is consistent with CASP-mediated HOG activation (Kelly *et al.*, 2009) Such an cross-talk of signaling pathways would not come as a surprise, since a tight regulation of cell wall homeostasis under normal growth conditions, as well as stress such as surface damage is essential for viability and cellular growth control.

Acknowledgements

We thank all laboratory members for helpful discussions and critical comments on the manuscript. We appreciate the technical support of Nathalie Landstetter and Anna Wächter. Dominique Sanglard is acknowledged for the kind gift of Posaconazole, and Yue Fu for sharing the Candida *als1* strain. This work was supported by the EU-FP6 project EURESFUN (STREP-CT-518199) to KK and SR, and in part by the Christian Doppler Society and the FP7-Integrated Project UNICELLSYS to KK.

References

Balashov, S.V., Park, S., and Perlin, D.S. (2006). Assessing resistance to the echinocandin antifungal drug caspofungin in *Candida albicans* by profiling mutations in *FKS1.* Antimicrob Agents Chemother *50*, 2058-2063.

Bastidas, R.J., Heitman, J., and Cardenas, M.E. (2009). The protein kinase Tor1 regulates adhesin gene expression in *Candida albicans*. PLoS Pathog *5*, e1000294.

Bockmuhl, D.P., and Ernst, J.F. (2001). A potential phosphorylation site for an A-type kinase in the Efg1 regulator protein contributes to hyphal morphogenesis of *Candida albicans*. Genetics *157*, 1523-1530.

Bruno, V.M., Kalachikov, S., Subaran, R., Nobile, C.J., Kyratsous, C., and Mitchell, A.P. (2006). Control of the *C. albicans* cell wall damage response by transcriptional regulator Cas5. PLoS Pathog *2*, e21.

Calderone, R.A., and Fonzi, W.A. (2001). Virulence factors of *Candida albicans*. Trends Microbiol *9*, 327-335.

Castillo, L., Calvo, E., Martinez, A.I., Ruiz-Herrera, J., Valentin, E., Lopez, J.A., and Sentandreu, R. (2008). A study of the *Candida albicans* cell wall proteome. Proteomics *8*, 3871-3881.

Castillo, L., Martinez, A.I., Garcera, A., Garcia-Martinez, J., Ruiz-Herrera, J., Valentin, E., and Sentandreu, R. (2006). Genomic response programs of *Candida albicans* following protoplasting and regeneration. Fungal Genet Biol *43*, 124-134.

Copping, V.M., Barelle, C.J., Hube, B., Gow, N.A., Brown, A.J., and Odds, F.C. (2005). Exposure of *Candida albicans* to antifungal agents affects expression of *SAP2* and *SAP9* secreted proteinase genes. J Antimicrob Chemother *55*, 645-654.

De Pauw, B.E. (2000). New antifungal agents and preparations. Int J Antimicrob Agents *16*, 147-150.

Denning, D.W. (2003). Echinocandin antifungal drugs. Lancet *362*, 1142-1151.

Diez-Orejas, R., Molero, G., Navarro-Garcia, F., Pla, J., Nombela, C., and Sanchez-Perez, M. (1997). Reduced virulence of *Candida albicans MKC1* mutants: a role for mitogen-activated protein kinase in pathogenesis. Infect Immun *65*, 833-837.

Douglas, C.M., D'Ippolito, J.A., Shei, G.J., Meinz, M., Onishi, J., Marrinan, J.A., Li, W., Abruzzo, G.K., Flattery, A., Bartizal, K., Mitchell, A., and Kurtz, M.B. (1997). Identification of the *FKS1* gene of *Candida albicans* as the essential target of 1,3-beta-D-glucan synthase inhibitors. Antimicrob Agents Chemother *41*, 2471-2479.

Eisen, M.B., Spellman, P.T., Brown, P.O., and Botstein, D. (1998). Cluster analysis and display of genome-wide expression patterns. Proc Natl Acad Sci U S A *95*, 14863-14868.

Fonzi, W.A., and Irwin, M.Y. (1993). Isogenic strain construction and gene mapping in *Candida albicans*. Genetics *134*, 717-728.

Frohner, I.E., Bourgeois, C., Yatsyk, K., Majer, O., and Kuchler, K. (2009). *Candida albicans* cell surface superoxide dismutases degrade host-derived reactive oxygen species to escape innate immune surveillance. Mol Microbiol *71*, 240-252.

Fu, Y., Ibrahim, A.S., Sheppard, D.C., Chen, Y.C., French, S.W., Cutler, J.E., Filler, S.G., and Edwards, J.E., Jr. (2002). *Candida albicans* Als1p: an adhesin that is a downstream effector of the *EFG1* filamentation pathway. Mol Microbiol *44*, 61-72.

Garcia-Effron, G., Park, S., and Perlin, D.S. (2009). Correlating echinocandin MIC and kinetic inhibition of *fks1* mutant glucan synthases for *Candida albicans*: implications for interpretive breakpoints. Antimicrob Agents Chemother *53*, 112-122.

Garcia, R., Rodriguez-Pena, J.M., Bermejo, C., Nombela, C., and Arroyo, J. (2009). The high osmotic response and cell wall integrity pathways cooperate to regulate transcriptional responses to Zymolyase-induced cell wall stress in *Saccharomyces cerevisiae.* J Biol Chem *284*, 10901-10911.

Gerami-Nejad, M., Berman, J., and Gale, C.A. (2001). Cassettes for PCR-mediated construction of green, yellow, and cyan fluorescent protein fusions in *Candida albicans*. Yeast *18*, 859-864.

Gillum, A.M., Tsay, E.Y., and Kirsch, D.R. (1984). Isolation of the *Candida albicans* gene for orotidine-5'-phosphate decarboxylase by complementation of *S. cerevisiae ura3* and *E. coli* pyrF mutations. Mol Gen Genet *198*, 179-182.

Harcus, D., Nantel, A., Marcil, A., Rigby, T., and Whiteway, M. (2004). Transcription profiling of cyclic AMP signaling in *Candida albicans*. Mol Biol Cell *15*, 4490-4499.

Hnisz, D., Schwarzmuller, T., and Kuchler, K. (2009). Transcriptional loops meet chromatin: a dual-layer network controls white-opaque switching in *Candida albicans*. Mol Microbiol *74*, 1-15.

Kelly, J., Rowan, R., McCann, M., and Kavanagh, K. (2009). Exposure to caspofungin activates Cap and Hog pathways in *Candida albicans*. Med Mycol *47*, 697-706.

Klotz, S.A., Gaur, N.K., Lake, D.F., Chan, V., Rauceo, J., and Lipke, P.N. (2004). Degenerate peptide recognition by *Candida albicans* adhesins Als5p and Als1p. Infect Immun *72*, 2029-2034.

Kumamoto, C.A. (2005). A contact-activated kinase signals *Candida albicans* invasive growth and biofilm development. Proc Natl Acad Sci U S A *102*, 5576-5581.

Kurtz, M.B., and Douglas, C.M. (1997). Lipopeptide inhibitors of fungal glucan synthase. J Med Vet Mycol *35*, 79-86.

Kusch, H., Engelmann, S., Albrecht, D., Morschhauser, J., and Hecker, M. (2007). Proteomic analysis of the oxidative stress response in *Candida albicans*. Proteomics *7*, 686-697.

Leonard, W.R., Jr., Belyk, K.M., Conlon, D.A., Bender, D.R., DiMichele, L.M., Liu, J., and Hughes, D.L. (2007). Synthesis of the antifungal beta-1,3-glucan synthase inhibitor CANCIDAS (caspofungin acetate) from pneumocandin B0. J Org Chem *72*, 2335-2343.

Liu, T.T., Lee, R.E., Barker, K.S., Wei, L., Homayouni, R., and Rogers, P.D. (2005). Genome-wide expression profiling of the response to azole, polyene, echinocandin, and pyrimidine antifungal agents in *Candida albicans*. Antimicrob Agents Chemother *49*, 2226-2236.

Lo, H.J., Kohler, J.R., DiDomenico, B., Loebenberg, D., Cacciapuoti, A., and Fink, G.R. (1997). Nonfilamentous *C. albicans* mutants are avirulent. Cell *90*, 939-949.

Mamnun, Y.M., Schüller, C., and Kuchler, K. (2004). Expression regulation of the yeast *PDR5* ATP-binding cassette (ABC) transporter suggests a role in cellular detoxification during the exponential growth phase. FEBS Lett *559*, 111-117.

Monge, R.A., Roman, E., Nombela, C., and Pla, J. (2006). The MAP kinase signal transduction network in *Candida albicans*. Microbiology *152*, 905-912.

Munro, C.A., Selvaggini, S., de Bruijn, I., Walker, L., Lenardon, M.D., Gerssen, B., Milne, S., Brown, A.J., and Gow, N.A. (2007). The PKC, HOG and Ca2+ signalling pathways co-ordinately regulate chitin synthesis in *Candida albicans*. Mol Microbiol *63*, 1399-1413.

Navarro-Garcia, F., Eisman, B., Fiuza, S.M., Nombela, C., and Pla, J. (2005). The MAP kinase Mkc1p is activated under different stress conditions in *Candida albicans*. Microbiology *151*, 2737-2749.

Noble, S.M., and Johnson, A.D. (2005). Strains and strategies for large-scale gene deletion studies of the diploid human fungal pathogen *Candida albicans*. Eukaryot Cell *4*, 298-309.

Pardini, G., De Groot, P.W., Coste, A.T., Karababa, M., Klis, F.M., de Koster, C.G., and Sanglard, D. (2006). The CRH family coding for cell wall glycosylphosphatidylinositol proteins with a predicted transglycosidase domain affects cell wall organization and virulence of *Candida albicans*. J Biol Chem *281*, 40399-40411.

Pfaller, M.A., and Diekema, D.J. (2007). Epidemiology of invasive candidiasis: a persistent public health problem. Clin Microbiol Rev *20*, 133-163.

Plaine, A., Walker, L., Da Costa, G., Mora-Montes, H.M., McKinnon, A., Gow, N.A., Gaillardin, C., Munro, C.A., and Richard, M.L. (2008). Functional analysis of *Candida albicans* GPI-anchored proteins: roles in cell wall integrity and caspofungin sensitivity. Fungal Genet Biol *45*, 1404-1414.

Rauceo, J.M., Blankenship, J.R., Fanning, S., Hamaker, J.J., Deneault, J.S., Smith, F.J., Nantel, A., and Mitchell, A.P. (2008). Regulation of the *Candida albicans* cell wall damage response by transcription factor Sko1 and PAS kinase Psk1. Mol Biol Cell *19*, 2741-2751.

Reinoso-Martin, C., Schüller, C., Schuetzer-Muehlbauer, M., and Kuchler, K. (2003). The yeast protein kinase C cell integrity pathway mediates tolerance to the antifungal drug caspofungin through activation of Slt2p mitogen-activated protein kinase signaling. Eukaryot Cell *2*, 1200-1210.

Saldanha, A.J. (2004). Java Treeview--extensible visualization of microarray data. Bioinformatics *20*, 3246-3248.

Schuetzer-Muehlbauer, M., Willinger, B., Krapf, G., Enzinger, S., Presterl, E., and Kuchler, K. (2003). The *Candida albicans* Cdr2p ATP-binding cassette (ABC) transporter confers resistance to caspofungin. Mol Microbiol *48*, 225-235.

Singh, S.D., Robbins, N., Zaas, A.K., Schell, W.A., Perfect, J.R., and Cowen, L.E. (2009). Hsp90 governs echinocandin resistance in the pathogenic yeast *Candida albicans* via calcineurin. PLoS Pathog *5*, e1000532.

Smukalla, S., Caldara, M., Pochet, N., Beauvais, A., Guadagnini, S., Yan, C., Vinces, M.D., Jansen, A., Prevost, M.C., Latge, J.P., Fink, G.R., Foster, K.R., and Verstrepen, K.J. (2008). *FLO1* is a variable green beard gene that drives biofilm-like cooperation in budding yeast. Cell *135*, 726-737.

Smyth, G.K. (2004). Linear models and empirical bayes methods for assessing differential expression in microarray experiments. Stat Appl Genet Mol Biol *3*, Article3.

Sohn, K., Urban, C., Brunner, H., and Rupp, S. (2003). *EFG1* is a major regulator of cell wall dynamics in *Candida albicans* as revealed by DNA microarrays. Mol Microbiol *47*, 89-102.

Sonneborn, A., Tebarth, B., and Ernst, J.F. (1999). Control of white-opaque phenotypic switching in *Candida albicans* by the Efg1p morphogenetic regulator. Infect Immun *67*, 4655-4660.

Stoldt, V.R., Sonneborn, A., Leuker, C.E., and Ernst, J.F. (1997). Efg1p, an essential regulator of morphogenesis of the human pathogen *Candida albicans*, is a member of a conserved class of bHLH proteins regulating morphogenetic processes in fungi. EMBO J *16*, 1982-1991.

Verstrepen, K.J., and Klis, F.M. (2006). Flocculation, adhesion and biofilm formation in yeasts. Mol Microbiol *60*, 5-15.

Vinces, M.D., Haas, C., and Kumamoto, C.A. (2006). Expression of the *Candida albicans* morphogenesis regulator gene *CZF1* and its regulation by Efg1p and Czf1p. Eukaryot Cell *5*, 825-835.

Walker, L.A., Munro, C.A., de Bruijn, I., Lenardon, M.D., McKinnon, A., and Gow, N.A. (2008). Stimulation of chitin synthesis rescues *Candida albicans* from echinocandins. PLoS Pathog *4*, e1000040.

Wettenhall, J.M., and Smyth, G.K. (2004). limmaGUI: a graphical user interface for linear modeling of microarray data. Bioinformatics *20*, 3705-3706.

Xu, D., Jiang, B., Ketela, T., Lemieux, S., Veillette, K., Martel, N., Davison, J., Sillaots, S., Trosok, S., Bachewich, C., Bussey, H., Youngman, P., and Roemer, T. (2007). Genome-wide fitness test and mechanism-of-action studies of inhibitory compounds in *Candida albicans*. PLoS Pathog *3*, e92.

Yin, Z., Stead, D., Walker, J., Selway, L., Smith, D.A., Brown, A.J., and Quinn, J. (2009). A proteomic analysis of the salt, cadmium and peroxide stress responses in *Candida albicans* and the role of the Hog1 stress-activated MAPK in regulating the stress-induced proteome. Proteomics *9*, 4686-4703.

FIGURE LEGENDS

Figure 1. *C. albicans* flocculation in response to CASP

A. *C. albicans* wild type strain (SC5314) growing in the exponential growth phase at 30°C in YPD or RPMI 1640 was treated with 50ng/ml CASP for two hours or left untreated. Cultures were photographed 2 min after vortex-mixing of the culture tubes.

B. High sugar inhibits CASP-induced flocculation. Wild type cells were grown to exponential growth phase in YPD or YPD supplemented with indicated concentrations of mannose. CASP was added at a final concentration of 100ng/ml. After a 3h CASP treatment the optical density of the cultures was measured directly after vortex-mixing. Some 15min later, the same tubes were measured again without mixing. All treatments and measurements were done in triplicates and standard deviations are shown as error bars.

C. High sugar concentrations increase viability in the presence of CASP. Wild type cells were grown to exponential growth phase in YPD or YPD+ 10% mannose, respectively before treatment with 100ng/ml CASP. After 3h, cells were strained with FUN1 and Calcofluor White (CFW) and microscopy pictures taken.

D. Cells were grown to an OD_{600nm} of about 1 in YPD, YPD+10% glucose or YPD +10% mannose. The cultures were split in two halves and one half was treated with CASP for 5h, whereas the other half remained as untreated control. All cultures where then diluted 1:1000 in normal YPD and incubated overnight. We determined the optical density of the overnight cultures. The experiment was performed in triplicates and the average OD_{600nm} for each condition is given in the graph with standard deviations as error bars.

Figure 2. High salt concentration improves survival

C. albicans wild type strain was grown to the early exponential growth phase at 30°C in YPD. Cells were then diluted to an OD_{600nm} of 0.1 in YPD, YPD+10% glucose or YPD +0.5M NaCl and incubated for 2h at 30°C. After adding 100ng/ml CASP, cultures were incubated at 30°C for another 16h with shaking. Pictures of each culture were taken over a time period of 5min.

Figure 3. Survival and flocculation of *mkc1*Δ/Δ mutant cells

A. Wild type cells were grown to an OD_{600nm} of about 1 in either YPD, YPD supplemented with additional 10% glucose or YPD plus 10% mannose before CASP [10ng/ml] was added. Samples were taken at indicated time points. Cell extracts were separated in a 10% SDS-PAGE gel. Immunoblotting was carried out using phospho-specific p44/42 antibodies to visualize activated Mkc1. Polyclonal antibodies recognizing Pgk1 were used to detect the loading control.

B. Wild type CA-IF100 and the corresponding *mkc1*Δ/Δ strain were grown to an OD_{600nm} of 1, before exposing to CASP at concentrations of 10ng/ml and 80ng/ml, respectively. After 3h, cells were strained with FUN1 and Calcofluor White (CFW), and inspected by microscopy.

C. For each condition from Figure 3B, living and dead cells were counted from 15 microscopy pictures. Average percentages of living cells versus to total number of cells are given for each condition.

Figure 4. Mkc1-dependent response to CASP

A. Wild type and *mkc1*Δ/Δ cells were grown to the exponential growth phase before treatment with 10ng/ml CASP for 1h and microarray experiments of treated versus untreated cells were performed. Expression data of genes upregulated in wild type but not or less in the *mkc1* mutant were clustered.

B. Northern analysis of Mkc1-dependent genes. Wild type and *mkc1*Δ/Δ cells were grown to the exponential growth phase before treatment with 10ng/ml CASP for 1h. Total RNA was isolated and mRNA levels of *MKC1, CHR11, PGA31* and the control *ACT1* were analyzed by Northern blotting.

Figure 5. *ALS1* is required for flocculation

A. The Wild type, *als1*Δ/Δ and the *ALS1* re-constituted strains were grown to the exponential growth phase at 30°C in glass tubes before 80ng/ml CASP was added for two hours. Cultures were photographed 2 min after vortex-mixing.

B. To quantify flocculation, the optical density of the cultures was measured directly after vortex-mixing. The same tubes were measured again without prior mixing 5min, 10min, 15min and 20min after the first measurement. Treatments and measurements were done in triplicates and standard deviations are included as error bars.

C. Northern analysis of *ALS1* expression. Wild type and *efg1*Δ/Δ strains were grown to the exponential growth phase followed by treatment with 10ng/ml CASP. Samples were taken at indicated time points. Total RNA was isolated and mRNA levels of *ALS1* were detected by Northern blotting. *CHR11* served as control for an Efg1-independent CASP-responsive gene and *ACT1* as a loading control.

D. Efg1 is required for CASP tolerance and flocculation. Wild type and *efg1*Δ/Δ cells growing in the exponential growth phase at 30°C in glass tubes were treated with 80ng/ml CASP for two hours. Cultures were photographed 2 min after vortex-mixing.

E. To quantify flocculation, the OD_{600nm} of cultures was measured directly after mixing. The same tubes were measured again without prior mixing 5min, 10min, 15min and 20min after the first measurement. Treatments and measurements were done in triplicates and standard deviations are indicated as error bars.

F. Identical volumes of ten-fold serial dilutions of exponentially growing cells of wild type and cells lacking Efg1 in two *C. albicans* background strains (SC5314, SN152) were spotted onto YPD plates containing 250ng/ml CASP and incubated at 30°C. Colony growth was inspected after 48 h incubation time.

Figure 6. *orf19.7350/RCT1* is required for CASP tolerance

A. Northern analysis of the *orf19.7350* / *RCT1* transcript in wild type and *efg1* mutant strains. Exponentially growing wild type cells and cells lacking Efg1 were treated with 10ng/ml CASP. Samples were taken at indicated time points. Total RNA was isolated and mRNA levels of *RCT1* detected by Northern blotting. *ACT1* served as loading control.

B. Strain CA-CG06 (*RCT1-GFP*) was grown to an OD_{600nm} of 1 before adding 10ng/ml CASP. Samples were taken at indicated time points. Cell extracts equivalent to 0.5 OD_{600nm} per lane were separated through a

10% SDS-PAGE gel. Immunoblotting was carried out using monoclonal anti-GFP antibodies and polyclonal antibodies detecting Pgk1 as loading control.

C. Exponentially growing wild type cells were treated with 50µg/ml Posaconazole or left untreated. Samples were taken at indicated time points. Total RNA was isolated and mRNA levels of *RCT1 and RTA2* were visualized by Northern blotting. *ACT1* served as loading control.

D. Identical volumes of ten-fold serial dilutions of exponentially growing *rct1*□/□ cells were spotted along with the corresponding wild type strains and the restored *rct1*□/□::*RCT1* strain onto YPD plates containing the indicated CASP concentrations. Colony growth was inspected after 48h incubation at 30°C.

E. Strain CA-CG06 (*RCT1-GFP*) was grown to the exponential growth phase, followed by adding 10ng/ml CASP to one half of the culture. The other half remained as untreated control. DAPI was added to both cultures to stain DNA. After a 2h treatment, pictures of live cells were taken on an Olympus microscope. Since GFP- fusion protein levels are lower in unstressed cells brightness of this GFP picture was enhanced when compared to the picture of CASP-treated cells.

Figure 7. Model for a CASP-activated signaling response in *C. albicans*

CASP–induced cell wall damage activates Hog1-, calcineurin-, Mkc1-, and Efg1- dependent signaling pathways, each driving expression of a distinct subset of genes implicated in cell wall remodelling and repair. Cell wall genes are upregulated to compensate for impaired β-glucan deposition into the cell wall and cell-cell adhesion is induced. The partial overlap of target genes ensures sustained response under many adverse conditions affecting cell wall integrity or function.

Table 1: Fungal strains used in this study

Strains	Short Names	Genotypes	Reference
SC5314			(Gillum *et al.*, 1984)
SN152		*arg4Δ/arg4Δ, leu2Δ/leu2Δ, his1Δ/his1Δ, URA3/ura3Δ*	(Noble and Johnson, 2005)
CA-IF100		*arg4Δ/arg4Δ, leu2Δ/leu2Δ::cmLEU2, his1Δ/his1Δ::cdHIS1, URA3/ura3Δ,*	(Frohner *et al.*, 2009)
CAI4		*ura3Δ::imm434/ura3Δ::imm43*	(Fonzi and Irwin, 1993)
HLC67	*efg1*Δ/Δ	CAI4, *efg1Δ::hisG/efg1Δ::hisG*	(Lo *et al.*, 1997)
DHCA216	*efg1*Δ/Δ	SC5314*, efg1Δ*::FRT/*efg1Δ*::FRT	(Hnisz *et al.*, 2009)
CAYC2	*als1*Δ/Δ	CAI4, *als1Δ::hisG/als1Δ::hisG-URA3-hisG*	(Fu *et al.*, 2002)
CAYFR3	*als1*Δ/Δ::*ALS1*	CAI4, *als1Δ::hisG/als1Δ::hisG-URA3-hisG(ALS1)*	(Fu *et al.*, 2002)
CA-CG02	*mkc1*Δ/Δ	SN152, *mkc1*Δ::*cmLEU2*/*mkc1*Δ::*CdHIS1*	This study
CA-CG03	*orf19.7350*Δ/+	SN152, *orf19.7350* ::*cmLEU2*/*ORF19.7350*	This study
CA-CG04	*orf19.7350*Δ/Δ	SN152, *orf19.7350*Δ::*cmLEU2*/*orf19.7350*Δ::*CdHIS1*	This study
CA-CG05	*orf19.7350*Δ/Δ*:: ORF19.7350*	SN152, *orf19.7350*Δ::*cmLEU2*/*orf19.7350*Δ::*CdHIS1*:: *ORF19.7350-FRT*	This study
CA-CG06		SN152*, ORF19.7350-GFP::CdHIS1*	This study

WT+C / WT	ORF	*NAME*	*S.c. Gene*	Functional Annotation
11,39	orf19.2125			Predicted ORF
10,56	orf19.24	*RTA2*	*RSB1*	Stress-associated protein; ketoconazole, caspofungin induced; Plc1p-regulated
6,84	orf19.7350		*YNL208W*	Predicted ORF in Assemblies 19 and 20; soluble protein in hyphae; fluconazole-induced; decreased mRNA abundance in an *efg1* homozygous null mutant
6,54	orf19.3740	*PGA23*	*YFL067W*	Putative GPI-anchored protein; transcription is negatively regulated by Rim101p; regulated by Cyr1p;
6,54	orf19.675		*YEL077C*	Similar to cell wall proteins; induced in core stress response, core caspofungin response;
6,23	orf19.5302	*PGA31*		Putative GPI-anchored protein; expression is regulated upon white-opaque switching; induced during cell wall regeneration
6,11	orf19.4255	*ECM331*		Putative GPI-anchored protein; caspofungin induced;
5,82	orf19.4082	*DDR48*		Immunogenic stress-associated protein; regulated by filamentous growth pathways; induced by benomyl, caspofungin
4,92	orf19.4477	*CSH1*		Member of aldo-keto reductase family, similar to aryl alcohol dehydrogenases
4,08	orf19.6840			Predicted ORF
3,46	orf19.5126			Predicted ORF
3,36	orf19.6877			Predicted ORF; upregulated in response to ciclopirox olamine or ketoconazole; gene of core caspofungin response
3,32	orf19.5741	*ALS1*		Adhesin; ALS family of cell-surface glycoproteins; adhesion
3,16	orf19.4765	*PGA6*		Putative GPI-anchored cell-wall protein
3,03	orf19.1287			Predicted ORF
3,03	orf19.4096		*TAZ1*	Predicted ORF
3,03	orf19.4287			Predicted ORF
2,93	orf19.5732		*NOG2*	Predicted ORF
2,85	orf19.5462			ORF Predicted
2,75	orf19.6041	*RPO41*	*RPO41*	Predicted ORF; downregulated during core stress response
2,69	orf19.7489		*LRG1*	Predicted ORF
2,68	orf19.7411		*OAC1*	Predicted ORF

2,64	orf19.5170	*ENA21*		Predicted ORF; similar to *S. cerevisiae* sodium transporters Ena1p and Ena5p; Gcn4p-regulated; flucytosine, amphotericin B, or ketoconazole-induced; osmotic stress-induced
2,51	orf19.7349	*CHS4*	*SKT5*	Activator of Chs3p chitin synthase; required for wild-type wall chitin content, but not for hyphal growth; mutant resistant to Calcofluor white; prenylation and 2 transmembrane segments predicted; functional homolog of *S. cerevisiae* Chs4p
2,43	orf19.6417		*TSR1*	Predicted ORF
2,39	orf19.23	*RTA3*		Similar to *S. cerevisiae* Rta1p (role in 7-aminocholesterol resistance) and Rsb1p (flippase); putative membrane protein; putative drug-responsive regulatory site; induced by fluphenazine, estradiol, ketoconazole, caspofungin

Table 2a. CASP-upregulated genes in *C. albicans*

WT+C / WT	ORF	*NAME*	*S.c. Gene*	Functional Annotation
-29,04	orf19.7514	*PCK1*	*PCK1*	Phosphoenolpyruvate carboxykinase; role in gluconeogenesis;
-26,91	orf19.1354		*YER067W*	Transcriptionally regulated by iron or by yeast-hyphal switch;
-16,91	orf19.2430			Predicted ORF
-9,19	orf19.4631	*ERG251*		Predicted ORF; ketoconazole-induced; amphotericin B, caspofungin repressed
-9,00	orf19.7218	*RBE1*	*PRY1*	Putative cell wall protein; transcription is negatively regulated by Rim101p, Efg1p, Ssn6p;
-8,11	orf19.3707	*YHB1*	*YHB1*	Nitric oxide dioxygenase; acts in nitric oxide scavenging/detoxification; role in virulence in mouse
-7,11	orf19.5267			Putative cell wall protein; downregulated in core caspofungin response;
-6,54	orf19.2608	*ADH5*		Putative alcohol dehydrogenase;
-6,19	orf19.3066	*ENG1*	*DSE4*	Endo-1,3-beta-glucanase required for cell separation after division, caspofungin repressed
-6,11	orf19.4907		*YCR061W*	Predicted ORF
-6,06	orf19.449		*YKR070W*	Predicted ORF; possible phosphatidyl synthase;
-5,90	orf19.2451	*PGA45*		Putative GPI-anchored protein; downregulated in core caspofungin response;
-5,66	orf19.3669	*SHA3*	*SKS1*	Protein similar to *S. cerevisiae* Sha3p, fluconazole-induced; ketoconazole-repressed
-5,46	orf19.4737	*TPO3*	*TPO2*	Possible role in polyamine transport; MFS-MDR family;
-5,31	orf19.3893	*SCW11*	*SCW11*	Cell wall protein; downregulated in core caspofungin response;
-5,13	orf19.3419	*MAE1*	*MAE1*	Malic enzyme, mitochondrial;
-5,10	orf19.3441	*FRP6*		Transcription is regulated by Nrg1p and Tup1p
-5,10	orf19.5079	*CDR4*		Putative transporter of ATP-binding cassette (ABC) superfamily; caspofungin repressed;
-5,06	orf19.2655	*BUB3*	*BUB3*	Protein similar to *S. cerevisiae* Bub3p
-5,06	orf19.3325		*GLG2/GLG1*	Protein described as glycogen synthesis initiator; regulated by Efg1p and Efh1p;
-5,03	orf19.5674	*PGA10*		Plasma membrane protein involved in heme-iron utilization; allows utilization of hemin and hemoglobin as iron sources in host tissues; predicted GPI anchor;
-4,72	orf19.2877	*PDC11*	*PDC1*	Protein similar to pyruvate decarboxylase;; regulated by Gcn4p, Efg1p, Efh1p;

-4,72	orf19.4342		*SUT1*	Predicted ORF
-4,63	orf19.6881	*YTH1*	*YTH1*	Protein described as an mRNA cleavage and polyadenylation specificity factor;
-4,59	orf19.2048			Transcription is positively regulated by Sfu1p
-4,52	orf19.2023	*HGT7*		Putative glucose transporter, major facilitator superfamily
-4,50	orf19.4617		*MAK3*	Predicted ORF
-4,29	orf19.1433			Predicted ORF, shows colony morphology-related gene regulation by Ssn6p
-4,14	orf19.3712			Predicted ORF
-4,14	orf19.5334			Predicted ORF; transcription regulated upon yeast-hyphal switch
-4,06	orf19.4777	*DAK2*	*DAK2*	Protein described as similar to dihydroxyacetone kinase; caspofungin repressed

Table 2b. CASP-downregulated genes in *C. albicans*

Figure 1

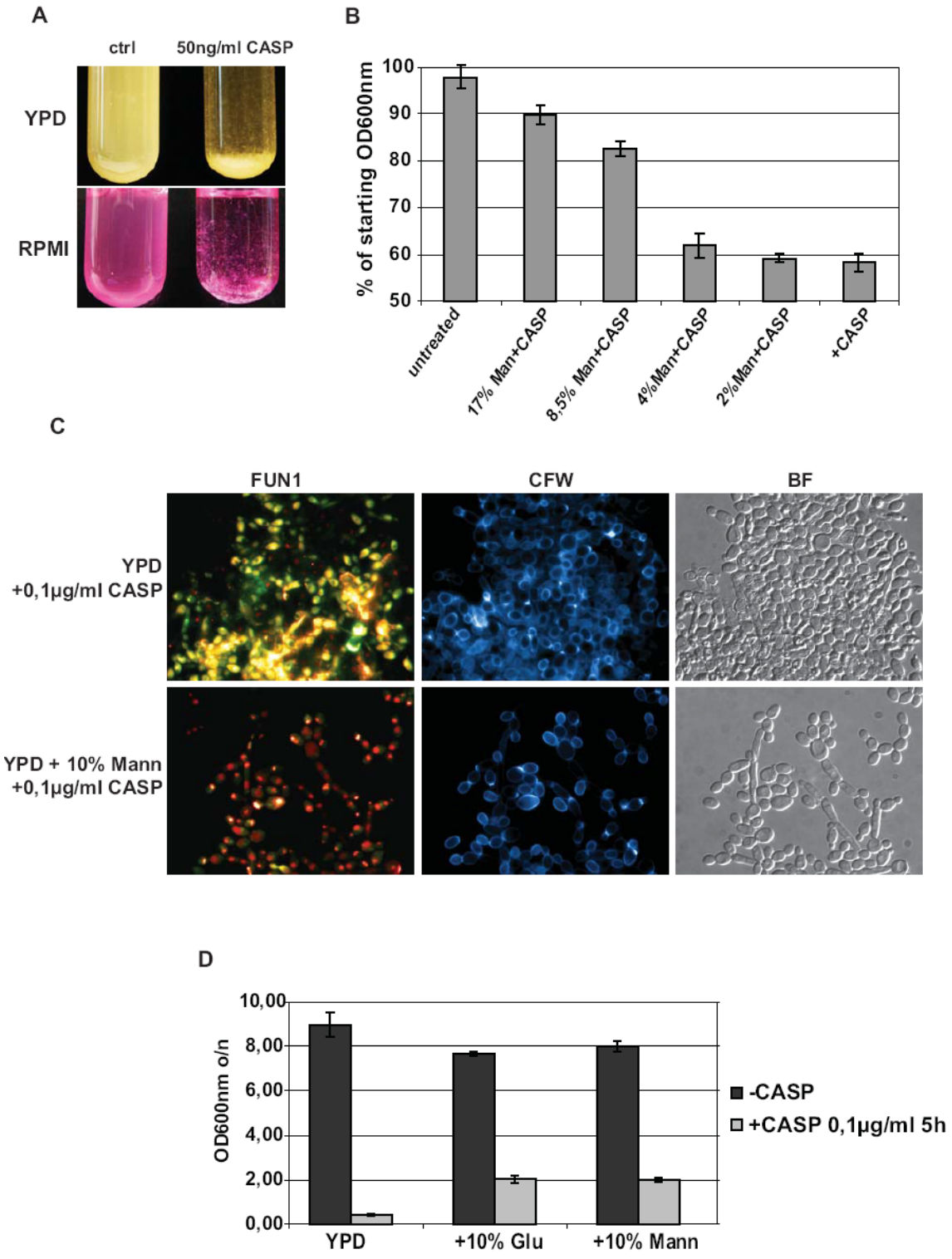
A
ctrl
50ng/ml CASP
YPD
RPMI
B
% of starting OD600nm
100
90
80
70
60
50
untreated
17% Man+CASP
8,5% Man+CASP
4%Man+CASP
2%Man+CASP
+CASP
C
FUN1
CFW
BF
YPD
+0,1µg/ml CASP
YPD + 10% Mann
+0,1µg/ml CASP
D
OD600nm o/n
10,00
8,00
6,00
4,00
2,00
0,00
YPD
+10% Glu
+10% Mann
-CASP
+CASP 0,1µg/ml 5h

Figure 2

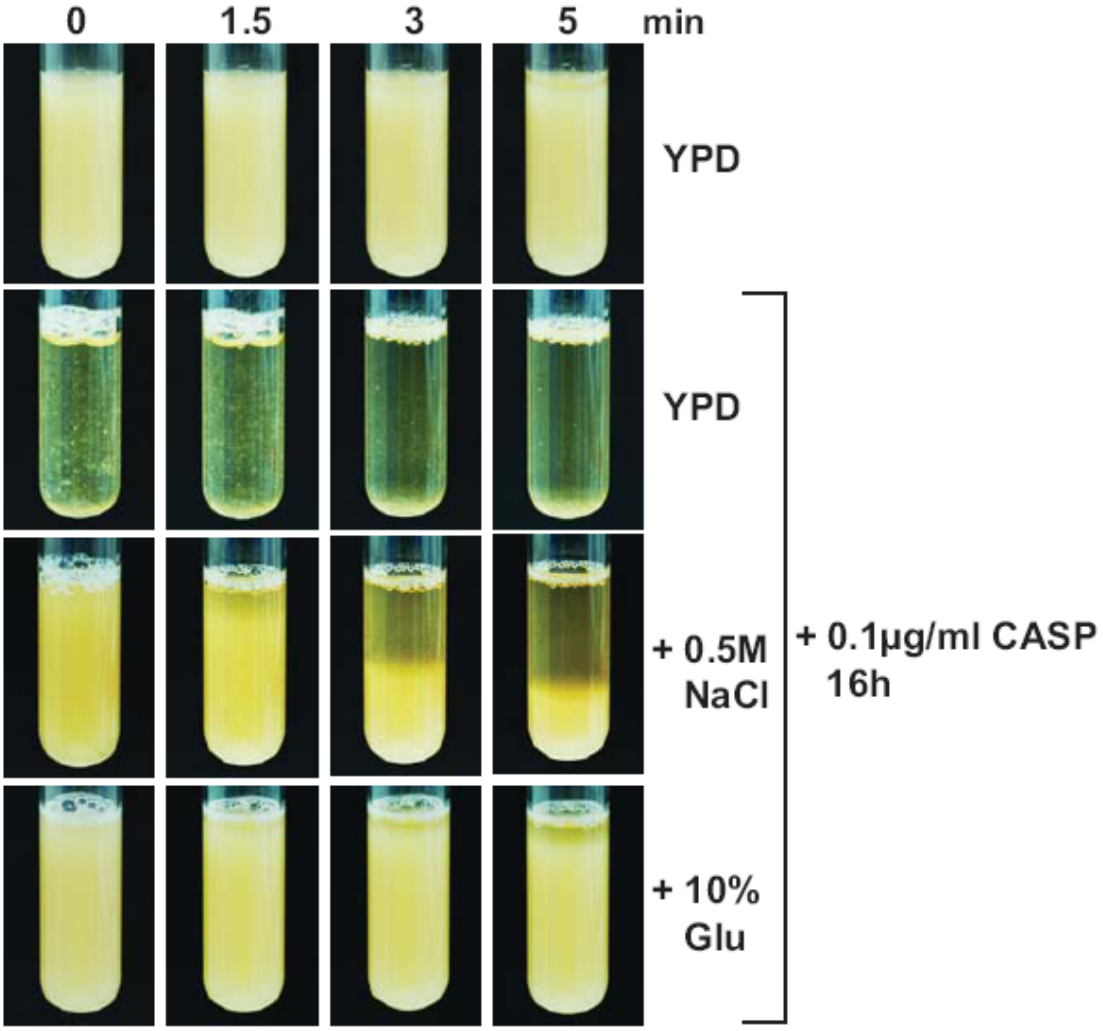

Figure 3

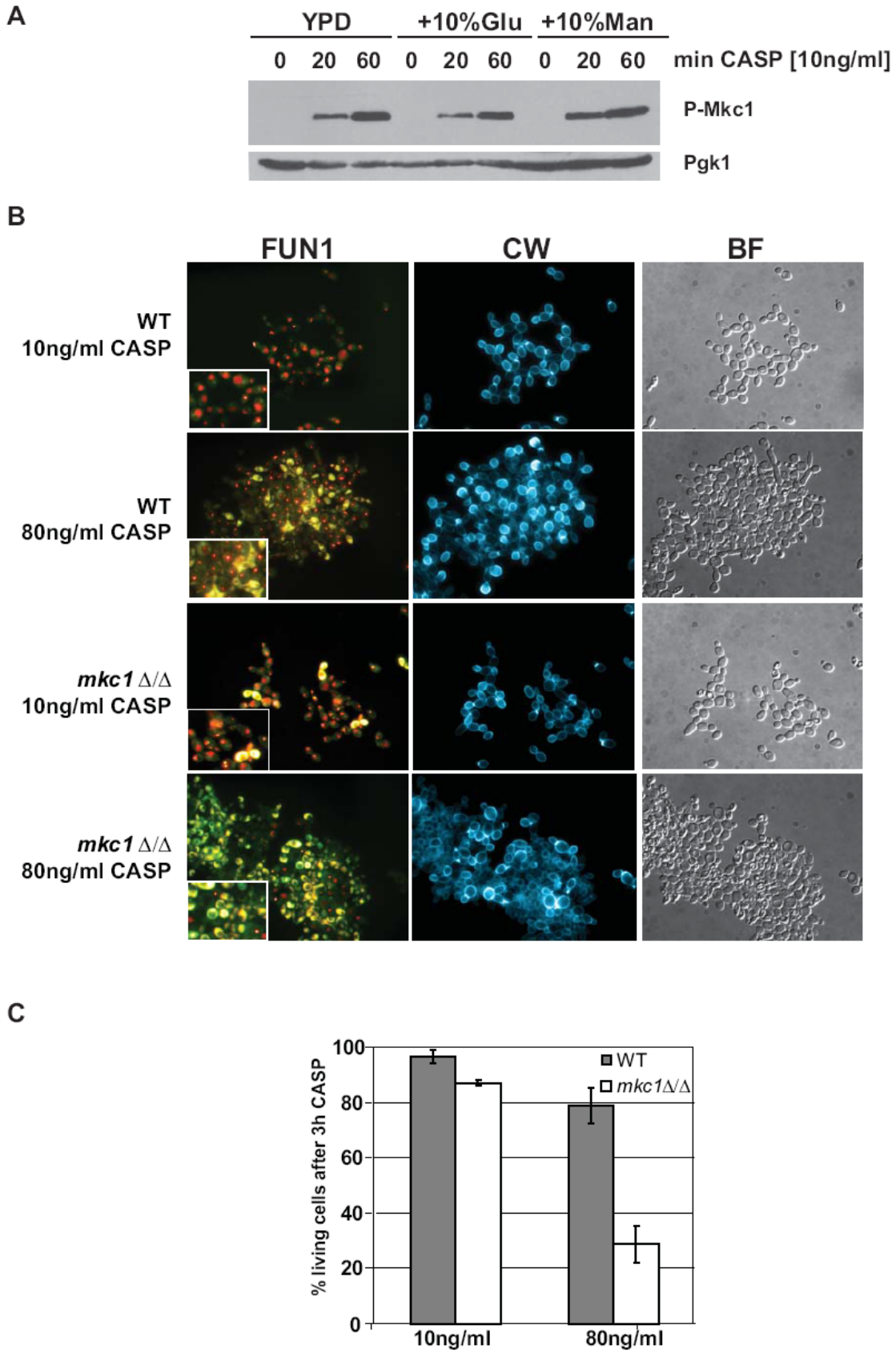
A
YPD
+10%Glu
+10%Man
0 20 60 0 20 60 0 20 60
min CASP [10ng/ml]
P-Mkc1
Pgk1
B
FUN1
CW
BF
WT
10ng/ml CASP
WT
80ng/ml CASP
mkc1 Δ/Δ
10ng/ml CASP
mkc1 Δ/Δ
80ng/ml CASP
C
% living cells after 3h CASP
100
80
60
40
20
0
WT
mkc1Δ/Δ
10ng/ml
80ng/ml

Figure 4

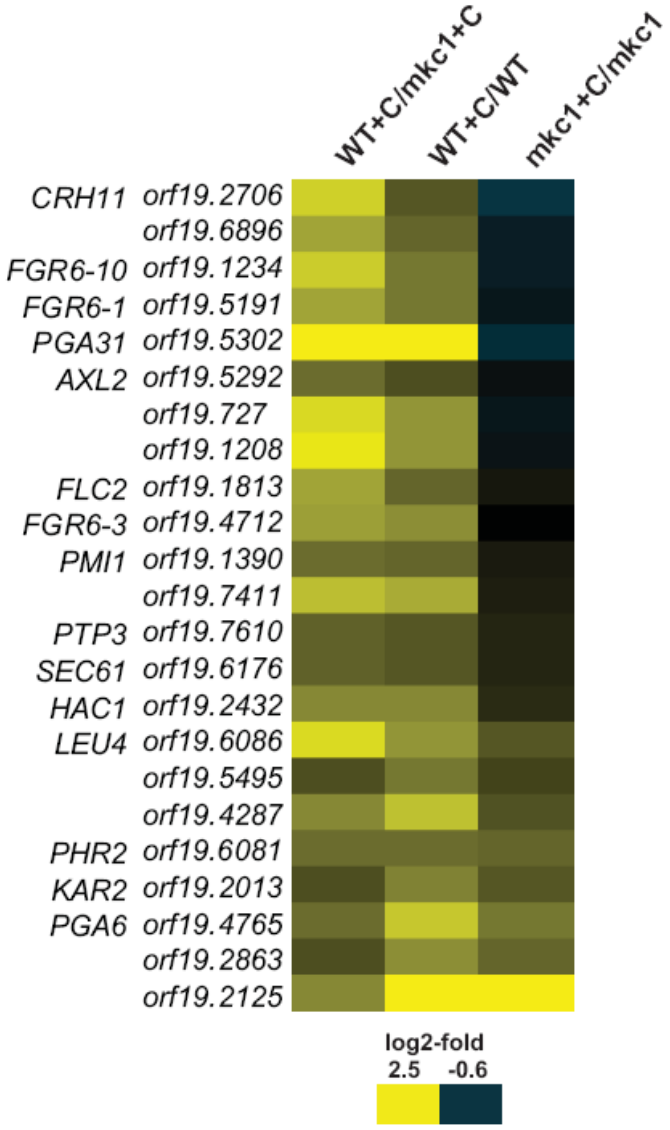
WT+C/mkc1+C
WT+C/WT
mkc1+C/mkc1
CRH11 orf19.2706
orf19.6896
FGR6-10 orf19.1234
FGR6-1 orf19.5191
PGA31 orf19.5302
AXL2 orf19.5292
orf19.727
orf19.1208
FLC2 orf19.1813
FGR6-3 orf19.4712
PMI1 orf19.1390
orf19.7411
PTP3 orf19.7610
SEC61 orf19.6176
HAC1 orf19.2432
LEU4 orf19.6086
orf19.5495
orf19.4287
PHR2 orf19.6081
KAR2 orf19.2013
PGA6 orf19.4765
orf19.2863
orf19.2125
log2-fold
2.5 -0.6

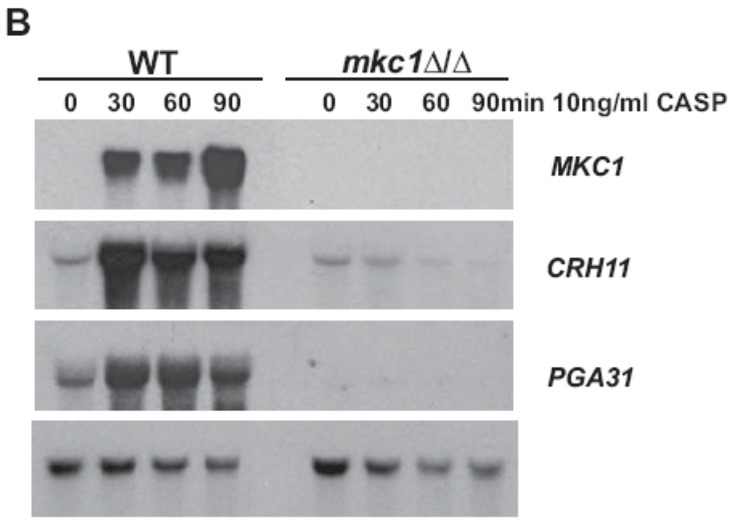
B
WT
mkc1Δ/Δ
0 30 60 90 0 30 60 90min 10ng/ml CASP
MKC1
CRH11
PGA31

Figure 5

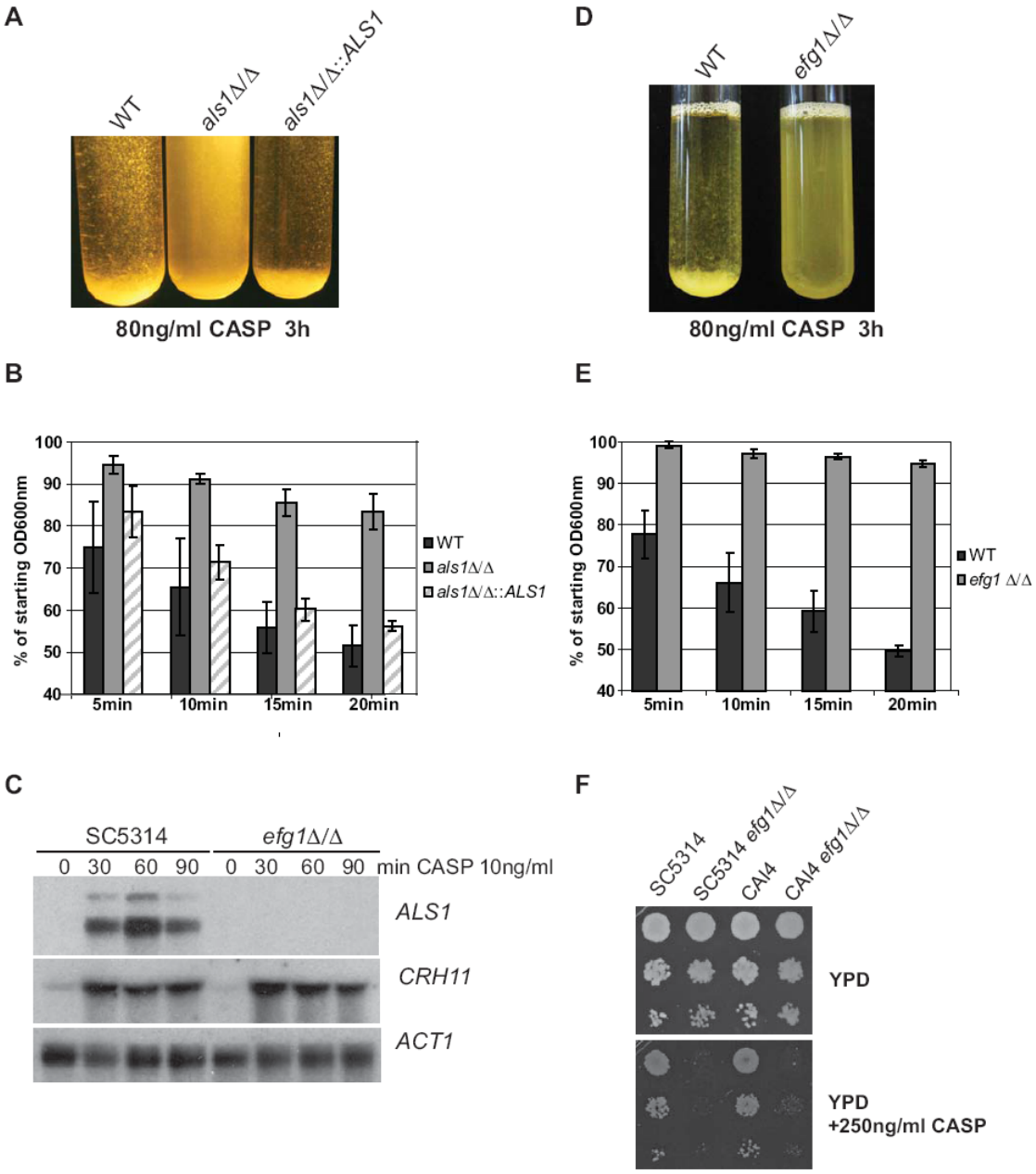
A
WT
als1Δ/Δ
als1Δ/Δ::ALS1
80ng/ml CASP 3h
D
WT
efg1Δ/Δ
80ng/ml CASP 3h
B
% of starting OD600nm
100
90
80
70
60
50
40
5min
10min
15min
20min
WT
als1Δ/Δ
als1Δ/Δ::ALS1
E
% of starting OD600nm
100
90
80
70
60
50
40
5min
10min
15min
20min
WT
efg1 Δ/Δ
C
SC5314
efg1Δ/Δ
0 30 60 90 0 30 60 90 min CASP 10ng/ml
ALS1
CRH11
ACT1
F
SC5314
SC5314 efg1Δ/Δ
CAI4
CAI4 efg1Δ/Δ
YPD
YPD
+250ng/ml CASP

Figure 6

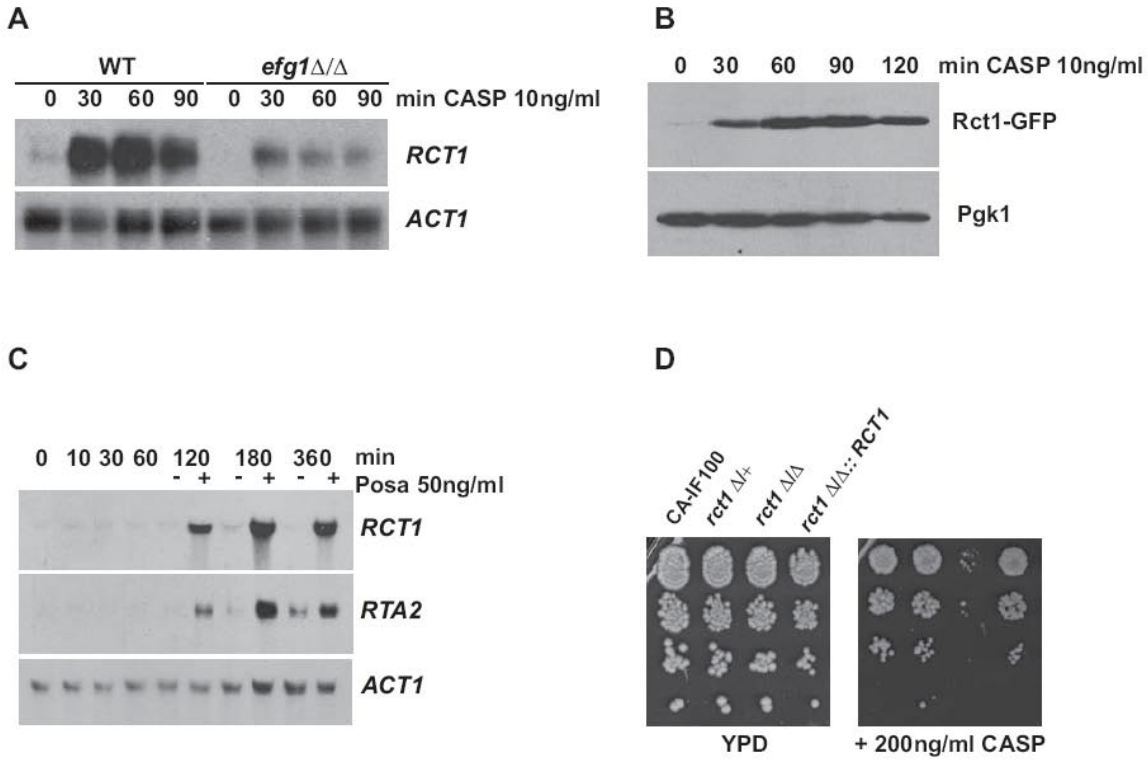
A
WT
efg1Δ/Δ
0 30 60 90 0 30 60 90 min CASP 10ng/ml
RCT1
ACT1
B
0 30 60 90 120 min CASP 10ng/ml
Rct1-GFP
Pgk1
C
0 10 30 60 120 180 360 min
- + - + - +
Posa 50ng/ml
RCT1
RTA2
ACT1
D
CA-IF100
rct1 Δ/+
rct1 Δ/Δ
rct1 Δ/Δ::RCT1
YPD
+ 200ng/ml CASP
E
GFP
DAPI
merge
BF
- CASP
+CASP 10ng/ml

Figure 7

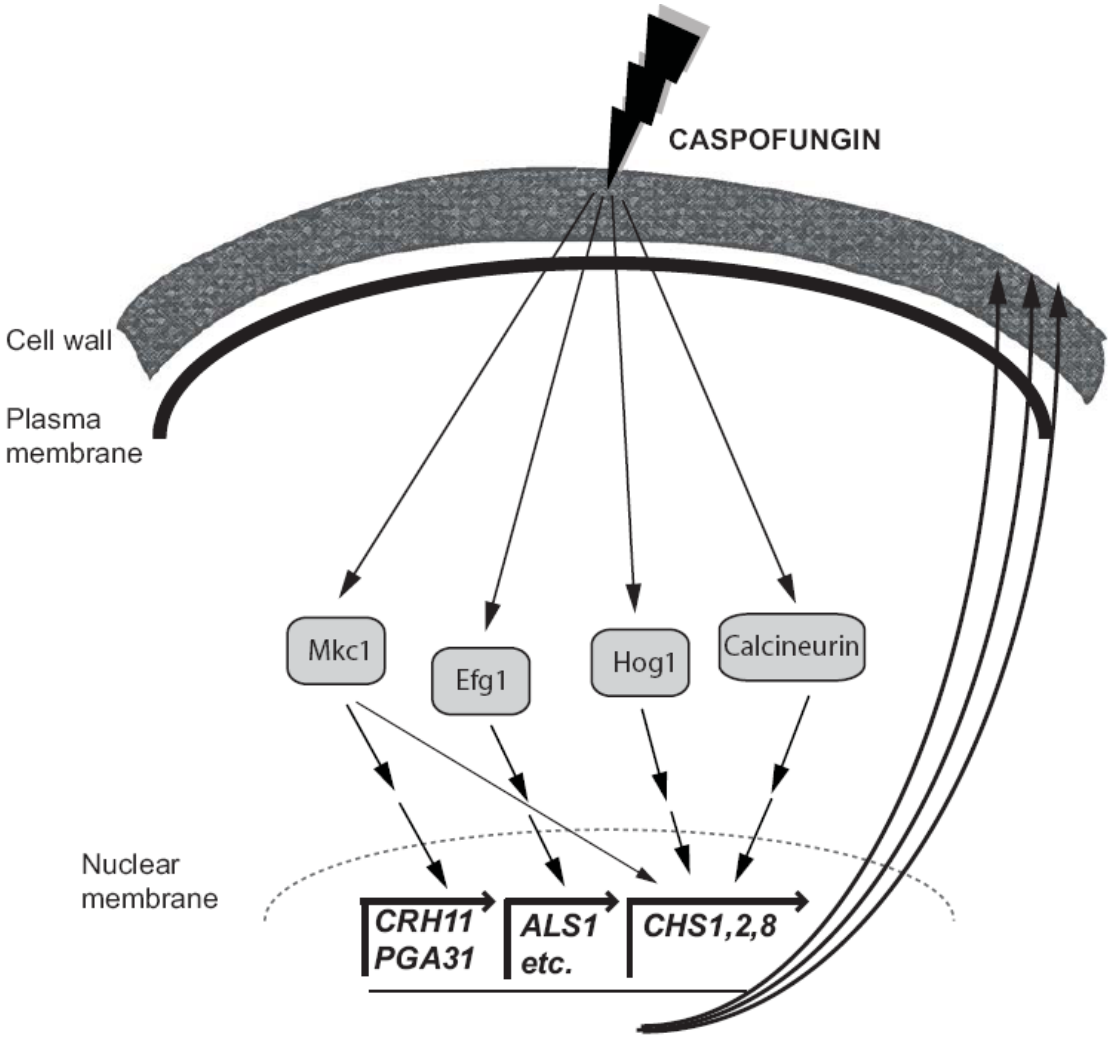
CASPOFUNGIN
Cell wall
Plasma membrane
Mkc1
Efg1
Hog1
Calcineurin
Nuclear membrane
CRH11 PGA31
ALS1 etc.
CHS1,2,8

The Set3/Hos2 Histone Deacetylase Complex Attenuates cAMP/PKA Signaling to Regulate Morphogenesis and Virulence of *Candida albicans*

Denes Hnisz[1], Olivia Majer[1], **Ingrid E Frohner**[1], Vukoslav Komnenovic[2], Karl Kuchler[†1]

[1]Medical University Vienna, Christian Doppler Laboratory for Infection Biology, Max F. Perutz Laboratories, A-1030 Vienna, Austria

[2]Institute of Molecular Biotechnology of the Austrian Academy of Sciences, A-1030 Vienna, Austria

Running title:
Set3/Hos2 Complex in *Candida albicans*

Keywords
Candida albicans, morphogenesis, cAMP signaling, filamentation, chromatin, SET3, HOS2

[†] To whom all correspondence should be addressed:
Karl Kuchler
Medical University Vienna, Max F. Perutz Laboratories
Department of Medical Biochemistry
Dr. Bohr-Gasse 9/2; A-1030 Vienna, Austria
Ph: +43-1-4277-61807; FAX: +43-1-4277-9618;
e-mail: karl.kuchler@meduniwien.ac.at

Accepted in PLoS Pathogens March 2010

ABSTRACT

Candida albicans like other pleiomorphic fungal pathogens is able to undergo a reversible transition between single yeast-like cells and multicellular filaments. This morphogenetic process has long been considered as a key fungal virulence factor. Here, we identify the evolutionarily conserved Set3/Hos2 histone deacetylase complex (Set3C) as a crucial repressor of the yeast-to-filament transition. Cells lacking core components of the Set3C are able to maintain all developmental phases, but are hypersusceptible to filamentation-inducing signals, because of a hyperactive cAMP/Protein Kinase A signaling pathway. Strikingly, Set3C-mediated control of filamentation is required for virulence *in vivo*, since *set3*Δ/Δ cells display strongly attenuated virulence in a mouse model of systemic infection. Importantly, the inhibition of histone deacetylase activity by trichostatin A exclusively phenocopies the absence of a functional Set3C, but not of any other histone deacetylase gene. Hence, our work supports a paradigm for manipulating morphogenesis in *C. albicans* through alternative antifungal therapeutic strategies.

AUTHOR SUMMARY

Candida albicans is the most prevalent human fungal pathogen causing disease in immunocompromised individuals. One key virulence factor, shared by many other microbial pathogens, is its ability to undergo morphogenetic transitions between unicellular and filamentous forms, which interact differentially with the host immune system. Morphogenesis in *C. albicans* is controlled by several signaling pathways, of which the Protein Kinase A (PKA) nutrient sensing pathway is of pivotal importance. Here, we identify a role for a conserved histone deacetylase complex (Set3C) as a key negative regulator of PKA signaling, controlling both morphogenesis and virulence. The genetic removal of the Set3C histone deacetylase complex causes cells to hyperfilament both *in vitro* and *in vivo*, and triggers the activation of PKA signaling. Moreover, cells lacking Set3 show strongly attenuated virulence in a mouse infection model. These results provide novel insights about the interplay of chromatin modification and signaling pathways, as exemplified by the control of morphogenesis of pleiomorphic fungi. Furthermore, our work establishes histone deacetylases as potential novel targets for antifungal drug discovery to improve therapeutic approaches combating life-threatening fungal infections.

INTRODUCTION

The human fungal pathogen *Candida albicans* is a harmless commensal of the mucosal surfaces and gastrointestinal tract of most healthy individuals. However, it can cause severe superficial and disseminated infections, particularly when the immune system of the human host is compromised [1]. A major virulence trait of *C. albicans* is the ability to switch between several distinct morphologies, including the unicellular yeast-like and the filamentous pseudohyphal and hyphal forms. Since several other fungal pathogens are also dimorphic or even pleiomorphic, including *Blastomyces dermatitidis* or *Coccidioides immiti*, morphogenesis has been considered a key component of fungal virulence and host invasion [2,3].

The switch from the yeast to filamentous forms in *C. albicans* is triggered by a broad range of environmental or host stimuli, including serum, an elevated growth temperature to 37^{o}C *in vitro*, and more specific inducers such as N-acetylglucosamine or estradiol [4,5]. The control of this morphological transition involves several signaling pathways and transcription factors [6,7]. The most prominent positive regulators are a mitogen-activated protein (MAP) kinase pathway and its downstream transcription factor Cph1 [8], as well as the cyclic adenosine monophosphate (cAMP)/protein kinase A (PKA) pathway and its downstream target transcription factor Efg1 [9,10]. In addition, filamentation is also under negative control by the transcriptional repressor Tup1 [11]. Tup1-mediated repression requires an interaction between Tup1 with sequence-specific DNA-binding factors such as Nrg1 and Rfg1 [12,13,14].

In addition to the yeast-filament transition, diploid *C. albicans* cells homozygous for the Mating Type Locus (*MTL*) can also reversibly switch between two distinct cell types termed white and opaque. White cells have a round, yeast-like shape and form dome-shaped colonies on solid agar, while opaque cells display an elongated morphology and form flattened colonies [15]. Furthermore, white cells are unable to mate, whereas opaque cells are mating-competent [16]. Switching between the two phases is believed to enable *C. albicans* to better adapt to various host niches. For example, white cells are more virulent in a murine systemic infection model, whereas opaque cells colonize the skin more efficiently than white cells [17,18].

White-opaque switching is reversible and regulated by several transcription factors. The *C. albicans* diploid genome harbors the Mating Type Locus (*MTL*) with two alleles known as **a** and α [19]. The master regulator of switching is *WOR1*, which in *MTL* heterozygous cells is stably repressed by a heterodimeric **a**/α repressor [16,20,21]. *MTL* homozygous white cells are devoid of detectable Wor1 expression. By contrast, opaque cells maintain high Wor1 levels for many generations due to multiple positive feed-back loops [22]. Interestingly, *EFG1* is a key negative regulator of *WOR1*, since *MTL* homozygous *efg1*Δ/Δ cells exist predominantly in the opaque phase [23,24].

Recently, we have shown that several histone-modifier enzymes, including the evolutionarily conserved Set3/Hos2 histone deacetylase complex (SetC) also modulate the white-opaque transition [25]. The related Set3 and Hos2 proteins in *Saccharomyces cerevisiae* are parts of a similar multiprotein complex (Set3C) that possesses histone deacetylase activity, with multiple functions, including meiosis-

specific repression of sporulation [26], promotion of Ty1 retrotransposons integration at tRNA genes [27], as well as signaling secretory stress through the PKC cell integrity pathway [28].

In this study, we discover a unique and novel composite phenotype caused by the deletions of key subunits of the Set3/Hos2 complex in *C. albicans*. On solid media, *set3*Δ/Δ and *hos2*Δ/Δ mutants display a hyperfilamenous phenotype at elevated temperatures, and specifically in the opaque phase. Surprisingly, in the filamentous forms of *set3*Δ/Δ and *hos2*Δ/Δ cells, Efg1-dependent target genes are induced as a result of an activated cAMP/PKA pathway. Our results establish the Set3C as a PKA-antagonist that fine-tunes the threshold of the yeast-filament conversion. We also show that *set3*Δ/Δ cells display strongly attenuated virulence in a murine model of systemic infection, which is associated with hyperfilamentation *in vivo*. Strikingly, we demonstrate that inhibition of histone deacetylation by trichostatin A exclusively phenocopies the lack of Set3C but not of any other histone deacetylase in *Candida albicans.* Hence, these data suggest a novel approach for developing antifungal drugs by manipulating the morphogenetic ability of *Candida albicans* through inhibition of chromatin modification.

RESULTS

MTL homozygous *set3*Δ/Δ mutants filament specifically in the opaque phase

The Set3 histone deacetylase complex (Set3C) of *Saccharomyces cerevisiae* comprises of four core (Set3, Hos2, Snt1, Sif2) and three peripheral subunits (Hos4, Hst1, Cpr1), of which Hos2 and Hst1 display catalytic activities. Disruption of any of the core subunit genes prevents complex assembly, whereas the disruption of peripheral subunit genes has no such effect [26]. Reciprocal BLAST searches of the *S. cerevisiae* and *C. albicans* proteomes revealed a strong conservation of the core proteins and suggested an analogous architecture of the putative CaSet3C (Table 1).

In a previous study, we reported that *SET3* and *HOS2* are key regulators of white-opaque switching in *MTL* homozygous *C. albicans* strains [25]. Surprisingly, *MTL***a**/**a** *set3*Δ/Δ opaque cells show an additional phenotype: they form wrinkled colonies on Lee's agar plates as opposed to the smooth colonies formed by wild type opaque cells and *SET3*/*set3*Δ heterozygotes (Figure 1A). Reintegration of one copy of *SET3* at the *RP10* locus rescued the phenotype, whereas the integration of a control vector at the *RP10* locus did not (Figure 1A).

Microscopic inspection revealed that wrinkled opaque colonies formed by *set3*Δ/Δ cells consisted of mostly filamentous structures with pseudohyphal characteristics [29]. Namely, the cells were elongated and longer than wild type opaque cells, and constrictions were visible at mother-daughter cell junctions (Figure 1B and S2B). In addition, *set3*Δ/Δ opaque cells expressed the filament-specific gene *ECE1* [30] at high levels, indicating an active filamentation program (Figure 1C).

Given the strong conservation of the yeast Set3C in *C. albicans*, we tested whether hyperfilamentation occurs upon deletion of other subunit-genes of the putative complex. Opaque cells lacking the core subunit Hos2 also gave rise to wrinkled colonies consisting of mostly pseudohyphae (Figure 1D). On the other hand, opaque cells lacking the peripheral subunit Hst1 formed smooth colonies,

whereas opaque *set3*Δ/Δ *hst1*Δ/Δ cells displayed wrinkled colonies, which reverted to smooth ones upon complementing the *SET3*-deletion (Figure 1D). Thus, in *C. albicans* the Set3C is likely to be of similar architecture as in *S. cerevisiae*. Importantly, the data indicate that loss of a functional Set3C triggers hyperfilamentation of opaque phase cells.

Loss of *SET3* promotes filamentation at an elevated temperature

SET3 has been previously identified in a large-scale haploinsufficiency screen as a modulator of filamentation in *MTL* heterozygous *C. albicans* cells [31]. Thus, we constructed several independent hetero- and homozygous *SET3* deletion strains in an *MTL***a**/α background, and compared the morphologies of wild type and deletion mutants on several standard liquid and solid laboratory media. Most notably, the *set3*Δ/Δ strain displayed hyperfilamentous growth on solid YPD at 37°C (Figure 2A). YPD at 30°C was used as standard medium supporting yeast phase growth, whereas YPD supplemented with 10% fetal calf serum (FCS) were standard conditions that promote filamentation (Figure 2A). *set3*Δ/Δ mutants showed a mild hyperfilamentation phenotype on filament-inducing Lee and Spider plates at 37°C. However, wild type and *set3*Δ/Δ did not show any apparent differences in liquid cultures of all conditions tested (Figure S1). In addition, *set3*Δ/Δ cells were more invasive on some solid media (Figure S1). Notably, a haploinsufficiency phenotype of *SET3*/*set3*Δ cells as reported earlier [31] was not observed in our experimental settings (Figure 1A and 2A), but we observed a mild haploinsufficiency effect at temperatures above 37°C (data not shown).

Microscopic inspection revealed that wrinkled *set3*Δ/Δ colonies on YPD plates at 37°C consisted of mainly filaments characterized by parallel cell walls and perpendicular septa, the hallmarks of true hyphae (Figure 2B and S2A) [29]. Furthermore, under these conditions, filament-specific *ECE1* mRNA levels in *set3*Δ/Δ colonies were upregulated, confirming an active filamentation program (Figure 2C).

Cells lacking the putative core subunits Hos2, Snt1 and Sif2 also gave rise to wrinkled colonies consisting of mostly true hyphae on YPD at 37°C (Figure 2D), and *hos2*Δ/Δ cells expressed *ECE1* at comparable levels as *set3*Δ/Δ cells (Figure 2C). By contrast, *hst1*Δ/Δ cells formed smooth colonies under these conditions. Moreover, the *set3*Δ/Δ *hst1*Δ/Δ double mutant formed wrinkled colonies, which was reverted upon restoring *SET3* (Figure 2D), confirming the notion of a conserved Set3C architecture in *C. albicans*.

As expected, the hyperfilamentation on YPD at 37°C was independent of *MTL*-zygosity. Indeed, *MTL***a**/**a** wild type and mutant white phase strains showed the same characteristics as the respective *MTL***a**/α isolates (Figure S2C), supporting the general view that the same genetic mechanisms regulate filamentation in both *MTL* heterozygous and *MTL* homozygous white phase cells.

If loss of Set3C function is the cause of the hyperfilamenting phenotype, biochemical inhibition of the catalytic activity should mimic the loss of the catalytic subunit. Therefore, we examined the morphological development of wild type *C. albicans* strains in the presence of the histone deacetylase inhibitor Trichostatin A (TSA) [32]. Surprisingly, we found that 10 μg/ml TSA supplementation of solid YPD medium strongly induced filamentation at 37°C (Figure 2E). We then examined single deletion *C. albicans* strains

lacking all putative histone deacetylase under identical growth conditions in the absence of TSA. Most strikingly, only the loss of the Set3 and Hos2 deacetylase genes induced the yeast-hyphae morphogenetic conversion (Figure 2E). These results demonstrate that inhibition of histone deacetylase activity by TSA is phenocopied by the loss of the Set3 and Hos2 core subunits of the *C. albicans* Set3C but not of any other histone deacetylase. Taken together, these data strongly suggest that lack of a functional Set3C causes a hyperfilamentation phenotype in *set3*Δ/Δ and *hos2*Δ/Δ mutants.

Several transcription factors involved in morphogenesis, including the positive regulator *EFG1*, as well as the negative regulators *NRG1* or *SSN6,* are themselves regulated at the transcriptional level upon serum-induced yeast-to-hypha transition [12,33,34]. Therefore, we tested whether repression of *SET3* or *HOS2* is associated with the morphological conversion of wild type cells. However, we found no significant differences between *SET3* and *HOS2* mRNA levels in yeast and hyphal cells (Figure S3). These results confirm that a mechanism other than transcriptional inactivation of *SET3* or *HOS2* must constitute a trigger driving yeast-to-hypha conversion.

Deletion of *EFG1* suppresses the hyperfilamentation of *set3*Δ/Δ and *hos2*Δ/Δ mutants

Does the Set3C represent an independent pathway regulating morphogenesis or is it a component of a previously characterized signaling pathway? To investigate the epistatic relationships between *SET3*, *HOS2* and the previously characterized positive regulators *CPH1* and *EFG1* [8,9], we analyzed the phenotypes of relevant double deletion mutants. The *cph1*Δ/Δ *set3*Δ/Δ and *cph1*Δ/Δ *hos2*Δ/Δ double mutants formed hyphae on YPD plates at 37^{o}C, as well as in response to serum. Thus, the combined loss of *CPH1* and *SET3* or *CPH1* and *HOS2* resembled the single deletion phenotypes of *set3*Δ/Δ and *hos2*Δ/Δ cells (Figure 3A and B). On the other hand, the *efg1*Δ/Δ *set3*Δ/Δ and *efg1*Δ/Δ *hos2*Δ/Δ double mutants failed to filament, even upon induction with serum; therefore, loss of *EFG1* was epistatic to the deletion of *SET3* or *HOS2* (Figure 3A and B).

In addition, we analyzed the genetic relationship between *SET3*, *HOS2* and *SET1*. *C. albicans SET1* is a histone methyltransferase gene [35], acting in the same pathway as *SET3* and *HOS2* regulating the frequency of white opaque switching [25]. Whereas in white-opaque switching regulation, *SET1* is epistatic to *SET3* and *HOS2* [25], we noticed a slight enhancement in filament formation in *set1*Δ/Δ *set3*Δ/Δ and *set1*Δ/Δ *hos2*Δ/Δ double mutants (Figure 3A). Furthermore, loss of *EFG1* was epistatic to the loss of *SET3* in opaque phase cells, as well (Figure 3C and 3D). Taken together, these results suggest that *SET3* and *HOS2* are acting in a different pathway than *CPH1* or *SET1.* Nevertheless, Set3C may interfere with Efg1-dependent signaling, resulting in hyperfilamentatation phenotypes of *set3*Δ/Δ and *hos2*Δ/Δ single mutants.

Loss of *SET3* or *HOS2* enhances the induction of *EFG1*-dependent target genes

The epistasis relations excluded the involvement of a Cph1-dependent mechanism contributing to the effect of *SET3* and *HOS2* deletions, but *EFG1* remained as a possibility. In addition, we also wanted to investigate whether the lack of *SET3* or *HOS2* interferes with the function of Tup1, a known transcriptional

repressor promoting yeast-phase growth in *C. albicans* [11]. Notably, Tup1 in *S. cerevisiae* was shown to directly interact with Hos2, and loss of Hos2 was shown to compromise Tup1-dependent gene repression [36].

Therefore, we chose several marker genes whose expression is regulated by Efg1, Tup1 or both of them, and analyzed their mRNA levels in *set3*Δ/Δ and *hos2*Δ/Δ mutants (Figure 4A) using qRT-PCR. *HWP1* is a filament-specific gene strongly induced by serum [37] or lack of *TUP1* [38]. In addition, serum induction of *HWP1* is strictly *EFG1*-dependent (Figure 4B) [37]. In the absence of *SET3* or *HOS2,* cells express high *HWP1* levels even on YPD at 37^{o}C, with about 15-fold differences between wild type and *set3*Δ/Δ or *hos2*Δ/Δ cells (P<0.01), indicating an active hyphal program. Moreover, elevated *HWP1*-expression is completely abolished once *EFG1* is also deleted in *set3*Δ/Δ or *hos2*Δ/Δ cells (Figure 4B). In addition, qualitatively identical results were obtained using additional hyphae-specific markers such as *ECE1* and *FRE2* (Figure S4).

RBT2 is a gene repressed by Tup1. However, *RBT2* expression does not change upon serum induction, excluding an Efg1-mediated control of *RBT2* (Figure 4C) [39]. In the absence of *SET3* or *HOS2,* cells express low levels of *RBT2* under all conditions tested, comparable to wild type cells, indicating that their absence does not interfere with Tup1-mediated repression of *RBT2*. Moreover, *DDR48* mRNA levels also show a qualitatively identical expression pattern in these mutants (Figure S4).

Finally, *SOD5* is expressed at low levels in yeast phase but is induced in an *EFG1*-dependent manner in serum-induced hyphae, and induction is maintained in *tup1*Δ/Δ cells (Figure 4D) [40]. Interestingly, we found that *set3*Δ/Δ and *hos2*Δ/Δ cells express *SOD5* at levels higher than wild type cells on YPD at 37^{o}C (about 3.5-fold relative to wild type, P<0.01) or in the presence of serum at 37^{o}C (about 3.3-fold relative to wild type, P<0.01) (Figure 4D). Most importantly, the elevated *SOD5* mRNA levels, both in *set3*Δ/Δ and *hos2*Δ/Δ cells, required *EFG1* (Figure 4D). Taken together, these results demonstrate that loss of *SET3* or *HOS2* strongly enhances the expression of *EFG1*-dependent genes. In other words, genes repressed by Efg1 in yeast phase cells are induced upon loss of *SET3* or *HOS2*, with *TUP1*-dependent targets remaining unaffected.

Hyperfilamentation of *set3*Δ/Δ cells is suppressed by adenine supplementation

In a previous study, we have shown that adenine is an environmental factor that modulates the frequency of the opaque to white transition *in vitro* requiring *SET3* [25]. We also made the striking observation that opaque isolates of the *MTL***a**/**a** *set3*Δ/Δ cells did not form pseudohyphae on adenine-supplemented Lee's medium at 25^{o}C (Figure 5A and B). The effect of adenine was both dose-dependent and specific; 100µg/ml adenine completely reverted cells to yeast phase growth, while the same concentration of uridine failed to do so (Figure 5A and B).

To analyze the effect of adenine supplementation at the gene expression level, we first confirmed the induction of the *EFG1*-dependent targets in opaque *MTL***a**/**a** *set3*Δ/Δ mutants. As expected, *HWP1* was strongly induced in *set3*Δ/Δ opaque but not in white cells (around 200-fold relative to wild type, P<0.01); nevertheless, *HWP1* expression was reduced back to wild type levels by deleting *EFG1* or upon addition of

adenine to the medium (Figure 5C). In addition, *ECE1* levels showed a qualitatively similar pattern (Figure S4). Furthermore, *SOD5* was also induced in *set3*Δ/Δ opaque cells (around 2.6-fold relative to wild type, P<0.01), and its induced expression was also reduced in *efg1*Δ/Δ *set3*Δ/Δ cells or *set3*Δ/Δ cells grown in the presence of adenine (Figure 5D). The expression level of the Tup1-target *RBT2* was again unaffected (Figure 5E).

Is the hyperfilamentation phenotype of white *set3*Δ/Δ cells on YPD at 37°C also reverted by adenine supplementation? Unfortunately, it is not possible to address this question directly, because the yeast extract present in YPD contains adenine [41]. Hence, as expected, additional 100µg/ml adenine supplementation on YPD had no effect on the phenotype of *set3*Δ/Δ cells at 37°C (Figure 5F). However, if the strains were cultured on SD medium, which has defined components and is devoid of adenine yet supports yeast-phase growth of wild type cells, we observed hyperfilamentation of *MTL***a**/α *set3*Δ/Δ cells at 37°C. This was reverted by adding 100 µg/ml adenine to SD or complementation of one allele of *SET3* (Figure 5G). Taken together, these results demonstrate that both the opaque and white filamentation phenotypes of *set3*Δ/Δ cells can be suppressed by exogenous adenine provided in the growth medium.

The *set3*Δ/Δ cells have a hyperactive cAMP/PKA pathway

Why are the Efg1-dependent target genes activated upon disruption of the Set3C? Efg1 receives input information from two signaling cascades. First, Efg1 is a downstream target of the cAMP/protein kinase A (PKA) signaling pathway. Briefly, this pathway transmits nutritional signals and involves the activation of the adenylyl-cyclase Cdc35 initiating cAMP synthesis, thereby activating PKA. *C. albicans* harbors two functional PKA catalytic subunits, Tpk1 and Tpk2 [42]. Second, Mkc1, the central MAP kinase of the protein kinase C (PKC) cell integrity pathway sensing cell wall damage, is also proposed to regulate Efg1-dependent morphogenesis [43]. Consequently, we tested the contribution of PKA and PKC signaling to the hyperfilamenting phenotypes of *set3*Δ/Δ (Figure 6A).

To assess activation of the PKC pathway, we performed Western blot analysis of the active, phosphorylated form of Mkc1. As expected, under filament-inducing conditions, both wild type and *set3*Δ/Δ cells harbored activated and thus phosphorylated Mkc1 (Figure 6B). Surprisingly, a high level of phosphorylated Mkc1 was also apparent in the *set3*Δ/Δ colonies after three days of incubation on YPD at 37°C, indicating a hyperactive PKC pathway (Figure 6B). However, we subsequently found that a lack of *SET3* was epistatic to the deletion of *MKC1*, since the *mkc1*Δ/Δ *set3*Δ/Δ double mutant displayed filamentous growth on solid YPD at 37°C similar to the *set3*Δ/Δ mutant (Figure 6C). These data demonstrate that although the PKC pathway appears active in *set3*Δ/Δ cells on YPD at 37°C, it is not the cause, but rather a consequence of the active filamentation program.

To address whether an active cAMP/PKA pathway is required for the hyperfilamenting phenotype of *set3*Δ/Δ cells, we performed epistasis experiments of *SET3* with *CDC35* encoding the adenylyl-cyclase, as well as *TPK1* and *TPK2* encoding the two PKA catalytic subunits. As shown on Figure 6C, lack of *CDC35* prevented both serum- and temperature-induced filamentation of wild type and *set3*Δ/Δ cells which was reverted upon supplementing the media with 10mM cAMP. These data demonstrates that

hyperfilamentation of *set3*Δ/Δ cells requires a functional cAMP/PKA pathway. On the other hand, deletion of *SET3* was epistatic to the deletion of either *TPK1* or *TPK2*, yet these results can be explained by the functional redundancy of the two PKA genes.

To link hyperfilamentation in the absence of Set3C with an increased activity of the cAMP/PKA pathway, we measured the trehalose content of wild type and mutant cultures. Trehalose is a disaccharide present in many yeast species; it is degraded by the neutral trehalase enzyme, which is activated by PKA [44,45]. As expected, we did not observe differences in the trehalose contents of wild type, *set3*Δ/Δ, *set3*Δ/Δ::*SET3* and *hos2*Δ/Δ cells after growth for two and three days on solid YPD at 30^{o}C supporting yeast phase growth (Figure S5A). Surprisingly, we failed to detect any differences between the four strains on solid YPD at 37^{o}C, where *set3*Δ/Δ and *hos2*Δ/Δ cells readily filament (Figure 6D, S5A). However, *set3*Δ/Δ cells contained around 3-fold less ($P<0.05$) trehalose than wild type or *set3*Δ/Δ::*SET3* heterozygous colonies when grown for three days on filament-inducing, FCS-supplemented plates (Figure 6D, S5A). Therefore, we concluded that differences in trehalose levels between yeast cells and filamentous forms may not be detectable because the colonies contain a mixture of both (Figure S2A). Consequently, we developed a filtration-based method to separate the yeast-phase and filamentous cells of colonies, to yeast and hyphal fractions. Strikingly, we found about 4-fold more trehalose in the yeast fraction when compared to the hyphae fraction ($P<0.05$, Figure 6D) derived from the same colonies of wild type, *set3*Δ/Δ and *set3*Δ/Δ::*SET3* cells when grown on filament-inducing FCS medium at 37^{o}C. Hence, a decreased trehalose content may reflect a history of PKA-activation, once the yeast-filament conversion has been initiated. In good agreement with this suggestion, a similar decrease in trehalose content was also detectable between the yeast and hyphal fractions of *set3*Δ/Δ cells grown on YPD medium at 37^{o}C ($P<0.05$, Figure 6D).

To directly assess whether at some stage of differentiation an elevated PKA activity can be detected in the hyperfilamentous *set3*Δ/Δ cells, we performed PKA activity assays using total cell extracts derived from wild type, *set3*Δ/Δ and *set3*Δ/Δ::*SET3* cells grown on YPD at 37^{o}C. In these experiments, a fluorescently labeled peptide is phosphorylated by PKA, followed by electrophoretic separation of phosphorylated and non-phosphorylated peptides and quantification by spectrophotometry (see Figure S5B and details in Materials and Methods). Surprisingly, we detected about 2-fold higher PKA activity of the yeast fraction of *set3*Δ/Δ cells when compared to the wild type ($P<0.05$, Figure 6E), indicating that this fraction contains a subset of cells harboring an elevated level of active PKA, although this difference is undetectable when comparing whole colonies (Figure 6E). Taken together, these results demonstrate that the hyperfilamentous phenotype of *set3*Δ/Δ cells requires functional cAMP/PKA signaling; differentiated hyphae are associated with a decrease in trehalose, while a subset of *set3*Δ/Δ cells harbor an elevated level of active PKA when compared to wild type cells.

Finally, we tested if suppression of hyperfilamentation in *set3*Δ/Δ cells by exogenous adenine can be rescued by stimulating the cAMP/PKA pathway with exogenous cAMP. Surprisingly, *set3*Δ/Δ cells indeed displayed a hypersensitive morphogenetic potential in the presence of both exogenous adenine and cAMP

(Figure 6F), indicating that both adenine and the Set3C can modulate cAMP/PKA signaling, albeit through antagonistic mechanisms.

Non-fermentable carbon sources revert hyperfilamentation of *set3*Δ/Δ cells

In *S. cerevisiae*, a known substrate of the cAMP/PKA pathway is glucose. Cells cultured on fermentable carbon sources (that can be degraded through glycolysis) are associated with a higher activity of cAMP/PKA signaling, while cells grown on non-fermentable carbon sources are characterized with a lower activity of cAMP/PKA signaling and activation of gluconeogenesis [44] (Figure 6A). Consequently, we tested if limiting cAMP/PKA signaling by non-fermentable carbon sources reverts the hyperfilamentation of *set3*Δ/Δ cells. Indeed, the hyperfilamentation effect was only observed if cells were grown on saccharides whose enzymatic degradation yields glucose. By contrast, *set3*Δ/Δ cells reverted to wild type morphologies in the presence of the non-fermentable carbon sources such as glycerol (Figure 7). A similar suppression was observed when the cells were grown on raffinose as a carbon source (Figure 7). Since yeasts, including *Candida* species do not have a β-lactamase enzyme, they fail to degrade raffinose (consisting of a glucose, galactose and fructose molecule) to fermentable monosaccharides. These results demonstrate that metabolic conditions normally associated with low cAMP/PKA signaling are sufficient to revert the hyperfilamentation effect of the *SET3*-deletion.

***set3*Δ/Δ cells have a hypersensitive cAMP/PKA signaling pathway**

N-acetylglucosamine (GlcNAc) can activate the cAMP/PKA pathway, and thus is a potent inducer of the yeast-filament transition [5,46]. To test whether activation of the cAMP/PKA pathway in the hyperfilamentous *set3*Δ/Δ cells result from a pathway being hypersensitive to filament-inducing stimuli, we analyzed the morphological development of wild type and *set3*Δ/Δ cells on solid media containing a gradient of GlcNAc. At 30^{o}C, wild type cells required high amounts (5-10mM) of GlcNAc to trigger filamentous growth (Figure 8A). By contrast, *set3*Δ/Δ cells displayed massive filamentation already at much lower (0.5-1mM) concentrations, demonstrating that the cAMP/PKA pathway in this mutant is hypersensitive to inducing stimuli when compared to wild type cells (Figure 8A).

The *set3*Δ/Δ mutant shows attenuated virulence in a murine infection model

The above results demonstrate that the Set3C moderates cAMP/PKA signaling, thereby promoting yeast phase growth. To address whether Set3C-dependent restriction of filamentation is important for virulence of *C. albicans in vivo*, we tested the *set3*Δ/Δ mutant in a mouse model of systemic infection. Consequently, wild type, *set3*Δ/Δ and complemented *set3* strains were injected into the tail vein of 6-8 week old male BALB/c mice. As shown on Figure 9A, 9 out of 10 mice infected with the wild type strain and 10 out of 10 mice infected with the complemented *set3* strain died until day seven after injection. By contrast, mice injected with the *set3*Δ/Δ strain started succumbing to the infection only on day 11, and 6 out of 10 mice were still alive after three weeks ($P<0.001$, Log rank test). We reproduced the infection experiment once more with another group of 10 mice per *C. albicans* genotype essentially yielding

identical results (data not shown). The results unequivocally demonstrate a strongly attenuated virulence of *set3*Δ/Δ cells. To confirm that the virulence defect of *set3*Δ/Δ cells is not caused by a reduced growth rate, we measured the generation times of wild type, heterozygous and homozygous *set3* mutants *in vitro*, but found no significant differences between any of the strains (Figure 9B).

Next, we performed histopathology experiments to address whether the virulence defect of *set3*Δ/Δ mutants is associated with altered morphological development or unusual tissue invasion *in vivo.* In the kidneys of mice infected with wild type *C. albicans*, fungal cells were present as a mixture of both unicellular and filamentous forms on day one after infection. By contrast, *set3*Δ/Δ cells were displaying hyperfilamentous morphologies (Figure 9C). These data demonstrate that *set3*Δ/Δ mutants, despite hyperfilamenting *in vivo*, display attenuated virulence in a murine infection model. These data suggest that the virulence defect is not caused by slower growth but rather by the interference with the morphogenetic conversion.

DISCUSSION

The Set3C is a cAMP/PKA-antagonistic repressor of filamentation

Here, we identify the Set3C, an evolutionary conserved histone deacetylase complex, as a repressor of the cAMP/PKA pathway regulating the yeast-to-hypha conversion in *Candida albicans*. We provide several lines of evidence that the hyperfilamentation resulting from removing the Set3C is linked to interference with the cAMP/PKA signaling pathway. First, deletion of the pathway genes *CDC35* and *EFG1* is epistatic to the deletion of *SET3* or *HOS2*. Although, *SET3* appears epistatic to both PKA genes *TPK1* and *TPK2,* it can be explained by the functional redundancy of the Tpk1 and Tpk2 enzymes [47]. Second, we found that differentiated hyphae contain around 4-times less trehalose than yeast-phase cells. Thus, trehalose content is a possible readout to detect the history of PKA activation during the yeast-to-hypha conversion of *C. albicans*. Seemingly contradicting this suggestion, an elevated PKA activity level was detected in the yeast phase fraction of filamentous wrinkled *set3*Δ/Δ colonies; however, this discrepancy appears logical because of the shortcomings of the filtering procedure used for the separation of morphologies. Namely, in filamentous colonies the differentiated hyphae stick together, yet short filaments are still passing through the filter pores and are found in the yeast fraction (data not shown). We believe that during growth on solid surfaces, a subset of cells reaches a yet undefined age or metabolic state, and then commit to the yeast-to-hypha conversion through activation of the cAMP/PKA pathway. This subset of cells that are “poised” to initiate germ tube formation is enriched in the yeast fraction of the filamentous colonies, thus enabling detection of subtle differences in PKA activity. Third, growth on non-fermentable carbon sources, which is associated with low cAMP/PKA signaling, is sufficient to revert the hyperfilamentation effect of the *SET3*-deletion.

In this study, we analyzed two distinct filamentation phenotypes of *set3*Δ/Δ cells to elucidate the mechanism of action of the Set3C, and we propose the following model, which we refer to as the “threshold shift model” (Figure 8B). In wild type cells, the cAMP/PKA pathway and its target transcription

factor Efg1 regulate morphogenesis in response to several environmental stimuli [9,10]. Naturally, molecules triggering morphogenetic conversions do not show a homogenous concentration *in vivo*; therefore, the regulatory pathway must have a certain *sensitivity* to input signals, which in the case of the cAMP/PKA pathway, is determined by (at least) two factors: the concentration of key regulatory components inside the cell and a Set3C-dependent attenuation mechanism. For instance, *EFG1* is rapidly downregulated upon yeast-to-hyphae conversion by serum and elevated temperature [10]. Efg1 binds to its own promoter, and in the absence of Efg1, the endogenous *EFG1* promoter is activated [34]. This auto-inhibitory loop appears crucial for a stable commitment to hyphal growth, because ectopic overexpression of *EFG1* causes hyphal cells to revert to yeast growth by lateral budding [34]. At the same time, the results presented in this study suggest that in the absence of a functional Set3C, the cAMP/PKA pathway responds to milder stimuli to initiate conversion to the filamentous growth (Figure 8A and B).

In our belief, this simple "threshold shift" model is coherent with both phenotypes of the *set3*Δ/Δ mutant for the following reasons. First, white phase *set3*Δ/Δ cells grow predominantly as hyphae on YPD at 37^{o}C as opposed to the wild type cells growing as yeasts (Figure 2, S2A). In this system, YPD at 30^{o}C, YPD 37^{o}C and YPD+serum at 37^{o}C in this order represent three conditions on the horizontal axis of the model analogous to a stimulus-gradient (Figure 8B). Wild type cells, whose cAMP/PKA signaling has wild type *sensitivity,* perceive the YPD at 37^{o}C as being below the threshold required for hyphal conversion. By contrast, *set3*Δ/Δ mutants perceive YPD at 37^{o}C as an environment whose inductive effect is already above the threshold required to switch to hyphal growth. Second, opaque phase *set3*Δ/Δ mutants grow predominantly as pseudohyphae on Lee's medium at 25^{o}C as opposed to *set3*Δ/Δ white cells as well as wild type white or opaque cells (Figure 1). In this system, however, Lee's medium at 25^{o}C already represents an environmental scenario close to the threshold point, which is supported by the fact that Lee's medium at 37^{o}C drives hyphal growth [30,37,48]. Why do *set3*Δ/Δ cells filament only in the opaque but not in the white phase? Opaque cells express *EFG1* at lower levels than white cells [23], because in opaque cells *EFG1* is repressed directly by the master opaque regulator Wor1, and indirectly by the transcription factor Czf1 [22]. Therefore, filamentation of opaque *set3*Δ/Δ cells is most probably resulting from the increased cAMP/PKA pathway sensitivity due to the lack of Set3C, and the inhibition of the *EFG1* locus by Wor1 and Czf1 mimicking the effect of the *EFG1*-autoinhibitory loop (the latter being absent in the white phase). Notably, Lee's medium at 25^{o}C is not a strong enough signal to induce true hyphal growth. This is in complete agreement with a recently proposed hypothesis, according to which weak filament-inducing signals turn on a set of genes required for pseudohyphal growth, while a stronger signal of the same nature turns on a set of additional genes triggering hyphal growth [49].

At which level of the pathway does the Set3C act on the molecular level? Recently, it was shown that *C. albicans* Efg1 binds to the promoters of filament-specific genes in both yeast and hyphal cells, and recruits the NuA4 histone acetyltransferase complex and the Swi/Snf chromatin remodeling complex upon hyphal induction [50]. Given that the *S. cerevisiae* Set3C possesses histone deacetylase activity [26], and that all subunits of the complex show strong evolutionary conservation (Table 1), it seems reasonable to propose that Set3C interferes with Efg1-dependent gene expression in *C. albicans* by effecting the

chromatin status at Efg1 target loci. On the other hand, the PKA hyperactivity in *set3*Δ/Δ cells as judged from trehalose quantification and PKA activity assays (Figure 6D and 6E) apparently contradicts this notion, and implies that the Set3C acts either at the level or upstream of PKA (see Figure 6A). Nevertheless, a chromatin-based regulatory effect at Efg1 target loci would still be possible, if Efg1 coordinated a feed-back mechanism affecting the activity of PKA. We are developing molecular tools to address these possibilities directly. In this context, it is interesting to note that in a previous study, we found the histone methyltransferase *SET1* to be epistatic to *SET3* or *HOS2* to regulate white-opaque switching in *C. albicans* [25]. We interpreted these data in a way that the PHD domain of Set3 recognizes methylation marks generated by Set1 at its target loci. Indeed, such a recognition was subsequently demonstrated in *S. cerevisiae, in vivo* [51]. Consequently, since deletion of *SET1* and *SET3* showed a synergistic effect in repressing filamentation (Figure 3A), it is reasonable to hypothesize that at genetic loci where Set3C antagonizes filamentation, it does not depend on the methylation marks generated by Set1. Alternatively, it is also possible that the Set3C targets as yet unknown transcription factor(s), rather than histone proteins. This will have to be explored in more detail in future studies.

Adenine as a morphogenetic signal

Along with serum and nitrogen-limitation, filamentation of *C. albicans* can be triggered by numerous specific stimuli, including human hormones, N-acetylglucosamine and bacterial peptidoglycans [4,52]. We identify adenine as a potential signal that also has a modulatory effect on the yeast-filament conversion *in vitro*. Namely, exogenous adenine attenuated the hyperfilamentation phenotypes of *set3*Δ/Δ cells and suppressed the upregulation of filament-specific genes (Figure 5 and S4). Similar to the Set3C, adenine may also influence cAMP/PKA dependent signaling events in a negative way, since cAMP supplementation in the presence of adenine rescued the phenotype of *set3*Δ/Δ cells (Figure 6F). Since adenine in itself did not have an influence on the morphogenesis or marker gene expression in wild type cells (Figure 5), it appears likely that its importance as a metabolic factor is limited to specific conditions *in vivo*, which are partially mimicked by the disruption of the Set3C. In this context, it is interesting to note that limitation of nicotinic acid (like adenine, a NAD precursor) in a urinary tract infection model regulates cell adhesion through a chromatin-dependent mechanism in the fungal pathogen *Candida glabrata* [53].

In summary, although the specific nature of the adenine signal will have to be explored in further studies, it provides an additional argument that both white and opaque filamentation phenotypes of *set3*Δ/Δ mutants are caused by an interference with the same genetic mechanism. In addition, we have shown earlier that exogenous adenine also modulates opaque-to-white transition [25], which, together with the results provided here, indicate the need to study the role of purine-metabolism in the regulation of *C. albicans* morphogenesis.

Morphogenesis as a virulence factor

Most human fungal pathogens including *Candida albicans, Cryptococcus neoformans, Blastomyces dermatitidis* or *Histoplasma capsulatum* are dimorphic. Therefore, morphogenesis has been extensively

studied as a potential virulence trait [2]. For example, locking *Candida albicans* cells in the yeast form by the combined deletion of *CPH1* and *EFG1* abolishes virulence [9]. Likewise, locking cells in a filamentous form by deleting *TUP1* had a similar effect [11]. These data led to the general view that virulence is determined by the ability to change morphologies rather than the individual growth forms *per se*. Although this view is widely accepted, supporting evidence remains indirect, because the mutants tested so far are either locked in a specific growth form or display pleiotropic alterations of other cellular functions unrelated to morphogenesis. For instance, deletion of the transcriptional repressor *NRG1* locks cells in a filamentous state and *nrg1*Δ/Δ cells are avirulent [14]. Deletion of the hypha-specific cyclin *HGC1* locks cells in the yeast form and the *hgc1*Δ/Δ mutant is also avirulent [54]. Deletion of the transcriptional repressor *SSN6* permits yeast and pseudohyphal growth, but not true hyphal growth. Lack of *SSN6* affects generation time, and *ssn6*Δ/Δ cells are avirulent [33]. The most direct evidence addressing the contribution of a specific growth form to virulence came from two recent studies on the transcription factors *UME6* and *NRG1.* The ectopic overexpression of *UME6* converted cells to the hyphal growth mode *in vivo* rendering cells hypervirulent [49]. Conversely, ectopic overexpression of *NRG1* inhibited hyphal growth *in vivo* causing attenuated virulence [55]. These studies demonstrated the pivotal role of the hyphal morphology during infection.

In this study we describe a novel phenotype caused by the ablation of key components of the Set3C. The *C. albicans set3*Δ/Δ mutant is able to maintain both normal yeast and filamentous growth modes but is hyperfilamenting both *in vitro* and *in vivo*. Strikingly, the s*et3*Δ/Δ mutant shows attenuated virulence in a murine systemic infection model. However, we cannot rule out that loss of *SET3* alters expression of other yet unknown virulence genes whose functions are unrelated to morphogenesis. We are currently performing whole genome microarray analyses to address this possibility. Nevertheless, the virulence defect of s*et3*Δ/Δ cells *in vivo* as yet appears to highlight the importance of maintaining the yeast phase growth during certain stages of dissemination in the host. Since mice infected with s*et3*Δ/Δ cells recover from the infection more efficiently than mice infected with wild type cells, it appears that the adequate timing for filamentation in a given niche is crucial for full virulence. The ability to maintain the unicellular yeast morphology in host environments being important for virulence is not surprising, since several pleiomorphic pathogens are virulent mainly in the yeast form. For instance, both in the case of *Histoplasma capsulatum* and *Cryptococcus neoformans*, yeast phase cells are required for human infections [2,56].

Regardless of other possible defects caused by impaired Set3C function, targeting the complex with specific deacetylase inhibitors can have a unique therapeutic potential. In fact, impairing the morphogenetic ability has been postulated as a promising area for antifungal drug discovery [55]. Trichostatin A (TSA), a known histone deacetylase inhibitor was recently shown to alter drug sensitivity and to inhibit serum-induced morphogenesis of some *C. albicans* strains [57,58]. In addition, a novel fungal Hos2-inhibitor has entered clinical trials to prove therapeutic potential used in combination with the antifungal fluconazole [59]. Here, we show that TSA is a potent trigger of the yeast-to-hyphae conversion of *C. albicans*. Most importantly, out of all putative histone deacetylase genes, only the

deletion of Hos2, the second catalytic subunit of the Set3C can phenocopy TSA treatment, providing compelling evidence that inhibition of the Set3C by TSA is causing the morphogenetic defects. Currently, we are investigating a possible therapeutic potential of TSA and related compounds to modulate morphogenesis and virulence *in vivo*.

In conclusion, we establish the Set3C as a novel key regulator of morphogenesis in *C. albicans*. We propose that compromising the complex activity leads to a "threshold shift" in the susceptibility to morphogenetic signals, and a consequent virulence defect. Since the complex appears well conserved from yeast to mammals [60], it will be fascinating to investigate the roles of the Set3C in the morphogenesis and virulence of other fungal pathogens. Indeed, the homologues of *SET3* and *HOS2* have recently been indentified as factors enhancing virulence of the human fungal pathogen *Cryptococcus neoformans* [61]. Taken together, our results emphasize the role of morphogenesis as a virulence factor and highlight the role of chromatin in regulating the activity of signaling pathways to orchestrate developmental changes in a simple eukaryotic model system.

MATERIALS AND METHODS

Media and growth conditions

Rich medium (YPD) and complete synthetic medium (SD) was prepared as previously described [41]. Modified Lee's medium was prepared as described [48]. Unless indicated otherwise, *MTL* heterozygous and homozygous strains were routinely grown at 30^{o}C and 25^{o}C, respectively. GlcNAc, adenine and cAMP were purchased from Sigma.

Strain construction

The complete list of *C. albicans* strains, primers and plasmids used in this study are listed in Supplementary Tables 1, 2 and 3, respectively. All strains were derived from SN152 [62], a leucine, histidine, arginine auxotrophic derivative of the clinical isolate SC5314 [63]. *SET3, HOS2, MKC1, CDC35, TPK1, TPK2, SNT1* and *SIF2* were deleted in SN152 using the fusion PCR strategy with the *C.m.LEU2* and *C.d.HIS1* markers [62]. The *cph1*Δ/Δ strain (JKC19) has been previously described [8]. All *MTL***a**/**a** strains were constructed in the DHCA202 background, which is a *MTL***a**/**a** derivative of SN152 [25]. The deletion mutants *set3*Δ/Δ, *hos2*Δ/Δ, *set1*Δ/Δ, *hst1*Δ/Δ, *efg1*Δ/Δ *set3*Δ/Δ, *efg1*Δ/Δ *hos2*Δ/Δ, *set1*Δ/Δ *set3*Δ/Δ and *set1*Δ/Δ *hos2*Δ/Δ in the DHCA202 background were described earlier [25]. *SET3* was deleted in the JKC19 and the *MTL***a**/**a** *hst1*Δ/Δ strains to create the *cph1*Δ/Δ *set3*Δ/Δ and *hst1*Δ/Δ *set3*Δ/Δ mutants, respectively, using the pDH104 plasmid [25] linearized by PvuI restriction. *HOS2* was deleted in the JKC19 background to create the *cph1*Δ/Δ *hos2*Δ/Δ mutant using the pDH102 plasmid [25] linearized by digestion with PvuI. *SET3* was deleted in the *mkc1*Δ/Δ background using the fusion PCR strategy with the *C.d.ARG4* marker and the linearized pDH104 plasmid to create the *mkc1*Δ/Δ *set3*Δ/Δ strain. *CDC35, TPK1* and *TPK2* were deleted in the *set3*Δ/Δ background using the fusion PCR strategy with the *C.d.ARG4* and *SAT1* markers to create the *cdc35*Δ/Δ *set3*Δ/Δ, *tpk1*Δ/Δ *set3*Δ/Δ and *tpk2*Δ/Δ *set3*Δ/Δ strains. Except for the

*cph1*Δ/Δ *set3*Δ/Δ, *cph1*Δ/Δ *hos2*Δ/Δ and *hst1*Δ/Δ *set3*Δ/Δ, *mkc1*Δ/Δ *set3*Δ/Δ *cdc35*Δ/Δ *set3*Δ/Δ and *tpk1*Δ/Δ *set3*Δ/Δ double mutants, at least two independent homozygous deletion strains were constructed from independent heterozygote isolates. Transformation was performed via electroporation as described [64]. Genomic integration events were verified with PCR and Southern blot analyses.

Gene complementation mutants were constructed using three approaches. In the *MTL***a**/α *set3*Δ/Δ strains and the *MTL***a**/**a** *hst1*Δ/Δ mutant, the *SET3* ORF was reintegrated into its endogenous locus using the pDH112 complementation plasmid [25] linearized by PvuI digestion. In the *MTL***a**/**a** *set3*Δ/Δ strains, the *SET3* ORF was integrated into one allele of the *RP10* locus. To target the *RP10* locus, 5´ and 3´ homology regions corresponding to about +/-1kb up- and downstream of the start and stop codon of the *RP10* ORF, respectively, were amplified from SC5314 genomic DNA. The upstream fragment was cloned using the HindIII and BamHI restriction sites; the downstream fragment was cloned using the SacI and SacII sites into the pAG36 [65] plasmid harboring a nourseothricin acetyltransferase (*NAT1*) resistance marker, to yield the plasmid pRP53. The *SET3* ORF with its endogenous promoter was cloned into pRP53 using ApaI and NheI restriction sites introduced into pRP53 on the 3´ primer of the upstream RP10 cloning fragment, to create the complementation vector p7221. The pRP53 empty vector and the p7221 integration constructs were linearized by AgeI-digestion prior to transformation. Gene complementation construct for the *HOS2* ORF was created using the *SAT1* marker cassette of the plasmid pSFS2A and the fusion PCR strategy exactly as described [25]. Transformation was performed via electroporation as described [64]. Correct genomic integration of the complementation plasmids was verified by PCR analysis.

Colony morphology analysis and microscopy

Colony morphology was analyzed using a Discovery V12 Stereoscope equipped with an Axiocam MR5 camera (Zeiss) Microscopic analysis was performed using an Olympus IX81 microscope equipped with a Hamamatsu Orca ER camera (Olympus). For fluorescence microscopy, cells were fixed in 70% ethanol for five minutes, washed three times with distilled water, stained with 10µM Calcofluor White and 1µg/ml DAPI (4',6-Diamidino-2-phenylindole dihydrochloride) for five minutes, washed three times with distilled water and deposited onto glass slides.

Generation time analysis

Strains were streaked from -80^{o}C frozen stocks on YPD agar plates and incubated three days at 30^{o}C. Single colonies were inoculated in liquid YPD and grown overnight, diluted to an OD_{600} of 1-2 and incubated three hours at 30^{o}C. Cultures were diluted into fresh YPD to an OD_{600} of 0.1-0.3; subsequently, OD_{600} values were measured every hour. The generation times were calculated by fitting an exponential function on the exponential parts of the growth curves using the Origin 6.1 software (MicroCal).

RNA isolation and quantitative qRT-PCR

Strains were streaked from -80°C frozen stocks onto YPD agar plates and incubated three days at 30°C. Opaque phase cultures, as well as the white isolates of the corresponding genotypes were streaked from -80°C frozen stocks on YPD agar plates containing 5µg/ml Phloxin B and incubated three days at 25°C. Single colonies were suspended in distilled water and spread at low densities onto media indicated at each experiment, and incubated using conditions described for each experiment. Colonies (1-3) were scraped off plates and suspended in 500µl TRI Reagent (Molecular Research Center). After addition of around 200µl glass beads (425-600µm, Sigma), cells were broken at 5m/s for 45 seconds on a FastPrep instrument (MP Biomedicals). Tubes were centrifuged and the supernatant (around 300µl) was transferred to a fresh tube, 500µl TRI Reagent and 160µl chloroform was added. After centrifugation at 14000g for 15 min at 4°C, the aqueous phase was extracted once with phenol:chloroform:isoamylalcohol. RNA was precipitated in 70% ethanol at -20°C overnight, washed once with 70% ethanol and dissolved in distilled water. About 5-10µg total RNA was treated with DNaseI (Fermentas). Subsequently, about 1-5µg of total RNA was reverse-transcribed with the First Strand cDNA synthesis kit (Fermentas). cDNA amplification was monitored quantitatively by SYBR Green incorporation in a Realplex Mastercycler (Eppendorf) using the MesaGreen Master mix (Eurogentec). Amplification curves were analyzed using the Realplex Software (Eppendorf). Statistics analysis (Student's t-test) was performed in Excel (Microsoft).

Western blot analysis

Colonies were scraped off plates and cells were washed three times with ice-cold distilled water. About 20 mg (±0.5 mg) wet weight of cells of each culture were measured and total cell extracts were prepared exactly as previously described [25]. For Western blot analysis, extracts from 0.5 mg wet cells were separated by SDS-PAGE. The phosphorylated forms of the Mkc1 and Cek1 MAP Kinases were detected with a phospho-p44/42 antibody (#9101, Cell Signaling). Loading controls were visualized using a monoclonal anti-tubulin antibody (DM1A, Sigma). Western blot experiments were repeated three times.

Trehalose determination

Colonies were scraped off plates and cells were washed three times with ice-cold distilled water. About 20 mg (±0.5 mg) wet weight of cells of each culture were frozen in liquid nitrogen. For the separation of yeast and hyphal phases, the colonies were filtered through a 70µm cell strainer (BD Falcon) prior to the washing steps. The pellets were resuspended in 0.5 ml of 0.25 M Na_2CO_3 per 20 mg of cells, boiled at 95°C for 20 min, and centrifuged at 14.000g for 5 min. A 10µl aliquot of the supernatant was neutralized by the addition of 6.5 µl 1M acetic acid. For each reaction, 5 µl of buffer T (300 mM NaAc, 30 mM $CaCl_2$, pH 5.5) and 3 µl of porcine kidney trehalase was added (3.7 U/ml, Sigma), and the volume was adjusted to 43 µl with distilled water. Reactions were incubated at 37°C for 45 min. The glucose liberated was measured in 25 µl of each reaction using the glucose assay kit from Sigma according to the manufacturer's instructions.

Protein Kinase A activity assay

Colonies were scraped off agar plates and about 100 mg (±50 mg) wet weight of cells of each culture was washed twice with ice-cold distilled water. For the separation of yeast and hyphal phases, the colonies were filtered through a 70μm cell strainer (BD Falcon) prior to the washing steps. Crude cell extracts were prepared as previously described [66]. Briefly, cell pellets were resuspended in 250 μl of 10mM sodium phosphate buffer (pH 6.8) containing 1mM EGTA, 1mM EDTA, 10 mM β-mercaptoethanol. Protease inhibitor tablets (Roche) were added prior to use. After resuspension, glass beads were added (425-600μm, Sigma), and cells were broken at 4m/s for 30 seconds on a FastPrep instrument (MP Biomedicals). Tubes were centrifuged twice at 14000 rpm at 4°C for 15 minutes and the supernatant was transferred to a fresh tube. Total protein concentrations were adjusted with the Bradford method, and extracts containing 10μg of total protein were immediately used for the enzymatic assay. Total PKA activity was measured following the guidelines of the PepTag cAMP-dependent protein kinase assay kit (Promega) in a total volume of 50 μl, containing 20mM Tris-HCl (pH 7.4), 10mM $MgCl_2$, 1mM ATP and 2μg of PepTag A1 Peptide. 10μM cAMP and 250μM H-89 (LC Laboratories) were added when indicated. Reactions were incubated at 30°C for 30 minutes, heat-inactivated at 95°C for 10min and separated on a 0.8% agarose gel in 50mM Tris (pH 8.0) buffer (Figure S5B). Quantification of the phosphorylated
PepTag peptide fractions excised from the gels was performed by spectrophotometry according to the manufacturer's instructions.

Virulence assays

Strains were streaked from -80°C frozen stocks on YPD agar plates and incubated two-three days at 30°C. Single colonies were inoculated in liquid YPD and grown until the mid-exponential growth phase (around OD_{600} 1). Cells were washed twice with PBS and the concentrations were adjusted with a hemocytometer. About $5*10^5$ cells were injected in 100-110 μl suspensions in PBS through the lateral tail vein into 6-8 week old male BALB/c mice. The mice all weighed between 17 and 20 grams and 10 mice per *C. albicans* genotype were used, except for the PBS control for which only three mice were injected. Survival was monitored over a three week period. Curves were plotted and statistical analysis (Log-rank test) was carried out using the Prism software (GraphPad). The virulence assay was repeated twice.

For histopathology, *C. albicans* cells were prepared and injected exactly as described for the survival experiments. Three 6-8 week old male BALB/c mice were injected per each *C. albicans* genotype, plus two mice were injected with PBS. Animals were sacrificed on Day 1 after the injection. Kidneys were fixed in 4% paraformaldehyde and embedded in paraffin. Serial sections (2μm) were stained with Grocott staining using the Bio-Optica Kit according to the manufacturer's instructions. All animal experiments were performed according to the guidelines of the Austrian Ministry of Science and Research and were approved by the animal ethics committee of the Medical University Vienna under the protocol number BMWF-68.205/0233-II/10b/2009.

ACKNOWLEDGEMENTS

We thank all laboratory members for critical and helpful discussions, Alexander Johnson for providing the strain SN152 and plasmids, Steffen Rupp for providing the strain JKC19. We are indebted to Patrick Van Dijck for helpful discussions and for providing the trehalose measurement protocol, Christa Gregori for sharing the *mkc1*Δ/Δ strain, and Christoph Schüller for critical reading of the manuscript. *C. albicans* sequence data were obtained from the Stanford Genome Center (http://www.candidagenome.org).

REFERENCES

1. Odds FC (1988) *Candida* and Candidosis: A Review and Bibliography. London: Baillière Tindall.
2. Rooney PJ, Klein BS (2002) Linking fungal morphogenesis with virulence. Cell Microbiol 4: 127-137.
3. Gow NA, Brown AJ, Odds FC (2002) Fungal morphogenesis and host invasion. Curr Opin Microbiol 5: 366-371.
4. Brown AJ, Gow NA (1999) Regulatory networks controlling *Candida albicans* morphogenesis. Trends Microbiol 7: 333-338.
5. Ernst JF (2000) Transcription factors in *Candida albicans* - environmental control of morphogenesis. Microbiology 146 (Pt 8): 1763-1774.
6. Whiteway M, Bachewich C (2007) Morphogenesis in *Candida albicans*. Annu Rev Microbiol 61: 529-553.
7. Liu H (2001) Transcriptional control of dimorphism in *Candida albicans*. Curr Opin Microbiol 4: 728-735.
8. Liu H, Kohler J, Fink GR (1994) Suppression of hyphal formation in *Candida albicans* by mutation of a STE12 homolog. Science 266: 1723-1726.
9. Lo HJ, Kohler JR, DiDomenico B, Loebenberg D, Cacciapuoti A, et al. (1997) Nonfilamentous *C. albicans* mutants are avirulent. Cell 90: 939-949.
10. Stoldt VR, Sonneborn A, Leuker CE, Ernst JF (1997) Efg1p, an essential regulator of morphogenesis of the human pathogen *Candida albicans*, is a member of a conserved class of bHLH proteins regulating morphogenetic processes in fungi. Embo J 16: 1982-1991.
11. Braun BR, Johnson AD (1997) Control of filament formation in *Candida albicans* by the transcriptional repressor TUP1. Science 277: 105-109.
12. Braun BR, Kadosh D, Johnson AD (2001) *NRG1*, a repressor of filamentous growth in *C.albicans*, is down-regulated during filament induction. EMBO J 20: 4753-4761.
13. Kadosh D, Johnson AD (2001) Rfg1, a protein related to the S*accharomyces cerevisiae* hypoxic regulator Rox1, controls filamentous growth and virulence in *Candida albicans*. Mol Cell Biol 21: 2496-2505.
14. Murad AM, Leng P, Straffon M, Wishart J, Macaskill S, et al. (2001) *NRG1* represses yeast-hypha morphogenesis and hypha-specific gene expression in *Candida albicans*. EMBO J 20: 4742-4752.
15. Slutsky B, Staebell M, Anderson J, Risen L, Pfaller M, et al. (1987) "White-opaque transition": a second high-frequency switching system in *Candida albicans*. J Bacteriol 169: 189-197.
16. Miller MG, Johnson AD (2002) White-opaque switching in *Candida albicans* is controlled by mating-type locus homeodomain proteins and allows efficient mating. Cell 110: 293-302.
17. Kvaal C, Lachke SA, Srikantha T, Daniels K, McCoy J, et al. (1999) Misexpression of the opaque-phase-specific gene *PEP1* (*SAP1*) in the white phase of *Candida albicans* confers increased virulence in a mouse model of cutaneous infection. Infect Immun 67: 6652-6662.
18. Kvaal CA, Srikantha T, Soll DR (1997) Misexpression of the white-phase-specific gene *WH11* in the opaque phase of *Candida albicans* affects switching and virulence. Infect Immun 65: 4468-4475.
19. Hull CM, Johnson AD (1999) Identification of a mating type-like locus in the asexual pathogenic yeast *Candida albicans*. Science 285: 1271-1275.
20. Huang G, Wang H, Chou S, Nie X, Chen J, et al. (2006) Bistable expression of *WOR1*, a master regulator of white-opaque switching in *Candida albicans*. Proc Natl Acad Sci U S A 103: 12813-12818.
21. Zordan RE, Galgoczy DJ, Johnson AD (2006) Epigenetic properties of white-opaque switching in *Candida albicans* are based on a self-sustaining transcriptional feedback loop. Proc Natl Acad Sci U S A 103: 12807-12812.

22. Zordan RE, Miller MG, Galgoczy DJ, Tuch BB, Johnson AD (2007) Interlocking transcriptional feedback loops control white-opaque switching in *Candida albicans*. PLoS Biol 5: e256.
23. Sonneborn A, Tebarth B, Ernst JF (1999) Control of white-opaque phenotypic switching in *Candida albicans* by the Efg1p morphogenetic regulator. Infect Immun 67: 4655-4660.
24. Srikantha T, Tsai LK, Daniels K, Soll DR (2000) *EFG1* null mutants of *Candida albicans* switch but cannot express the complete phenotype of white-phase budding cells. J Bacteriol 182: 1580-1591.
25. Hnisz D, Schwarzmuller T, Kuchler K (2009) Transcriptional loops meet chromatin: a dual-layer network controls white-opaque switching in *Candida albicans*. Mol Microbiol 74: 1-15.
26. Pijnappel WW, Schaft D, Roguev A, Shevchenko A, Tekotte H, et al. (2001) The *S. cerevisiae* SET3 complex includes two histone deacetylases, Hos2 and Hst1, and is a meiotic-specific repressor of the sporulation gene program. Genes Dev 15: 2991-3004.
27. Mou Z, Kenny AE, Curcio MJ (2006) Hos2 and Set3 promote integration of Ty1 retrotransposons at tRNA genes in *Saccharomyces cerevisiae*. Genetics 172: 2157-2167.
28. Cohen TJ, Mallory MJ, Strich R, Yao TP (2008) Hos2p/Set3p deacetylase complex signals secretory stress through the Mpk1p cell integrity pathway. Eukaryot Cell 7: 1191-1199.
29. Sudbery P, Gow N, Berman J (2004) The distinct morphogenic states of *Candida albicans.* Trends Microbiol 12: 317-324.
30. Birse CE, Irwin MY, Fonzi WA, Sypherd PS (1993) Cloning and characterization of *ECE1*, a gene expressed in association with cell elongation of the dimorphic pathogen Candida albicans. Infect Immun 61: 3648-3655.
31. Uhl MA, Biery M, Craig N, Johnson AD (2003) Haploinsufficiency-based large-scale forward genetic analysis of filamentous growth in the diploid human fungal pathogen *C.albicans*. EMBO J 22: 2668-2678.
32. Yoshida M, Kijima M, Akita M, Beppu T (1990) Potent and specific inhibition of mammalian histone deacetylase both *in vivo* and *in vitro* by trichostatin A. J Biol Chem 265: 17174-17179.
33. Hwang CS, Oh JH, Huh WK, Yim HS, Kang SO (2003) Ssn6, an important factor of morphological conversion and virulence in *Candida albicans*. Mol Microbiol 47: 1029-1043.
34. Tebarth B, Doedt T, Krishnamurthy S, Weide M, Monterola F, et al. (2003) Adaptation of the Efg1p morphogenetic pathway in *Candida albicans* by negative autoregulation and PKA-dependent repression of the *EFG1* gene. J Mol Biol 329: 949-962.
35. Raman SB, Nguyen MH, Zhang Z, Cheng S, Jia HY, et al. (2006) *Candida albicans SET1* encodes a histone 3 lysine 4 methyltransferase that contributes to the pathogenesis of invasive candidiasis. Mol Microbiol 60: 697-709.
36. Watson AD, Edmondson DG, Bone JR, Mukai Y, Yu Y, et al. (2000) Ssn6-Tup1 interacts with class I histone deacetylases required for repression. Genes Dev 14: 2737-2744.
37. Sharkey LL, McNemar MD, Saporito-Irwin SM, Sypherd PS, Fonzi WA (1999) HWP1 functions in the morphological development of *Candida albicans* downstream of *EFG1, TUP1*, and *RBF1*. J Bacteriol 181: 5273-5279.
38. Braun BR, Johnson AD (2000) *TUP1, CPH1* and *EFG1* make independent contributions to filamentation in *Candida albicans*. Genetics 155: 57-67.
39. Braun BR, Head WS, Wang MX, Johnson AD (2000) Identification and characterization of *TUP1*-regulated genes in *Candida albicans*. Genetics 156: 31-44.
40. Martchenko M, Alarco AM, Harcus D, Whiteway M (2004) Superoxide dismutases in *Candida albicans*: transcriptional regulation and functional characterization of the hyphal-induced *SOD5* gene. Mol Biol Cell 15: 456-467.
41. Kaiser C, Michaelis S, Mitchell A (1994) Methods in Yeast Genetics. A Laboratory Course Manual. New York: Cold Spring Harbor Laboratory Press.
42. Biswas S, Van Dijck P, Datta A (2007) Environmental sensing and signal transduction pathways regulating morphopathogenic determinants of *Candida albicans*. Microbiol Mol Biol Rev 71: 348-376.
43. Kumamoto CA (2005) A contact-activated kinase signals *Candida albicans* invasive growth and biofilm development. Proc Natl Acad Sci U S A 102: 5576-5581.
44. Thevelein JM, de Winde JH (1999) Novel sensing mechanisms and targets for the cAMP-protein kinase A pathway in the yeast *Saccharomyces cerevisiae*. Mol Microbiol 33: 904-918.
45. Uno I, Matsumoto K, Adachi K, Ishikawa T (1983) Genetic and biochemical evidence that trehalase is a substrate of cAMP-dependent protein kinase in yeast. J Biol Chem 258: 10867-10872.

46. Castilla R, Passeron S, Cantore ML (1998) N-acetyl-D-glucosamine induces germination in *Candida albicans* through a mechanism sensitive to inhibitors of cAMP-dependent protein kinase. Cell Signal 10: 713-719.
47. Bockmuhl DP, Krishnamurthy S, Gerads M, Sonneborn A, Ernst JF (2001) Distinct and redundant roles of the two protein kinase A isoforms Tpk1p and Tpk2p in morphogenesis and growth of *Candida albicans*. Mol Microbiol 42: 1243-1257.
48. Bedell GW, Soll DR (1979) Effects of low concentrations of zinc on the growth and dimorphism of *Candida albicans*: evidence for zinc-resistant and -sensitive pathways for mycelium formation. Infect Immun 26: 348-354.
49. Carlisle PL, Banerjee M, Lazzell A, Monteagudo C, Lopez-Ribot JL, et al. (2009) Expression levels of a filament-specific transcriptional regulator are sufficient to determine *Candida albicans* morphology and virulence. Proc Natl Acad Sci U S A 106: 599-604.
50. Lu Y, Su C, Mao X, Raniga PP, Liu H, et al. (2008) Efg1-mediated recruitment of NuA4 to promoters is required for hypha-specific Swi/Snf binding and activation in *Candida albicans*. Mol Biol Cell 19: 4260-4272.
51. Kim T, Buratowski S (2009) Dimethylation of H3K4 by Set1 recruits the Set3 histone deacetylase complex to 5' transcribed regions. Cell 137: 259-272.
52. Xu XL, Lee RT, Fang HM, Wang YM, Li R, et al. (2008) Bacterial peptidoglycan triggers *Candida albicans* hyphal growth by directly activating the adenylyl cyclase Cyr1p. Cell Host Microbe 4: 28-39.
53. Domergue R, Castano I, De Las Penas A, Zupancic M, Lockatell V, et al. (2005) Nicotinic acid limitation regulates silencing of *Candida adhesins* during UTI. Science 308: 866-870.
54. Zheng X, Wang Y (2004) Hgc1, a novel hypha-specific G1 cyclin-related protein regulates *Candida albicans* hyphal morphogenesis. EMBO J 23: 1845-1856.
55. Saville SP, Lazzell AL, Monteagudo C, Lopez-Ribot JL (2003) Engineered control of cell morphology in vivo reveals distinct roles for yeast and filamentous forms of *Candida albicans* during infection. Eukaryot Cell 2: 1053-1060.
56. Hull CM, Heitman J (2002) Genetics of *Cryptococcus neoformans.* Annu Rev Genet 36: 557-615.
57. Simonetti G, Passariello C, Rotili D, Mai A, Garaci E, et al. (2007) Histone deacetylase inhibitors may reduce pathogenicity and virulence in *Candida albicans*. FEMS Yeast Res 7: 1371-1380.
58. Smith WL, Edlind TD (2002) Histone deacetylase inhibitors enhance *Candida albicans* sensitivity to azoles and related antifungals: correlation with reduction in CDR and ERG upregulation. Antimicrob Agents Chemother 46: 3532-3539.
59. Turner B, Murch L (2009) Interscience Conference on Antimicrobial Agents and Chemotherapy--49th annual meeting. Part 1. 11-15 September 2009, San Francisco, CA, USA. IDrugs 12: 667-669.
60. Guenther MG, Lane WS, Fischle W, Verdin E, Lazar MA, et al. (2000) A core SMRT corepressor complex containing HDAC3 and TBL1, a WD40-repeat protein linked to deafness. Genes Dev 14: 1048-1057.
61. Liu OW, Chun CD, Chow ED, Chen C, Madhani HD, et al. (2008) Systematic genetic analysis of virulence in the human fungal pathogen *Cryptococcus neoformans*. Cell 135: 174-188.
62. Noble SM, Johnson AD (2005) Strains and strategies for large-scale gene deletion studies of the diploid human fungal pathogen *Candida albicans*. Eukaryot Cell 4: 298-309.
63. Gillum AM, Tsay EY, Kirsch DR (1984) Isolation of the *Candida albicans* gene for orotidine-5'-phosphate decarboxylase by complementation of *S. cerevisiae ura3* and *E. coli pyrF* mutations. Mol Gen Genet 198: 179-182.
64. Reuss O, Vik A, Kolter R, Morschhauser J (2004) The *SAT1* flipper, an optimized tool for gene disruption in *Candida albicans*. Gene 341: 119-127.
65. Goldstein AL, McCusker JH (1999) Three new dominant drug resistance cassettes for gene disruption in *Saccharomyces cerevisiae*. Yeast 15: 1541-1553.
66. Cassola A, Parrot M, Silberstein S, Magee BB, Passeron S, et al. (2004) *Candida albicans* lacking the gene encoding the regulatory subunit of protein kinase A displays a defect in hyphal formation and an altered localization of the catalytic subunit. Eukaryot Cell 3: 190-199.
67. Roman E, Nombela C, Pla J (2005) The Sho1 adaptor protein links oxidative stress to morphogenesis and cell wall biosynthesis in the fungal pathogen *Candida albicans.* Mol Cell Biol 25: 10611-10627.

FIGURE LEGENDS

Figure 1. *MTL* homozygous *set3*Δ/Δ cells filament specifically in the opaque phase

(A) Colony morphologies. *MTL***a**/**a** *set3*Δ/Δ cells grow as wrinkled colonies in the opaque but not in the white phase at 25°C on Lee's agar plates containing 5µg/ml Phloxin B, staining opaque cells pink. Images were taken after 5 days of incubation. Scale bar corresponds to 2mm.

(B) Opaque phase filaments of *MTL***a**/**a** *set3*Δ/Δ cells on Lee's medium display pseudohyphal characteristics. Cells are elongated and constrictions are visible where two daughter cells stay attached after cell division. Bold arrowheads indicate nuclei stained with DAPI. Cell wall is stained with Calcofluor White. Empty arrowheads indicate cell wall constrictions. Scale bar corresponds to 5µm.

(C) The *MTL***a**/**a** *set3*Δ/Δ mutant expresses the filament-specific *ECE1* transcript at high levels in the opaque phase. qRT-PCR analysis was performed with cDNA samples derived from colonies shown in Figure 1A. In addition, *ECE1* expression level in white phase *MTL***a**/**a** wild type cells grown on Lee's medium at 37°C for three days is added as a control. Transcript levels were normalized against the expression level of *RIP1*. qRT-PCR reactions were performed in triplicates and RNA isolated from two independent cultures were analyzed. Data are shown as mean + SD.

(D) Colony morphologies of additional mutants of the putative Set3/Hos2 complex. Opaque phase *MTL***a**/**a** cells deleted for the core subunit *HOS2* (see text) form wrinkled colonies on Lee's medium at 25°C, similar to *set3*Δ/Δ cells, whereas mutants lacking the peripheral subunit *HST1* form smooth colonies. In addition, *SET3* is epistatic to *HST1*. Images were taken after five days of incubation. Scale bar corresponds to 2mm.

Figure 2. Loss of *SET3* promotes filamentation in *C. albicans*

(A) Colony morphologies. *set3*Δ/Δ cells form wrinkled colonies on YPD at 37°C. Strains were grown for three days. FCS stands for YPD supplemented with 10% fetal calf serum. Scale bar corresponds to 2mm.

(B) The filaments of *set3*Δ/Δ cells on YPD at 37°C display true hyphal characteristics: parallel cell walls with perpendicular septa. Bold arrowheads indicate nuclei stained with DAPI. Cell wall is stained with Calcofluor White. Empty arrowheads indicate the septa. Scale bar corresponds to 5µm.

(C) *set3*Δ/Δ and *hos2*Δ/Δ mutants express the filament-specific *ECE1* transcript at high levels on YPD at 37°C. qRT-PCR analysis was performed with cDNA samples derived from the colonies shown in Figure 2A. Transcript levels were normalized against the expression level of *RIP1*. qRT-PCR reactions were performed in triplicates and RNA isolated from two independent cultures were analyzed. Data are shown as mean + SD.

(D) Colony morphologies of additional mutants of the Set3 Complex. Cells deleted for the core subunits *HOS2, SNT1* and *SIF2* form wrinkled colonies on YPD at 37°C, whereas the deletion cells lacking the peripheral subunit *HST1* form smooth colonies. In addition, *SET3* is epistatic to *HST1*. Images were taken after three days of incubation. Scale bar corresponds to 2mm.

(E) (left panel) Trichostatin A treatment enhances filamentation. The displayed strain is a *MTL***a**/**a** strain. (right panel) Trichostatin A treatment is phenocopied by genetic disruption of the Set3C, but none of the

other putative histone deacetylases. Images were taken after three days of incubation at 37°C. Scale bar corresponds to 2mm.

Figure 3. Lack of *EFG1* suppresses hyperfilamentation of *set3*Δ/Δ and *hos2*Δ/Δ mutants

(A) Colony morphologies of mutant strains with the indicated genotypes. Loss of *CPH1* or *EFG1* compromises the ability of cells to form filaments even under serum induction. *EFG1* deletion is epistatic to the deletion of *SET3* or *HOS2*, whereas *CPH1* deletion is hypostatic. Deletion of *SET1* in *set3*Δ/Δ and *hos2*Δ/Δ mutants has a mild synergistic effect. Strains were grown for three days on the media indicated. FCS stands for YPD supplemented with 10% fetal calf serum. Scale bar corresponds to 2mm.

(B) Microscopic analysis of the colonies shown on Figure 3A. On YPD at 37°C the wrinkled colonies of *cph1*Δ/Δ *set3*Δ/Δ cells consists of a mixture of yeast cells and hyphae, while *efg1*Δ/Δ *set3*Δ/Δ show the slightly elongated morphology of *efg1*Δ/Δ cells irrespective of the presence of serum. Scale bar corresponds to 5μm.

(C) Colony morphologies of mutant strains with the indicated genotypes. In opaque phase cells, *EFG1* deletion is epistatic to the loss of *SET3*. Strains were grown at 25°C on Lee's agar plates containing 5μg/ml Phloxin B. Images were taken after 5 days of incubation. Scale bar corresponds to 2mm.

(D) Microscopic analysis of the colonies shown in Figure 3C. Contrary to opaque *set3*Δ/Δ cells, no filamentous structures are present in the colonies formed by opaque *efg1*Δ/Δ or *efg1*Δ/Δ *set3*Δ/Δ cells. Scale bar corresponds to 5μm.

Figure 4. Loss of *SET3* or *HOS2* enhances induction of *EFG1*-dependent target genes

(A) Scheme of the experimental approach. Expression profiles of the genes in parentheses are shown on Figure S4. qRT-PCR analysis was performed with cDNA samples derived from the colonies shown in Figure 2A and 3A. Transcript levels were normalized against the expression level of *RIP1*. qRT-PCR reactions were performed in triplicates and RNA isolated from two independent cultures were analyzed. Data are shown as mean + SD.

(B) The expression of *HWP1* is strongly induced in *set3*Δ/Δ and *hos2*Δ/Δ cells even on YPD at 37°C. *HWP1* expression is abolished once *EFG1* is deleted both in wild type and *set3*Δ/Δ or *hos2*Δ/Δ cells. Double asterisk indicates statistical significance of $P<0.01$ relative to wild type cells cultured under identical conditions (Student's t-test).

(C) *RBT2* is repressed by Tup1, but not by Set3 or Hos2 under all conditions tested.

(D) The expression of *SOD5* is strongly induced in *set3*Δ/Δ and *hos2*Δ/Δ cells upon a mild (YPD, 37°C) or strong (FCS, 37°C) inductive stimulus. Elevated *SOD5* expression requires *EFG1*. Double asterisk indicates statistical significance of $P<0.01$ relative to wild type cells cultured under identical conditions (Student's t-test).

Figure 5. Adenine supplementation suppresses hyperfilamentation of *set3*Δ/Δ mutants

(A) Colony morphologies of opaque phase *MTL***a**/**a** strains. Opaque *set3*Δ/Δ cells form smooth colonies on Lee's medium supplemented with adenine. Images were taken after five days of incubation at 25^{o}C on Lee's agar plates containing 5µg/ml Phloxin B.

(B) Microscopy of the colonies shown in Figure 5A. The opaque *MTL***a**/**a** *set3*Δ/Δ cells do not filament in the presence of 100µg/ml adenine. Scale bar corresponds to 5µm.

In panels (C), (D) and (E), the logic for the expression analysis is described in Figure 4A. qRT-PCR analysis was performed with cDNA samples derived from the colonies shown in Figure 3C and Figure 5A. Transcript levels were normalized against the expression level of *RIP1*. qRT-PCR reactions were performed in triplicates and RNA isolated from two independent cultures were analyzed. Data are shown as mean + SD.

(C) *HWP1* expression is strongly induced in opaque phase *set3*Δ/Δ cells, but the induction is suppressed by deletion of *EFG1* or by supplementing the medium with 100µg/ml adenine. Double asterisk indicates statistical significance of P<0.01 relative to wild type cells of the same phase cultured under identical conditions (Student's t-test).

(D) Expression of *SOD5* is induced in *set3*Δ/Δ opaque cells, but the induction is suppressed by deletion of *EFG1* or by supplementing the medium with 100µg/ml adenine. Double asterisk indicates statistical significance of P<0.01 relative to wild cells of the same phase cultured under identical conditions (Student's t-test).

(E) *RBT2* is repressed by Tup1, but not by Set3 or Hos2.

(F) Colony morphologies on YPD medium without or with 100µg/ml adenine added. Scale bar corresponds to 2mm.

(G) Colony morphologies on SD medium without or with 100µg/ml adenine added. Scale bar corresponds to 2mm.

Figure 6. The *set3*Δ/Δ and *hos2*Δ/Δ cells have a hyperactive cAMP/PKA pathway

(A) Simplified scheme of signaling pathways converging at Efg1. Dashed lines indicate implied or indirect connections.

(B) Western blot analysis of phosphorylated MAP kinases. Deletion of *SET3* is associated with increased level of phosphorylated Mkc1, indicating active PKC signaling (compare lanes 8 and 11). The antibody also recognizes phosphorylated Cek1, the upstream MAP kinase of Cph1 [67].

(C) Colony morphologies of mutant strains with the indicated genotypes. *SET3* is epistatic to *MKC1, TPK1* and *TPK2* but hypostatic to *CDC35*. Images were taken after three days of incubation except for the *cdc35*Δ/Δ and *cdc35*Δ/Δ *set3*Δ/Δ strains, which were incubated for four days. FCS stands for YPD supplemented with 10% fetal calf serum. Scale bar corresponds to 2mm.

(D) Trehalose content of colonies grown on YPD at 37^{o}C (left panel). Although the total colonies have similar trehalose levels, the hyphal fraction of the *set3*Δ/Δ cells contains about 4-times less trehalose as the yeast fraction, indicating a history of elevated PKA activity. When grown on plates supplemented with FCS at 37^{o}C (right panel), *set3*Δ/Δ colonies contain about 3-times less trehalose than wild type or

*set3*Δ/Δ::*SET3* colonies. Moreover, all filamentous fractions contain about 4-times less trehalose than the corresponding yeast fractions, indicating a history of elevated PKA activity. "T": total, "Y": yeast, "H": hyphal fraction. Data are displayed as mean + SD of three independent experiments. Asterisk indicates statistical significance of P<0.05 (Student's t-test).

(E) Protein kinase A activities of cell extracts derived from the indicated colonies. Data are normalized against the activity level of wild type extracts, and are displayed as mean + SD of three independent experiments. "T": total, "Y": yeast, "H": hyphal fraction. Asterisk indicates statistical significance of P<0.05 (Student's t-test).

(F) Colony morphologies. Exogenous cAMP rescues the sensitized morphogenetic potential of *set3*Δ/Δ cells in the presence of adenine. Cultures were grown for 5 days at 37°C on SD medium. Scale bar corresponds to 2mm.

Figure 7. Hyperfilamentation of *set3*Δ/Δ is reverted by non-fermentable carbon sources

Colony morphologies on YP medium supplemented with 2% of the indicated carbon sources. *set3*Δ/Δ display wild type morphology on media containing non-fermentable carbon sources. Since *Candida spp.* do not have a β-lactamase, the cells fail to convert raffinose into fermentable monosaccharides. "F:" fermentable, "NF": non-fermentable. Cultures were grown for 3 days at 37°C. Scale bar corresponds to 2mm.

Figure 8. *set3*Δ/Δ cells are a hyperreactive to cAMP/PKA induction by GlcNAc

(A) Colony morphologies of wild type and *set3*Δ/Δ cells grown on YPD at 30°C for 3 days in the presence of the indicated amounts of N-acetylglucosamine (GlcNAc). Scale bar corresponds to 2mm.

(B) The "threshold shift" model for Set3C function in triggering morphogenesis. The cAMP/PKA signaling pathway transmits environmental information, thereby shaping the morphogenetic change. In wild type cells (left panel), the sensitivity of the pathway to adequate signals is antagonized by the SetC. If the Set3C is disrupted or impaired (right panel), the threshold for morphogenetic conversion is shifted, and the pathway responds to milder inducing stimuli by triggering filamentation. In addition, metabolites such as adenine also modulates the activity of the pathway through as yet undisclosed mechanisms.

Figure 9. The *set3*Δ/Δ mutant shows attenuated virulence in a murine infection model

(A) Kaplan-Meier survival curves of mice receiving tail vein injections of *MTL***a**/α wild type, *set3*Δ/Δ and *set3*Δ/Δ::*SET3 C. albicans* strains. Ten mice per *C. albicans* genotype were injected; survival was monitored over three weeks. Statistical significance was determined using the Log-rank test.

(B) *set3*Δ/Δ strains do not have a growth defect *in vitro*. Generation times of wild type and *set3*Δ/Δ cells were measured in YPD medium at 30°C as described in Materials and Methods.

(C) Histopathology of the cortical part of kidneys of mice infected with wild type or *set3*Δ/Δ *C. albicans* strains on day one after infection. The *set3*Δ/Δ displays hyperfilamentous growth. Tissues were stained with Grocott staining to visualize fungal cells. Counterstaining was performed with Hematoxilin.

Table 1. Components of the *S. cerevisiae* and *C. albicans* Set3 Complex components

S.c. Gene	*S.c.* Systematic name	required for structural integrity (S.c.)	*C.a.* ORF	Length (*C.a.*, aa)	Homology value (aa)
SET3	YKR029C	+	19.7221	1069	2.00E-47
HOS2	YGL194C	+	19.5377	454	< 1E-150
SNT1	YCR033W	+	19.5241	1001	6.00E-37
SIF2	YBR103W	+	19.132	593	1.00E-34
HOS4	YIL112W	-	19.4728	1380	4.00E-31
HST1	YOL068C	-	19.4761	657	5.00E-105
CPR1	YDR155C	-	19.6472	162	1.00E-73

In the absence of the subunits required for structural integrity, no complex can assemble in *S. cerevisiae* [26]. The BLAST E-values of the protein sequences indicate that every subunit is evolutionary conserved (E-value <10^{-30}) in *C. albicans*. "aa": amino acid

Figure 1

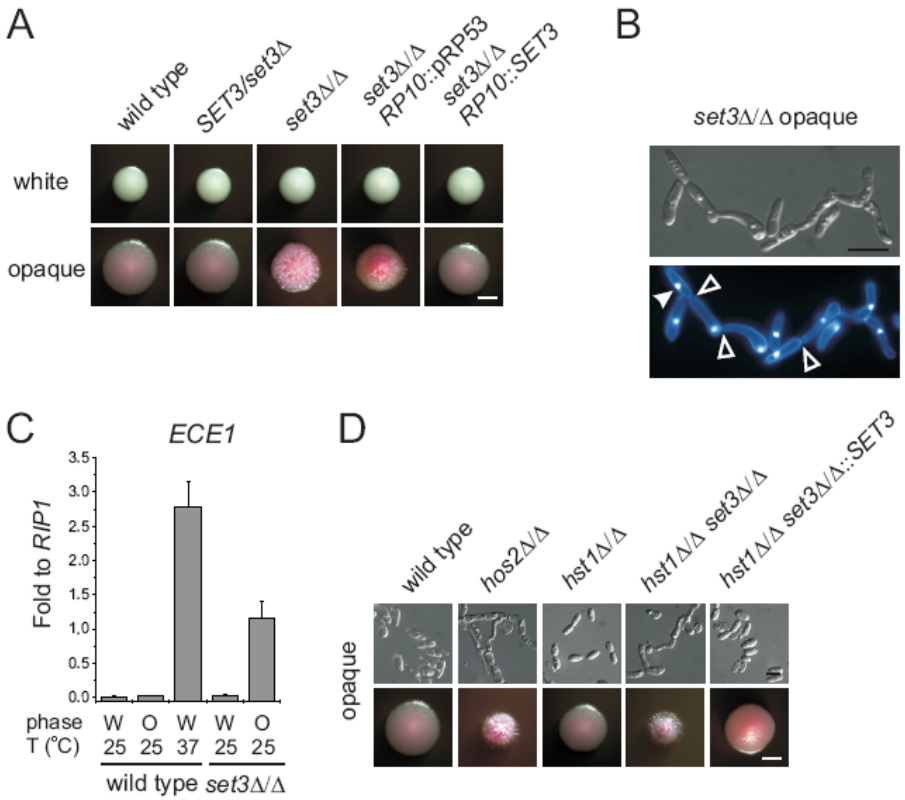

Figure 2

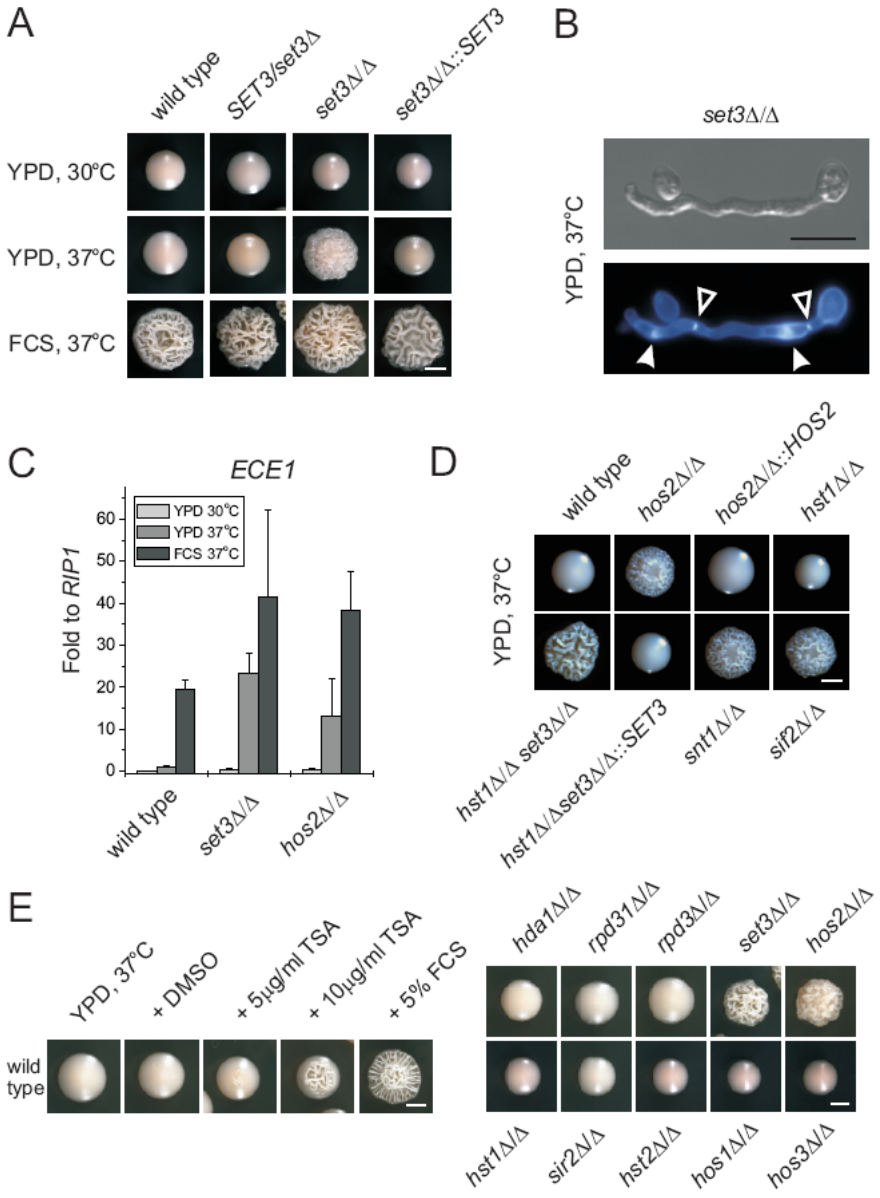
A
wild type
SET3/set3Δ
set3Δ/Δ
set3Δ/Δ::SET3
YPD, 30°C
YPD, 37°C
FCS, 37°C
B
set3Δ/Δ
YPD, 37°C
C
ECE1
YPD 30°C
YPD 37°C
FCS 37°C
Fold to RIP1
0
10
20
30
40
50
60
wild type
set3Δ/Δ
hos2Δ/Δ
D
wild type
hos2Δ/Δ
hos2Δ/Δ::HOS2
hst1Δ/Δ
YPD, 37°C
hst1Δ/Δ set3Δ/Δ
hst1Δ/Δset3Δ/Δ::SET3
snt1Δ/Δ
sif2Δ/Δ
E
YPD, 37°C
+ DMSO
+ 5µg/ml TSA
+ 10µg/ml TSA
+ 5% FCS
wild type
hda1Δ/Δ
rpd31Δ/Δ
rpd3Δ/Δ
set3Δ/Δ
hos2Δ/Δ
hst1Δ/Δ
sir2Δ/Δ
hst2Δ/Δ
hos1Δ/Δ
hos3Δ/Δ

Figure 3

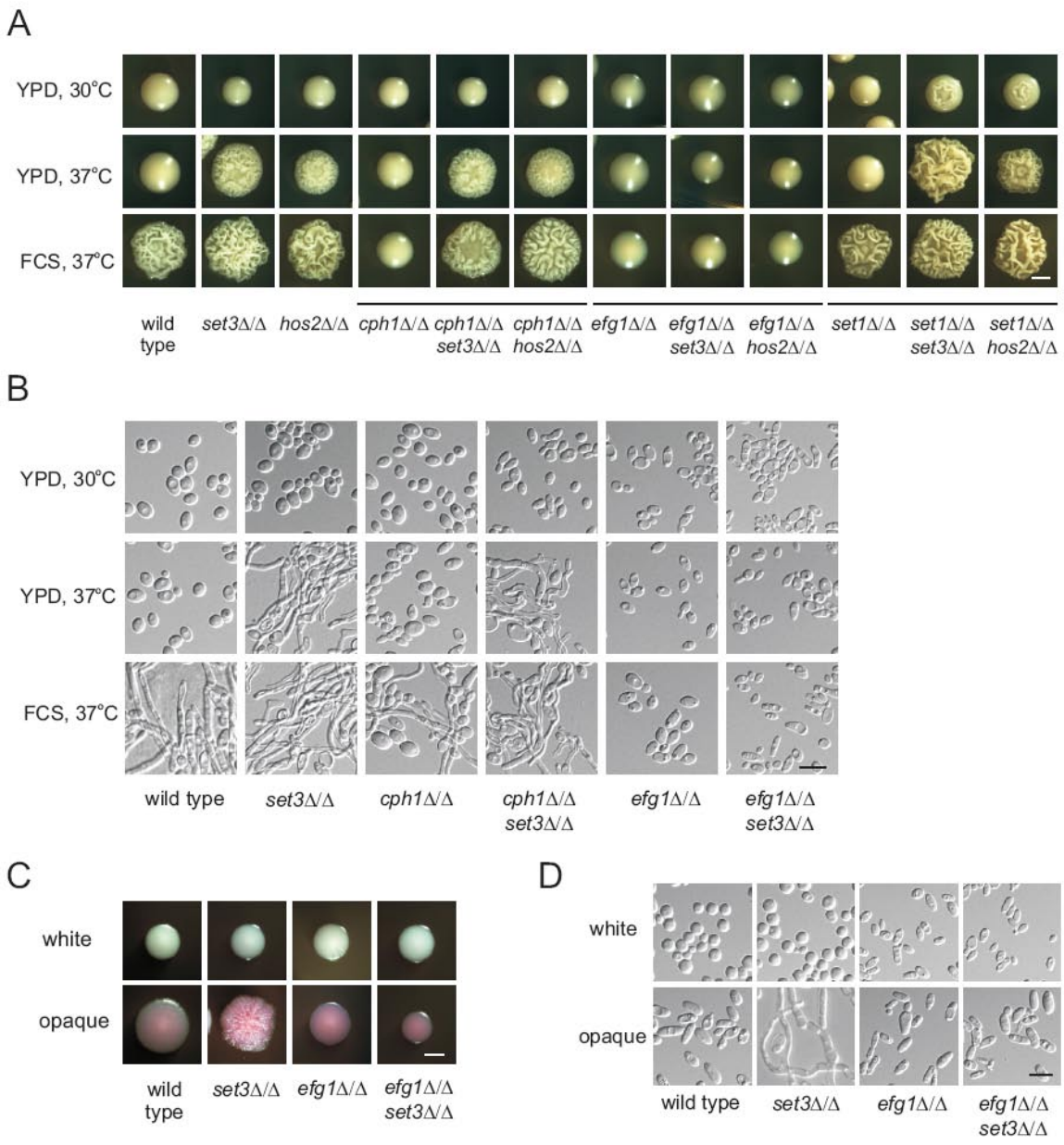
A
YPD, 30°C
YPD, 37°C
FCS, 37°C
wild type
set3Δ/Δ
hos2Δ/Δ
cph1Δ/Δ
cph1Δ/Δ set3Δ/Δ
cph1Δ/Δ hos2Δ/Δ
efg1Δ/Δ
efg1Δ/Δ set3Δ/Δ
efg1Δ/Δ hos2Δ/Δ
set1Δ/Δ
set1Δ/Δ set3Δ/Δ
set1Δ/Δ hos2Δ/Δ
B
YPD, 30°C
YPD, 37°C
FCS, 37°C
wild type
set3Δ/Δ
cph1Δ/Δ
cph1Δ/Δ set3Δ/Δ
efg1Δ/Δ
efg1Δ/Δ set3Δ/Δ
C
white
opaque
wild type
set3Δ/Δ
efg1Δ/Δ
efg1Δ/Δ set3Δ/Δ
D
white
opaque
wild type
set3Δ/Δ
efg1Δ/Δ
efg1Δ/Δ set3Δ/Δ

Figure 4

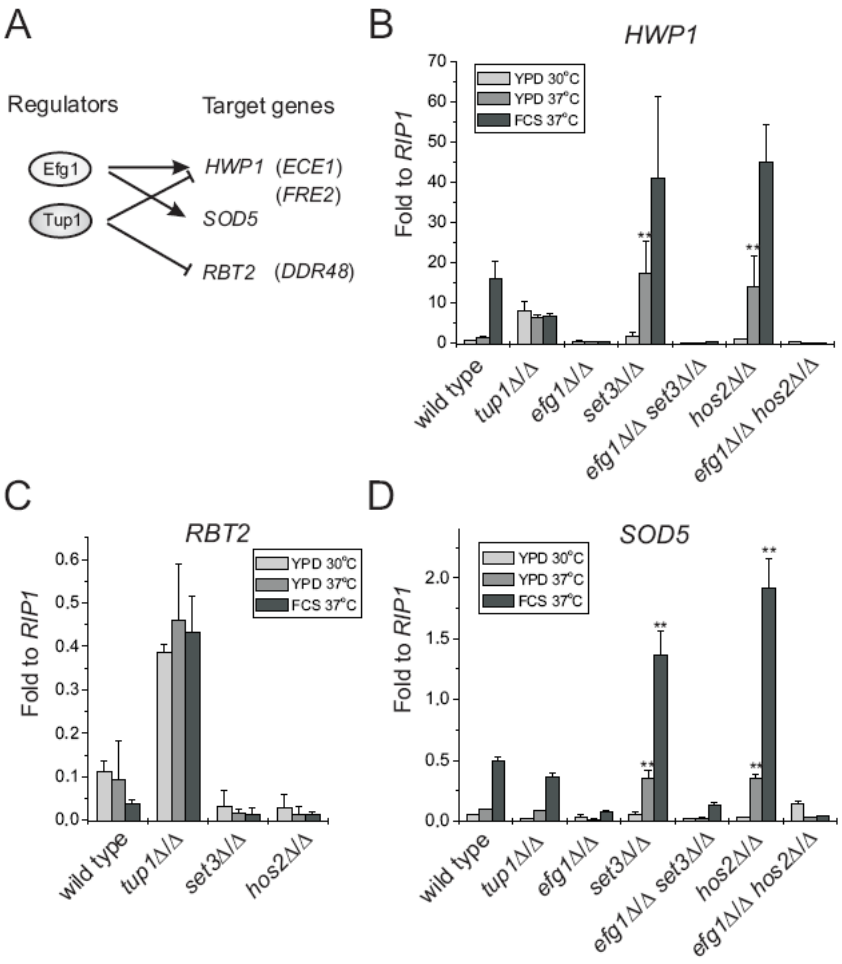
A
Regulators
Target genes
Efg1
Tup1
HWP1 (ECE1)
(FRE2)
SOD5
RBT2 (DDR48)
B
HWP1
YPD 30°C
YPD 37°C
FCS 37°C
Fold to RIP1
wild type
tup1Δ/Δ
efg1Δ/Δ
set3Δ/Δ
efg1Δ/Δ set3Δ/Δ
hos2Δ/Δ
efg1Δ/Δ hos2Δ/Δ
C
RBT2
D
SOD5

Figure 5

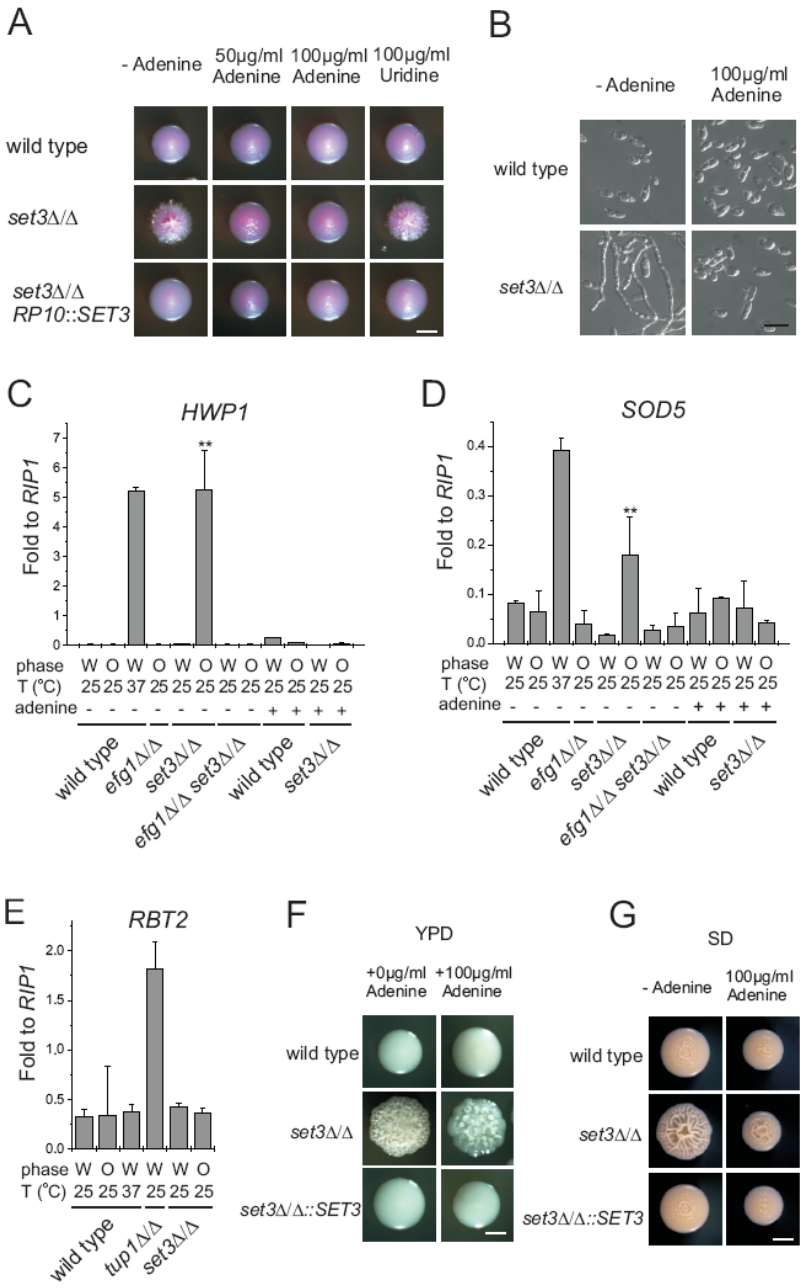
A
- Adenine
50µg/ml Adenine
100µg/ml Adenine
100µg/ml Uridine
wild type
set3Δ/Δ
set3Δ/Δ RP10::SET3
B
- Adenine
100µg/ml Adenine
wild type
set3Δ/Δ
C
HWP1
Fold to RIP1
phase W O W O W O W O W O W O
T (°C) 25 25 37 25 25 25 25 25 25 25 25 25
adenine - - - - - - - - + + + +
wild type
efg1Δ/Δ
set3Δ/Δ
efg1Δ/Δ set3Δ/Δ
wild type
set3Δ/Δ
D
SOD5
Fold to RIP1
phase W O W O W O W O W O W O
T (°C) 25 25 37 25 25 25 25 25 25 25 25 25
adenine - - - - - - - - + + + +
wild type
efg1Δ/Δ
set3Δ/Δ
efg1Δ/Δ set3Δ/Δ
wild type
set3Δ/Δ
E
RBT2
Fold to RIP1
phase W O W W W O
T (°C) 25 25 37 25 25 25
wild type
tup1Δ/Δ
set3Δ/Δ
F
YPD
+0µg/ml Adenine
+100µg/ml Adenine
wild type
set3Δ/Δ
set3Δ/Δ::SET3
G
SD
- Adenine
100µg/ml Adenine
wild type
set3Δ/Δ
set3Δ/Δ::SET3

Figure 6

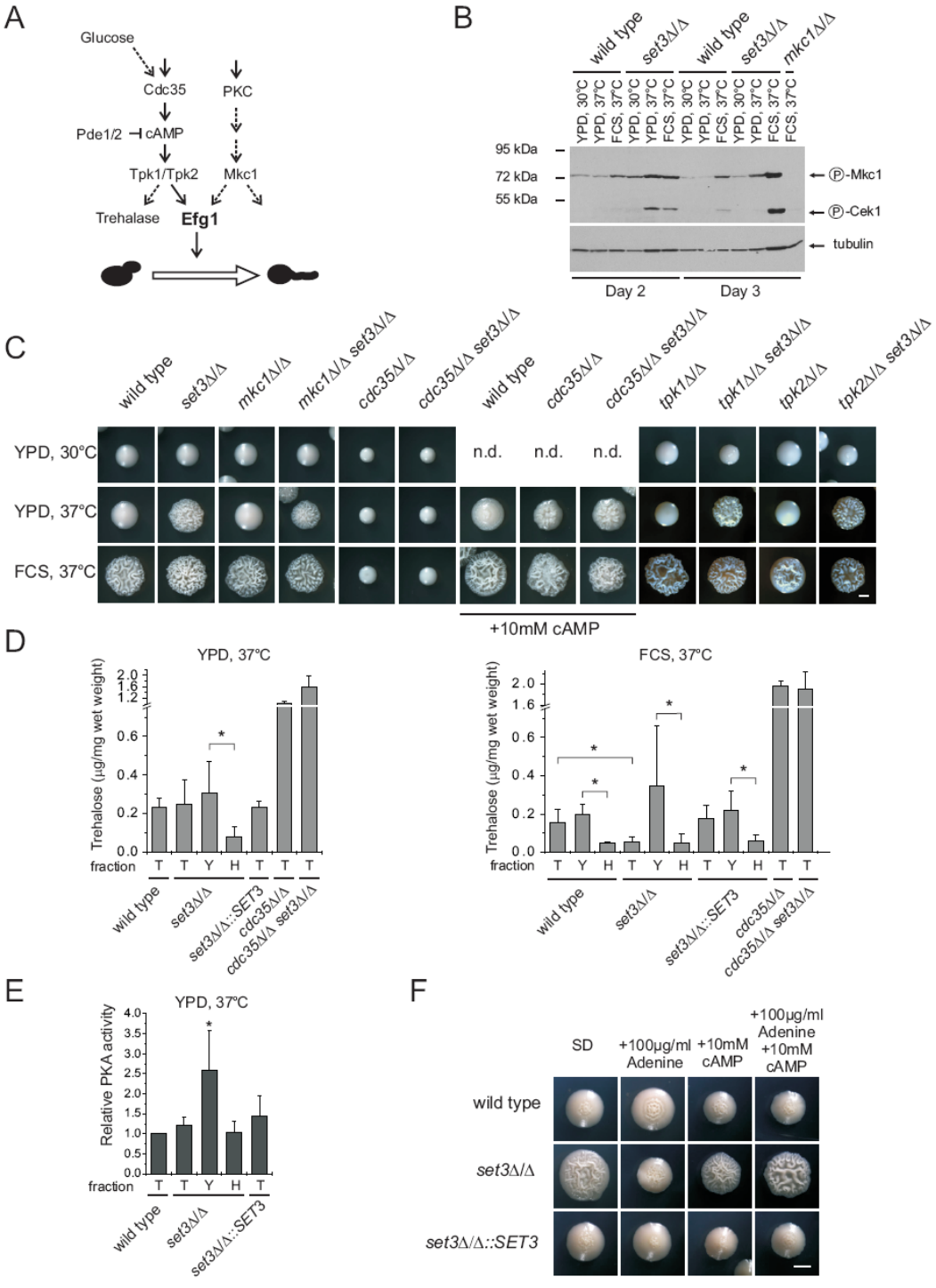
A
Glucose
Cdc35
PKC
Pde1/2
cAMP
Tpk1/Tpk2
Mkc1
Trehalase
Efg1
B
wild type
set3Δ/Δ
wild type
set3Δ/Δ
mkc1Δ/Δ
YPD, 30°C
YPD, 37°C
FCS, 37°C
95 kDa
72 kDa
55 kDa
Ⓟ-Mkc1
Ⓟ-Cek1
tubulin
Day 2
Day 3
C
wild type
set3Δ/Δ
mkc1Δ/Δ
mkc1Δ/Δ set3Δ/Δ
cdc35Δ/Δ
cdc35Δ/Δ set3Δ/Δ
wild type
cdc35Δ/Δ
cdc35Δ/Δ set3Δ/Δ
tpk1Δ/Δ
tpk1Δ/Δ set3Δ/Δ
tpk2Δ/Δ
tpk2Δ/Δ set3Δ/Δ
YPD, 30°C
YPD, 37°C
FCS, 37°C
n.d.
n.d.
n.d.
+10mM cAMP
D
YPD, 37°C
FCS, 37°C
Trehalose (µg/mg wet weight)
fraction
T
Y
H
wild type
set3Δ/Δ
set3Δ/Δ::SET3
cdc35Δ/Δ
cdc35Δ/Δ set3Δ/Δ
E
YPD, 37°C
Relative PKA activity
F
SD
+100µg/ml Adenine
+10mM cAMP
+100µg/ml Adenine +10mM cAMP
wild type
set3Δ/Δ
set3Δ/Δ::SET3

Figure 7

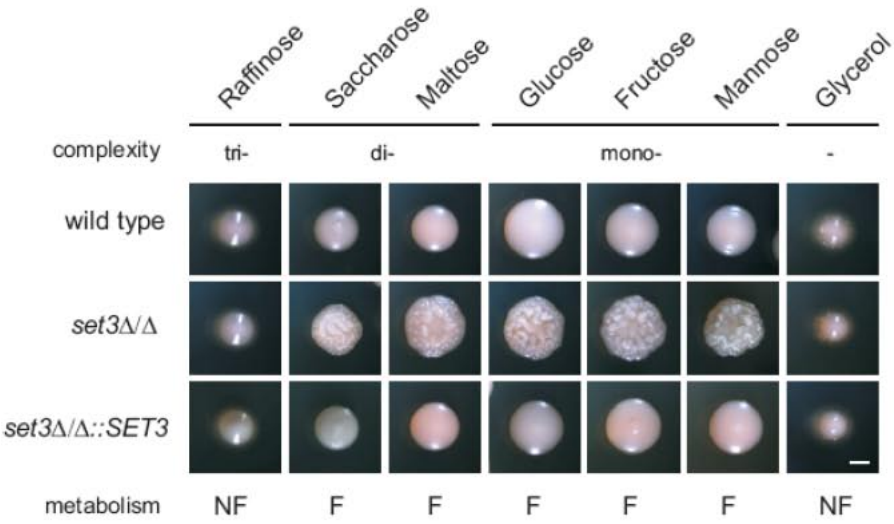

Figure 8

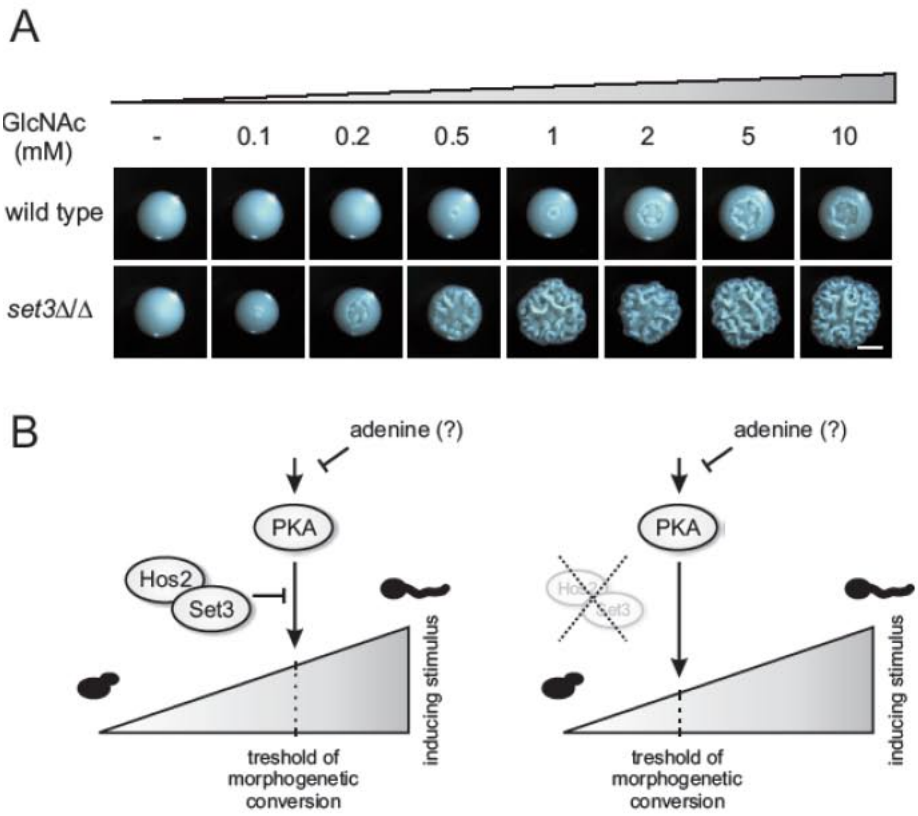

Figure 9

A

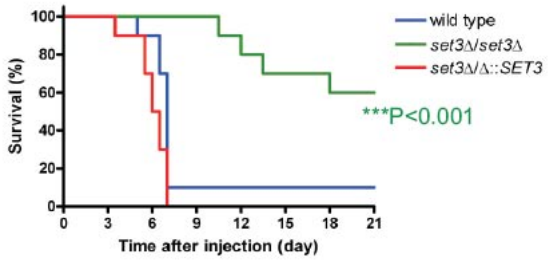

B

Strain	Generation time (min)
wild type	58.5 ± 1.7
SET3/*set3*Δ	59.1 ± 1.5
*set3*Δ/Δ (#1)	59.8 ± 1.5
*set3*Δ/Δ::*SET3*	56.7 ± 2.1
*set3*Δ/Δ (#2)	59.6 ± 1.2

C

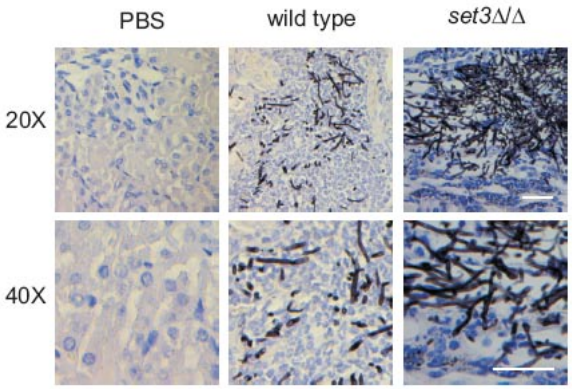

Acknowledgments

I would like to thank all people who have supported me in all possible ways during the time of my PhD thesis. They made it possible for me to have an unforgettable time in- and outside of the Lab.

Special thanks to my parents for their love, moral support and faith in me.

I thank my supervisor Karl for the opportunity to work on this interesting topic in his lab and for all his support.

I want to give a special thank you to all present and former members of the “KaKu-Versum” for creating such a pleasant and unique working atmosphere. In particular I thank my colleagues working in the 2.509 and 2.507 Labs for scientific and private chats during our famous coffee breaks, and diverse outside entertaining. Furthermore, I’d like to say thanks to my co-workers sitting in 2.107 Lab, for their support and enthusiasm about new ideas and experiments. I give my thanks to Christelle for her great supervision and encouragement. I thank Regina and Maria for their administrative support and for always having an open ear. Especially I want to thank Christa, Conny, Nathie, Kritstina, Flo, Olivia and Tobi for being great colleagues and friends.

I say thank you to all my friends outside of the Lab, in particular Dani, Gina, Gerhard, Julia, Christina and Sabine for always being around when I needed them and for memorable evenings.

I give my deepest thanks to Doris for spending a lot of time deciphering and improving my scientific English and for her care and support.

Curriculum Vitae

Name:	Ingrid Elisabeth Frohner
Birthday:	July 26, 1980

Education

Aug 2005 - May 2010	**PhD thesis** in Genetics-Microbiology at the University Of Vienna
Oct 1999 - May 2005	**Master of Science** Microbiology and Genetics at the University of Vienna

Research and Professional Experience

Since Aug 2005: Role of infection	**Ph.D thesis at the Institute of Medical Biochemistry**, Prof. Dr. Karl Kuchler: oxidative stress in macrophages and dendritic cells through *Candida spp*.
Dec 2003 - March 2005 Kuchler:	**Diploma thesis at the Institute of Medical Biochemistry**, Prof. Dr. Karl Functional Analysis of the Yeast Transcription Factor War1p
Oct 2003: PCR	I**nternship at the Institute of Medical Biochemistry**, Prof. Dr. Karl Kuchler – based gene tagging in *Candida albicans*.
Mai 2003: The role	**Internship at the Institute of Medical Biochemistry,** Dr. Christian Seiser – of Histone Deacetylases during mouse embryonic development, mouse tissues and fibroblast cells.
Oct 2003 - Jan 2004	Part time job at the Institute of Medical Biology, Prof. Silvia Hagemann
Aug 2000 - Sept 2003	Part time job at the Institute of Medical Biology, Dr. Wolfgang Miller

Teaching Experience

Oct 2008 to Oct 2009	Supervision of the Diploma Thesis of Kristina Yatsyk: Visualization of Superoxide Dismutase Sod5 Localization in Opportunistic Human Pathogen *Candida albicans*
Nov 2007 between	Supervision of the Internship of Roland Baumgartner: The interactions C*andida albicans* and cells of the innate immune system and the role of superoxide dismutases *SOD4* and *SOD5* in *Candida albicans*
Nov 2006	Supervision of the Internship of Sophia Millonigg: The role of different Superoxid Dismutases of *Candida albicans*
May 2003 and 2004:	Tutorial assistant at Medical University of Vienna – Seminar: Evolution of Mankind and its Diseases

Organising Experience

Jan 2009 – Oct2009	Member of the organising committee of the 1st MFPL PhD and PostDoc recess in Krumbach, Austria
June 2006- July 2007	Chair of the organising committee of the 7th FEBS-YSF Meeting ("Molecular Network") with up to 100 participants in Vienna, Austria
March 2006 and 2008	Assisting crew of the 1st and 2nd FEBS Special Meeting in Innsbruck on ABC Proteins ("ABC Proteins: From Multidrug Resistance to Genetic Disease")with up to 350 participants in Innsbruck, Austria.

Courses and Summer Schools

January 2007:	LaCi, The 2nd Luminy Advanced Course in Immunology, Marseille
November 2005:	Medical Mycology Course, Austrian Society of Medical Mycology

Scholarships and Awards

Aug 2005 – July 2008	Vienna Biocenter International PhD Programme Fellowship funded by the Austrian Science Fund (FWF).
March 2009	"Young Investigator Award" awarded for a talk presentation at the Fungal Genetics, Asilomar, March 2009 Title: *Candida albicans* cell surface superoxide dismutases degrade host-derived reactive oxygen species to escape innate immune surveillance. Counselor: Prof Dr. Karl Kuchler

Languages

German:	First language
English:	Excellent skills fluent in speech and writing
Italian:	Basic skills

Scientific Publications

The Set3/Hos2 Histone Deacetylase Complex Attenuates cAMP/PKA Signaling to Regulate Morphogenesis and Virulence of *Candida albicans*
Denes Hnisz, Olivia Majer, **Ingrid E Frohner,** Vuksolav Komnenovic, Karl Kuchler
PLOS Pathogens, Accepted March 2010,

In vitro systems for studying the interaction of fungal pathogens with primary cells from the mammalian innate immune system.
Bourgeois C, Majer O, **Frohner I**, Kuchler K.
Methods Mol Biol. 2009;470:125-39.

Candida albicans cell surface superoxide dismutases degrade host-derived reactive oxygen species to escape innate immune surveillance.
Frohner IE, Bourgeois C, Yatsyk K, Majer O, Kuchler K.
Mol Microbiol. 2009 Jan;71(1):240-52. Epub 2008 Nov 4.

Weak organic acids trigger conformational changes of the yeast transcription factor War1 in vivo to elicit stress adaptation.
Gregori C, Schüller C, **Frohner IE**, Ammerer G, Kuchler K.
J Biol Chem. 2008 Sep 12;283(37):25752-64. Epub 2008 Jul 11.

Abstract publication: *Candida albicans* yeast form and hyphae form trigger ROS production in primary macrophages
I. Frohner, C. Bourgeois, O. Majer and K. Kuchler
The FEBS Journal Vol.274 Supplement 1 July 2007

Oral Presentations

Medical Mycology - From Basic Science to Clinical Needs, Vienna, December 4-5, 2009
Candida albicans cell surface superoxide dismutases degrade host-derived reactive oxygen species to escape innate immune surveillance.
Frohner IE, Bourgeois C, Yatsyk K, Majer O, Kuchler K.

Fungal Genetics, Asilomar, March 2009
Candida albicans cell surface superoxide dismutases degrade host-derived reactive oxygen species to escape innate immune surveillance.
Frohner IE, Bourgeois C, Yatsyk K, Majer O, Kuchler K.

VBC student symposium, Vienna, October 2007
Candida spp-induced Oxidative Stress Response in Innate Immune Cells
Ingrid Frohner, Christelle Bourgeois, Olivia Majer & Karl Kuchler